THE EFFECT OF MICROSTRUCTURE ON THE PROPERTIES OF FOAMED CONCRETE

MADELEINE VISAGIE

A dissertation submitted in partial fulfilment of the requirements for the degree of

MASTER OF ENGINEERING (STRUCTURAL ENGINEERING)

In the

FACULTY OF ENGINEERING

UNIVERSITY OF PRETORIA

May 2000

SUMMARY

THE EFFECT OF MICROSTRUCTURE ON THE PROPERTIES OF FOAMED CONCRETE

M VISAGIE

Supervisor: Doctor E. P. Kearsley

Department: Civil Engineering

University: University of Pretoria

Degree: Master of Engineering (Structural engineering)

Foamed concrete is produced when a foaming agent is added to cement-based slurry, consisting of cement, water, cement extender and filler. This lightweight building material can contribute significantly to uplift disadvantaged communities when used during the development of infrastructure. To achieve this goal, in depth research into the structural properties of the material is essential.

Since 1992 tests to determine structural properties of foamed concrete have been conducted at the University of Pretoria. The results show that the compressive strength of foamed concrete is a function of age, ash/cement ratio and porosity and for a given porosity and age there is an optimum ash content, resulting in the maximum compressive strength. The focus of this research is therefore on foamed concrete mixtures with target densities varying between 700 kg/m^3 and 1500 kg/m^3 where the question that needed to be answered is: what is the influence of the microstructure on the physical and structural properties of these mixtures?

The study is restricted to the effect of the microstructure on the relation between the physical properties (such as density, ash / cement ratio and porosity), and the structural property (compressive strength) of foamed concrete.

In order to evaluate the influence of the microstructure on these relationships it was necessary to develop parameters to explain and quantify the microstructure of foamed concrete. An

image processing and analysis system was applied to develop the air-void size distribution parameters and the air-void spacing parameters. These parameters were used to represent the microstructure (entrained air-void structure) of the foamed concrete mixtures. It was therefore now possible to plot graphs showing the effect of the microstructure on the physical and structural properties of foamed concrete.

It was established that the 28-day dry densities have an influence on the air-void size distribution. In turn the air-void size distribution has an influence on the average % porosities and 28-day compressive strength of foamed concrete. The 28-day dry densities have no influence on the spacing of air-voids and in turn the spacing of the air-voids does not have any influence on the average % porosity and 28-day compressive strength.

SAMEVATTING VAN

DIE EFFEK VAN DIE MIKRO-STRUKTUUR OP DIE EIENSKAPPE VAN SKUIMBETON

M VISAGIE

Promotor: Doktor E. P. Kearsley

Departement: Siviele Ingenieurswese

Universiteit: Universiteit van Pretoria

Graad: Magister in Ingenieurswese (Struktuur Ingenieurswese)

Skuimbeton word vervaardig deur 'n skuimmiddel by sement, water en sementaanvuller te voeg. Hierdie liggewig beton kan met welslae gebruik word in die opbou van infra struktuur by minder bevoorregte gemeenskappe. Om hierdie doel te bereik is dit nodig om die strukturele eienskappe van die boumateriaal te ondersoek.

Sedert 1992 word daar by die Universiteit van Pretoria navorsing gedoen oor die strukturele eienskappe van skuimbeton. Daar is gevind dat die druksterkte 'n funksie is van die ouderdom van die skuimbeton, die as / sement verhouding en die porositeit. Die maksimum druksterkte by 'n spesifieke ouderdom van die skuimbeton word verkry by 'n optimum as hoeveelheid in die mengsel. Die doel van hierdie navorsing is om te bepaal of die mikro-struktuur van skuimbeton enige invloed het op die fisiese en strukturele einskappe van die materiaal. Slegs mengsels met teiken digthede tussen 700 kg/m³ en 1500 kg/m³ word bestudeer in hierdie navorsing.

Die studie word beperk tot die effek van die mikro-struktuur op die fisiese eienskappe (as / sement verhouding, digtheid en porositeit) en strukturele eienskappe (28 dae druksterkte) van die spesifieke mengsels.

'n Fotografiese beeld prossesering en analitiese stelsel is gebruik om parameters te ontwikkel om die mikro-struktuur van skuimbeton te kwantifiseer. Twee parameters is ontwikkel, die een om die verdeling van die grote van die ingemengde lug borrels aan te dui en die ander een

om die spasiëring van die ingemengde lug borrels in die mengsel aan te dui. Aangesien hierdie parameters die mikro-struktuur van skuimbeton verteenwoordig was dit nou moontlik om die effek van die mikro-struktuur op die fisiese- en strukturele eienskappe van skuimbeton te bepaal.

Die resultate van die studie dui aan dat die 28-dae droë digtheid wel 'n invloed het op die verdeling van die grote van die lug borrels. Die verdeling van die grote van die lug borrels het weer 'n effek op die gemiddelde porositeit en 28-dae druk sterkte. Die 28-dae droë digtheid het geen invloed op die spasiëring van die lug borrels en die die spasiëring van die lug borrels op sy beurt het ook nie 'n invloed op die gemiddelde porositeit en 28-dae druk sterkte nie.

ACKNOWLEDGEMENT

I wish to express my appreciation to the following organisations and persons who made this dissertation possible:

- Grinaker, for the donation of the materials used in this investigation.

- Doctor EP Kearsley, my promoter, for her guidance and support.

- The following persons for their assistance during the course of the study:

  Mr. D. Mostert
  Mr. J. Pretorius
  Mrs. J. Callanan
  Miss B. Le Roux
  Miss G. Veldman
  Personnel of the concrete laboratory of the Civil Engineering department of the University of Pretoria.

- My family, especially my husband and two children for their encouragement and all the sacrifices they made.
- To my creator.

TABLE OF CONTENTS

APPENDIX G Summary of exponential fits for the cumulative % oversize graphs for specific ash / cement ratios

LIST OF TABLES

LIST OF FIGURES

1. INTRODUCTION

1.1 BACKGROUND

Foamed concrete is one of few building materials combining good mechanical strength with low thermal conductivity and ease of application. It is used extensively to reduce the weight of precast concrete building units and also improving the insulating properties of these units. This lightweight building material when used during the development of infrastructure can therefore contribute significantly to uplift disadvantaged communities. To achieve this goal, in depth research into the structural properties of the material is essential.

Foamed concrete is produced when a foaming agent is added to cement-based slurry, consisting of cement, water, cement extender and filler. The foaming agent, consisting of hydrolized protiens is diluted with water and aerated to create the foam (Neville, 1987). The cement paste sets around the foam bubbles and when the foam begins to degenerate, the paste has sufficient strength to maintain its shape around the void. To ensure that the desired persentage of air is entrained in the mixture, pre-foaming, where the foaming agent is aerated before being added to the mixture, is recommended (Kearsley, 1996).

Cost is always a major factor in the development of infrastructure. Mixtures can be designed to use fly ash as a cement replacement thereby optimizing strength and minimizing cost. Fly ash is readily available at low cost in South Africa (Krüger, 1998).

Since 1992 tests to determine structural properties of foamed concrete have been conducted at the University of Pretoria. The results showed that the compressive strength of foamed concrete is a function of age, ash / cement ratio and porosity and for a given porosity and age there is an optimum ash content, resulting in the maximum compressive strength. All the tests were conducted on foamed concrete mixtures with target densities higher than 1000 kg/m^3. In addition the effect of the microstructure (air-void structure) on the properties of these spesific mixtures was found to be minimal (Kearsley, 1999).

The focus of this research is on foamed concrete mixtures with target densities varying between 700 kg/m³ and 1500 kg/m³ where the question that needs to be answered is: what is the influence of the microstructure on the physical and structural properties of these mixtures?

1.2 OBJECTIVES OF STUDY

The objective of this investigation is to:

- Determine the influence of the physical properties of foamed concrete mixtures with target densities varying between 700 kg/m³ and 1500 kg/m³ on the structural properties of these mixtures.
- Develop parameters to explain and quantify the microstructure of foamed concrete.
- Determine the effect of the microstructure on the properties of foamed concrete mixtures with target densities varying between 700 kg/m³ and 1500 kg/m³.
- Determine the possible influence of the microstructure on the optimum ash content of the mixtures with target densities varying between 700 kg/m³ and 1500 kg/m³.

1.3 SCOPE OF STUDY

The scope of this investigation covers foamed concrete mixtures manufactured using rapid hardening Portland cement, unclassified ash (pozz-fill), a South African pre-foaming agent "Foamtech" consisting of hydrolyzed protiens and 2 kg/m^3 of chopped 6.7 Dtex fibrillated polypropylene fibers (12 mm long). Only one source of each material is used in this project and no inert filler (such as sand) is used in any of the mixtures. A cost analysis for design mixtures does not form part of the investigation.

The pore structure of foamed concrete consists of gel and capillary pores, entrained air-voids and entrapped air-voids. For the scope of this study only the entrained air-void structure is identified to represents the microstructure of foamed concrete. The influence therefore of the gel and capillary pores as well as the entrapped air-voids on the properties of foamed concrete is not covered by this research.

The study is restricted to the effect of the microstructure on the 28-day dry density, ash / cement ratio, average % porosity and the 28-day compressive strength of the foamed concrete mixtures. The determination of the influence of the microstructure on the shrinkage, creep, water absorption, permeability, ultimate strength, durability and volume stability of the mixtures is therefore beyond the scope of this investigation. The effect of the method of casting and the curing of the foamed concrete mixtures on microstructure is not covered by this research.

1.4 STUDY METHODOLOGY

Foamed concrete mixtures with different ash / cement ratios (zero to four) and different target densities between 700 kg/m³ and 1500 kg/m³ were used in this investigation. A pre-foamed protein based foaming agent was used for the mixtures to ensure predictable densities.

The physical properties (28-day dry density and average % porosity) as well as a spesific structural property (the 28-day compressive strength) of the foamed concrete mixtures were obtained first, before the relationships between these properties were determined.

In order to evaluate the influence of the microstructure on these relationships it was necessary to develop parameters to explain and quantify the microstructure of foamed concrete. An image processing and analysis system was applied to develop the air-void size distribution parameters and the air-void spacing parameters. These parameters were used to represent the microstructure (entrained air-void structure) of the foamed concrete mixtures. It was therefore now possible to plot graphs showing the effect of the microstructure on the physical and structural properties of foamed concrete.

1.5 ORGANISATION OF DISSERTATION

The dissertation has been divided into the following sections:

- Chapter 1 serves as an introduction to the thesis.

- The composition and material properties of foamed concrete are discussed in Chapter 2 and the most important physical and structural properties are identified.
- The methods of measurement of air-void parameters as used for hardened conventional concrete are evaluated in Chapter 3.
- In Chapter 4 the experimental procedure is discussed.
- The results are listed in Chapter 5.
- In Chapter 6 the air-void structure parameters (the air-void size distribution and the air-void spacing) are developed.
- The influence of the microstructure on the physical and structural properties is evaluated in Chapter 7.
- Chapter 8 contains the conclusions and the recommendations of the study.
- References are given in Chapter 9.
- Various results are provided in the different appendices. These appendices are referred to in the main body of the dissertation.

2. COMPOSITION AND PROPERTIES OF FOAMED CONCRETE

2.1 INTRODUCTION

Lightweight concrete's density is appreciably lower than the usual range of concretes made with normal weight aggregates. Three types of lightweight concrete are produced namely (Neville, 1987):

a) Lightweight aggregate concrete
b) Aerated concrete: Foamed - or Gas concrete
c) No-fines concrete

In essence, the decrease in density of the concrete in each type is obtained by the presence of voids either in the aggregate or in the mortar or in the openings between the coarse aggregate particles (Neville, 1987).

This study is only concerned with aerated concrete in particular foamed concrete, which is produced by introducing large voids (0.01mm to 1.0mm) in size, into the cement paste. The cement paste consists of cement, water and cement replacement. Depending on the required properties it can be produced with or without lightweight aggregate such as sand, stone dust, fine gravel etc. (Taylor, 1974). The introduction of the voids is achieved by adding foam to the mixture. A foaming agent consisting of hydrolized proteins is diluted with water and aerated to form the foam.

The aim of this research is to investigate the microstructure of the material as the primary factor influencing the relationship between the physical properties and the structural properties of foamed concrete. In this chapter the composition of the material and the relationships between the physical properties and the structural properties of foamed concrete are evaluated.

2.2 MATERIAL COMPOSITION

2.2.1 Cement paste

Factory made steam-cured foamed concrete was first successfully produced in 1928 using cement as a basic binding material. Subsequently, countries like

USSR, USA and Germany developed new technologies based on different binding materials, depending on their availability and their relative costs. Maximum economy would result if lime is used as the base since lime is the cheapest binding material, but studies done at Ennore, Madras show that cement in the binder is necessary to optimize setting time. As a result, at Ennore, Madras only a portion of the cement was replaced by fly ash, a waste product from the Basin Bridge powerhouse nearby (Chitharanjan, 1978).

During the manufacturing of the product the cement paste starts setting around the air-bubbles and when the foam begins to degenerate after approximately three quarters of an hour, the paste must have sufficient strength to maintain its shape around the air-void (Kearsley 1996). Using a combination of cement and fly ash the required strength of the cement paste can be attained if the free CaO content in the binder available for chemical reaction can be maintained. In other words the CaO in the fly ash is used to augment the reduction of CaO in the binder because of the removal of a portion of cement. Cement contains active lime in the form of CaO, which varies from 55 to 65 percent, and its activity varies with the quality of cement at the time of use. Therefore Chitharanjan (Chitharanjan, 1978) concluded that a theoretical prediction regarding the optimum percent of fly ash cannot be made, the optimum can only be reached experimentally.

The use of a lightweight aggregate, for example sand, as filler in the mixture will also influence the optimum percentage of fly ash. The filler will increase the silica content of the paste and that will change the final hydration product, namely the calcium silicate hydrates known as crystalline tobermorite (Chitharanjan, 1978).

It was found by Chitharanjan (Chitharanjan, 1978) that the optimum Basin Bridge powerhouse fly ash content for the maximum strength with minimum density and moisture content is 40 percent by weight of the specific binder. The replacement of cement with fly ash did not keep the quality of the foamed concrete the same, but in fact it improved the quality.

In large areas of South Africa fly ash is available at low cost and according to Kearsley (Kearsley, 1999) the South African fly ash (pozz-fill – unclassified ash) can be used as a cement replacement in foamed concrete with no negative

effect on the properties. Although the rate of gain in strength is reduced by use of large volumes of ash, up to 67 % of the cement can be replaced by ash without any significant reductions in long-term strength.

The composition of the mixture used by Kearsley (Kearsley, 1999) to determine the optimum ash / cement ratio is Portland cement, South African fly ash and foam manufactured with a pre-foaming agent. There seems to be an optimum ash content, resulting in the highest compressive strength for a given porosity. A compressive strength model (as discussed in 2.3.4) is developed for this type of mixtures to predict the optimum ash content theoretically. It was found that this optimum ash content increases with an increase in age.

Foamed concrete is more sensitive to water content than normal concrete. Concrete normally has a certain water demand to obtain a required workability and the strength of the concrete decreases as the water-cement ratio increases (Neville, 1987). For foamed concrete workability is not a problem but if the water in the mixture is not sufficient for initial reaction of the cement paste, the cement withdraws water from the foam, causing rapid degeneration of the foam. If too much water is added, segregation takes place, causing a variation in density (Kearsley, 1996).

Kearsley (Kearsley, 1996) did research on the optimum water/cement ratio for all the different foam contents and found that it is in the region of 0.38 when no fly ash was added. When South African fly ash was used in the binder the required water/cement ratio increased as the fly ash/cement ratio increased.

2.2.2 Foam

The density of the foamed concrete is a function of the volume of foam that is added to the cement paste. To ensure that the desired percentage air is entrained in the mixture, pre-foaming, where the foaming agent is aerated before being added to the mixture, is used (Kearsley, 1996).

The aerated foaming agent, on mixing with the cement-based slurry entrains a controlled quantity of air in uniformly dispersed discreet cavities. These voids

are typically spherical with diameters from 0.01 mm to 1.0 mm and are closely spaced being not more than 0.4 mm apart (Neville, 1987).

The foaming agent is surface active, which means that the molecules when placed into water are capable of splitting themselves into ions (see figure 2.1). The organic ions are built up of a long organic chain, which is uncharged, and an electrically charged part or the polar part. As water can be considered to consist of dipoles, the polar part of the organic ion will be attracted by that part of the water molecule, which has an opposite charge (Kreijger, 1967).

The chain is always pushed out of the water; this being hydrophobic (water hating) and the polar group is attracted to the water this being hydrophilic (water loving). If the polar part is charged positive, one speaks of a cat-ion: if it is charged negative, of an an-ion. Next to these two groups there are organic molecules, which can be presented also as a dipole (see figure 2.1). These are called non-ionic. (Kreijger, 1967).

The net result when mixing the foam, water and cement paste is that the foaming agent molecules orient themselves at any air / water interface thereby stabilizing themselves. The surface of the cement particles is made hydrophobic by the admixture and by means of the carbon chains the air-bubbles adhere to the cement particles and the sand grains. This combined effect stabilizes the air bubbles, which is the best condition for a regular distribution throughout the mixture (see figure 2.2) (Kreijger, 1967).

The pressure difference between the inside and outside of an air bubble is given by the following relationship (Uchikawa, 1991):

$$\Delta P = \frac{4\gamma}{D} \qquad \text{(Eq 2.1)}$$

Where:

ΔP = pressure difference between inside and outside of air-void

γ = surface tension

D = bubble diameter

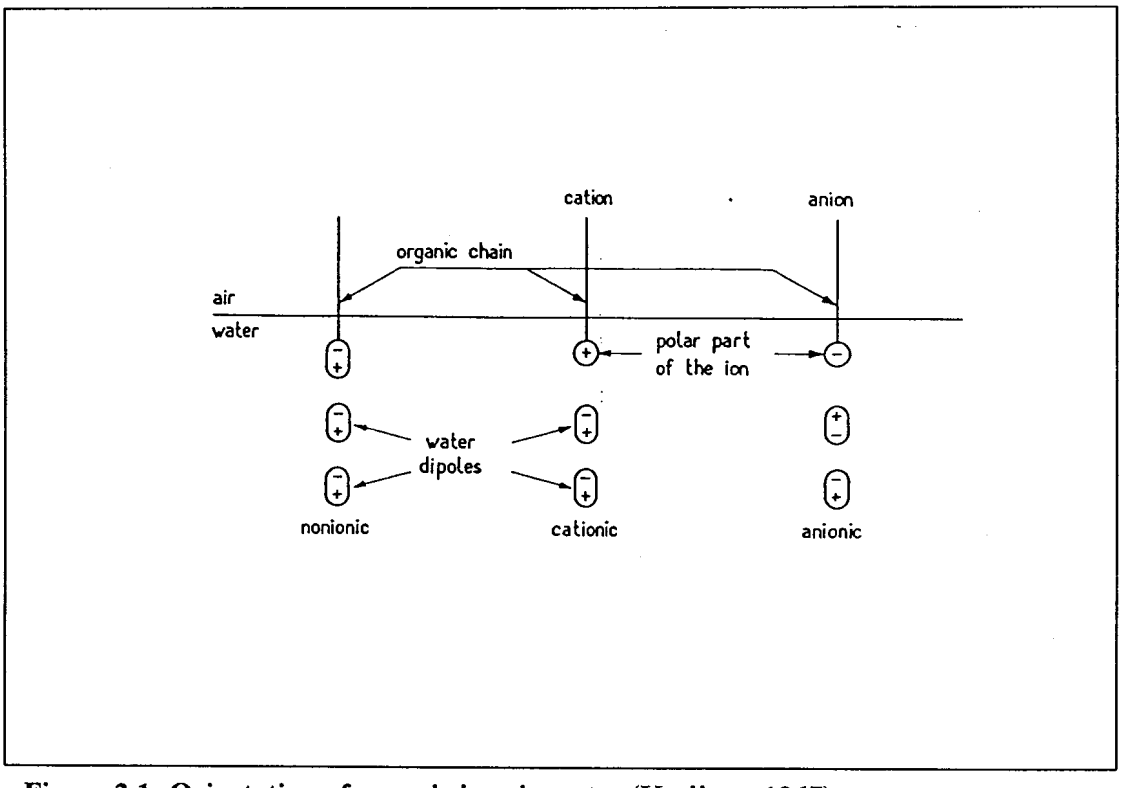

Figure 2.1: Orientation of organic ions in water (Kreijger, 1967).

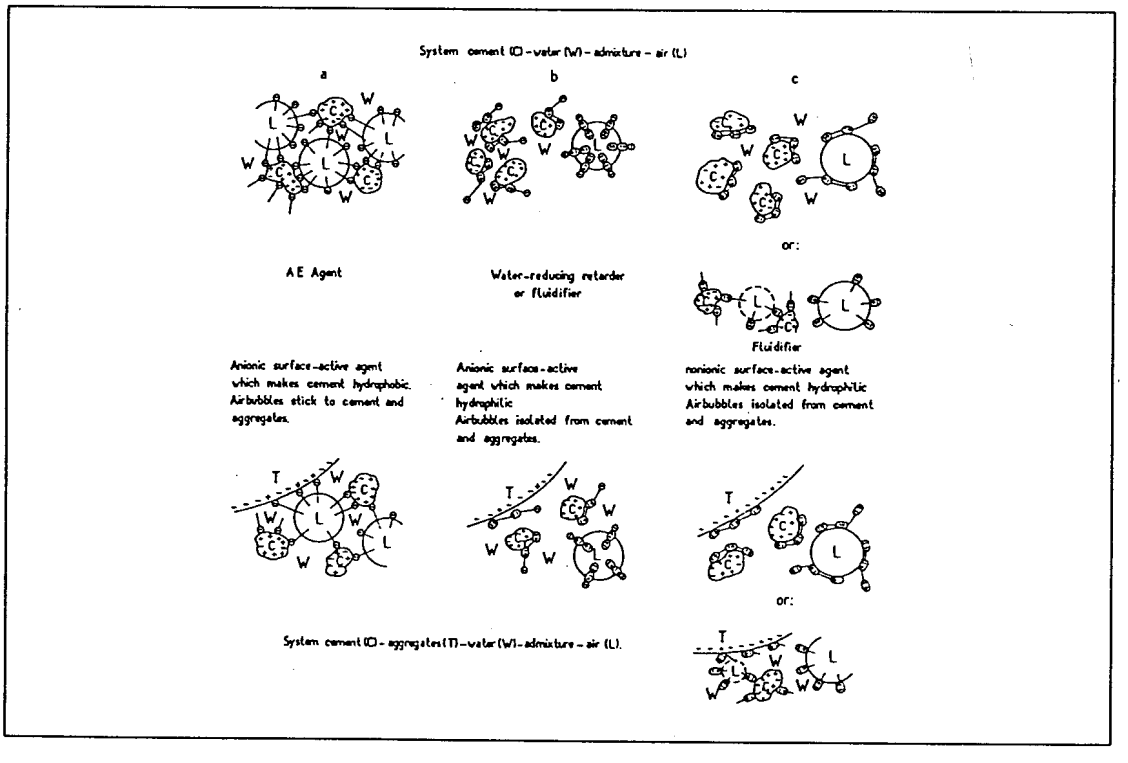

Figure 2.2: Scheme of the interactions between cement, air, water and molecules of foaming agent (Kreijger, 1967).

From equation 2.1 it is clear that small bubbles require the air in the bubble to be at a higher pressure than larger bubbles, and therefore there is a strong tendency for small bubbles to join to form larger bubbles to lower the air-pressure in the bubbles. The foaming agent is based on materials, which will lower the surface tension, and therefore it becomes easier to form smaller bubbles. The foaming agent also helps to maintain the bubble by slightly increasing viscosity and by forming a stabilized skin to the bubble.

The air-bubbles just after forming are not filled with products of hydration because they are separate from the capillary pore system in the cement paste as gel can only form in water (Neville, 1987).

The foaming agent is one of the most important elements of the material. A good quality foaming agent and therefore one which has the ability to form a stabilized skin to the air-bubbles will guarantee an evenly distributed air-void system.

2.3 MATERIAL PROPERTIES

In order to evaluate the relations between the physical properties and the structural properties of foamed concrete these properties have to be identified.

When undertaking the design of a foamed concrete mixture, a target casting density is determined and the dry density of the mixture is the most important factor affecting the properties of the mixture (Kearsley, 1999). The density is therefore identified as an important physical property that has to be investigated.

According to Kearsley (Kearsley, 1999) porosity, ash / cement ratio, and age are also variables, which will influence the structural characteristics of foamed concrete.

Strength, durability, impermeability and volume stability are the most important structural characteristics of concrete. Nevertheless strength usually gives an overall picture of the quality of concrete and it is directly related to the structure of the cement paste (Neville, 1987). Therefore in the rest of this

investigation only the compressive strength will be use as the structural property indicating the quality of foamed concrete.

The required target casting density can be determined by using chosen water / cement (w/c) and sand / cement (s/c) ratios (ACI, 1975) and the relative densities of the materials the mass of the cement and the volume of foam that should be added to obtain the required density. By assuming that V_f liters of foam should be added per cubic meter of foamed concrete and that the cement content of the mixture is x kg/m^3 the following equations can be used for calculating the actual mixture compositions:

$$\rho_m = x + xw/c + xs/c + RD_f V_f \qquad \text{(Eq. 2.2)}$$

$$1000 = \frac{x}{RD_c} + xw/c + \frac{xs/c}{RD_s} + V_f \qquad \text{(Eq. 2.3)}$$

Where:

ρ_m = Target casting density (kg/m^3)

RD_f = Relative density of foam

RD_c = Relative density of cement

RD_s = Relative density of sand

In mixtures where the sand has been replaced by ash an ash / cement ratio (a/c) is used instead of the sand / cement ratio and the relative density of sand is replaced with the relative density of ash (Kearsley, 1999).

From these equations it's clear that the density of foamed concrete is directly related to the percentage foam that is added to the slurry. The maximum compressive strength of the material decreases as the foam content increases (Kearsley, 1997).

2.3.1 Relation between density and compressive strength

According to Vine-Lott (Vine-Lott, 1985) the compressive strength of foamed concrete is an inverse function of the density of the material. This relationship

between density and compressive strength is exponential, the value of the exponent varying with the size and distribution of the air-voids.

2.3.2 Relation between density and porosity

The porosity of a porous material is defined as the fraction of its bulk volume occupied by voids therefore the porosity of foamed concrete is defined as the relative volume of pores or voids in the cement paste.

Kearsley (Kearsley, 1999) found that porosity is largely dependent on the dry density and not on ash type or ash content. The porosity of foamed concrete as a function of dry densities between 800 kg/m^3 and 2000 kg/m^3 can best be described using the following equation:

$$\rho = 18665\gamma_d^{-0.844} \qquad \text{(Eq. 2.4)}$$

Where:

ρ = porosity (%)

γ_d = dry density (kg/m^3)

2.3.3 Relation between porosity and compressive strength

Several equations have been suggested to express the relationship between porosity and strength of porous solids. According to Fagerlund and Rößler (Fagerlund, 1973 and Rößler, 1985) the following equation can be used successfully to express the relationship between porosity and strength of cement paste:

$$\sigma = \sigma_0(1-P)^n \qquad \text{(Eq 2.5)}$$

Where:

σ = strength

σ_0 = strength at zero porosity

P = porosity

n = empirical constant

Hoff (Hoff, 1972) investigated the relationship between porosity and compressive strength of foamed concrete. The foamed concrete investigated was made using only Portland cement, water, and preformed foam, which provided the air, content. Foamed concrete can be shown by the simple model in figure 2.3 as being composed of air, evaporable water, non-evaporable water and cement. As such, foamed concrete can be considered as a cement paste with a large void content or high porosity and equation 2.5 can be used to express the relationship between porosity and strength.

Hoff (Hoff, 1972) defined the theoretical porosity as the fractional portion of the total volume that is air plus evaporable water. From weight-volume considerations, the porosity can be expressed as follows:

$$P = 1 - \frac{d_c(1 + 0.20\rho_c)}{(1+k)\rho_c\gamma_w} \qquad \text{(Eq 2.6)}$$

Where:

d_c = concrete density

k = water / cement ratio

ρ_c = Specific gravity of cement

γ_w = unit weight of water

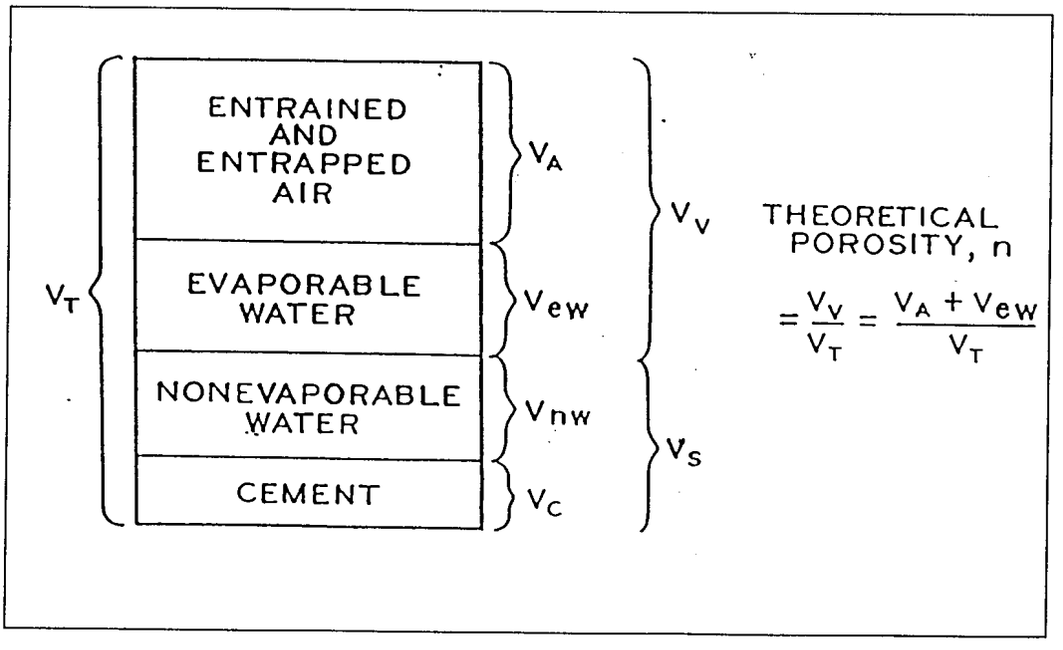

Figure 2.3: Simple model of the composition of foamed concrete as used in the investigation by (Hoff, 1972).

Substituting this equation for porosity in the strength-porosity equation 2.5 for cement paste will give the following expression:

$$\sigma = \sigma_0[\frac{d_c(1+0.20\rho_c)}{(1+k)\rho_c\gamma_w}]^n \qquad \text{(Eq 2.7)}$$

$$\sigma = \sigma_0(\frac{d_c}{1+k})^n(\frac{1+0.20\rho_c}{\rho_c\gamma_w})^n \qquad \text{(Eq 2.8)}$$

The last term of (Eq 2.8) stays the same for a given cement, and hence:

$$\sigma \propto \sigma_0(\frac{d_c}{1+k})^n \qquad \text{(Eq 2.9)}$$

Where:

σ = strength

σ_0 = strength at zero porosity

n = empirical constant

d_c = concrete density

k = water / cement ratio

These equations only hold true for foamed concrete containing only air, water and cement. Kearsley (Kearsley, 1999) made modifications to equation 2.6 so that the theoretical porosity of mixtures containing ash could be determined. The water binder ratio and the binder specific gravity were used in equation 2.6, where the term binder is defined as all the cementitious material in the mixture. The binder specific gravity is calculated by dividing the total binder weight by the total binder volume. The theoretical porosity of foamed concrete mixtures containing a cement extender, one year after casting is therefore expressed by the following equation (Kearsley, 1999):

$$P = 1 - \frac{d_c(1+0.2\rho_b)}{(1+k)\rho_b\gamma_w} \qquad \text{(Eq 2.10)}$$

Where:

d_c = concrete dry density

k = water / binder ratio

ρ_b = Spesific gravity of binder

γ_w = unit weight of water

2.3.4 Effect of ash content, porosity and age on compressive strength

The compressive strength of foamed concrete is not only a function of porosity and therefore dry density but also of mixture age and ash content. The compressive strength of foamed concrete is represented by the following equation (Kearsley, 1999):

$$f_c = (\lambda + \beta Ln(t))(1 - p)^{\alpha} \quad \text{(Eq. 2.11)}$$

With:

$$\beta = \beta_1 + \beta_2 (a/c) + \beta_3 (a/c)^2 \quad \text{(Eq. 2.12)}$$

$$\lambda = \lambda_1 + \lambda_2 (a/c) + \lambda_3 (a/c)^2 \quad \text{(Eq. 2.13)}$$

Where:

f_c = compressive strength (MPa)

t = time since casting (days)

p = porosity (as a fraction)

a/c = ash / cement ratio (by weight)

α β and λ = constants

Kearsley (Kearsley, 1999) determined different values for the constants (α β and λ) for pulverized fuel ash (Pfa) and pozz-fil (unclassified fly ash) respectively (see Table 2.1).

For the scope of this research only South African pozz-fil (unclassified fly ash) is used as a cement extender.

Although high fly ash content results in a reduction in compressive strength at early ages, the long-term strength (say after one year) is improved by replacing up to 75 % of the cement (by weight) with ash.

Table 2.1: Constants for Compressive Strength Model (Kearsley, 1999).

Constant	Pfa	Pozz-fill
α	3.7	3.7
β_1	24.91	23.74
β_2	52.89	56.78
β_3	-12.27	-14.31
λ_1	172.8	176.9
λ_2	-196.0	-229.7
λ_3	34.02	46.04

The 365 day strengths for mixtures with dry densities between 800 kg/m^3 and 2000 kg/m^3 indicate an optimum ash content with maximum strength obtained at ash / cement ratios in the region of 1.5 (Kearsley, 1999).

2.4 MICROSTRUCTURE

It is clear that the physical properties (dry density, porosity and ash content) as well as the age have an influence on the structural property (compressive strength). The question arises, what effect the microstructure of foamed concrete has on these properties? The same porosity as well as density can be achieved for many small air-voids or for fewer larger air-voids in the mixture; therefore the air-void structure may influence these properties.

Compressive strength of normal concrete appears to depend not so much on the chemical composition as on the physical structure of the products of hydration of cement and on their relative volumetric proportions. In particular, it is the presence of flaws, discontinuities and pores that influence the strength of the concrete (Neville, 1987).

Olorunsogo (Olorunsogo, 1990) stated that the pore structure of a cementitious material, pre-determined by its porosity, mean radius and pore size distribution, is a very important micro-structural characteristic as it influences the strength of the material. The properties are dependent mainly on the distribution of the pores within the hardened cement paste.

The pore structure of air-entrained cement paste consists of water – and air-voids as shown in Figure 2.4. The water voids comprises of the gel pore space corresponding to the space between the C-S-H layers and the capillary pore space whose formation depends on the evaporation of the water used in the pastes. The capillary pores remain unfilled with hydrates in the hardened specimens. Hence the different mixture preparation (w/c ratio, compaction) as well as curing conditions (time, temperature, relative humidity) and type of cement used are all parameters influencing the gel- and capillary pore structure of the paste (Atzeni, 1987).

The air-voids include the entrained air formed by the air-entraining agent and the entrapped air as a result of the mixing process (Uchikawa, 1991).

The gel pore shapes are usually represented as platy cylindrical however, the hydraulic radius can also represent it. The shape of the capillary pores is also cylindrical but with small contractions and enlargements along their lengths as shown in figure 2.4 (Cebeci, 1980). Meanwhile the shape of air-voids are spherical or polyhedral resembling spherical (Uchikawa, 1991).

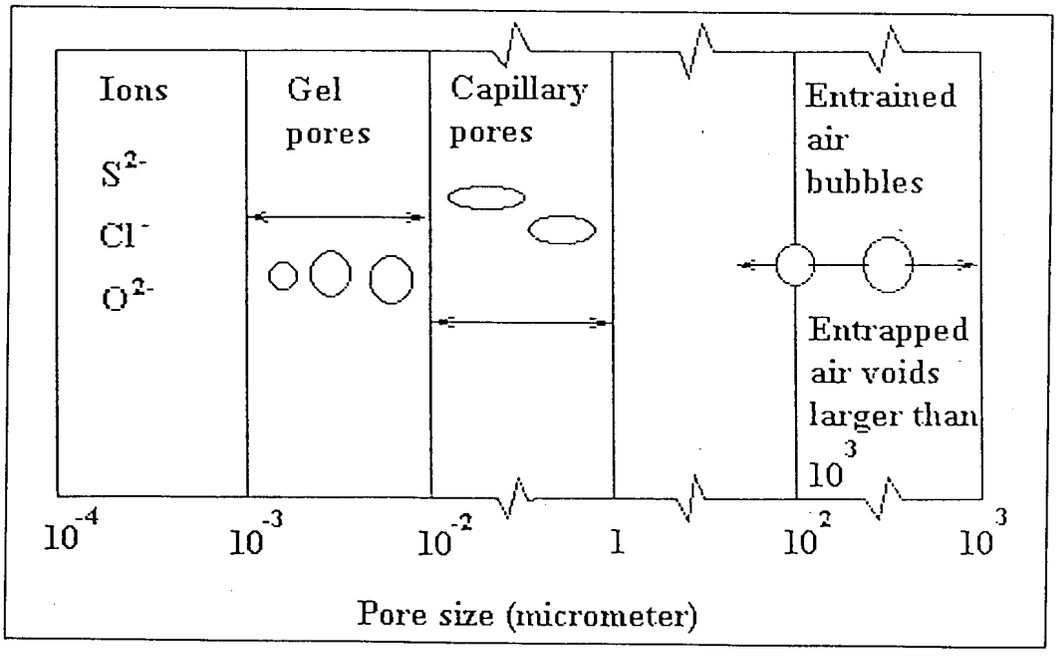

Figure 2.4: Dimensional range of pores in hardened air entrained cement paste (Gowripalan, 1990 and Uchikawa, 1991).

Odler and Rössler (Odler and Rössler, 1985) correlate compressive strength of hardened cement pastes with gel- and capillary pore distribution by means of the following equation:

$$\sigma_c = \sigma_0 - aP_{<10nm} - bP_{10-100nm} - cP_{>100nm} \qquad \text{(Eq. 2.14)}$$

Where:

σ_c = compressive strength

σ_0 = strength at zero capillary porosity

$P_{<10nm}$ = volume of pores with radii r < 10 nm (in %)

$P_{10-100nm}$ = volume of pores with radii r = 10-100 nm (in %)

$P_{>100}$ = volume of pores with radii r > 100 nm (in %)

Correlation results showed however that some of the constants were negative, implying paradoxically, that increased porosity enhanced strength. This can be explained by the fact that as hydration progresses there is a greater number of smaller size pores. As a result, for certain curing times the smaller size ranges appear to increase and because of the greater number of hydrated phases, strengths are higher too. It is for this reason that (Atzeni, 1987) used a different approach for taking into account the effect of pore distribution by correlating strength with an original parameter, named the 'mean distribution radius', defined as follows:

$$\ln r_m = \frac{\sum V_i \ln r_i}{\sum V_i} \qquad \text{(Eq. 2.15)}$$

Where:

r_m = mean distribution radius

V_i = volume of pore

r_i = radius of pore

As r_m decreases, compressive strength increases, gradually at first and then abruptly above the threshold of 10 nm. According to (Atzeni, 1987) the pore distribution parameter (r_m) does not give an adequate correlation of compressive strength properties of hardened cement pastes. Therefore Atzeni (Atzeni, 1987) combined total porosity (P) and strength at zero porosity (σ_0)

as defined in 2.3.3, with the pore distribution parameter (r_m), which leads to the following relation:

$$\sigma = K\frac{\sigma_0(1-P)}{\sqrt{r_m}} \qquad \text{(Eq.2.16)}$$

Compressive strength is directly proportional to a parameter, which incorporates the fraction of gel and capillary pores, the mean distribution radius of these pores and the characteristic strength of the cement paste.

Cebeci (Cebeci, 1981) investigated the effect of air entrainment on the pore structure of hardened cement paste and found that air-entraining only introduces the large air-voids and does not alter the characteristic fine pore structure of hardened cement paste appreciably. Kearsley (Kearsley, 1999) on the other hand found that at high porosities (low target densities) of foamed concrete the calculated paste porosity is higher than the porosity of the cement paste containing no foam. It is therefore possible that some of the water added to mixtures as part of the foam is increasing the effective water / binder ratio in other words changing the gel and capillary pore structure of the paste surrounding the entrained air- voids. The assumption can be made that the gel and capillary pore structure as well as the air-void structure will have an influence on the properties of foamed concrete.

The air-void structure of foamed concrete is for the scope of this investigation identified as the more important micro-structural characteristic and will be investigated in chapter three.

2.5 CONCLUSIONS

- The density of foamed concrete is directly related to the percentage foam that is added to the slurry.
- The compressive strength of foamed concrete is an inverse function of the density of the material.
- Compressive strength of foamed concrete is a function of ash content, porosity and mixture age (physical properties).
- There seems to be an optimum ash content, resulting in the highest compressive strength for a given porosity.

- The air-void structure is a very important micro-structural property influencing the properties of foamed concrete.

3. MEASUREMENT OF AIR-VOID PARAMETERS

3.1 INTRODUCTION

The air-void structure of foamed concrete is identified as one of the most important micro-properties influencing the properties of foamed concrete. In search of a way to describe the air-void structure of foamed concrete, the methods of determination of the air-void parameters for air-entrained hardened concrete are evaluated in this chapter.

Stereology is the foundation of image analysis. It represents the mathematical methods for reconstructing the three-dimensional parameters defining the structure from measurements obtained on sections of the structure (Chan, 1987).

The following methods for measurement of air-void parameters in air-entrained concrete are based on stereology as well as the fact that the essential feature of entrained air-voids, is that they are spherical and, therefore, circular in section, whereas other features will generally be irregular in shape.

3.2 METHODS FOR MEASUREMENT OF AIR-VOID PARAMETERS IN AIR-ENTRAINED HARDENED CONCRETE

3.2.1 Linear traverse method

The American Standard Test Method (ASTM C 457, 1990) and the new European Standard (prEN, 1993) describe a linear traverse method for measurement of air-void parameters.

According to this method, cubes or cylinders of minimum dimension 150 mm are cast from the air-entrained concrete under investigation. The samples are sectioned, such that the cut surfaces are perpendicular to the sample face that was uppermost during manufacture, to produce specimens for analysis.

The approximate dimensions of the specimens are 150 mm x 100 mm x 40 mm. The largest face of these prisms is then ground to produce a smooth flat

surface finish. The surface is further prepared in such a way that the voids are highlighted with a white powder and the rest of the matrix is inked black for microscopic investigation.

The prepared specimen is mounted under a stereoscopic microscope with a magnification of 100 x +/- 10 x. Using the linear-traverse method, the air-void structure is examined by scanning the specimen along a series of traverse lines running parallel to the original free upper surface during manufacture (see figure 3.1).

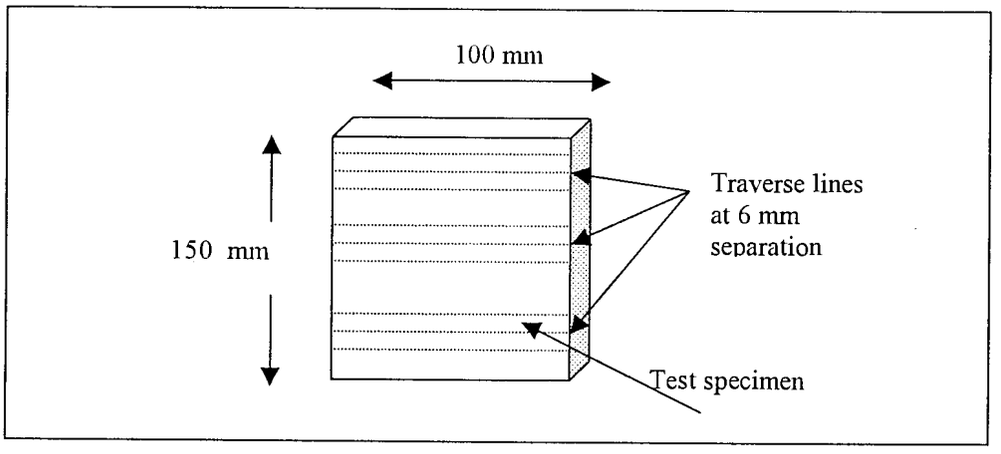

Figure 3.1: Distribution of traverse lines on the surface test specimen

The number of air-voids intersected by the traverse lines is recorded, as are the individual chord lengths of the traverse across the air-voids. The traverse length through paste and the total length of traverse are also recorded (see figure 3.2). These recorded data are then analysed according to the stereological linear analysis of Rosiwell. According to this analysis the areal fraction and consequently the volume fraction can be approximated by the intercept length fraction (Chan, 1987).

3.2.1.1 Air-void structure parameters

With the results of this analysis the air-void structure is described by means of the following parameters:

a) **Total air content.** The proportion of the total volume of concrete taken up by air-voids expressed as a percentage by volume. Willis

(Willis, 1949) derived the following equation to determine the air content by chord intercept measurements:

$$A = n\bar{l} \qquad \text{(Eq. 3.1)}$$

Where:

n = the number of bubbles intersected per unit length of traverse.

$\bar{l}$ = the arithmetic mean of the measured chord intercepts.

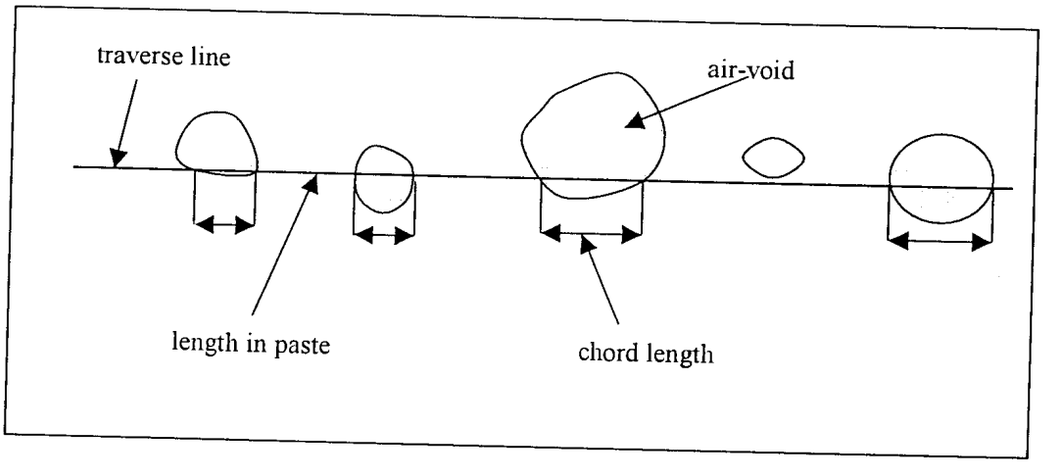

Figure 3.2 Determination of chord lengths and lengths in paste on traverse line

b) **Specific surface of entrained air.** A calculated parameter representing the total surface area of air-voids divided by their volume (boundary area of air-voids per unit volume of air). According to Willis (Willis, 1949) this parameter can also be determined from $\bar{l}$:

$$\alpha = \frac{4}{\bar{l}} \qquad \text{(Eq. 3.2)}$$

Where:

α = specific surface area

The equations for air content and specific surface are applicable to any system of spherical dispersoids whether the system is made up of single or multisized spheres.

c) **Spacing factor.** The calculation of this parameter assumes that all air-voids present are of uniform size and are evenly distributed through

the cement paste. It is distributed such that the model has the same volume of air per unit volume of concrete and the same specific surface of air bubbles as the system of random sized bubbles. Each hypothetical air-void is centrally imbedded in a cement paste cube.

The spacing factor is the distance from the corner of the cube to the surface of the sphere (hypothetical air-void) and can be calculated by knowing the spesific surface of entrained air, air-void content and cement paste content of the specimen (Chan, 1987).

d) **Air-void size distribution.** The European standard (prEN 1993) use the chord lengths to calculate the distribution of the number of air-void diameters within the cement paste.

During the linear traverse method only those air-voids intercepted by the traverse line will be counted in the chord distribution; a large number will not be intercepted and are therefore not included in the chord distribution. Calculations in (prEN 1993) Annex A provide a means to estimating the total number of voids from those intercepted by means of a statistical analysis.

A graphical representation of the distribution can be obtained by plotting the volume of air attributable to each size of void, either as a volume percentage of the cement paste or as a proportion of the total air content.

e) **Micro-air content.** A calculated parameter representing the air content attributed to air-voids of 0.3 mm diameter or less.

The determination of all these parameters was developed before the technology of image analysis exists. None of these factors has been proven to give an exact measure of the desired quantity (Willis, 1949). The calculations of the spacing factor for example inadequately assume uniform sized air-voids and neglect aggregates and therefore it is not representative of the distances between the air-voids.

Equation 2.1 gives the pressure difference between the inside and outside of an air bubble. According to (Uchikawa, 1991) if the assumption is made that the outside pressure is atmospheric pressure and γ is to be the surface tension of water the minimum diameter of an air-void is approximately 30 um. The maximum diameter of air-voids is 1 mm and the pores with diameters greater than 1 mm is defined as large entrapped air. The pores smaller than 30 um are defined as gel- and capillary pores. According to Wilk & Dobrolubov (Wilk & Dobrolubov, 1984) perfectly batched and mixed air-entrained concrete of high durability contains well-distributed spherical voids with diameters varying between 20 and 300 micrometer. The micro air parameter therefore does not represent a specific classification of pore type in the mixture, but indicates the quality of air entraining.

3.2.2 Modified point-count method

The American Standard Test Method (ASTM C 457, 1990) also describes a modified point-count method for the measurement of the air-void parameters. The preparation of the specimens is the same as for the linear traverse method. For this method the air-void structure is examined by scanning it along a regular imaginary grid system of points at which stops are made to determine the composition of the matrix.

The linear distance between stops, the number of stops in air-voids and paste are recorded. These recorded data are analysed by the stereology point analysis of Glagolev and Thomson. According to this analysis the areal fraction and therefore the volume fraction can be evaluated by the fraction of points (Chan, 1987).

The same air-void parameters as for the linear-traverse method are determined by the recorded data and they are used to describe the air-void system.

3.2.3 Image analysis in conjunction with linear traverse method.

Cahill (Cahill, 1994) developed a method where image acquisition and analysis are used in conjunction with the linear traverse method to determine the air-void system. It comprises a motorised X-Y stage, a microscope with

focus control, a high- resolution monochrome camera, a motor control box and the Kontron IBAS Image Analysis system.

The specimens are prepared in the same way as for the ASTM - and European methods (ASTM C 457, 1990 and prEN, 1993). The traverse of the camera over the polished surface of the concrete mimics the linear traverse method. Each of the images produced by the camera is analysed by placing it on a fine grid. The system examines every square, a number representing its place on a numerical scale ranging from 0 (black) to 255 (pure white) via intermediate numbers representing shades of grey. The image is then acquired and any void within the image is identified solely on the criterion of intensity of grey value. All occurrences of grey value above a threshold of e.g. 220 are assumed part of a void and are turned white. The background values 220 or below, is converted to black, so producing a binary black/white image. Once the image has been digitised and acquired in this way, the information is stored and can be analysed mathematically. A traverse line is placed across an image and the overlap of the traverse line with any air-void yields chord intercepts. The void chords are measured and the method of calculation of air-void parameters is taken directly from the European Standard (prEN, 1993). As discussed previously in paragraph 3.2.1.1 these parameters do not represent the actual quantities desired.

3.2.4 Image processing method

Nasser and Singh (Nasser and Singh, 1995) developed a new apparatus and method to determine the air-void characteristics of fresh and hardened concrete. The apparatus consists of an electronic video camera, lighting system, computer and image processing software. The method consists of video images taken of the concrete surface to be tested and these are analyzed to determine air-void parameters. It takes a short period of time to perform the test compared to the traditional standard methods.

There is no need to prepare the concrete surfaces of the specimens while using this method. The first step in the method is to expose the specimen to the video camera, which is set to magnify the image 30 times. Next the camera is focused and the image is monitored so as to obtain the best possible picture of

the concrete surface, which can be stored in the apparatus for immediate or future statistical analysis.

Image processing software is used to identify, extract, and measure different features from a frozen video image. The principal behind the air-void identification is that air-voids are darker than other features in the image and can be assigned a very low value of gray scale. The air-voids are selected having the same gray scale range. The software routines can calculate the area of the selected air-voids, their x-y coordinates and their diameters.

The image processing method of Nasser and Singh (Nasser and Singh, 1995) uses the calculated air-void area to determine the air-void diameter.

$$\text{Air-void diameter} = \sqrt{\frac{4A}{\pi}} \qquad \text{(Eq. 3.3)}$$

Where:

A = area of void.

By using the image processing method of Nasser and Singh the data of the air-voids are recorded. The air-void parameters as defined by the European Standard (prEN, 1993) can then be calculated by exporting the data to a spreadsheet that contains the required geometric formulae for calculations.

3.2.4.1 Air-void structure parameters

The fact that the software routines of the image processing method can calculate the area of the selected air-voids, their x-y coordinates and their diameters and then export it to a spreadsheet ensures the exact measurement of the actual quantity of the air-void parameters.

Nasser and Singh (Nasser and Singh, 1995) defined the following parameters:

- Total air content
- Specific surface of entrained air
- Spacing factor
- Air-void size distribution
- Shape of air-voids

These parameters will be discussed in the following paragraphs.

a) Total air content

Air content (%) = (sum of areas of air-voids / total area of image) * 100

This parameter does not give an accurate indication of the percentage air in the mixture, because it does not take the gel and capillary pores into consideration. The actual porosity of the mixtures can be determined by the vacuum saturation method as discussed in chapter 4 paragraph 4.4.

b) Specific surface of entrained air.

According to equation 3.2 the *specific area of the air-voids* = $\frac{4}{Diameter}$

This parameter is only dependent on the diameter of the air-void and therefore the diameter of the air-void as such can be used to evaluate relations between the properties of the mixtures and the microstructure.

c) Spacing factor.

A *spacing factor* defined as the distance from the center of an air-void to the center of the nearest air-void in the neighborhood is developed. The center to center spacing between any two air-voids is given by:

$$s = \sqrt{(x_1 - x_2)^2 + (y_1 - y_2)^2} \qquad \text{(Eq. 3.4)}$$

$x_{1,2}$ = x - coordinates of air-voids

$y_{1,2}$ = y - coordinates of air-voids

If the *spacing factor* is calculated in this manner the paste content and aggregate content between the air-voids are not taken into account. In other words this spacing factor is not representative of the minimum or maximum distances between the air-voids. A representative spacing factor for this investigation has to be developed.

d) Air-void size distribution.

Nasser and Singh (Nasser and Singh, 1995) obtained a histogram of the diameters of the *air-voids and their size distribution* from the exported data (see figure 3.3). The average diameter as determined from the histogram is used to represent the group of the individual values of the diameters of the air-voids. The question arises if this average diameter is really representative of the size distribution?

e) Shape of air-voids.

All these parameters are based on the essential feature that entrained air-voids are spherical and therefore circular in section. With the data obtained from the image processing method the shape of the air-voids can be determined and the circularity therefore be tested.

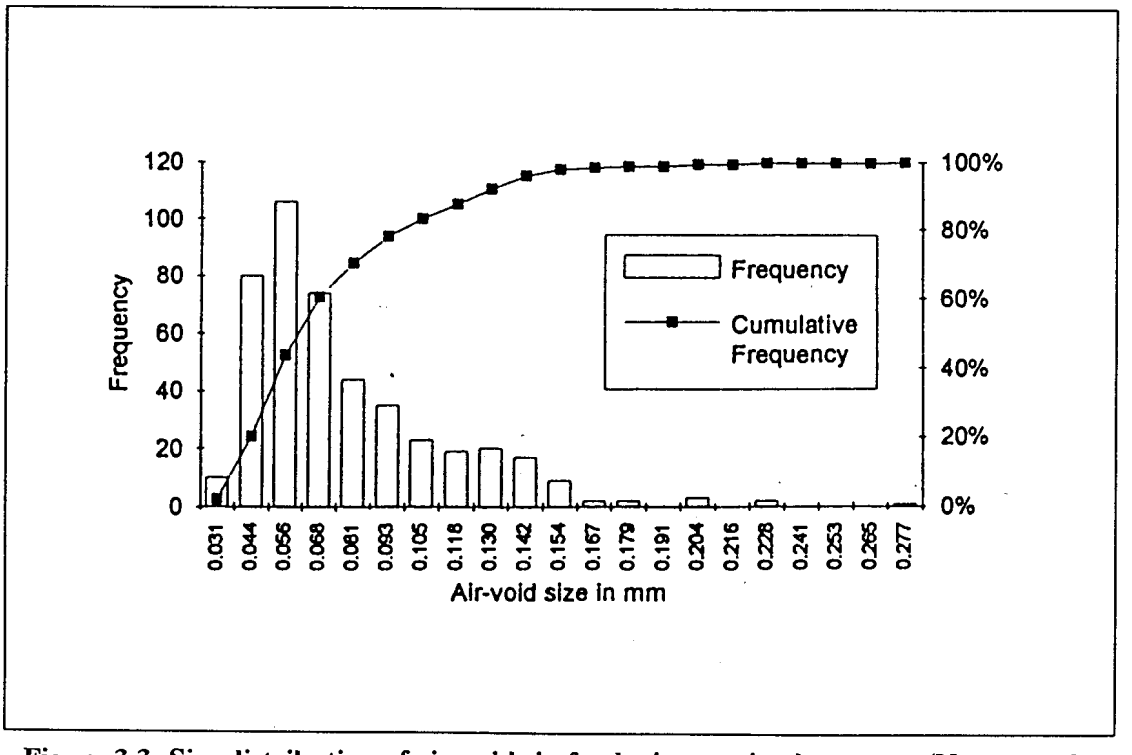

Figure 3.3: Size distribution of air-voids in fresh air entrained concrete (Nasser and Singh, 1995)

3.3 Rosin-Rammler distribution function

In searching for a parameter, which will provide a more representative description of the *air-void size distribution* than proposed by Nasser and Singh, the Rosin – Rammler distribution function was investigated.

From a probability point of view Rosin and Rammler investigated the particle size distribution of crushed coal and developed a function that describes the distribution as (Olorunsogo, 1990):

$$f(x) = \exp(-bx^n) \qquad \text{(Eq. 3.5)}$$

Where:

b = fineness characteristic measure of the material being analyzed.

n = a measure of the range of particle sizes.

Rosin and Rammler also found that the function does not only apply to crushed coal but also to various other powered materials.

The function was modified as follows:

$$RR = \exp\left(-\left(\frac{x}{x_0}\right)^n\right) \qquad \text{(Eq. 3.6)}$$

Where:

The weight function $f(x)$ is denoted as RR.

x_0 = the absolute size constant or position parameter (it represents the particle size above which 36.8 % of the particles are coarser).

Taking the double of the logarithm of equation 3.6, we obtain:

$$\ln\ln\left(\frac{1}{RR}\right) = n(\ln x - \ln x_0) \qquad \text{(Eq. 3.7)}$$

Equation 3.7 describes a straight line plot with a coordinate system made up of a log scale abscissa for the particle size x, and an ordinate with a double logarithm of the reciprocal of the residue RR. The slope of the straight line is n and the line intercept the horizontal axis at a value describing the particle

size x (Olorunsogo, 1990). A hypothetical example of the diagrammatic representation of the particle size distribution by the Rosin – Rammler distribution function is shown in figure 3.4.

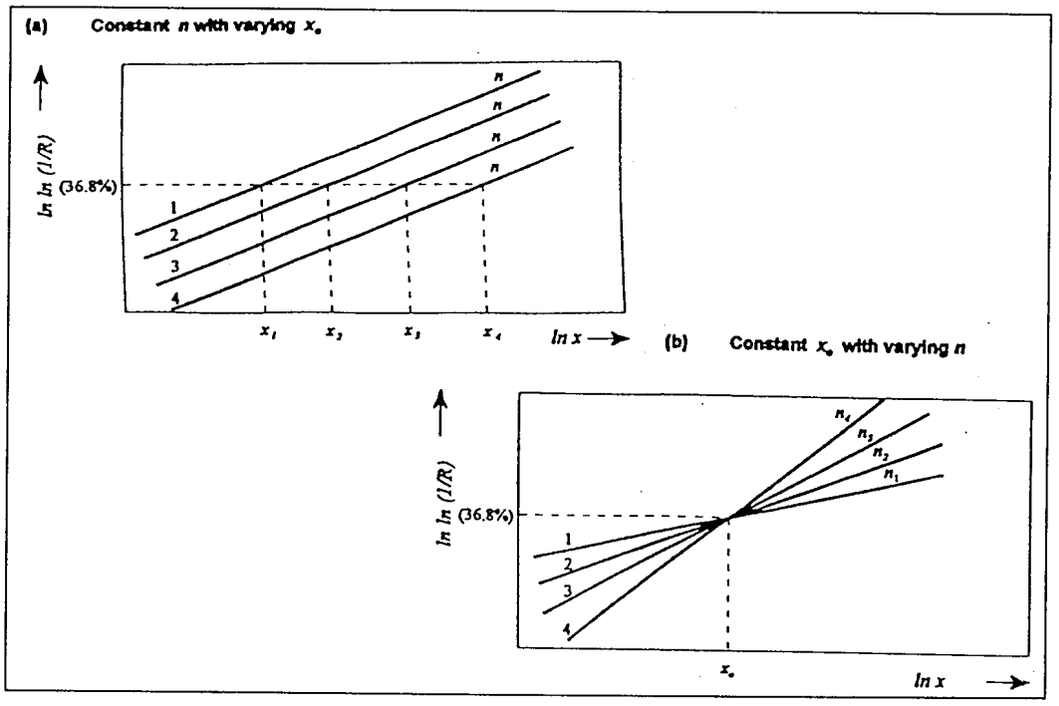

Figure 3.4: Diagrammatic representation of Rosin-Rammler distribution function (Wainwright and Olorunsogo, 1999).

Figure 3.4 (a) shows the typical particle size distribution of four different samples having the same n and different x_0. This illustration shows that the sample represented by the four plots might have similar ranges of size distribution (denoted by equal n) but with possible varying degrees of fineness (indicated by the various x_0). The sample represented by plot 1 being the finest and the one represented by plot 4 the coarsest of the four. Similarly, figure 3.4 (b) illustrates a situation whereby the four samples might be of the same fineness (because of the same x_0) but possibly with different size ranges (Wainwright and Olorunsogo, 1999).

Defining the air-voids as circular particles this distribution function can be used to provide an easy means of describing the air-void size distribution quantitatively.

3.4 CONCLUSIONS

- From the literature reviewed it can be concluded that the air-void structure can best be determined by the image processing and analysis method.
- The air-void structure of foamed concrete can fully be described by means of the shape of the air-voids, distances between air-voids and the air-void size distribution.
- The Rosin-Rammler distribution function can be evaluated as a method providing an easy means of describing the air-void size distribution quantitatively.

4. EXPERIMENTAL PROCEDURE

4.1 INTRODUCTION

Literature review indicates that by replacing percentages of cement with fly ash the properties of the cement paste in foamed concrete can be enhanced. Foamed concrete mixtures with different ash/cement ratios and different target densities are therefore used in this investigation. A pre-foamed protein based foaming agent is used for the mixtures to ensure predictable densities (Kearsley 1996).

All materials used in this research are produced in South Africa and a single source of the different materials was used.

This chapter describes the different methods used to determine the physical properties (the density, porosity and the air-void structure) as well as a specific structural property (the compressive strength) of the foamed concrete mixtures.

The vacuum saturation method is used to determine the actual porosity of the foamed concrete test specimens.

An image processing and analysis system was used to determine the air-void structure parameters. At present it proved to be the most accurate method. The apparatus differ slightly from the apparatus used by Nasser and Singh (Nasser and Singh, 1995) in that a high-resolution monochrome camera was used instead of an electronic video camera.

4.2 COMPOSITION OF FOAMED CONCRETE MIXTURES

The foamed concrete used in this research is produced under controlled conditions from cement, fly ash, water and a pre-foamed protein based foaming agent.

The cement used is rapid hardening Portland cement from PPC, Herculus, Pretoria. The cement can be classified as CEM I 42,5R according to the South African Specification SABS EVN 197- 1:1992. Unclassified ash (pozz-fill) is obtained in bulk from Letabo and used as a cement extender.

The foaming agent used is "Foamtech", consisting of hydrolyzed protiens and it's manufactured in South Africa. The foaming agent is diluted with water in a ratio of 1:40 and then aerated to a density of 70 kg/m^3.

It was not the aim of this investigation to establish the effect of fibers on the properties of foamed concrete and therefore 2 kg/m^3 of chopped 6.7 Dtex fibrillated polypropylene fibers (12 mm long) were used in all the mixtures. Research at the University of Pretoria showed that these fibers do not influence the compressive strength of foamed concrete but do have a significant effect on the tensile strength of foamed concrete (Kearsley, 1997).

4.3 DENSITY

The test specimens (cubes) cast for this study have a dimension of 100-mm x 100-mm x 100-mm. The initial density of the specimens as measured during manufacturing is the *casting density* and it can be compared with the design density or in other words the *target density.*

Test specimens are de-moulded within 24 hours of casting and the *de-mould density* of each specimen is determined. After de-moulding, each specimen is wrapped in plastic and cured in constant temperature room (22 ° C) and 60 % relative humidity for 28 days.

The density of each specimen is again determined after 28 days and this density is called the *28-day test density.*

For the measurement of the *28-day dry density* one specimen in every batch is cured for 28 days in the constant temperature room. There after the cube is weighed to determine the testing density. The cube is then placed in an oven at a temperature of 100 ° C for another 7 days and the *dry density* is then determined.

4.4 COMPRESSIVE STRENGTH

The 100-mm test cubes were cast in steel moulds and de–moulded after ± 24 hours. Then it was wrapped in polythene wrapping and kept in a constant temperature room (22 ° C) and 60 % relative humidity, up to the day of testing.

The cubes were crushed on a more sensitive press, (with a 50 MPa capacity), than usually used for normal concrete. Three cubes from the same mixture of foamed concrete were crushed and the average of the three results is used to define the strength of the mixture. The compressive strength were recorded to the nearest 0.1 MPa (Kearsley, 1999).

4.5 AIR-VOID STRUCTURE

4.5.1 Image analysis

The image processing and analysis system used in this research is shown in Figure 4.1.

It consists of a high-resolution monochrome camera connected to an optical microscope and computer with the image analysis software "Optimate 5.21". The microscope has a movable X,Y stage and by moving the specimen manually in both the X and Y directions, representative images of the specimen are collected.

The software has a function "Area Morphometry" (Optimate 5.21 Utilities menu) which allows the collection of data of a randomly selected image (or section of the specimen). A sub-function allows the defining of smaller areas of the image to be investigated by using a pointing device e.g. a mouse to trace

the perimeter of such an area, which will then be displayed on the monitor. Holding down the primary mouse button and following the perimeter of the area performs the trace. The trace will be displayed on the computer monitor as a thin red line.

The data of every defined area in the image is stored and analyzed separately. The output data is presented and stored in an ASCII file for use by any data processing computer program.

The output data of the encircled areas of a specific image consist of the total area in calibration units, total length of perimeter in calibration units, x - and y position of area centroid. The circularity, longest axis in calibration units, width perpendicular to longest axis, mean and standard deviation of the grey value of the pixels enclosed by the area are also part of the output data (Optimum 5.21 Utilities menu).

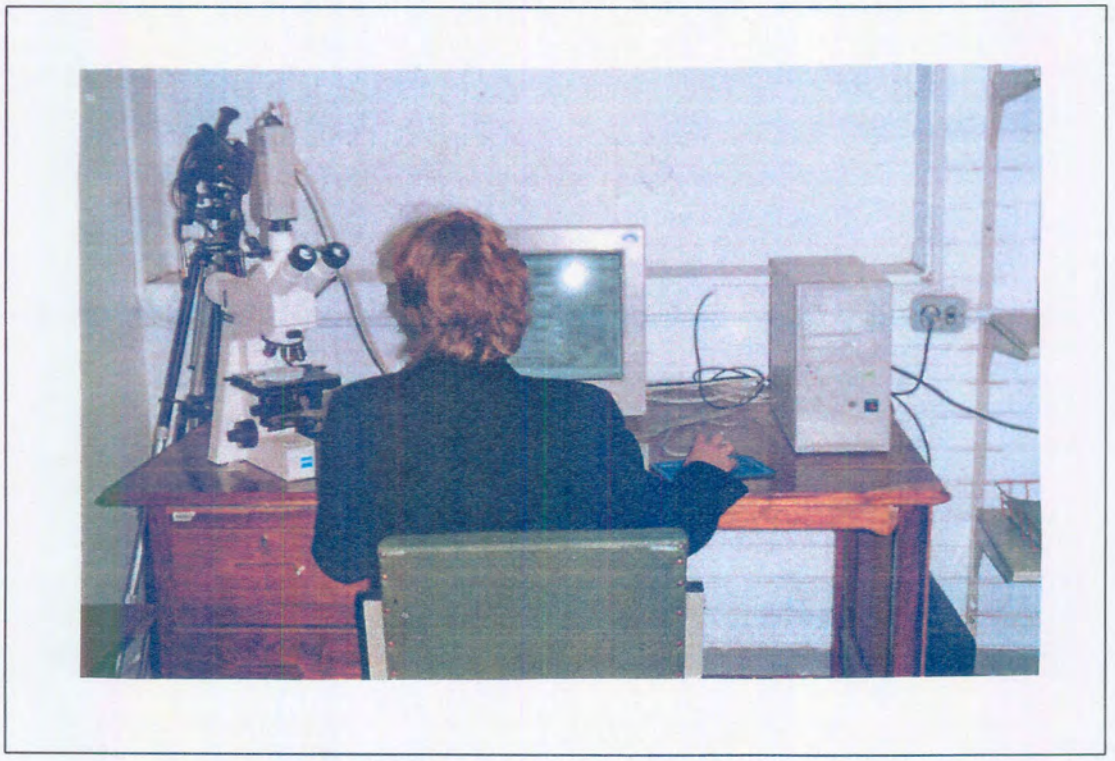

Figure 4.1: Image analysis system

4.5.2 Sample preparation

An extra cube for every mixture was cast for microscopic analysis purposes. Slices of the cube of between 12-mm and 15-mm thick are cut using a diamond saw (See Figure 4.2). The slices are cut perpendicular to the original free surface after which every slice is again cut in quarters. The dimensions of the specimens are 50-mm x 50-mm x 12-15-mm. The alignment of the specimens is kept the same throughout the whole experiment (See Figure 4.3).

The intended test surfaces of the specimens are wet ground using sandpaper with a 180 and 600 grit respectively, to produce a smooth flat surface (See Figure 4.4).

The specimens are cleaned with compressed air to remove any residue and prepared in the oven at 50 °C to ensure a dry surface for microscopic analysis (Visagie, M. 1997).

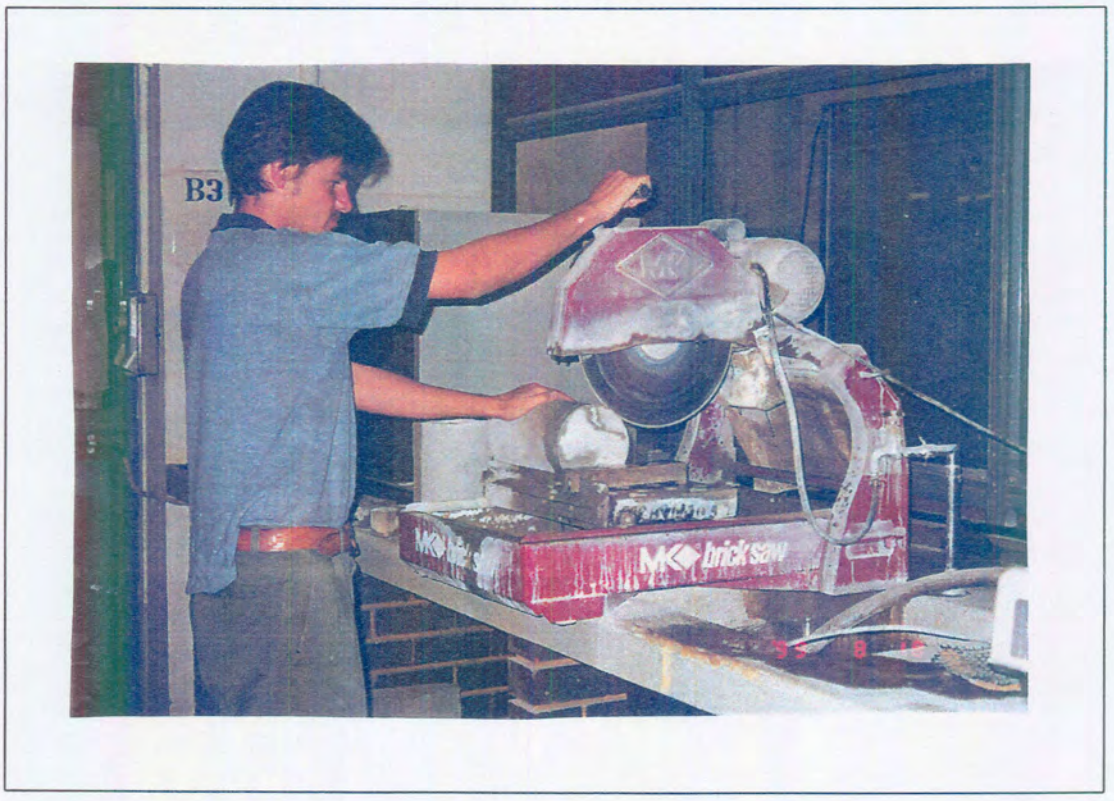

Figure 4.2: Diamond saw used for cutting of specimens

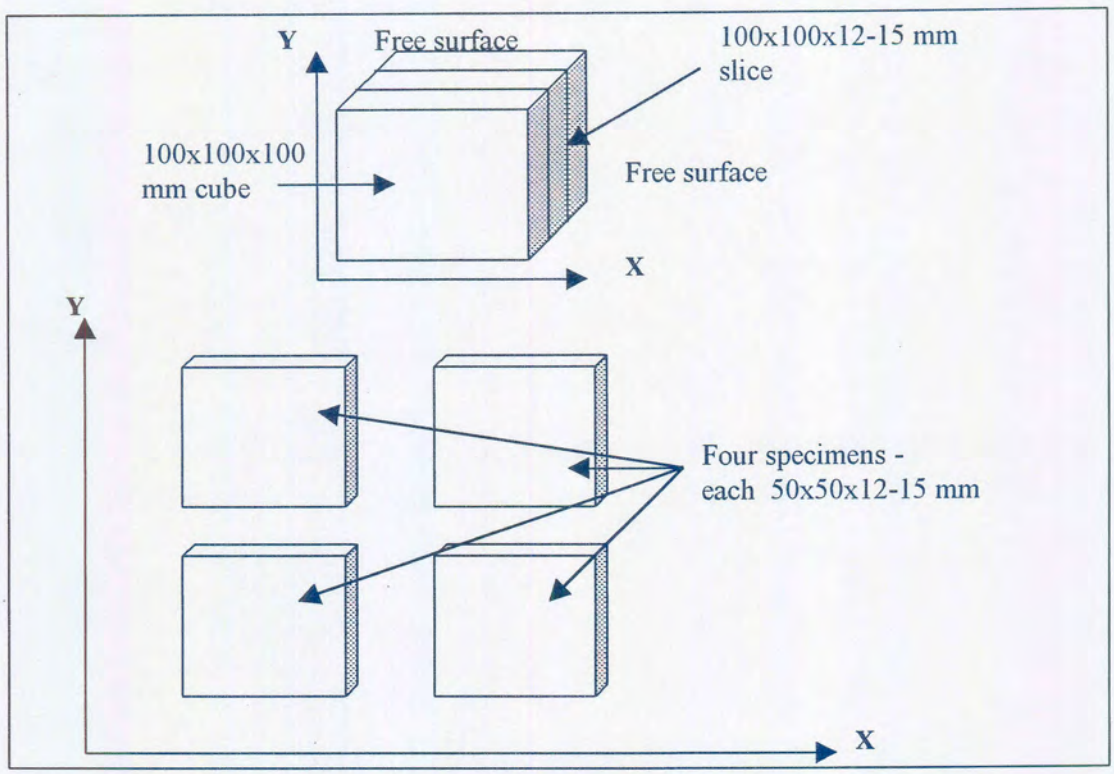

Figure 4.3: Preparation and alignment of specimens

Figure 4.4: Wet grounding of test surfaces of specimens

4.5.3 Identification of air-voids

According to the method used for identification of air-voids by the European Standard (PrEN 480-II:1993), the concrete surface is first inked black to reduce contrast between aggregate and paste and allowed to dry. Working a white zinc paste into the voids highlights them. Air-voids in foamed concrete is closer together than in normal concrete and therefore this method is not suitable for foamed concrete as not all the air-voids are filled with the paste.

In this study, no specific method was used to accentuate the contrast between air-voids and cement paste. The focus of the optical microscope was adjusted until the cement paste was in focus and all the air-voids are blurred on the computor monitor. This contrast is considered to be sufficient to distinguish between air-voids and cement paste.

Figure 4.5 shows the typical images produced by the camera. The air-voids can easily be identified. Every one of these images are digitized and stored by the computer.

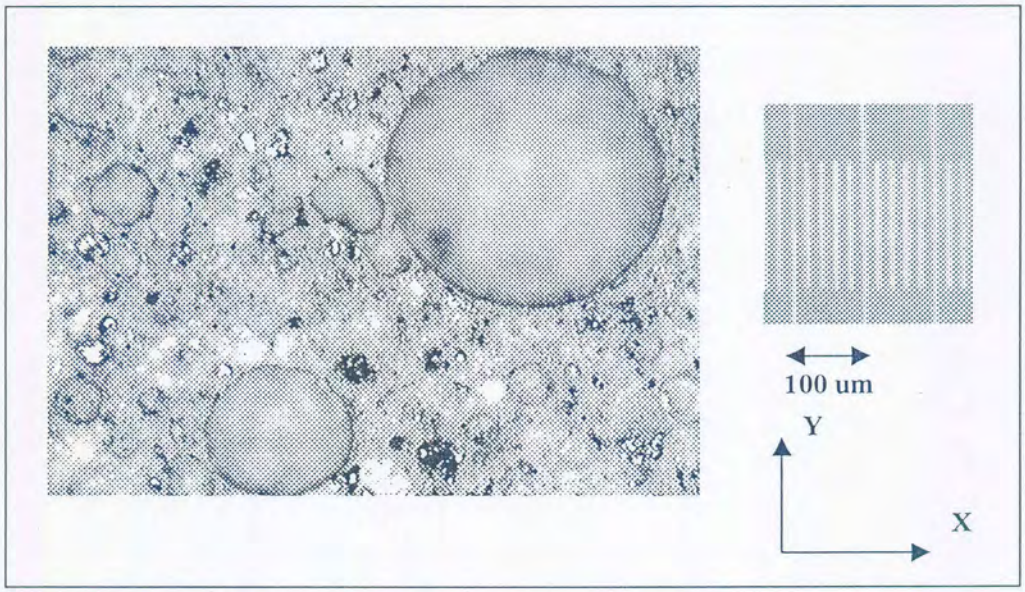

Figure 4.5: Image of foamed concrete as seen on computer monitor

The "Area Morphometry" function of the software allows the defining of air-voids in the photo by tracing the perimeter of the void on the computor monitor with the mouse. The trace is displayed as a thin red line on the

monitor (See Figure 4.6). The data for every defined area in the photo is stored and analyzed separately.

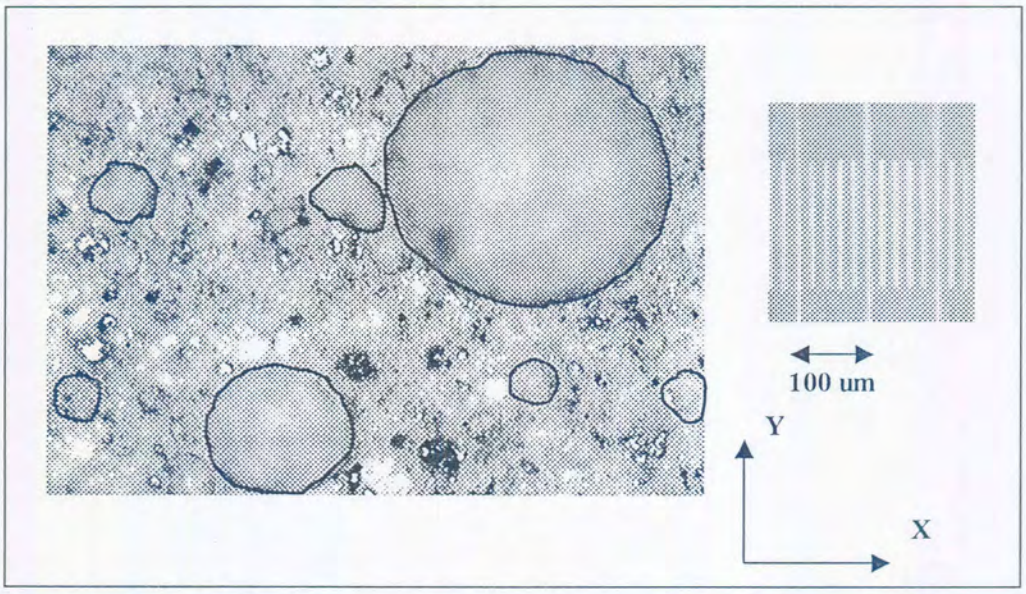

Figure 4.6: Manually traced air-voids as seen on computer monitor

Each photograph that was taken represented an area 1954 μm wide and 1872 μm high. Twenty photos of each mixture were analyzed resulting in more than 250 air-voids counted per mixture.

Air-voids were counted with diameters between 10 μm and a 1000 μm. By setting the boundaries it was ensured that only entrained air-voids was counted and not entrapped air or gel pores.

The output data of the software is presented and stored in an ASCII file. An extract of part of the file is shown in Table 4.1. The count is the number of air-voids counted in a spesific photo. The area is the total area of a spesific air-void in $(\mu m)^2$ units. The perimeter is the length in μm of the red line indicated on the computor monitor. The next two columns are the x- and y coordinates of the centroid of each air-void.

Table 4.1: Extract of software output data from "OPTIMUM 5.21"

Count	Area	Perimeter	X - Position	Y - Position
4	20991.37	577.19	64.3	1117.08
	30543.43	685.76	977.05	758.38
	12658.85	463.64	557.97	755.42
	34692.92	789.81	1267.8	593.96
8	4481.82	271.67	700.51	1132.35
	7015.42	368.07	512.13	1082.13
	9109.98	366.93	985.75	1042.1
	26092.1	641.91	704.35	954.54
	2847.63	227.92	922.69	821.08
	17543.11	512.65	1415.72	703.62
	137915	1567.1	281.09	600.62
	40711.36	761.77	1402.32	199.35
2	2091.51	184.93	267.94	375.39
	21116.37	586.9	798.62	151.87
6	15786.97	503.82	1179.44	912.46
	8347.76	352.81	1429.51	917.84
	12594.82	444.64	1374.66	720.46
	27064.69	651.57	1183.64	689.18
	5756.24	296.34	1177.62	130.71

4.6 POROSITY

There are different methods, which can be used to determine the actual porosity of concrete. According to Gaafer (Gaafer, 1995) the porosity that is calculated using the mercury porosimetry technique is always lower than that determined from the vacuum saturation technique. As foamed concrete contains relatively large percentage voids, that might not be easily accessible to water, (Kearsley, 1999) decided to use the vacuum saturation apparatus as developed by Cabrera and Lynnsdale at the University of Leeds to determine the porosity of foamed concrete.

4.6.1 Apparatus

The apparatus as developed by Cabrera and Lynnsdale at the University of Leeds (Gaafer, B.A. 1995) is used to determine the porosity of the mixturetures. Figure 4.7 shows the arrangement of the apparatus.

1. Vacuum desiccator

2. Vacuum pump
3. Three – way valve, to be connected to the desiccator
4. Bottle made from pyrex.
5. De-aerator
6. Tubing

4.6.2 Experimental procedure

The 50-mm x 50-mm x 12-15-mm specimens used for the microscopic analysis was also used for this test. The samples were dried at 100 ° C until all the evaporable water had evaporated and the weight had stabilized.

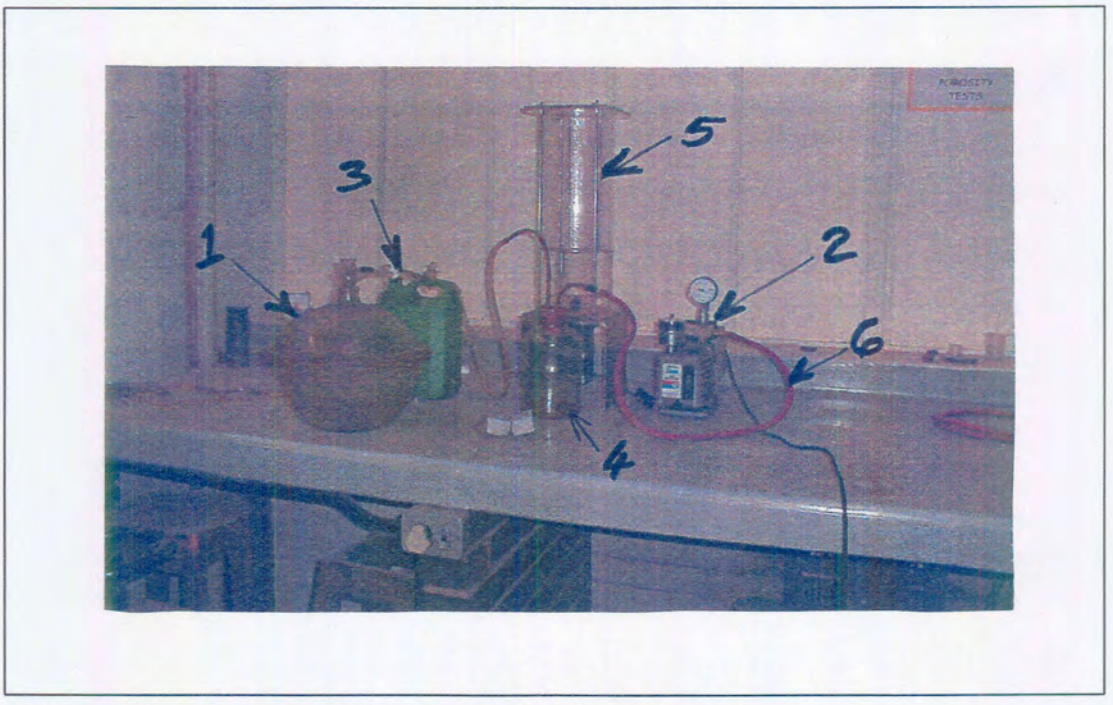

Figure 4.7: Arrangement of vacuum saturation apparatus

The dried samples were placed in the desiccator and the valve to the vacuum pump was opened. The samples were placed under vacuum for at least three hours; thereafter the valve to the bottle was opened to fill the dissicator with de-aired, distilled water. It was filled with water up to 300 mm above sample level and the vacuum pump was used for another three hours. At this stage the valve to the atmosphere was opened to provide extra pressure which pushes

water into the pores of the samples. The samples remained under water over night and the next day the saturated samples were weighed in air and water. The porosity was calculated with the following formula (Gaafer, 1995):

$$P = \frac{(W_{sat} - W_{dry})}{(W_{sat} - W_{wat})} * 100 \qquad \text{(Eq 4.1)}$$

Where:

P = Vacuum saturation porosity (%)

W_{sat} = Weight in air of saturated sample

W_{wat} = Weight in water of saturated sample

W_{dry} = Weight of oven dried sample.

5. RESULTS

5.1 MIXTURES

Thirty foamed concrete mixtures with different ash/cement ratios and target densities varying between 700 kg/m³ and 1500 kg/m³ are used in this investigation. Ash/cement ratios of zero, one, two, three and four are used to be able to determine the effect thereof on the properties of the mixtures. The compositions of the mixtures are listed in Table 5.1. The water/cement, ash/cement and water/binder ratios as indicated in Table 5.1 are weight ratios and the binder content is taken as the sum of the cement and the ash. The volumetric proportional composition of each mixture can be seen in Table 5.2.

5.2 RESULTS

The values of the different densities measured (as explained in Chapter 4) for every mixture is listed in Table 5.3.

Table 5.4 shows the porosity and the 28-day cube compressive strength of each mixture. The 28-day test and dry densities are listed with the porosity and the cube strength. The porosity as shown in the table presents the average value of the porosity of two samples tested for each mixture with the vacuum saturation method as described in the previous chapter. Each 28-day compressive strength value presents the average of three cubes tested for every mixture.

Table 5.1: Composition of foamed concrete mixtures

Mix number	Ash/ Cement ratio	Water/ Cement ratio	Water/ Binder ratio	Target density (kg/m^3)	Composition of mixture per (m^3)				
					cement (kg)	ash (kg)	water (l)	foam (l)	fibers (kg)
1	0	0.33	0.33	1500	1112	0	367	278	2
2	0	0.33	0.33	1200	879	0	290	429	2
3	0	0.33	0.33	1000	723	0	239	530	2
4	0	0.33	0.33	900	645	0	213	580	2
5	0	0.33	0.33	800	567	0	187	631	2
6	0	0.33	0.33	700	490	0	162	681	2
7	1	0.58	0.29	1500	574	574	334	221	2
8	1	0.58	0.29	1200	454	454	264	384	2
9	1	0.58	0.29	1000	373	373	219	492	2
10	1	0.58	0.29	900	333	333	195	546	2
11	1	0.58	0.29	800	294	294	173	598	2
12	1	0.58	0.29	700	252	252	149	654	2
13	2	0.87	0.29	1500	383	765	336	192	2
14	2	0.87	0.29	1200	302	605	266	361	2
15	2	0.87	0.29	1000	249	498	219	474	2
16	2	0.87	0.29	900	222	444	195	530	2
17	2	0.87	0.29	800	195	391	172	587	2
18	2	0.87	0.29	700	168	337	148	643	2
19	3	1.17	0.28	1500	291	873	320	189	2
20	3	1.17	0.28	1200	230	690	253	358	2
21	3	1.17	0.28	1000	189	568	208	472	2
22	3	1.17	0.28	900	169	507	186	528	2
23	3	1.17	0.28	800	149	446	163	585	2
24	3	1.17	0.28	700	128	385	141	641	2
25	4	1.6	0.27	1500	234	936	314	184	2
26	4	1.6	0.27	1200	185	740	248	355	2
27	4	1.6	0.27	1000	152	609	204	469	2
28	4	1.6	0.27	900	136	544	182	526	2
29	4	1.6	0.27	800	120	478	160	583	2
30	4	1.6	0.27	700	103	413	138	640	2

Table 5.2: Volume ratios of mixtures

Mix number	Ash/ Cement ratio	Water/ Cement Ratio (by weight)	Water/ Binder ratio (by weight)	Target density (kg/m^3)	Composition of mixture (per Volume)				
					cement (%)	ash (%)	water (%)	foam (%)	fibers (%)
1	0	0.33	0.33	1500	35.3	0.0	36.7	27.8	0.2
2	0	0.33	0.33	1200	27.9	0.0	29.0	42.9	0.2
3	0	0.33	0.33	1000	23.0	0.0	23.9	53.0	0.2
4	0	0.33	0.33	900	20.5	0.0	21.3	58.0	0.2
5	0	0.33	0.33	800	18.0	0.0	18.7	63.1	0.2
6	0	0.33	0.33	700	15.5	0.0	16.2	68.1	0.2
7	1	0.58	0.29	1500	18.2	26.1	33.4	22.1	0.2
8	1	0.58	0.29	1200	14.4	20.6	26.4	38.4	0.2
9	1	0.58	0.29	1000	11.8	16.9	21.9	49.2	0.2
10	1	0.58	0.29	900	10.6	15.1	19.5	54.6	0.2
11	1	0.58	0.29	800	9.3	13.4	17.3	59.8	0.2
12	1	0.58	0.29	700	8.0	11.5	14.9	65.4	0.2
13	2	0.87	0.29	1500	12.1	34.8	33.6	19.2	0.2
14	2	0.87	0.29	1200	9.6	27.5	26.6	36.1	0.2
15	2	0.87	0.29	1000	7.9	22.6	21.9	47.4	0.2
16	2	0.87	0.29	900	7.0	20.2	19.5	53.0	0.2
17	2	0.87	0.29	800	6.2	17.8	17.2	58.7	0.2
18	2	0.87	0.29	700	5.3	15.3	14.8	64.3	0.2
19	3	1.17	0.28	1500	9.2	39.7	32.0	18.9	0.2
20	3	1.17	0.28	1200	7.3	31.4	25.3	35.8	0.2
21	3	1.17	0.28	1000	6.0	25.8	20.8	47.2	0.2
22	3	1.17	0.28	900	5.4	23.0	18.6	52.8	0.2
23	3	1.17	0.28	800	4.7	20.3	16.3	58.5	0.2
24	3	1.17	0.28	700	4.1	17.5	14.1	64.1	0.2
25	4	1.6	0.27	1500	7.4	42.6	31.4	18.4	0.2
26	4	1.6	0.27	1200	5.9	33.6	24.8	35.5	0.2
27	4	1.6	0.27	1000	4.8	27.7	20.4	46.9	0.2
28	4	1.6	0.27	900	4.3	24.7	18.2	52.6	0.2
29	4	1.6	0.27	800	3.8	21.7	16.0	58.3	0.2
30	4	1.6	0.27	700	3.3	18.8	13.8	64.0	0.2

Table 5.3 Densities of mixtures

Mix number	Ash/ Cement ratio	Water/ Cement ratio	Water/ Binder ratio	Densities				
				Target density (kg/m^3)	Casting density (kg/m^3)	De-mould density (kg/m^3)	28-day Test density (kg/m^3)	28-day Dry density (kg/m^3)
1	0	0.33	0.33	1500	1488	1465	1460	1223
2	0	0.33	0.33	1200	1199	1200	1197	892
3	0	0.33	0.33	1000	1013	998	994	831
4	0	0.33	0.33	900	897	888	882	741
5	0	0.33	0.33	800	810	788	783	661
6	0	0.33	0.33	700	677	667	657	536
7	1	0.58	0.29	1500	1512	1478	1463	1235
8	1	0.58	0.29	1200	1170	1089	1071	901
9	1	0.58	0.29	1000	1014	1006	989	811
10	1	0.58	0.29	900	906	885	872	735
11	1	0.58	0.29	800	815	788	774	646
12	1	0.58	0.29	700	716	705	694	559
13	2	0.87	0.29	1500	1516	1475	1467	1230
14	2	0.87	0.29	1200	1208	1160	1156	958
15	2	0.87	0.29	1000	1018	995	988	790
16	2	0.87	0.29	900	900	879	865	713
17	2	0.87	0.29	800	788	784	767	612
18	2	0.87	0.29	700	722	707	691	555
19	3	1.17	0.28	1500	1514	1477	1469	1219
20	3	1.17	0.28	1200	1211	1189	1185	958
21	3	1.17	0.28	1000	1041	1016	1012	812
22	3	1.17	0.28	900	901	880	869	697
23	3	1.17	0.28	800	813	802	795	631
24	3	1.17	0.28	700	711	704	691	540
25	4	1.6	0.27	1500	1488	1456	1443	1168
26	4	1.6	0.27	1200	1214	1185	1173	941
27	4	1.6	0.27	1000	1012	994	985	771
28	4	1.6	0.27	900	917	884	875	726
29	4	1.6	0.27	800	797	772	759	689
30	4	1.6	0.27	700	719	687	676	518

Table 5.4: Porosity and 28-day compressive strength of mixtures

Mix number	Ash/ Cement ratio	Water/ Cement ratio	Water/ Binder ratio	Target density (kg/m^3)	28-day Test density (kg/m^3)	28-day Dry density (kg/m^3)	Porosity (%)	28-day Compressive Strength (MPa)
1	0	0.33	0.33	1500	1460	1223	43.5	22.00
2	0	0.33	0.33	1200	1197	892	55.1	9.40
3	0	0.33	0.33	1000	994	831	59.8	7.17
4	0	0.33	0.33	900	882	741	64.8	4.52
5	0	0.33	0.33	800	783	661	68.9	3.30
6	0	0.33	0.33	700	657	536	76.8	2.00
7	1	0.58	0.29	1500	1463	1235	41.7	24.20
8	1	0.58	0.29	1200	1071	901	53.5	6.25
9	1	0.58	0.29	1000	989	811	58.2	4.69
10	1	0.58	0.29	900	872	735	61.9	2.92
11	1	0.58	0.29	800	774	646	70.9	2.29
12	1	0.58	0.29	700	694	559	72.4	1.40
13	2	0.87	0.29	1500	1467	1230	41.9	20.50
14	2	0.87	0.29	1200	1156	958	51.7	5.84
15	2	0.87	0.29	1000	988	790	60.0	3.76
16	2	0.87	0.29	900	865	713	67.8	2.45
17	2	0.87	0.29	800	767	612	71.8	1.47
18	2	0.87	0.29	700	691	555	73.8	1.00
19	3	1.17	0.28	1500	1469	1219	40.7	10.56
20	3	1.17	0.28	1200	1185	958	49.8	5.07
21	3	1.17	0.28	1000	1012	812	55.1	2.43
22	3	1.17	0.28	900	869	697	67.5	1.61
23	3	1.17	0.28	800	795	631	71.3	1.14
24	3	1.17	0.28	700	691	540	72.5	0.72
25	4	1.6	0.27	1500	1443	1168	42.6	6.63
26	4	1.6	0.27	1200	1173	941	56.6	3.53
27	4	1.6	0.27	1000	985	771	60.3	1.71
28	4	1.6	0.27	900	875	726	66.1	1.25
29	4	1.6	0.27	800	759	689	70.7	0.77
30	4	1.6	0.27	700	676	518	74.2	0.53

6. AIR-VOID STRUCTURE PARAMETERS

6.1 INTRODUCTION

The aim of this research is to investigate the microstructure of the material as a primary factor influencing the relationship between the physical properties (such as density and porosity), and the structural property (compressive strength) of foamed concrete. In order to evaluate these relationships it was necessary to develop parameters to explain and quantify the microstructure of foamed concrete.

Literature review indicated that the air-void structure of foamed concrete is one of the most important micro-properties influencing the properties of the material. Therefore in this chapter the development of the air-void structure parameters are discussed.

From the literature it is found that the air-void structure of air-entrained concrete can be described in terms of the air-void shape, size distribution and spacing in the cement paste.

The Rosin-Rammler distribution and the oversize air-void diameter distribution are investigated to determine parameters for the air-void size distribution.

The perpendicular distance through the cement paste from one air-void to the nearest other air-void in the vicinity is used to describe the spacing of the air-voids. Specific parameters for these distances are developed and discussed in this chapter.

6.2 AIR-VOID SHAPE

The shape of the air-voids in the mixtures used in this investigation had to be determined first before parameters could be developed to describe the air-void structure of foamed concrete.

Twenty photographs (and therefore twenty images) were taken from a mixture with a target density of 900 kg/m^3 and an ash / cement ratio of two to investigate the shape and alignment of the air-voids. The total distance in μm of the cord in the direction of the x-axis through the centroid of the air-void is taken as the x-cord of the air-void. The total distance of the cord in the direction of the y-axis through the centroid of the air-void is taken as the y-cord of the air-void (See Figure 6.1). The x-cord and the y-cord were measured for every air-void in an image (See Table 6.1 for all the data).

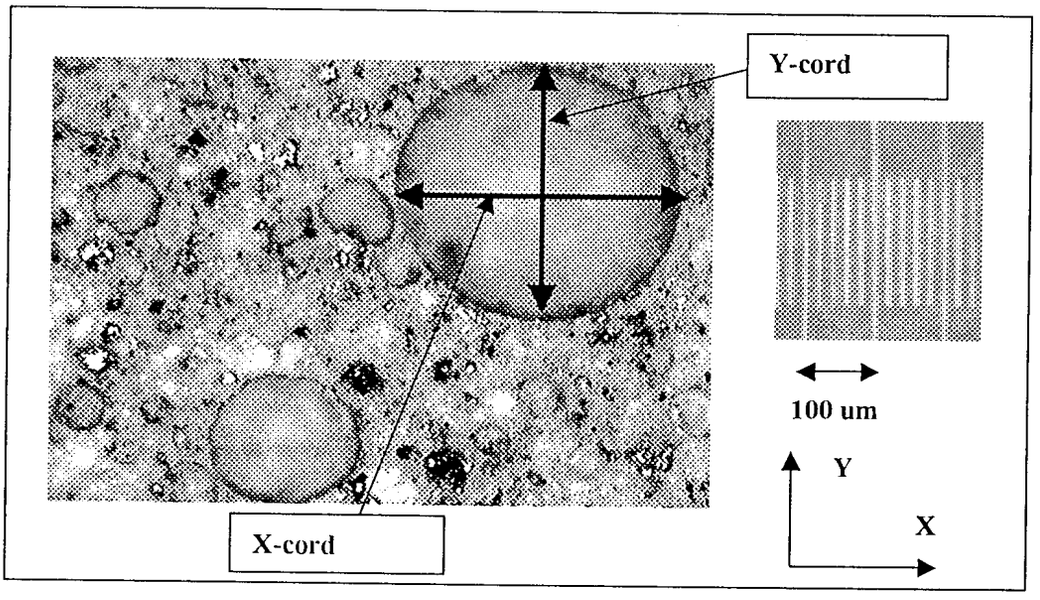

Figure 6.1: Determination of x-and y-cord of air-voids in images

The shape of the air-voids can be determined by evaluating the x- and y-cords of the air-voids. The air-void is circular if the x-cord of the air-void is equal to the y-cord of the air-void.

In Figure 6.2 the y-cords of the air-voids are plotted as a function of the x-cords and there is clearly no orientation of the air-voids in the x- or y-direction. From this graph it can also be seen that the air-voids with diameters smaller than 300 μm have a higher circularity in section than those with diameters greater than 300 μm in section. The most likely reason therefore is that the air bubbles merge if the diameter of the air-voids become greater than 300 μm.

Table 6.1: X- and Y-chords to determine shape of air-voids.

x-chord (um)	y- chord (um)	x- chord (um)	y- chord (um)	x- chord (um)	y- chord (um)	x- chord (um)	y- chord (um)
63	56	353	390	180	165	223	235
68	64	198	269	125	133	60	53
343	134	108	125	178	193	550	605
300	234	123	140	210	175	235	230
88	124	382	195	140	123	245	265
226	304	354	253	115	120	188	203
337	520	596	233	135	198	396	333
327	45	108	163	153	190	225	205
227	279	93	93	128	148	400	235
225	226	309	265	438	343	190	159
185	156	375	270	163	145	435	378
91	106	493	370	568	208	135	150
444	222	418	398	326	138	185	225
213	224	242	228	185	148	153	155
109	71	238	235	498	383	530	550
395	327	142	105	556	320	243	273
300	295	176	185	60	73	178	185
138	149	99	105	268	275	143	148
93	110	200	263	63	90	488	511
48	97	145	155	113	108	78	134
300	159	160	178	63	85	235	235
255	279	195	275	53	55	270	403
193	231	375	200	833	465	48	60
276	256	128	105	138	163		
62	56	140	130	119	155		
74	113	125	123	278	273		
317	267	626	380	168	145		
52	44	498	208	178	165		
358	435	230	215	70	110		
78	92	141	208	468	450		

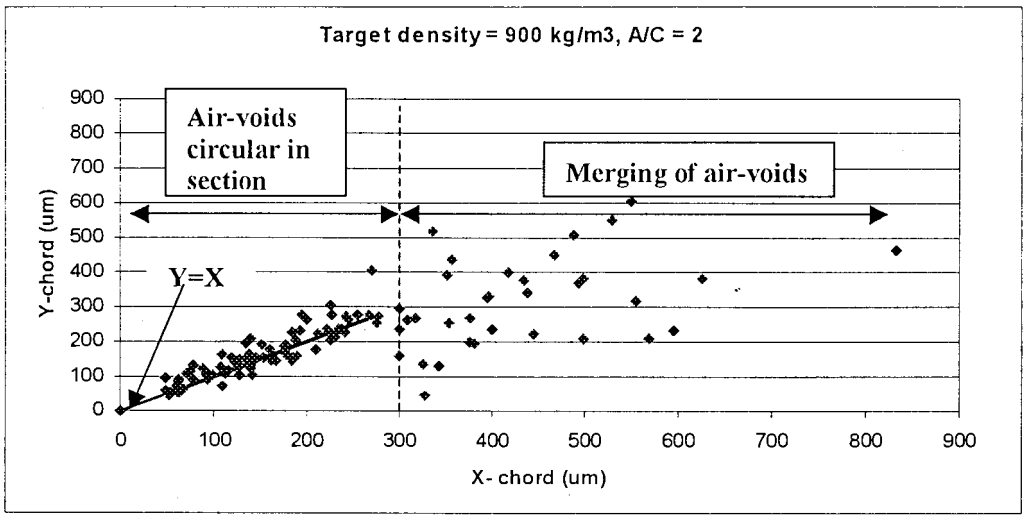

Figure 6.2: Shape of air-voids

Figure 6.3 shows the histogram of the x-chord / y-chord ratio of the air-voids with diameters smaller than 300 μm. The air-void is circular if the x-chord / y-chord ratio equals one. The mean and standard deviation of this histogram was found to be 0.96 and 0.024 respectively. The probability for a normal distribution with a standard normal variable of two is P = 0.954 (Van As and Joubert, 1996). 95.4% therefore of the x-chord / y-chord ratio values fall between 0.91 and 1.01. Based on this analysis and data the assumption was made that the majority of air-voids in the foamed concrete mixtures can be described as circular in section.

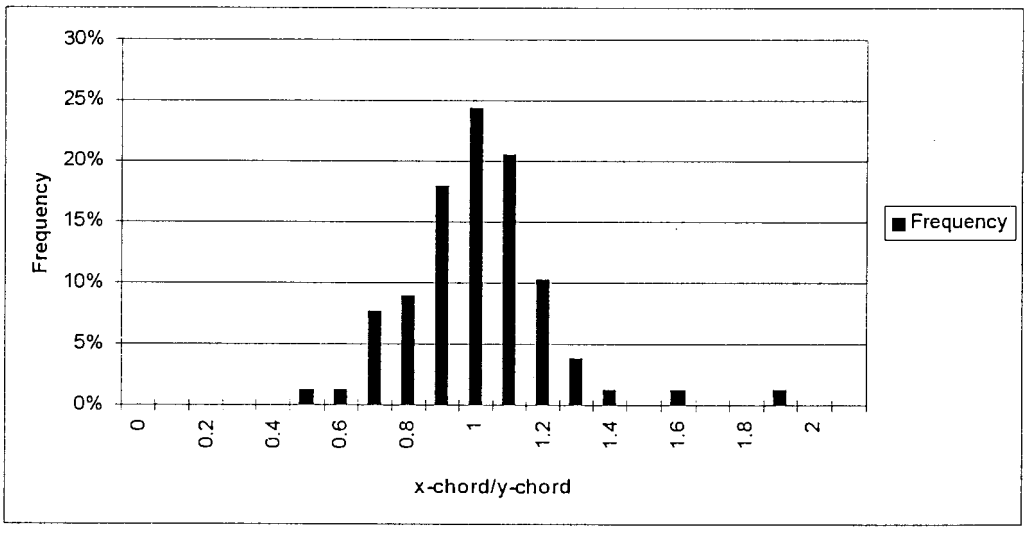

Figure 6.3: Histogram of x-chord / y-chord ratios of air-voids with diameters smaller than 300 μm

6.3 AIR-VOID SIZE DISTRIBUTION

Using the fact that the air-voids are circular in section and assuming that the air-voids are perfect spheres, an effective air-void diameter can be calculated using the measured area from the software output data (Visagie, 1997):

$$\text{Air-void diameter} = \sqrt{\frac{4A}{\pi}}$$

Where:

A = area of void.

The distribution of the air-void sizes was determined by plotting a histogram for the calculated air-voids counted in each mixture. Typical air-void diameter distributions are indicated in Figure 6.4 and the histograms plotted for all the other mixtures are attached in Appendix A. The percentage of the number of voids is plotted on the vertical axis and the air-void diameters are plotted on the horizontal axis. The cumulative persentage distribution is also plotted on this graph. The size distribution of air-voids for all the mixtures follows a log normal distribution (Visagie, 1997). The cumulative distribution shows the persentage of the voids that is smaller than a certain diameter.

From Figure 6.4 it appears that for lower densities there is an increase in the number of larger voids. Parameters had to be developed, in order to quantify these differences in air-void sizes and to compare the mixtures with each other. These parameters will also be used to evaluate the influence of air-void size distribution on the properties of foamed concrete.

6.3.1 Air-void size distribution parameters

By plotting the inverse of the cumulative percentage distribution, *the cumulative % oversize air-void diameter distribution* is obtained as shown in Figure 6.5. Provision was made for statistical outliers by not taking the five percent smallest diameters and five percent largest diameters into account. A cumulative plot as shown in figure 6.5 was drawn for each mixture (see Appendix B).

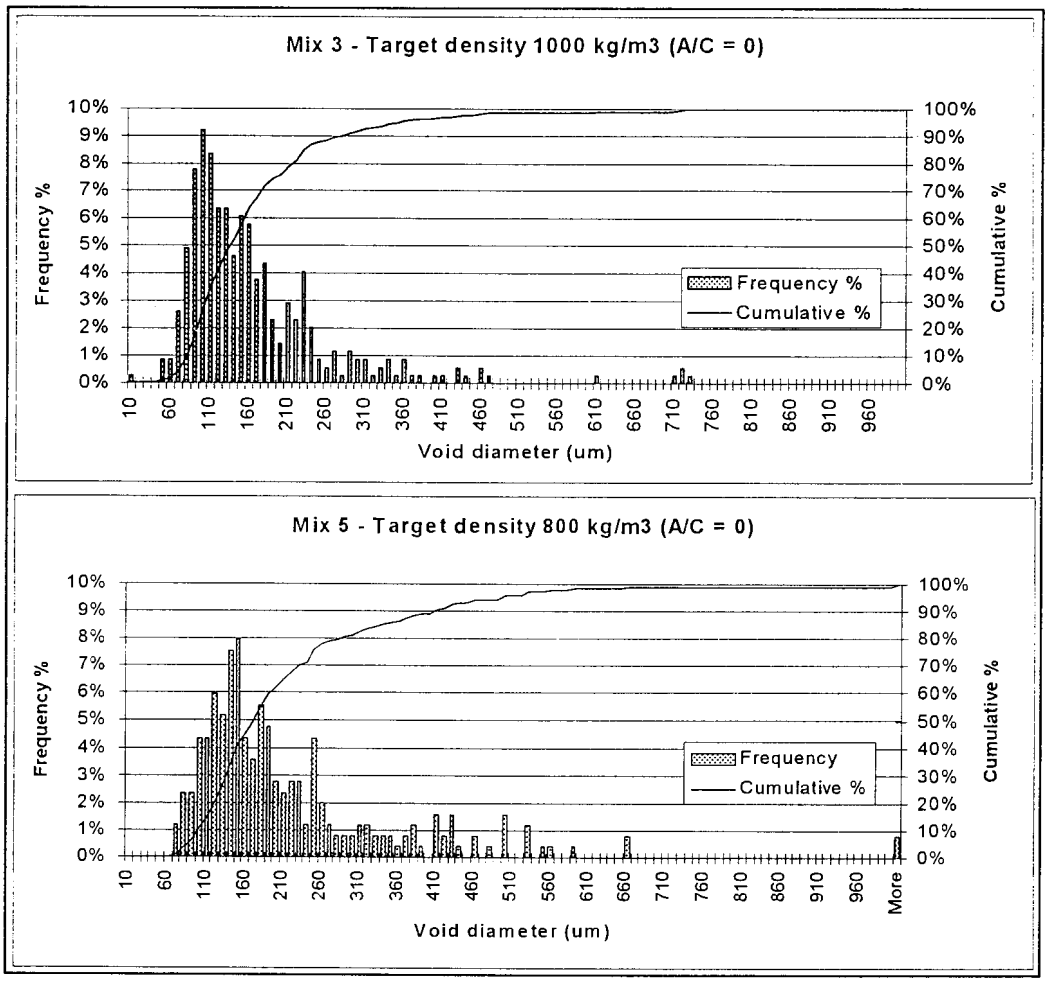

Figure 6.4: Typical air-void size distributions

For each mixture a trendline is added to the cumulative % oversize graph (see Figure 6.5).

The fitted trendline that best describe the measured values is an exponential function. The fitted functions for all the mixtures can be seen in Table 6.2. The statistical R-square value for all the mixtures of the exponential fit is between 0.96 and 0.998. The exponential equation is therefore a true representation of the *cumulative % oversize air-void diameter distribution*.

Both the constants in the equation vary with density and ash content and therefore the constants as such cannot be used to compare the mixtures (See Table 6.2).

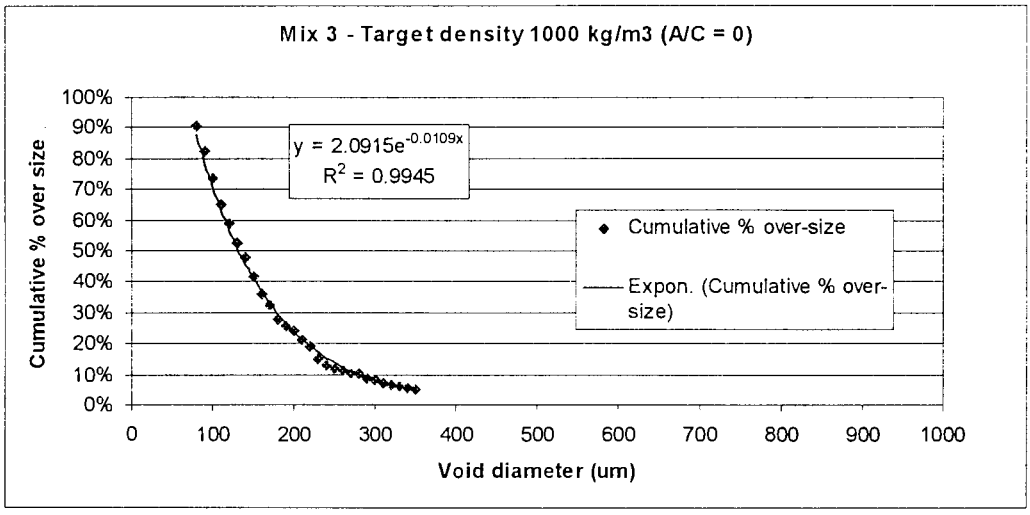

Figure 6.5: Exponential fit for cumulative percentage oversize air-voids

6.3.1.1 Rosin-Rammler air-void diameter distribution parameters

Defining the air-voids as circular areas in section the Rosin-Rammler distribution function (equation 3.6) can be used to provide a way of describing the air-void size distribution quantitatively.

The *cumulative % oversize air-void diameter distribution* as discussed in 6.3.1 can be represented as a Rosin-Rammler distribution. The reason is the trendlines fitted for all the mixtures' *cumulative % oversize air-void diameter distributions* are exponential equations and these equations are true representation of the distributions - see 6.3.1.

The Rosin-Rammler air-void size distribution parameters are listed in Table 6.3 and Figure 6.6 and 6.7 is an example of how the values in the Table were derived. The modified Rosin-Rammler distribution graph *ln ln (1/y)* versus *ln x* is plotted, with y the fitted functions $y = a\ e^{(bx)}$ (see Table 6.2) for the cumulative % oversize air-void diameter distribution and x the air-void diameter. A linear trendline and equation is also added to these graphs (see Figure 6.6). The slope and interception with the horizontal axis of the line is taken as the n value and ln x_0 value respectively of the modified Rosin-Rammler function. The Rosin-Rammler distribution for all the mixtures can be viewed in Appendix C.

Table 6.2: Fitted functions of oversize air-void diameter distribution

Mixture number	Ash/ Cement ratio	Water/ Cement ratio	Water/ Binder ratio	Target density (kg/m^3)	Fitted Function $y = a\,e^{(bx)}$		R^2
					a	b	
1	0	0.33	0.33	1500	1.4517	-0.0061	0.9752
2	0	0.33	0.33	1200	3.1625	-0.0137	0.9948
3	0	0.33	0.33	1000	2.0915	-0.0109	0.9945
4	0	0.33	0.33	900	1.8106	-0.0085	0.9948
5	0	0.33	0.33	800	1.6839	-0.0072	0.9918
6	0	0.33	0.33	700	1.6907	-0.004	0.9881
7	1	0.58	0.29	1500	1.9795	-0.0108	0.9966
8	1	0.58	0.29	1200	2.1509	-0.0109	0.9953
9	1	0.58	0.29	1000	1.954	-0.0095	0.9948
10	1	0.58	0.29	900	1.6416	-0.0073	0.9915
11	1	0.58	0.29	800	1.3041	-0.0053	0.9947
12	1	0.58	0.29	700	1.4722	-0.0043	0.9849
13	2	0.87	0.29	1500	2.5265	-0.0125	0.9936
14	2	0.87	0.29	1200	2.0025	-0.0125	0.9824
15	2	0.87	0.29	1000	1.4143	-0.0071	0.9733
16	2	0.87	0.29	900	2.1091	-0.0072	0.9888
17	2	0.87	0.29	800	1.8165	-0.0056	0.9824
18	2	0.87	0.29	700	1.655	-0.0057	0.9941
19	3	1.17	0.28	1500	2.0551	-0.0117	0.9829
20	3	1.17	0.28	1200	1.7065	-0.0111	0.96
21	3	1.17	0.28	1000	1.6738	-0.0064	0.985
22	3	1.17	0.28	900	1.6455	-0.0056	0.9935
23	3	1.17	0.28	800	2.1211	-0.0052	0.9756
24	3	1.17	0.28	700	2.04	-0.0035	0.9748
25	4	1.6	0.27	1500	5.333	-0.0183	0.9784
26	4	1.6	0.27	1200	5.01	-0.0168	0.9771
27	4	1.6	0.27	1000	3.2081	-0.0119	0.9899
28	4	1.6	0.27	900	1.61	-0.0052	0.9771
29	4	1.6	0.27	800	2.1105	-0.0071	0.9745
30	4	1.6	0.27	700	1.8457	-0.0041	0.9915

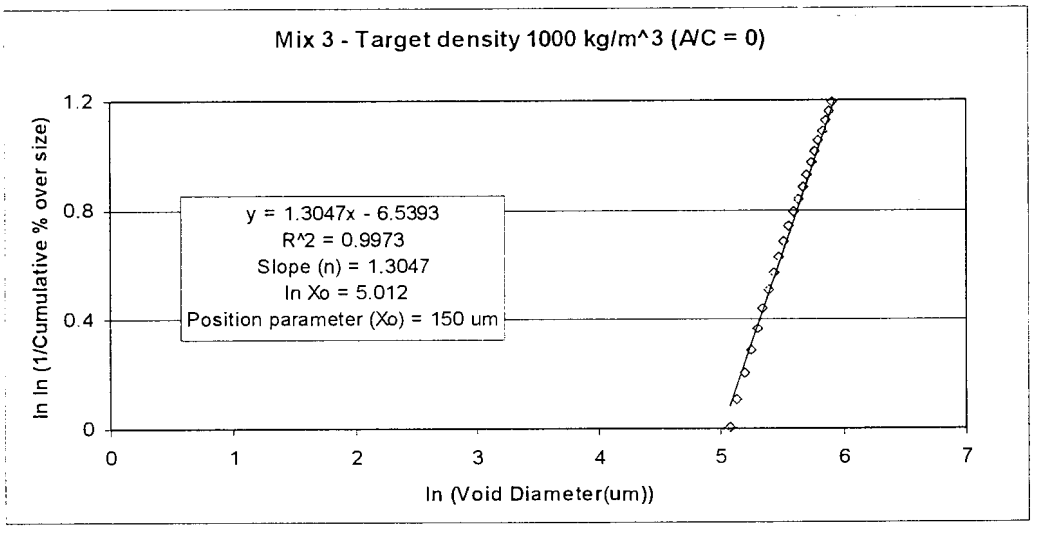

Figure 6.6: Rosin-Rammler distribution graph

36.8 % of the air-void diameters are greater than the x_0 value (position parameter in μm) This parameter is an indicator of the void size. The n value represents the range of the air-void diameter distribution of the air-void diameters greater than x_0 (See Figure 6.7).

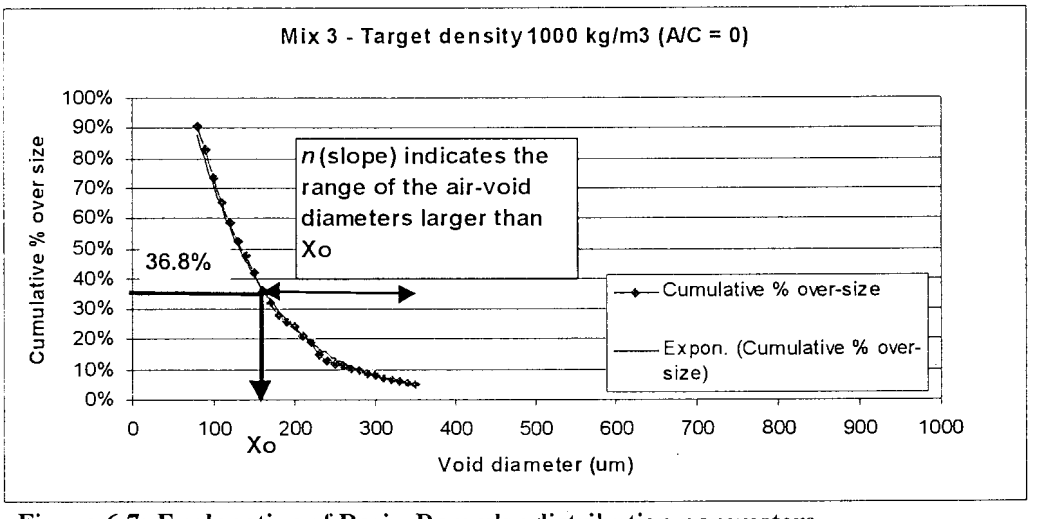

Figure 6.7: Explanation of Rosin-Rammler distribution parameters

The values of the slope n and the position parameter x_0 for all 30 mixtures can be seen in Table 6.3. The equations for the linear trendline fitted to the Rosin-Rammler distribution graph and the statistical R-square value of the linear fit are also listed in Table 6.3.

Table 6.3: Rosin-Rammler air-void size distribution parameters

Mixture number	Ash/ Cement ratio	Water/ Cement ratio	Water/ Binder ratio	Target density (kg/m^3)	Fitted function for Rosin-Rammler distribution graph y = cx + d		R^2	Rosin-Rammler distribution parameters	
					c	d		Position parameter x_0 (μm)	Slope n
1	0	0.33	0.33	1500	1.183	-6.3729	0.9993	219	1.183
2	0	0.33	0.33	1200	1.6407	-8.2473	0.9968	152	1.6407
3	0	0.33	0.33	1000	1.3047	-6.5393	0.9973	150	1.3047
4	0	0.33	0.33	900	1.2441	-6.4421	0.9981	176	1.2441
5	0	0.33	0.33	800	1.2117	-6.42	0.9986	198	1.2117
6	0	0.33	0.33	700	1.2918	-7.6459	0.999	372	1.2918
7	1	0.58	0.29	1500	1.3796	-6.9278	0.9984	152	1.3796
8	1	0.58	0.29	1200	1.4213	-7.1877	0.9984	157	1.4213
9	1	0.58	0.29	1000	1.3761	-7.0778	0.9985	171	1.3761
10	1	0.58	0.29	900	1.2794	-6.7807	0.9991	200	1.2794
11	1	0.58	0.29	800	1.1516	-6.2888	0.9996	235	1.1516
12	1	0.58	0.29	700	1.2172	-7.0058	0.9994	316	1.2172
13	2	0.87	0.29	1500	1.5112	-7.5665	0.9978	149	1.5112
14	2	0.87	0.29	1200	1.389	-6.7821	0.9984	132	1.389
15	2	0.87	0.29	1000	1.1973	-6.259	0.9994	186	1.1973
16	2	0.87	0.29	900	1.416	-7.7351	0.9984	236	1.416
17	2	0.87	0.29	800	1.333	-7.5034	0.9987	278	1.333
18	2	0.87	0.29	700	1.2818	-7.1157	0.999	258	1.2818
19	3	1.17	0.28	1500	1.4084	-6.9932	0.9983	143	1.4084
20	3	1.17	0.28	1200	1.3063	-6.411	0.9989	134	1.3063
21	3	1.17	0.28	1000	1.2918	-7.0329	0.999	231	1.2918
22	3	1.17	0.28	900	1.2811	-7.1319	0.999	262	1.2811
23	3	1.17	0.28	800	1.4198	-8.2239	0.9982	328	1.4198
24	3	1.17	0.28	700	1.4341	-8.8538	0.9986	480	1.4341
25	4	1.6	0.27	1500	1.9269	-9.5447	0.9955	142	1.9269
26	4	1.6	0.27	1200	1.8923	-9.4934	0.9956	151	1.8923
27	4	1.6	0.27	1000	1.6425	-8.493	0.9973	176	1.6425
28	4	1.6	0.27	900	1.2676	-7.1315	0.9991	277	1.2676
29	4	1.6	0.27	800	1.4194	-7.7762	0.9982	240	1.4194
30	4	1.6	0.27	700	1.341	-7.9768	0.9987	383	1.341

6.3.1.2 Oversize air-void diameter distribution parameters

The corresponding 50 % oversize air-void diameter (D50) in μm can be read from the exponential fit graph (see Figure 6.8). This diameter gives an indication of the average void size of each mixture. In the same way the 10 % oversize air- void diameter (D10), which shows the difference in number of larger voids in each mixture. The values of *the oversize air-void diameter distribution parameters* (D50) and (D10) can be seen in Table 6.4. These parameters can be compared for different mixture compositions.

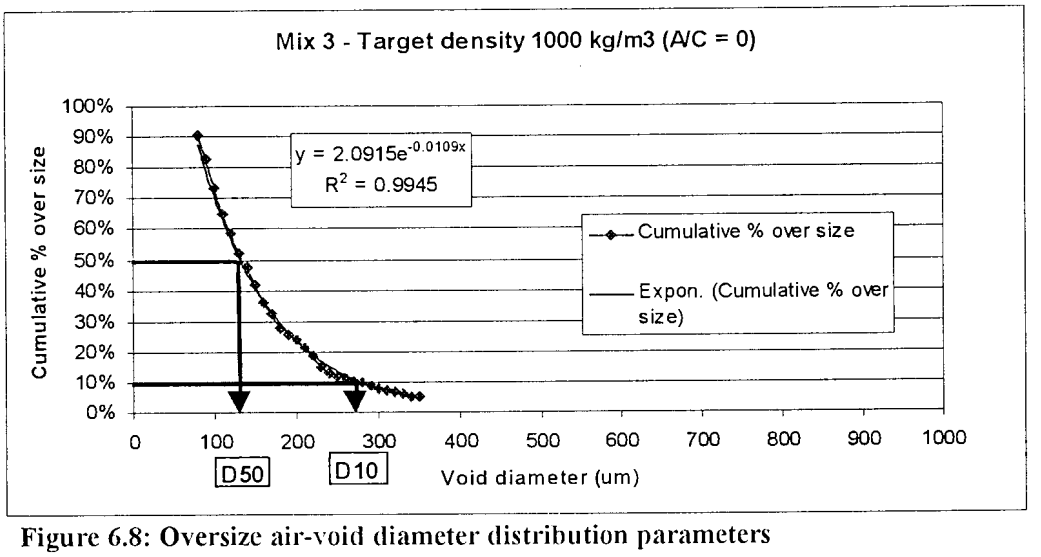

Figure 6.8: Oversize air-void diameter distribution parameters

6.4 AIR-VOID SPACING

The shape and size of the air-voids can not be the only aspects describing the air-void structure because the thickness of the paste around the air-voids may also have an influence on the properties of the material. Based on the principle that a chain is only as strong as its weakest link, the minimum paste thickness around each air-void was established (Kearsley, 1999).

The perpendicular distance through the cement paste from one air-void to the nearest other air-void in the vicinity is used to describe the spacing of the air-voids in other words the minimum paste thickness for each air-void - see the microscopic image in Figure 6.9.

Table 6.4: Fitted function and parameters of oversize air-void diameter distribution

Mixture number	Ash/ Cement ratio	Water/ Cement ratio	Water/ Binder ratio	Target density (kg/m^3)	Fitted Function $y = a\,e^{(bx)}$		R^2	Oversize air-void diameter distribution parameters	
					a	b		D50 (μm)	D10 (μm)
1	0	0.33	0.33	1500	1.4517	-0.0061	0.9752	175	439
2	0	0.33	0.33	1200	3.1625	-0.0137	0.9948	135	252
3	0	0.33	0.33	1000	2.0915	-0.0109	0.9945	131	279
4	0	0.33	0.33	900	1.8106	-0.0085	0.9948	151	341
5	0	0.33	0.33	800	1.6839	-0.0072	0.9918	169	392
6	0	0.33	0.33	700	1.6907	-0.004	0.9881	305	707
7	1	0.58	0.29	1500	1.9795	-0.0108	0.9966	127	276
8	1	0.58	0.29	1200	2.1509	-0.0109	0.9953	134	282
9	1	0.58	0.29	1000	1.954	-0.0095	0.9948	143	313
10	1	0.58	0.29	900	1.6416	-0.0073	0.9915	163	383
11	1	0.58	0.29	800	1.3041	-0.0053	0.9947	181	485
12	1	0.58	0.29	700	1.4722	-0.0043	0.9849	251	625
13	2	0.87	0.29	1500	2.5265	-0.0125	0.9936	130	258
14	2	0.87	0.29	1200	2.0025	-0.0125	0.9824	111	240
15	2	0.87	0.29	1000	1.4143	-0.0071	0.9733	146	373
16	2	0.87	0.29	900	2.1091	-0.0072	0.9888	200	423
17	2	0.87	0.29	800	1.8165	-0.0056	0.9824	230	518
18	2	0.87	0.29	700	1.655	-0.0057	0.9941	210	492
19	3	1.17	0.28	1500	2.0551	-0.0117	0.9829	121	258
20	3	1.17	0.28	1200	1.7065	-0.0111	0.96	111	256
21	3	1.17	0.28	1000	1.6738	-0.0064	0.985	189	440
22	3	1.17	0.28	900	1.6455	-0.0056	0.9935	213	500
23	3	1.17	0.28	800	2.1211	-0.0052	0.9756	278	587
24	3	1.17	0.28	700	2.04	-0.0035	0.9748	402	862
25	4	1.6	0.27	1500	5.333	-0.0183	0.9784	129	217
26	4	1.6	0.27	1200	5.01	-0.0168	0.9771	137	233
27	4	1.6	0.27	1000	3.2081	-0.0119	0.9899	156	291
28	4	1.6	0.27	900	1.61	-0.0052	0.9771	225	534
29	4	1.6	0.27	800	2.1105	-0.0071	0.9745	203	430
30	4	1.6	0.27	700	1.8457	-0.0041	0.9915	319	711

The method used to calculate the spacing of the air-voids is describe in view of

Figure 6.10 which represent a microscopic image of three air-voids. A x-coordinate, y-coordinate and a radius (R) represent each air-void. The coordinates of the centroids of the air-voids are found in the output data of the software. The radii were calculated from the measured areas by assuming that all air-voids are perfect spheres.

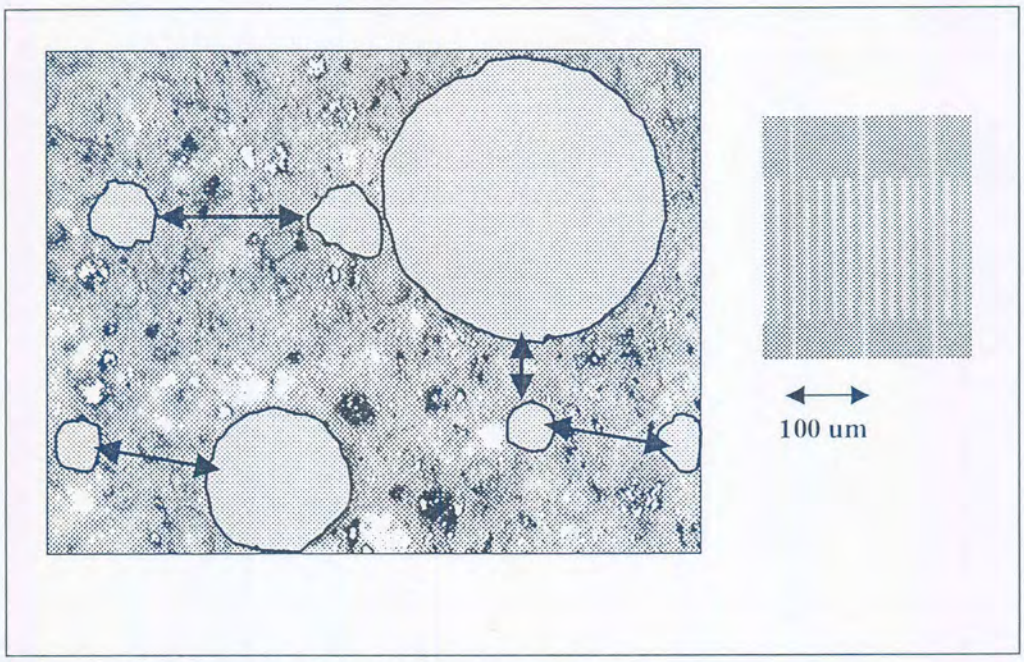

Figure 6.9: Minimum thickness of paste around air-voids

The distance ($S_{1,2}$) between void 1 and void 2 can be calculated using the following equation (Kearsley, 1999):

$$S_{1,2} = \sqrt{\left((x_1 - x_2)^2 + (y_1 - y_2)^2\right)} - R_1 - R_2 \qquad \text{(Eq. 6.1)}$$

Where:

$S_{1,2}$ = Minimum Perpendicular distance between void 1 and void 2.

$x_1\ x_2$ = x-coordinates of void 1 and void 2.

$y_1 y_2$ = y-coordinates of void 1 and void 2.

$R_1 R_2$ = radii of void 1 and void 2.

By sequentially replacing the properties of void 2 in Equation 6.1 with each of the air-voids on the photo the distance between void 1 and each of the of the other voids can be calculated. These distances are compared and the minimum distance is recorded as the space between void 1 and its closest neighbor. After

determining the minimum spacing for void 1 the procedure can be repeated for each of the other voids (Kearsley, 1999).

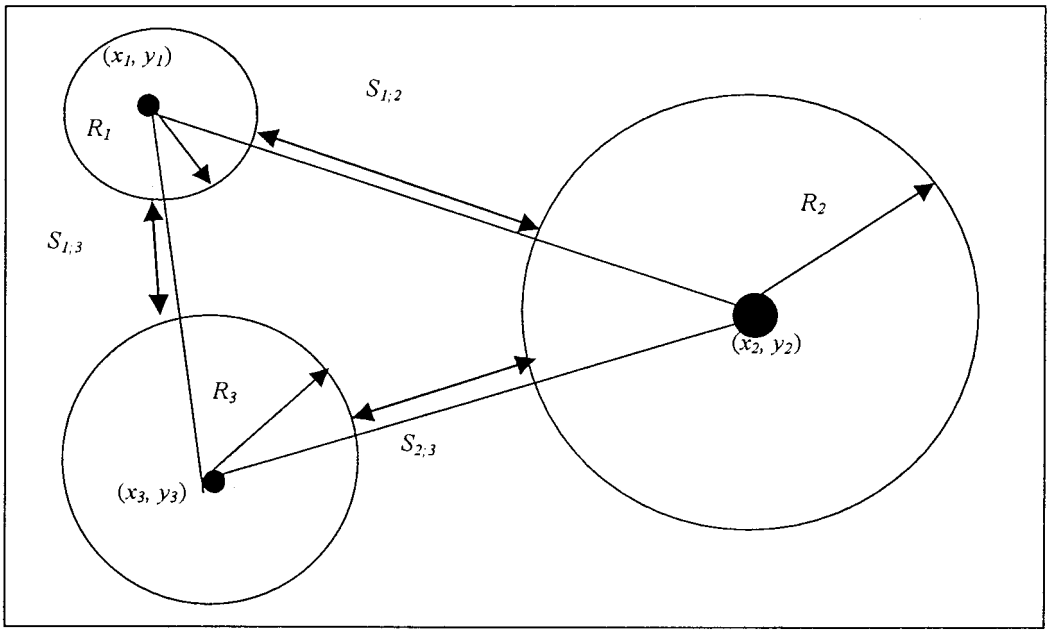

Figure 6.10: Spacing of air-voids (Kearsley, 1999)

The ASCII file of the photo data as produced by the analysis software for every photograph taken were imported into spreadsheets using Microsoft Excel. A macro was written in Excel (see Appendix D) to take each void and calculate the thickness of the paste between that void and all the other voids. The minimum value calculated was taken as the minimum thickness of the paste around that spesific void (Kearsley, 1999). The macro as written by Kearsley was changed for this investigation. A negative minimum value (air-voids touching each other) is recorded by the macro as zero.

The distribution of the minimum distances between the air-voids (the air-void spacing) was determined by plotting histograms for the calculated air-void spacings counted in each mixture. A typical distribution is indicated in Figure 6.11 and the histograms plotted for all the other mixtures are attached in Appendix E. The percentage of the number of minimum distances between air-voids is plotted on the vertical axis to compare the histograms of the different mixtures with each other and the air-void spacings are plotted on the horizontal axis. The *cumulative frequancy % distribution* for the air-void

spacing is also plotted on this graph. The spacing of the air-voids indicated, as zero on the graph is air-voids touching each other.

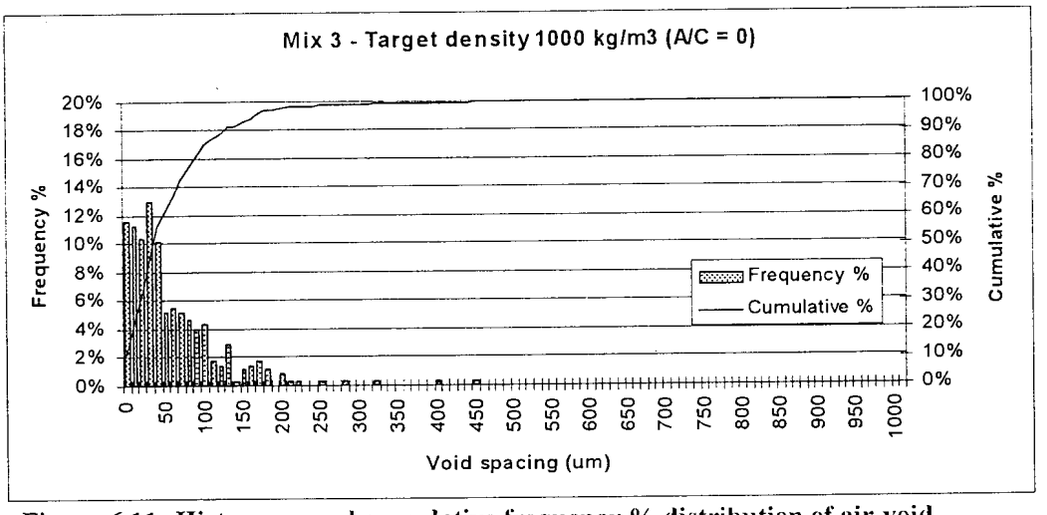

Figure 6.11: Histogram and cumulative frequency % distribution of air-void

The same method as was described for the *oversize air-void diameter distribution* was used to develop parameters for spacing of air-voids in order to compare mixtures.

The inverse of the *cumulative frequency % distribution* of the air-void spacing was obtained and an exponential function was fitted for the graph (see Figure 6.12). The exponential fit for the graphs for all the mixtures can be viewed in Appendix F. Provision was made for statistical outliers by omitting the top and bottom 5 %, in other words the 5 % voids with the smallest distance to their nearest neighbor and the 5 % voids with the largest distance to their nearest neighbor. The fitted functions for all the mixtures can be seen in Table 6.5. The statistical R-square value for all the mixtures of the exponential fit is between 0.89 and 0.998 (see Table 6.5). The exponential equation is therefore a true representation of the inverse of the *cumulative frequency % distribution.*

Both the constants in the equation vary with density and ash content and therefore the constants as such cannot be used to compare the mixtures (See Table 6.5).

The median distance between the air-voids *S50* (where 50% of the air-void spacing are smaller than the value) and *S90* distance (where 10 % of the void

spacing are smaller than the value) was calculated for each mixture by using the fitted functions (See Figure 6.12). *S50* and *S90* are also listed in Table 6.5.

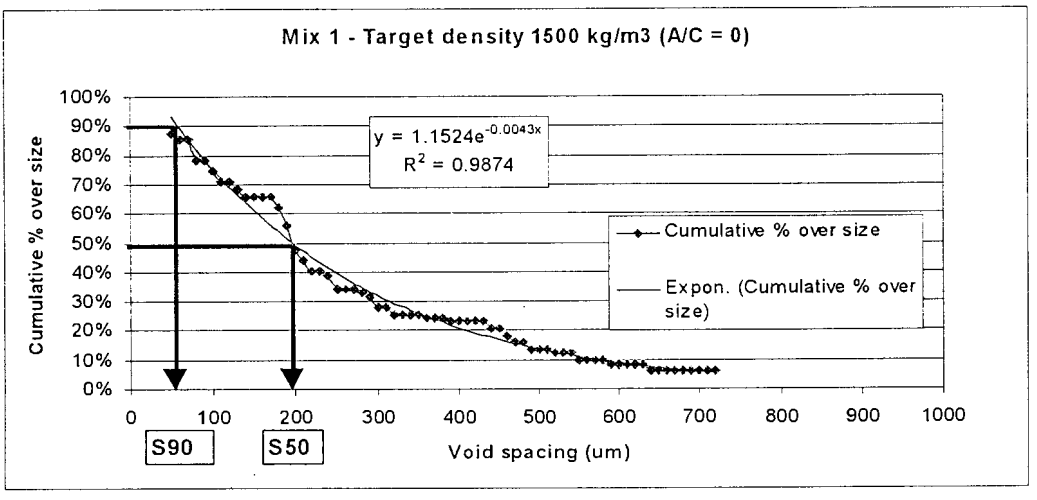

Figure 6.12: Air-void spacing parameters

6.5 CONCLUSIONS

6.5.1 Air-void shape

- The air-voids in these mixtures are approximately circular in section and it was assumed that the air-voids are perfect spheres, therefore the size of the air-voids are best described with an effective air-void diameter.

6.5.2 Air-void size and size distribution

- The air-void diameter distribution follows a log normal distribution.
- The Rosin-Rammler distribution parameters are used to describe the air-void size distribution. It consists of the position parameter (x_0), (this value indicates the air-void diameter in µm for which 36.8 % of the air-void diameters are larger) which gives an indication of the void size. The (n) value represents the range of the air-void diameter distribution of the air-void diameters greater than (x_0).

Table 6.5: Fitted functions and air-void spacing parameters.

Mixture number	Ash/ Cement ratio	Water/ Cement ratio	Water/ Binder ratio	Target density (kg/m^3)	Fitted Function $y = a\,e^{(bx)}$		R^2	Air-void spacing parameters	
					a	b		S50 (μm)	S90 (μm)
1	0	0.33	0.33	1500	1.2027	-0.0427	0.9874	190	7
2	0	0.33	0.33	1200	1.0481	-0.0134	0.996	60	11
3	0	0.33	0.33	1000	0.9042	-0.017	0.9975	30	0
4	0	0.33	0.33	900	0.9264	-0.0144	0.9953	40	2
5	0	0.33	0.33	800	0.921	-0.0157	0.99	70	2
6	0	0.33	0.33	700	0.9913	-0.0097	0.9889	70	10
7	1	0.58	0.29	1500	1.1256	-0.0056	0.9826	140	40
8	1	0.58	0.29	1200	1.239	-0.0097	0.9862	90	33
9	1	0.58	0.29	1000	1.1769	-0.0102	0.9928	80	26
10	1	0.58	0.29	900	1.081	-0.0072	0.9888	100	25
11	1	0.58	0.29	800	1.1069	-0.0069	0.9412	110	30
12	1	0.58	0.29	700	0.6975	-0.0058	0.963	60	0
13	2	0.87	0.29	1500	1.0495	-0.0043	0.9747	150	36
14	2	0.87	0.29	1200	0.9919	-0.0038	0.9704	180	26
15	2	0.87	0.29	1000	1.2805	-0.0076	0.9911	120	46
16	2	0.87	0.29	900	1.2951	-0.0084	0.9822	110	43
17	2	0.87	0.29	800	1.1853	-0.0091	0.987	90	30
18	2	0.87	0.29	700	1.3375	-0.0096	0.9863	100	41
19	3	1.17	0.28	1500	1.4157	-0.0091	0.9893	110	50
20	3	1.17	0.28	1200	1.2286	-0.0071	0.9853	130	44
21	3	1.17	0.28	1000	1.1899	-0.0085	0.9951	100	33
22	3	1.17	0.28	900	1.3901	-0.0098	0.9658	100	44
23	3	1.17	0.28	800	1.6036	0.00102	0.9718	110	57
24	3	1.17	0.28	700	1.0125	-0.0067	0.9664	100	18
25	4	1.6	0.27	1500	1.6886	-0.0044	0.9501	280	143
26	4	1.6	0.27	1200	1.2471	-0.0079	0.9951	120	41
27	4	1.6	0.27	1000	1.3124	-0.012	0.9784	80	31
28	4	1.6	0.27	900	1.2185	-0.0062	0.984	140	49
29	4	1.6	0.27	800	0.7782	-0.004	0.8923	110	0
30	4	1.6	0.27	700	1.3544	-0.0076	0.9736	130	54

- The *oversize air-void diameter distribution parameters* (D50) and (D10) are developed to quantify the air-void size distribution. The 50 % oversize air-void diameter (D50) in μm gives an indication of the average void size of each mixture. The 10 % oversize air-void diameter (D10) indicates the diameter for which only 10 % of the diameters are larger.

6.5.3 Air-void spacing

- The perpendicular distance through the cement paste from one air-void to the nearest other air-void in the vicinity is used to describe the spacing of the air-voids.
- The spacing parameters S50 and S90 are developed to quantify and describe the distances between air-voids. S50 is the median distance between the air-voids and S90 indicates the value where 10 % of the distance between the air-voids is smaller than the value.

7. DISCUSSION OF RESULTS

7.1 INTRODUCTION

The aim of this chapter is to investigate the effect of the air-void structure (air-void size distribution and air-void spacing) on the relation between physical properties (such as density, ash / cement ratio and porosity), and the structural property (compressive strength) of foamed concrete. The air-void structure parameters as developed in chapter 6 are used to determine the relationships.

7.2 EFFECT OF DENSITY ON AIR-VOID STRUCTURE

7.2.1 Air-void size distribution

Kearsley (1999) has published results of properties of foamed concrete as a function of dry density. In some references (Neopor and L.B. Chemicals, Product Information sheets) the properties of foamed concrete are related to the wet density. The relation between the wet and dry density of the mixtures is a linear relation (see Figure 7.1) and can be used to compare the results obtained from the different studies.

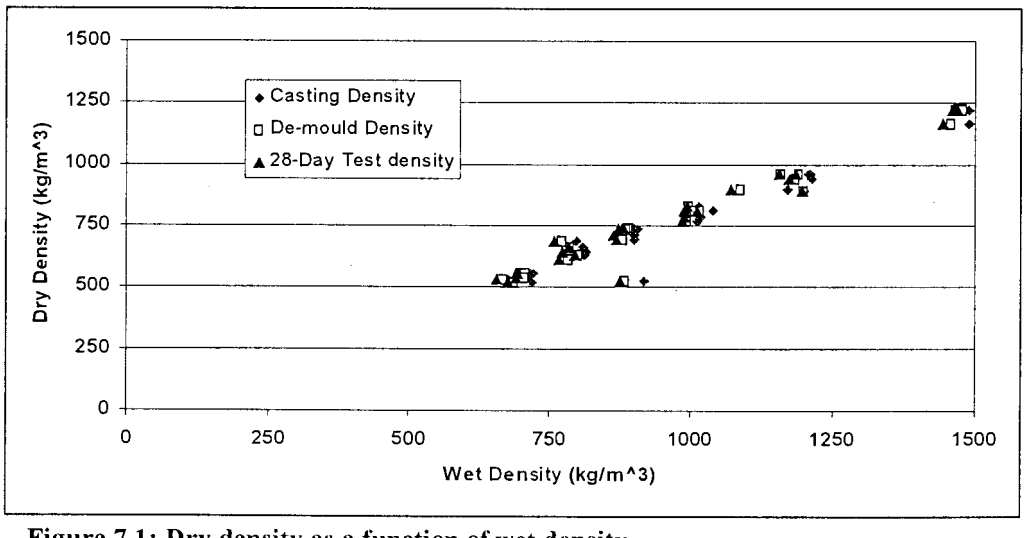

Figure 7.1: Dry density as a function of wet density

The effect of the 28-day dry density on the air-void size-distribution can be seen in Figure 7.2 and Figure 7.3. The Rosin-Rammler air-void size distribution parameters (as discussed in 6.3.1.1) are plotted as a function of the 28-day dry density.

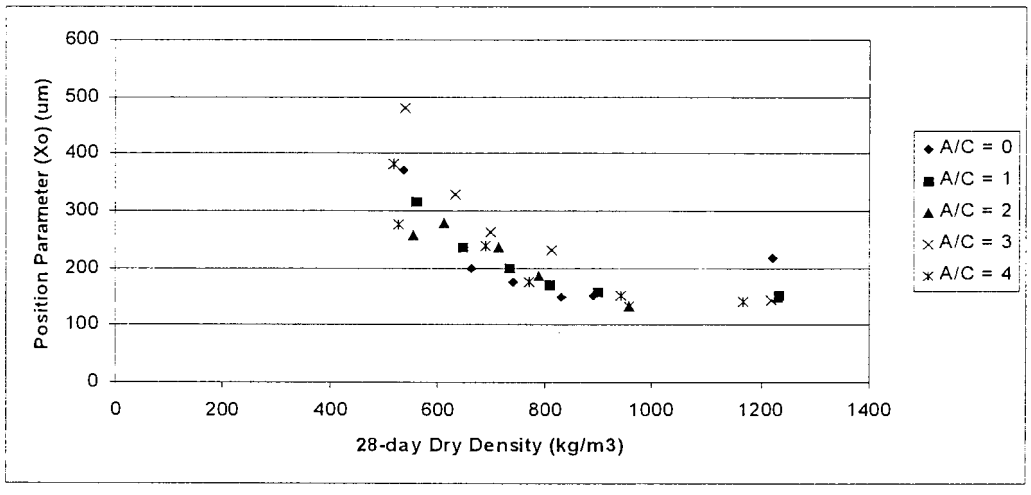

Figure 7.2: Relation between 28-day dry density and Rosin-Rammler distribution position parameter (x_o)

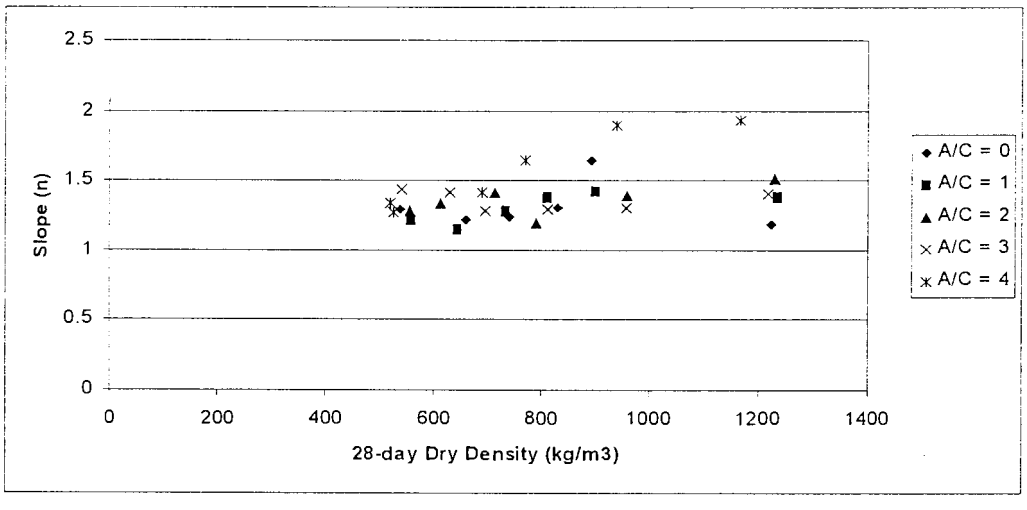

Figure 7.3: Relation between 28-day dry density and Rosin-Rammler distribution slope (n) parameter

The graph in Figure 7.2 indicates that the position parameter (x_o) and therefore the air-void diameters become smaller as the dry density increases.

In Figure 7.3 the slope (n) is plotted as a function of the dry density. From this graph it seems that the 28-day dry density does not have any influence on the

n value, which represents the range of the air-void diameter distribution of the air-void diameters greater than the position parameter (x_o).

The relevance of the Rosin-Rammler air-void size distribution parameters was evaluated by comparing the fitted functions for the cumulative % oversize air-void diameters for different 28-day dry densities for a spesific ash / cement ratio. The functions for ash / cement ratios of three are plotted in Figure 7.4. The rest of the void size distributions can be viewed in Appendix G.

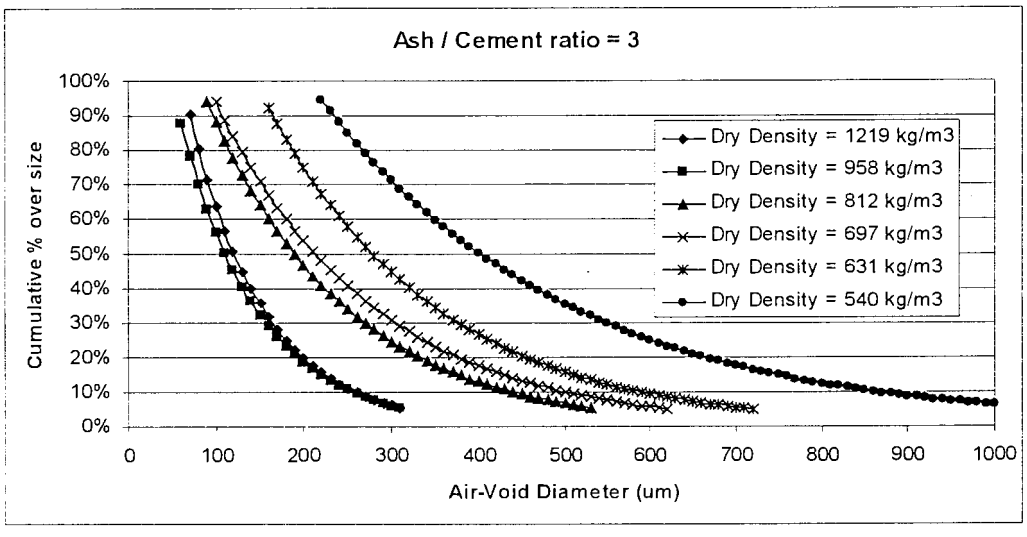

Figure 7.4: Summary of exponential fitted functions for the cumulative % oversize air-void diameters

According to Figure 7.4 the position parameter (x_o) and therefore the air-void diameters increase as the dry density decreases. On the other hand it is clear that the dry density has a *significant influence* on the range of the air-void diameters greater than the position parameter (x_o). The mixtures with lower densities seem to have more of the larger voids but this trend cannot be seen when comparing the Rosin-Rammler slope (n) parameters.

The Rosin-Rammler air-void size distribution parameters are therefore *not* representative of the air-void size distribution of the mixtures. The reason is the fact that the Rosin-Rammler parameters are insensitive towards the tail end of the *cumulative % oversize air-void diameter distribution.*

In Figure 7.5 the *oversize air-void diameter distribution parameters* (D50) and (D10) are plotted as a function of the 28-day dry density in order to find the influence of dry density on the air-void size distribution.

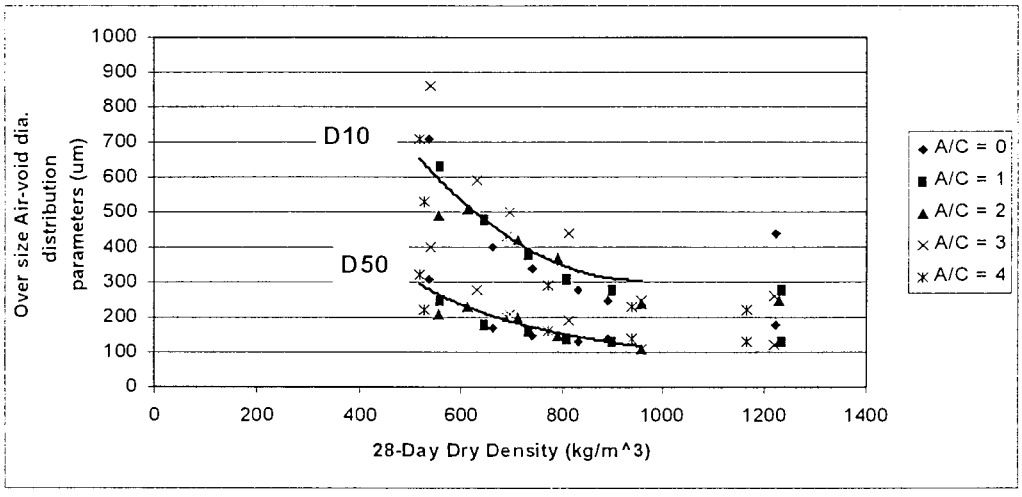

Figure 7.5: Relation between 28-day dry density and air-void size distribution parameters

As the *28-day dry density* increases the average void diameters became smaller. At higher densities the 10 % largest voids in the mixtures also become smaller. It is interesting to note that the distribution curves converge, indicating that the voids become smaller and more uniform in size at higher densities. The lower *28-day dry densities* (between 500 kg/m^3 and 1000 kg/m^3) do have an influence on the air-void size because the air-bubbles are close together just after casting and therefore have the opportunity to merge before setting of the paste around the air-voids. A limit is reached at a *28-day dry density* of 1000 kg/m^3, as the data obtained at higher densities do not display any clear pattern. It seems that the dry densities higher than 1000 kg/m^3 do not have an influence on the air-void size distribution because the air-voids are far apart in the paste and therefore do not have the ability to merge before setting of the paste around the bubbles.

7.2.2 Air-void spacing

The effect of the *28-day dry density* on the air-void spacing can be seen in Figure 7.6. For mixtures with dry densities lower than 1000 kg/m^3, 90 % of

the spacing distances are larger than 35 µm and 50 % of the spacing distances are larger than 100 µm. Spacing distances increase for the higher dry densities.

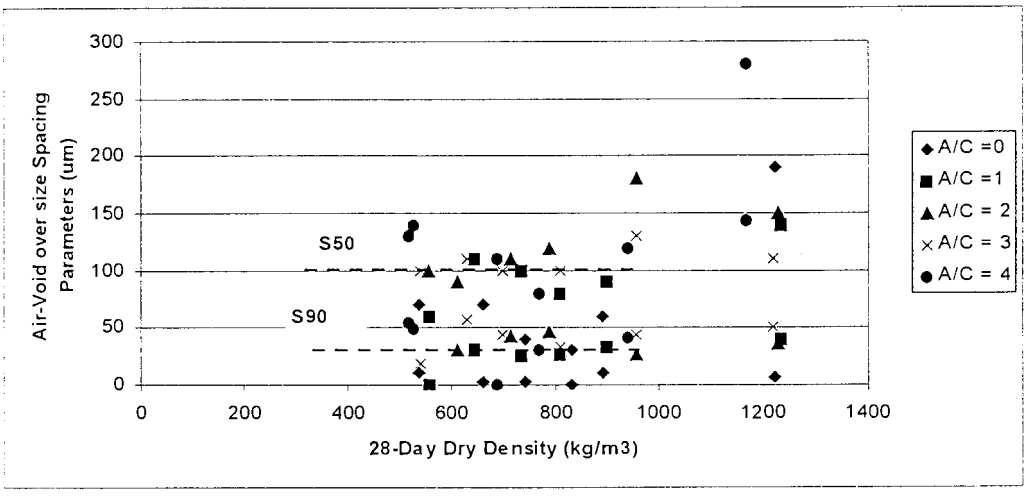

Figure 7.6: Relation between 28-day dry density and oversize air-void spacing parameters

The lower *28-day dry densities* don't have any influence on the air- void spacing. The higher *28-day dry densities* may have an influence on the air-void spacing but the data obtained in this investigation is not enough to determine if there is a relation or not.

7.3 EFFECT OF ASH / CEMENT RATIO ON AIR-VOID STRUCTURE

7.3.1 Air-void size distribution

In Figure 7.7 the *oversize air-void diameter distribution parameters* (D50) and (D10) are plotted as a function of the ash / cement ratio. Figure 7.7 shows the influence of ash / cement ratio on the air-void size distribution of mixtures with target densities between 1500 kg/m^3 and 700 kg/m^3.

The ash / cement ratio has an influence on the air-void size distribution range. According to Figure 7.7 the air-void size distribution range is the narrowest

for an ash / cement ratio of two and the widest for an ash / cement ratio of three.

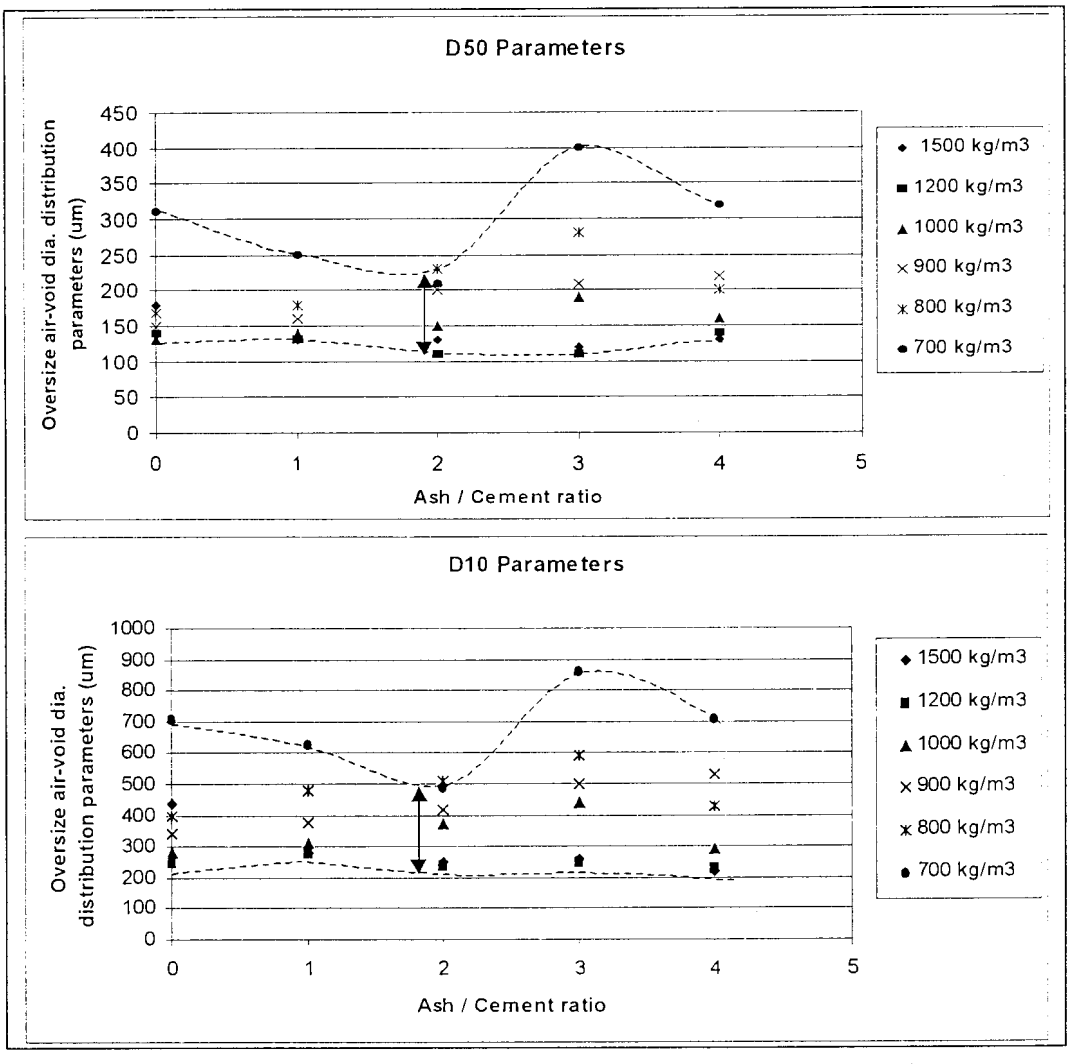

Figure 7.7: Relation between ash / cement ratio and air-void size distribution parameters

There is no mathematical trend to describe the effect of the ash / cement ratio on the air-void size distribution.

7.3.2 Air-void spacing

Figure 7.8 shows the effect of the ash / cement ratio on the air-void spacing of the mixtures with target densities lower than 1200 kg/m^3. The minimum distances between the air-voids are the largest for an ash / cement ratio of two.

Figure 7.8 also shows that for the mixtures with an ash / cement ratios of two and three, 90 % of the air-voids are not touching each other (minimum distances between the air-voids are not zero). There is no mathematical trend to describe the effect of the ash / cement ratio on the air-void spacing.

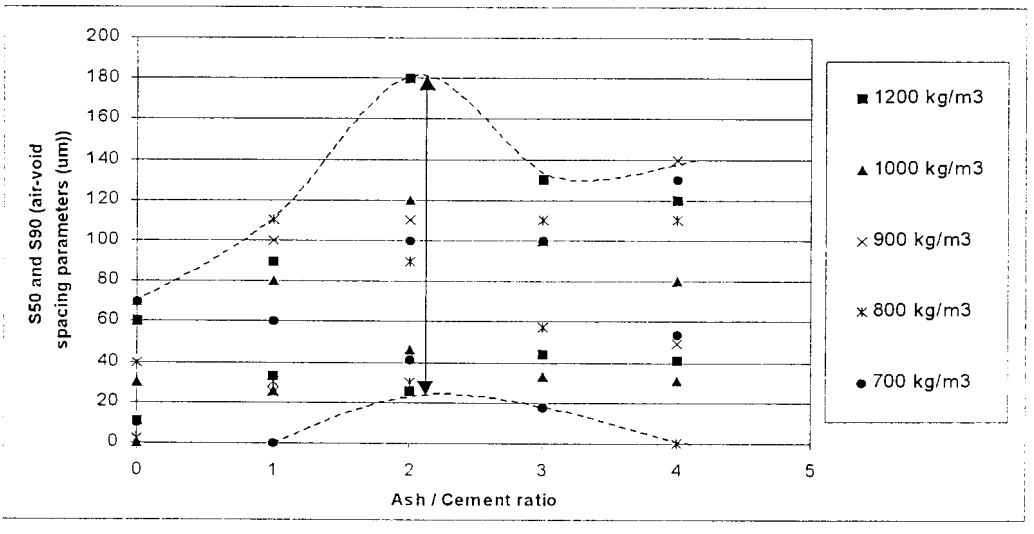

Figure 7.8: Relation between ash / cement ratio and spacing parameters

7.4 EFFECT OF AIR-VOID STRUCTURE ON POROSITY

7.4.1 Air-void size distribution

The porosity of foamed concrete is the sum of the air-voids and the voids in the paste. The relation between the *28-day dry density* and the *average % porosity* can be seen in Figure 7.9.

A power trendline was added to the graph in Figure 7.9 and the equation and R-square value displayed on the graph. The statistical R-square value for the equation is 0.9591 and therefore a relative strong relation exists between dry density and *average % porosity* for the mixtures.

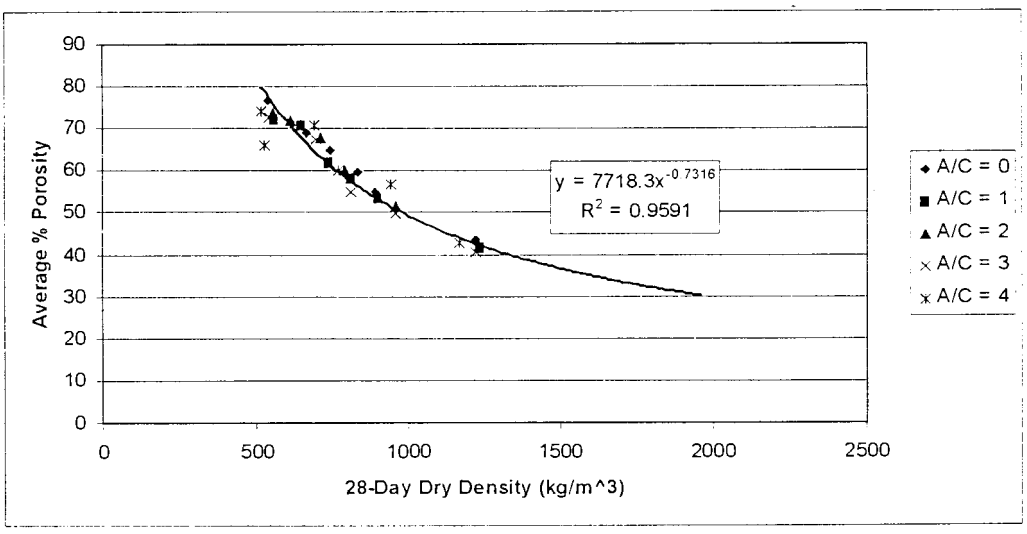

Figure 7.9: Relation between 28-day dry density and average % porosity

The relation between the air-void size distribution parameters and average % porosity (see Figure 7.10) indicates that an increase in the air-void diameter results in an increase in the *average % porosity*. Wider void distributions lead to higher porosities for the mixtures with porosities higher than 50 % (dry densities lower than 1000 kg/m^3). For mixtures with porosities lower than 50 % (dry densities higher than 1000 kg/m^3) the air-void size distribution does not seem to have an influence on the *average % porosity*.

7.4.2 Air-void spacing

The spacing parameters are plotted as a function of the porosity in Figure 7.11. The distances between air-voids do not have any influence on the porosity of the mixtures.

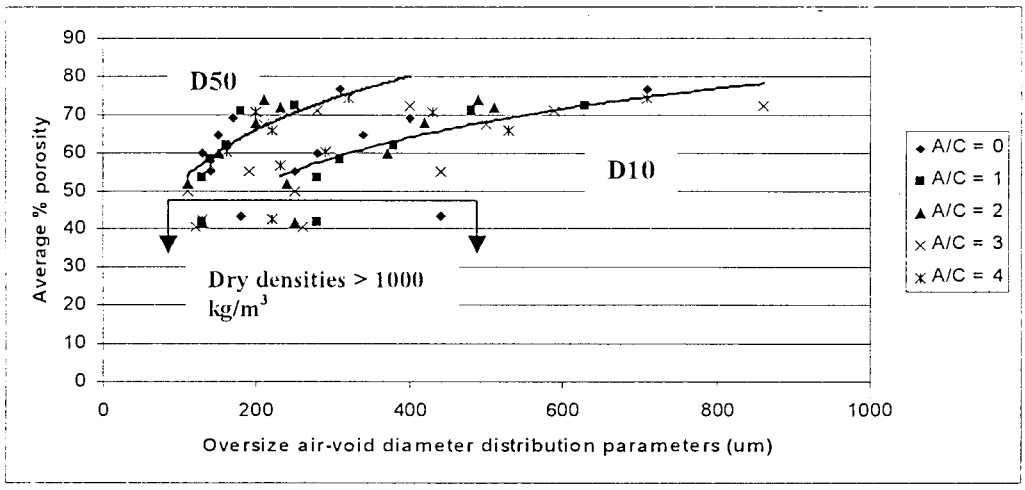

Figure 7.10: Relation between air-void size distribution parameters and average % porosity.

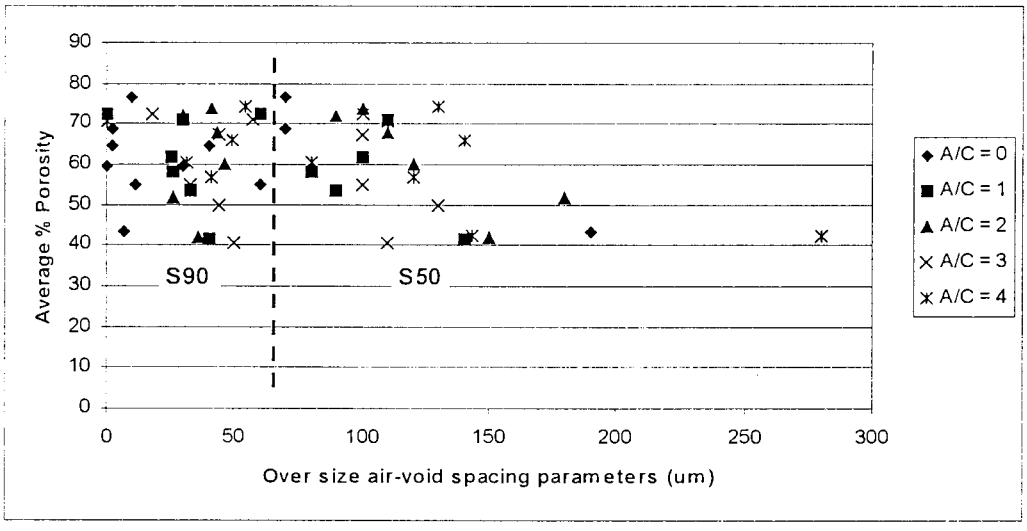

Figure 7.11: Relation between air-void spacing parameters and average % porosity

7.5 EFFECT OF AIR-VOID STRUCTURE ON COMPRESSIVE STRENGTH

7.5.1 Air-void size distribution

The *28-day compressive strength* is plotted as a function respectively of the *28-day dry density* and the *average % porosity* (see Figure 7.12 and 7.13).

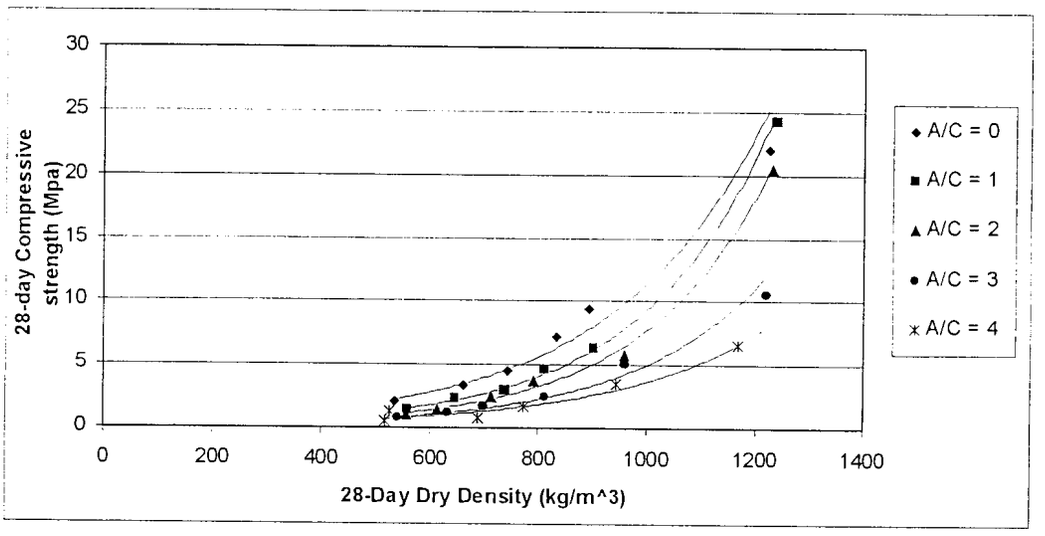

Figure 7.12: Relation between 28-day dry density and 28-day compressive strength

The relation between the *28-day dry density* and the *28-day compressive strength* of foamed concrete is an exponential relationship. The *28-day compressive strength* increases with an increase in the *28-day dry density*. The ash / cement ratio of the mixtures has a specific influence on this relationship. For the same *28-day dry density*, the *28-day compressive strength* decreases as the ash / cement ratio increases.

Table 7.1 lists the exponential fitted functions (as shown in Figure 7.12) for the relationship between the *28-day dry density* and the *28-day compressive strength* for different ash / cement ratios. The statistical R-square value of the exponential fit is also listed in Table 7.1.

Table 7.1: Fitted functions for the relationship between the 28-day dry density and the 28-day compressive strength

Mixture numbers	Ash/ Cement ratio	Fitted Function $y = a\,e^{(bx)*}$		R^2
		a	b	
1-6	0	0.5157	0.0024	0.9769
7-12	1	0.127	0.0036	0.9955
13-18	2	0.0833	0.0038	0.9884
19-24	3	0.0737	0.0035	0.9865
25-30	4	0.0638	0.0033	0.8538

* x = 28-day dry density

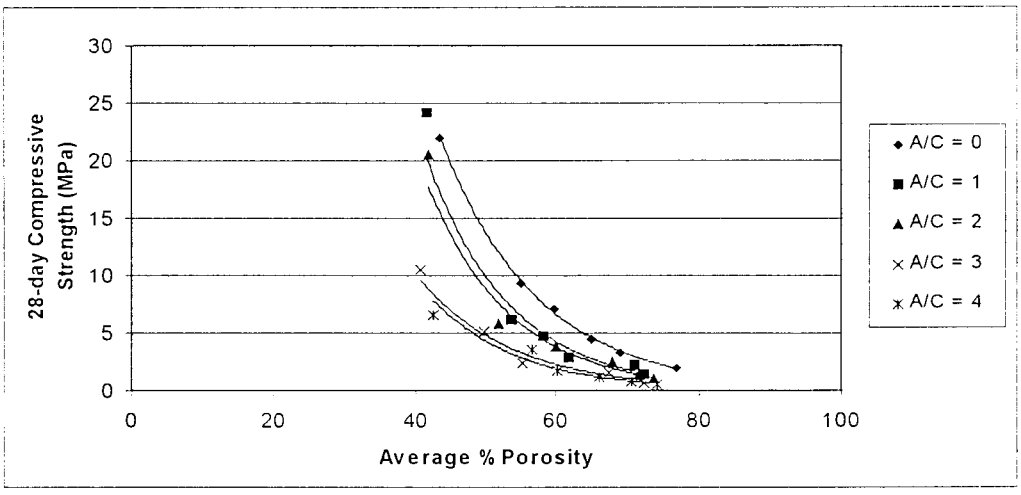

Figure 7.13: Relation between average % porosity and 28-day compressive strength

The relation between the *average % porosity* and the *28-day compressive strength* of foamed concrete is also an exponential relationship. The *28-day compressive strength* decreases with an increase in the *average % porosity*. The ash / cement ratio of the mixtures also has a specific influence on this relationship. For the same *average % porosity*, the *28-day compressive strength* decreases as the ash / cement ratio increases.

Table 7.2 lists the exponential fitted functions (as shown in Figure 7.13) for the relationship between the *average % porosity* and the *28-day compressive strength* for different ash / cement ratios. The statistical R-square value of the exponential fit is also listed in Table 7.2.

Table 7.2: Fitted functions for the relationship between the average % porosity and the 28-day compressive strength

Mixture numbers	Ash/ Cement ratio	Fitted Function $y = a\,e^{(bx)}$*		R^2
		a	b	
1-6	0	528.61	-0.073	0.9978
7-12	1	691.7	-0.0849	0.9572
13-18	2	629.96	-0.0853	0.97
19-24	3	203.79	-0.075	0.9559
25-30	4	249.97	-0.0813	0.961

* x = Average % porosity

Ash / cement ratios as well as dry densities lower than 1000 kg/m^3 have an effect on the air-void size distribution. The air-void size distribution has an influence on porosities higher than 50 %. On the other hand the dry density, ash / cement ratio and porosity have a definite effect on the compressive strength. As a result of these facts a relation has to exist between the air-void size distribution and compressive strength of foamed concrete.

The effect of the air-void size distribution on the *28-day compressive strength* can be determined from Figure 7.14. It displays a decrease in the *28-day compressive strength* with an increase in void diameter. Figure 7.14 indicates that smaller uniformed size air-voids in a mixture ensure higher *28-day compressive strengths*. Larger air-voids in a mixture give rise to lower *28-day compressive strengths*.

Wider air-void size distributions lead to lower *28-day compressive strengths* for mixtures with *28-day dry densities* lower than 1000 kg/m^3. The air-void size distribution does not seem to have an influence on the *28-day compressive strength* for the mixtures with *28-day dry densities* higher than 1000 kg/m^3. It seems that for the mixtures with *28-day dry densities* higher than 1000 kg/m^3 it is the composition of the paste that determines the compressive strength of the mixture because the air-voids are too far apart to have an influence on the compressive strength.

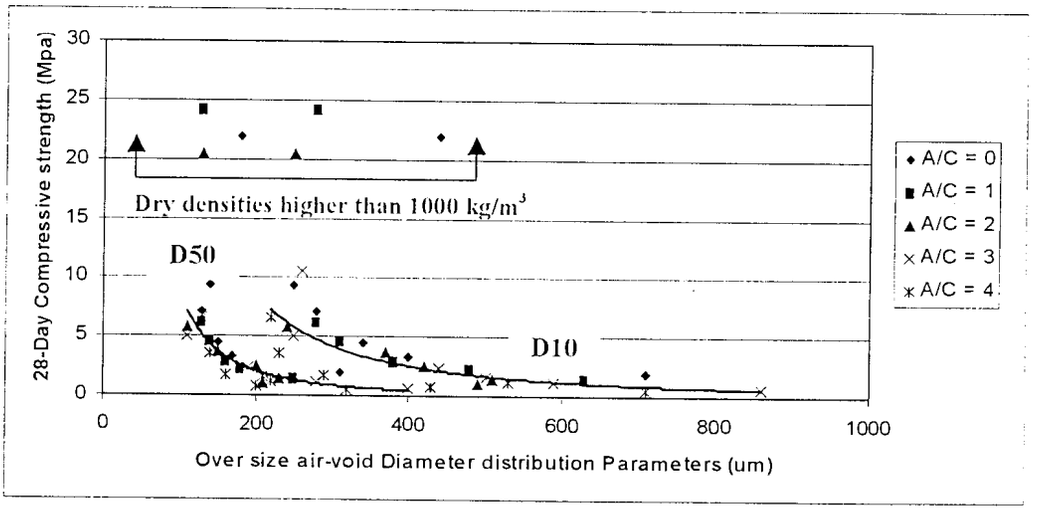

Figure 7.14: Relation between over size air-void distribution parameters and 28-day compressive strength

7.5.2 Air-void spacing

The spacing parameters are plotted as a function of the compressive strength in Figure 7.15. No real relation between the air-void spacing and the 28-day compressive strength can be found. This correlates with the fact that there is no relation between air-void spacing and the other physical properties of the mixtures.

7.6 EFFECT OF AIR-VOID STRUCTURE ON PREDICTED LONG TERM COMPRESSIVE STRENGTH

The measured porosities were used in equation 2.11, 2.12 and 2.13 to determine the 365-days predicted compressive strengths for the mixtures in this investigation. The constants in Table 2.1 for pozz-fill were used for these mixtures. All the values of the predicted 365-days compressive strengths for the mixtures are listed in Table 7.3. The only discrepancy in this table is mix no 6's predicted strength, it is lower than the 28-day compressive strength. The measured porosity is very high.

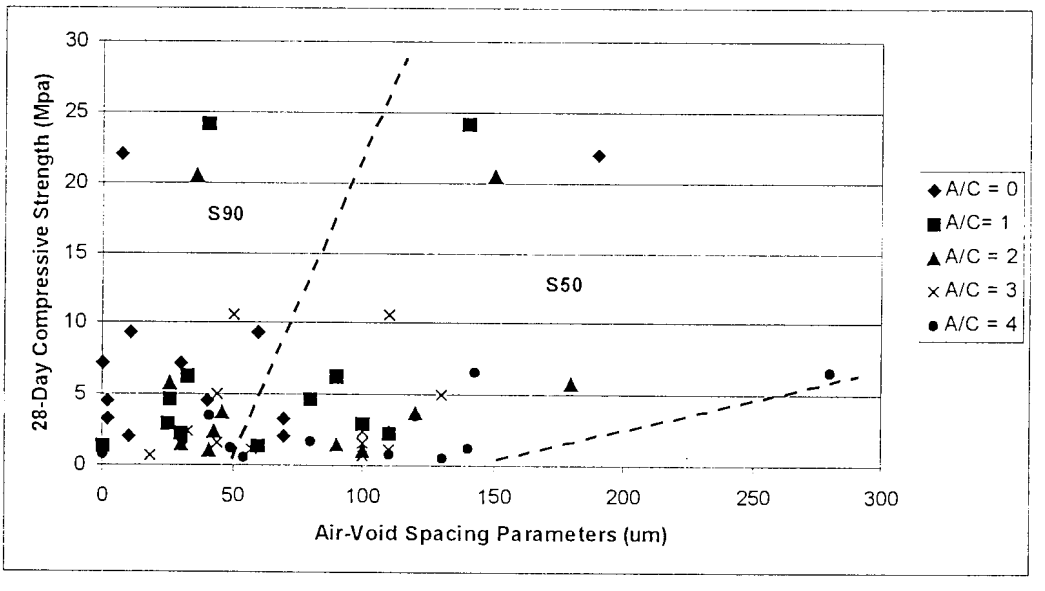

Figure 7.15: Relation between air-void spacing parameters and the 28-day compressive

Figure 7.16 indicates the relation between the ash / cement ratio and the predicted 365-days compressive strength of the mixtures with *target densities* lower than 1200 kg/m^3.

From this graph it seems that the optimum ash / cement ratio for this specific mixtures resulting in the highest predicted 365-day compressive strength is two. The question arises if the microstructure has any influence on this optimum design mixture.

For the mixtures with *28-day dry densities* lower than 1000 kg/m^3 narrower air-void size distributions lead to higher *28-day compressive strengths*, but the narrowest air-void size distribution is found at an ash / cement ratio of two (see Figure 7.7). It is possible that for a narrow air-void size distribution the particle packing is the best and therefore the long-term compressive strength of the mixture is a maximum.

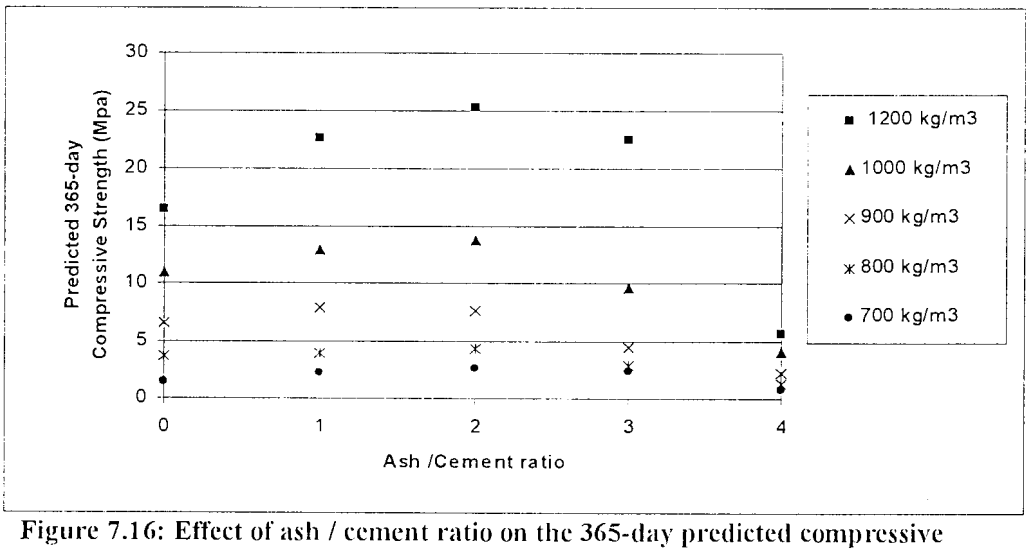

Figure 7.16: Effect of ash / cement ratio on the 365-day predicted compressive strength

The minimum distances between the air-voids are a maximum for an ash / cement ratio of two for mixtures with *28-day dry densities* lower than 1000 kg/m^3 (see Figure 7.8). From literature (Neville, 1987 and Kearsley, 1999) when ash is added to cement paste initially the gain in strength is caused by the hydration of the cement and the ash acts as filler. As time passes, the ash starts contributing towards the strength, an increasing percentage of the ash starts acting as a cement – extender.

Table 7.3: Predicted Compressive strengths of mixtures after 365 days

Mix nr	A/C ratio	Target density (kg/m^3)	28-day Compressive Strength (MPa)	λ	β	Measured porosity	t	365-day Predicted Strength (MPa)
1	0	1500	22.00	176.9	23.74	0.44	365	38.23
2	0	1200	9.40	176.9	23.74	0.55	365	16.45
3	0	1000	7.17	176.9	23.74	0.60	365	10.92
4	0	900	4.52	176.9	23.74	0.65	365	6.63
5	0	800	3.30	176.9	23.74	0.70	365	3.68
6	0	700	2.00	176.9	23.74	0.77	365	1.42 *
7	1	1500	24.20	-6.76	66.21	0.42	365	52.14
8	1	1200	6.25	-6.76	66.21	0.54	365	22.55
9	1	1000	4.69	-6.76	66.21	0.60	365	12.94
10	1	900	2.92	-6.76	66.21	0.65	365	7.89
11	1	800	2.29	-6.76	66.21	0.71	365	3.94
12	1	700	1.40	-6.76	66.21	0.75	365	2.27
13	2	1500	20.50	-98.34	80.06	0.42	365	50.25
14	2	1200	5.84	-98.34	80.06	0.52	365	25.28
15	2	1000	3.76	-98.34	80.06	0.59	365	13.81
16	2	900	2.45	-98.34	80.06	0.65	365	7.69
17	2	800	1.47	-98.34	80.06	0.70	365	4.35
18	2	700	1.00	-98.34	80.06	0.74	365	2.65
19	3	1500	10.56	-97.84	65.29	0.41	365	41.51
20	3	1200	5.07	-97.84	65.29	0.50	365	22.44
21	3	1000	2.43	-97.84	65.29	0.60	365	9.68
22	3	900	1.61	-97.84	65.29	0.68	365	4.49
23	3	800	1.14	-97.84	65.29	0.71	365	2.85
24	3	700	0.72	-97.84	65.29	0.73	365	2.42
25	4	1500	6.63	-5.26	21.9	0.43	365	15.88
26	4	1200	3.53	-5.26	21.9	0.57	365	5.64
27	4	1000	1.71	-5.26	21.9	0.60	365	4.08
28	4	900	1.25	-5.26	21.9	0.66	365	2.27
29	4	800	0.77	-5.26	21.9	0.71	365	1.33
30	4	700	0.53	-5.26	21.9	0.74	365	0.82

* The 365-day predicted strength is lower than the 28-day compressive strength. It is possible that the equations 2.11, 2.12 and 2.13 are not valid for mixtures with low densities and no ash added.

Based on the principle that a chain is as strong as its weakest link, the mixtures with a maximum cement paste around the air-voids (minimum air-void spacing) can develop the strongest links over a period of time.

It seems that the microstructure (air-void size distribution and air-void spacing) has an influence on the long-term strengths of foamed concrete. No mathematical relationship is possible with the existing data therefore further research is necessary.

From the literature review it is found that the relationship between the density and compressive strength of foamed concrete is an exponential relationship with the power varying with the size and distribution of the air-voids. Table 7.1 shows that the power for the mixtures with an ash / cement ratio of two is an optimum (0.0038).

In the light of the previous paragraphs it seems that the exponent of the exponential relationship between the 28-day dry density and the 28-day compressive strength can be an indicator of the microstructure (air-void size distribution and air-void spacing) of the mixtures. The exponent with the highest value indicates the narrowest air-void size distribution and the largest air-void spacing. Evaluation of the exponents in the relations can therefore result in a prediction of the optimum design (highest 365-day compressive strength) for the specific mixture. Also in this area further research is necessary.

7.7 CONCLUSIONS

- The Rosin-Rammler air-void size distribution parameters *cannot* be used because it is not representative of the air-void size distribution of the mixtures.
- The 28-day compressive strength increases with an increase in the 28-day dry density. The relation is an exponential relation. For the same 28-day dry density, the 28-day compressive strength decreases as the ash / cement ratio increases.
- The relation between the average % porosity and the 28-day compressive strength of foamed concrete is also an exponential relationship. The 28-

day compressive strength increases with a decrease in the average % porosity. For the same average % porosity, the 28-day compressive strength decreases as the ash / cement ratio increases.

- The 28-day dry densities between 500 and 1000 kg/m^3 have an influence on the air-void size distribution. The void diameters became smaller as the dry density increases.
- It seems (for 28-day dry densities higher than 1000 kg/m^3) the air-void size distribution is *not* influenced by density. A possible reason therefore is the fact that the air-voids in these mixtures are far apart in the paste and do not have the ability to merge before setting of the paste around the bubbles.
- The air-void size distribution for mixtures with dry densities between 500 and 1000 kg/m^3 has an influence on the average % porosities and 28-day compressive strength of foamed concrete. It displays an increase in porosity and a decrease in the 28-day compressive strength with an increase in void diameter.
- It seems that (for the mixtures with 28-day dry densities higher than 1000 kg/m^3) it is the composition of the paste that determines the compressive strength of the mixture and not the air-void size distribution. A possible reason therefore is that the air-voids are too far apart in the paste to have an influence on the 28-day compressive strength.
- The 28-day dry densities between 500 and 1000 kg/m^3 have no influence on the spacing of air-voids. The higher 28-day dry densities may have an influence on the air-void spacing but the data obtained in this investigation is not enough to determine if there is a relation or not.
- The spacing of the air-voids does not seem to have any influence on the porosity and 28-day compressive strength.
- The optimum ash / cement ratio for this specific mixtures resulting in the highest predicted 365-day compressive strength is two.
- The narrowest air-void size distribution and the maximum air-void spacing are found at an ash / cement ratio of two.
- It seems that the power of the exponential relationship between the dry density and the compressive strength can be an indication of the microstructure (air-void size distribution and air-void spacing) of the mixtures.

8. CONCLUSIONS AND RECOMMENDATIONS

8.1 CONCLUSIONS

The influence of the physical properties on the structural properties of the foamed concrete mixtures, as investigated in this research maybe summarized as follows:

- The 28-day dry density and the 28-day compressive strength of foamed concrete are related by an exponential relationship. The 28-day compressive strength increases with an increase in the 28-day dry density.
- The average % porosity and the 28-day compressive strength of foamed concrete are also related by an exponential relationship. The 28-day compressive strength increases with a decrease in the average % porosity
- The 28-day compressive strength reduces with increased ash / cement ratio. This is, however, not the ultimate strength and it is anticipated that with proper curing the strength of the mixtures with high ash contents will increase significantly after more than 28 days.

An image analysis system was used to developed the following parameters to explain and quantify the microstructure (air-void structure) of foamed concrete in order to evaluate the influence of the microstructure on the properties of the mixtures with low target densities:

- The shape of most of the air-voids in these mixtures is approximately circular in section and the assumption is made that the air-voids are perfect spheres, therefore the size of the air-voids are best described with an effective air-void diameter.
- The Rosin-Rammler distribution function is evaluated and it does *not* provide parameters that describe the air-void size distribution quantitatively.
- The *oversize air-void diameter distribution parameters* (**D50** and **D10**) are developed to quantify the air-void size distribution. The 50 % oversize air-void diameter (**D50**) gives an indication of the average void size of each mixture. The 10 % oversize air-void diameter parameter (**D10**) indicates the diameter of the air-voids for which only 10 % of the diameters are larger.

- The perpendicular distance through the cement paste from one air-void to the nearest other air-void in the vicinity is used to describe the spacing of the air-voids.
- The *spacing parameters* (**S50** and **S90**) are developed to quantify and describe the distances between air-voids. (**S50**) is the median distance between the air-voids and (**S90**) indicates the value for which 10 % of the void distances are smaller.

The effect of the air-void structure on the properties of foamed concrete mixtures with low target densities may be summarized as follows:

- (For 28-day dry densities between 500 and 1000 kg/m^3) the air-void size distribution is influenced by density. The void diameters become larger as the dry density decreases.
- It seems (for 28-day dry densities higher than 1000 kg/m^3) the air-void size distribution is *not* influenced by density. A possible reason therefore is the fact that the air-voids in these mixtures are far apart in the paste and do not have the ability to merge before setting of the paste around the bubbles.
- The air-void size distribution (for mixtures with dry densities between 500 and 1000 kg/m^3) has an influence on the average porosities and 28-day compressive strength of foamed concrete. The average air-void size increases with increased porosity and this decreased the 28-day compressive strength.
- It seems that the air-void size distribution (for the mixtures with 28-day dry densities higher than 1000 kg/m^3) has *no* influence on the average porosities and 28-day compressive strength of foamed concrete. The air-voids are too far apart in the paste to have an influence on the properties of these mixtures. It seems that the composition of the paste determines the 28-day compressive strength of these mixtures.
- At low densities (between 500 and 1000 kg/m^3) the 28-day dry density has no influence on the spacing of air-voids. The higher 28-day dry densities may have an influence on the air-void spacing but the data obtained in this investigation is not conclusive.
- The spacing of the air-voids does not have any influence on the average porosity or the 28-day compressive strength.

The possible influence of the air-void structure on the predicted long-term compressive strength of the foamed concrete mixtures with low dry densities (between 500 and 1000 kg/ m^3) is as follows:

- It seems that for ideal cured foamed concrete mixtures, with the narrowest air-void size distribution and the largest air-void spacing will ensure the highest 365-day compressive strength.
- It seems that the power of the exponential relationship between the 28-day dry density and the 28-day compressive strength can be an indicator of the microstructure (air-void size distribution and air-void spacing) of the mixtures. The power with the highest value indicates the narrowest air-void size distribution and the largest air-void spacing. Evaluation of the exponents in the relations can therefore result in a prediction of the optimum design (highest 365-day compressive strength) for the specific mixture.

8.2 RECOMMENDATIONS

This research was executed using single source materials and the effect of the different cement, ash and foam sources on the properties of foamed concrete with target densities lower than 1500 kg/m^3 should be investigated.

Further research is necessary on the influence of the microstructure on foamed concrete mixtures with dry densities higher than 1000 kg/m^3.

In this study no specific method was used to prepare the samples for microscopic analysis. Further research is needed into sample preparation to accentuate the contrast between air-voids and cement paste in order to simplify and speed up the image analysis.

The influence of the gel and capillary pores as well as the entrapped air-voids on the properties of foamed concrete needs investigation.

Only the 28-day properties of the mixtures were obtained in this study. Long-term properties of these mixtures need further investigation in order to determine if there is a mathematical relation between the air-void structure and the long-term compressive strength of the foamed concrete mixtures.

9. REFERENCES

ACI Committee 523. 1975. Guide for Cellular Concretes Above 50 pcf, and for Aggregate Concretes Above 50 pcf with Compressive Strengths Less Than 2500 psi. *ACI Journal*, February 1975, Title no. 72-7, pp. 50-66.

ASTM 1990. Standard Test Method for Microscopical determination of Parameters of the Air-void System in Hardened Concrete. *ASTM Annual Book*, Vol 04.02.

Atzeni, C. Massidda, L. and Sanna, U. 1987. Effect of pore distribution on the strength of hardend cement pastes. *Pore structure and materials properties,* Proceedings of the first international RILEM congress, Vol 1, first ed. Chapman and Hall Ltd, London and New York, pp 195-202

Cahill, J. Dolan, J.C. and Inward, P.W. 1994, The identification and measurement of entrained air in concrete using image analysis. *Petrography of cementitious materials*, ASTM STP 1215, Sharon M. Dehayes and David Stark, Eds., American Society for Testing and Materials, Philadelphia, pp 111-124

Cebeci, Ö.Z. 1981. Pore structure of air-entrained hardened cement paste. *Cement and concrete research.* Volume 11, 1981. pp. 257-265

Chan, S.L. 1987. Applications of stereological and image analytical methods for concrete testing. *Pore structure and materials properties,* Proceedings of the first international RILEM congress, Vol 1, first ed. Chapman and Hall Ltd, London and New York, pp 111-118.

Chitharanjan, N. Ramakrishnan, V.S. and Ganesan, S. October 1978. A new production technology for the manufacture of cellular concrete. *Indian concrete Journal,* pp. 266-271.

Fagerlund, G. 1973. Strength and porosity of concrete. *Pore Structure* Proceedings of the International RILEM Symposium, Prague, 1973, Part 2, pp. D51-D73.

Gaafer, B.A. 1995. The effect of environmental curing condition on the gas and water permeability of concrete. *PhD thesis,* University of Leeds.

Gowripalan, N. Cabrera, J.G. Cusens, A.R. and Wainwright, P.J. February 1990. Effect of curing on Durability. *Concrete International.*pp.47-54.

Hoff, G.C. 1972. Porosity-Strength Considirations for Cellular Concrete. *Cement and Concrete Research.* Volume 2, 1972, pp. 91-100.

Kearsley, E.P. 1996. The use of foamcrete for affordable development in third world countries. *Proceedings conference on concrete in service of mankind (Congress on appropriate concrete technology)*, Dundee, UK, 1996. E & FN Spon, London, UK, pp. 233 - 243

Kearsley, E.P. The use of Foamcrete in Southern Africa, *Proceedings of the Third CANMET/.ACI International Conference on High Performance Concrete,* Kuala Lumpur, Malaysia, December 1997. American Concrete Institute, 1997, pp. 919 – 934.

Kearsley, E.P. 1999. The effect of high volumes of ungraded fly ash on the properties of foamed concrete, 1999, *PhD thesis,* University of Leeds.

Kreijger, P.C. 1967. Action of air-entraining agents and water-reducing agents and the difference between them. *Topic II: Physico-chemical principles of the action of the admixtures with various cements and concretes.* Proceedings of the international RILEM symposium on admixtures for mortar and concrete, Brussels, 1967, pp 33-37

Krüger, E 1998. Guides on the use of South African fly ash as a cement extender. *Guide I An Overview.* The South African Coal Ash Association (SACAA), 1998, p 5

Nasser, K.W. and Singh, B.P. 1995. A new method and apparatus for determining the air-void parameters in fresh and hardened concrete. *Adam Neville symposium on concrete technology,* 1995, pp. 239-256

Neopor System GMBH. Neopor lightweight Cellular-Concrete. *Product Information sheet,* Nürtingen, Germany

Neville, A.M. Brooks, J.J. 1987. *Concrete technology,* First ed. Longman Group, UK Limited. pp. 95,127, 291,357

Odler, I. and Rößler, M. 1985. Investigations on the Relationship between Porosity, Structure and Strength of Hydrated Portland Cement Pastes. II Effect of Porestructure and of degree of hydration. *Cement and Concrete Research.* Volume 15, pp 401-410.

Olorunsogo, F.T. 1990. Effect of particle size distribution of ground granulated blast furnace slag on some properties of slag cement mortar. *PhD thesis,* University of Leeds.

Optimate 5.21 Utilities menu.

PrEN 480-II:1993, Admixtures for concrete, mortar and grout – Test methods - Determination of air void characteristics in hardened concrete. *European standard.*

Rößler, M. and Odler, I. 1985. Investigations on the Relationship between Porosity, Structure and Strength of Hydrated Portland Cement Pastes. I Effect of Porosity. *Cement and Concrete Research.* Volume 15, pp 320-330.

Taylor, W.H. February 1974. The production, properties and uses of foamed concrete. *Precast Concrete.* pp. 83-96

Uchikawa, H. Uchida, S. and Hanehara, S. April/June 1991. Measuring method of pore structure in hardened cement paste, mortar and concrete. *Il Cemento.* Volume 88, no 2: pp 67-90

Van As, S.C. and Joubert, H.S. 1996. *Applied Statistics For Engineers.* Department of Civil Engineering University of Pretoria. Edition 1996. pp 6-10 – 6-12

Vine-Lott, K. November 1985. Production of 'foam' concrete by microcomputer. *Concrete.* pp. 12-14

Visagie, M. 1997. The effect of microstructure on the properties of foamed concrete. *Proceedings of the young concrete engineers' and technologists conference*, Midrand, SA, pp. 101-109

Wainwright, P.J. and Olorunsogo, F.T. 1999. Effects of PSD of GGBS on some durability properties of slag cement mortars. *Journal of the South African Institution of Civil Engineering.* Volume 41, Number 1 First Quarter 1999. pp 9-17

Wilk, W. and Dobrolubov, G. 1984. Microscopic Quality Control of Concrete during Construction. *Proceedings of the Sixth International Conference on the Microscopic*, Albuquerque, 1984, pp. 330-343.

Willis, T.F. 1949. Discussion of "The air requirement of frost-resistant concrete" by T.C. Powers. *Proceedings Highway Research Board.* Volume 29, Bulletin No. 33, Portland Cement Assn. pp. 203-211

APPENDIX A

AIR-VOID SIZE DISTRIBUTION OF MIXES

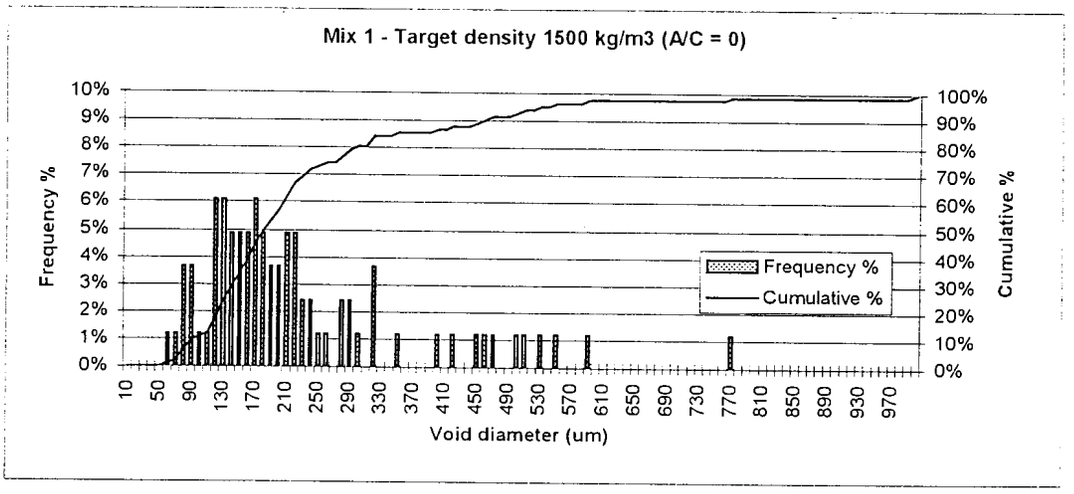
Mix 1 - Target density 1500 kg/m3 (A/C = 0)
Frequency %
Cumulative %
Void diameter (um)
Frequency %
Cumulative %

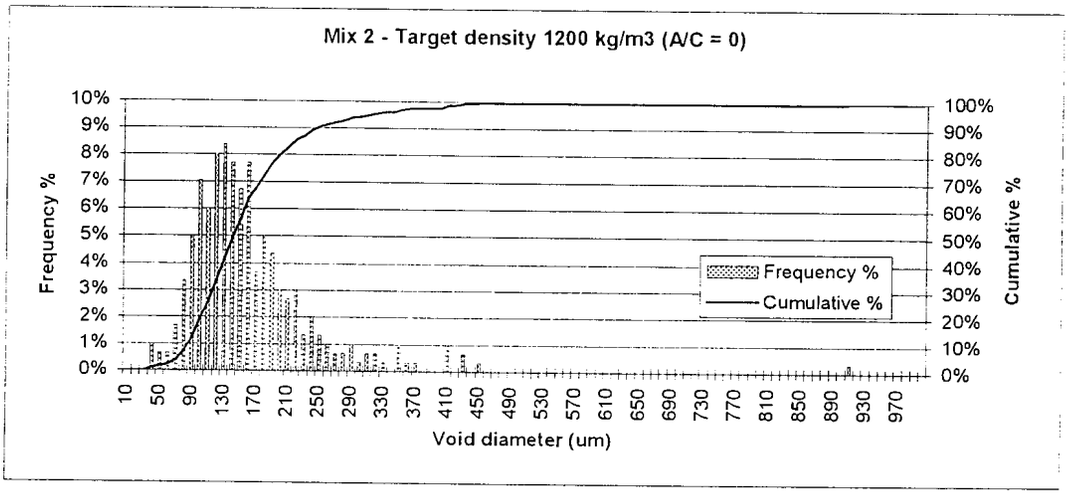
Mix 2 - Target density 1200 kg/m3 (A/C = 0)
Frequency %
Cumulative %
Void diameter (um)
Frequency %
Cumulative %

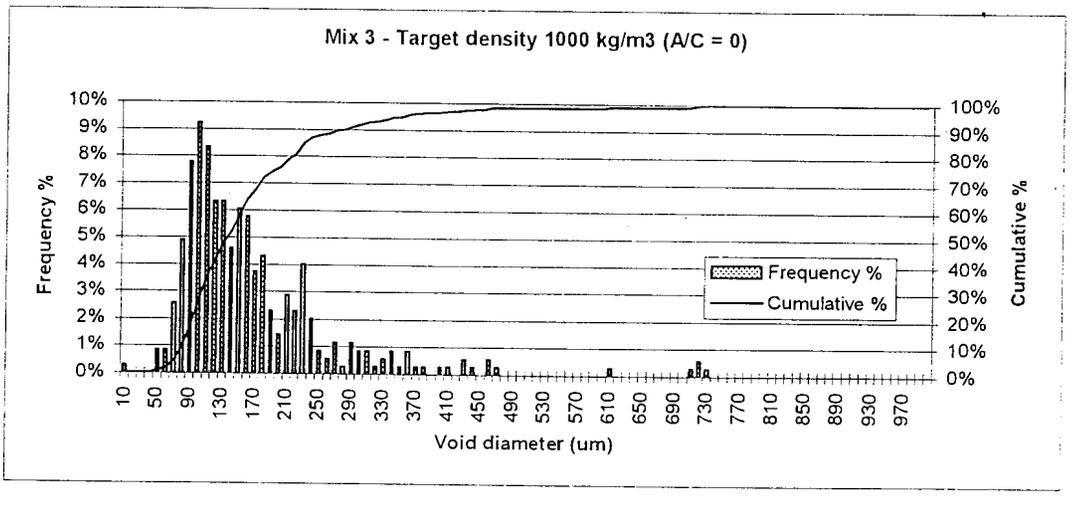
Mix 3 - Target density 1000 kg/m3 (A/C = 0)
Frequency %
Cumulative %
Void diameter (um)
Frequency %
Cumulative %

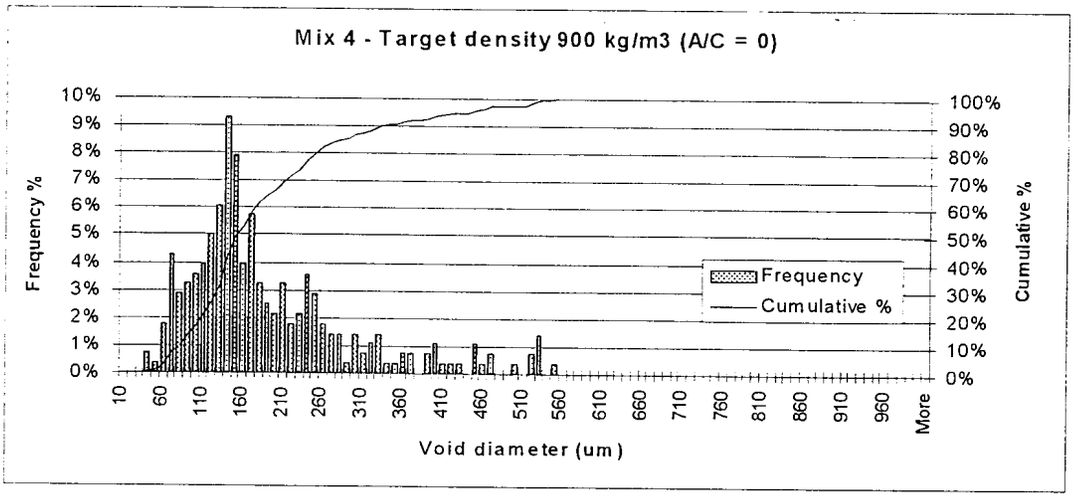
Mix 4 - Target density 900 kg/m3 (A/C = 0)
Frequency %
Cumulative %
Frequency
Cumulative %
Void diameter (um)
10
60
110
160
210
260
310
360
410
460
510
560
610
660
710
760
810
860
910
960
More

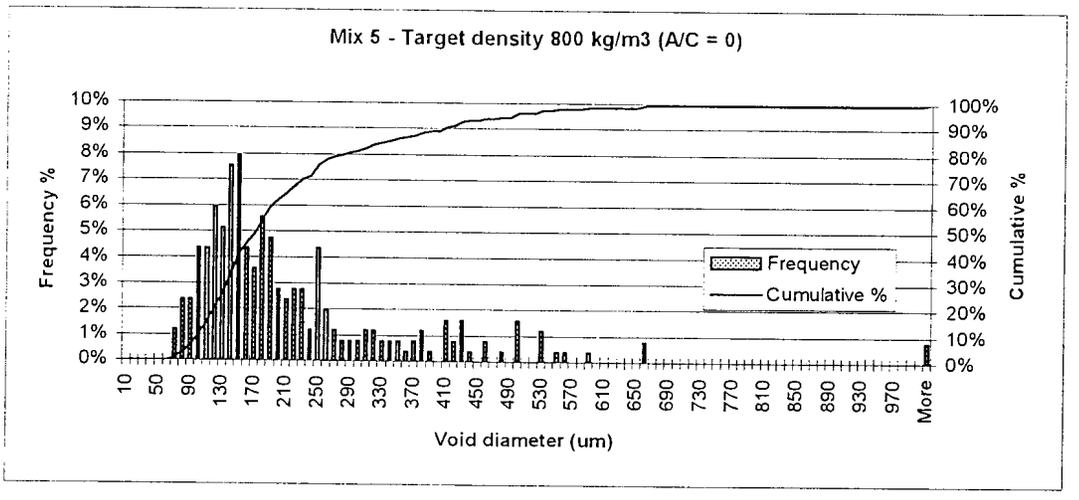
Mix 5 - Target density 800 kg/m3 (A/C = 0)
Frequency %
Cumulative %
Frequency
Cumulative %
Void diameter (um)
10
50
90
130
170
210
250
290
330
370
410
450
490
530
570
610
650
690
730
770
810
850
890
930
970
More

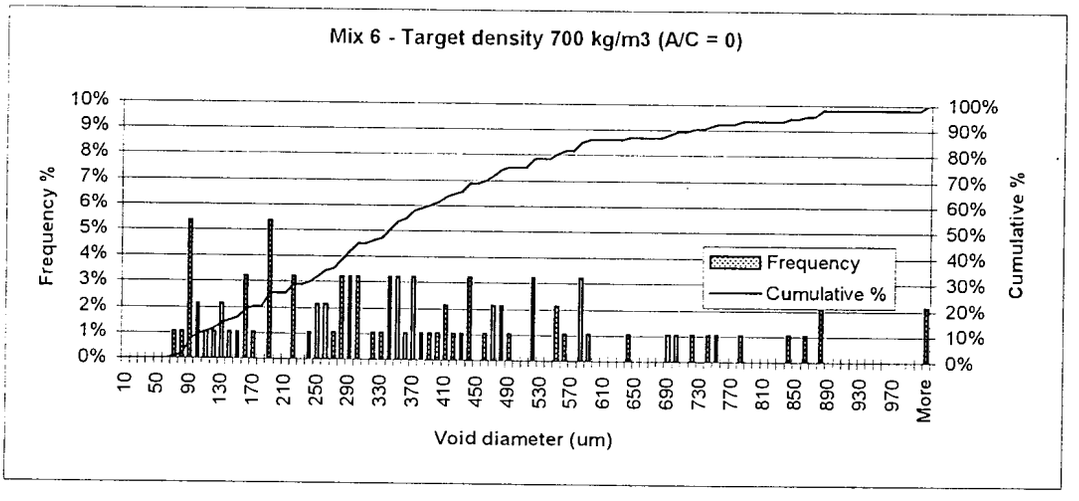
Mix 6 - Target density 700 kg/m3 (A/C = 0)
Frequency %
Cumulative %
Frequency
Cumulative %
Void diameter (um)
10
50
90
130
170
210
250
290
330
370
410
450
490
530
570
610
650
690
730
770
810
850
890
930
970
More

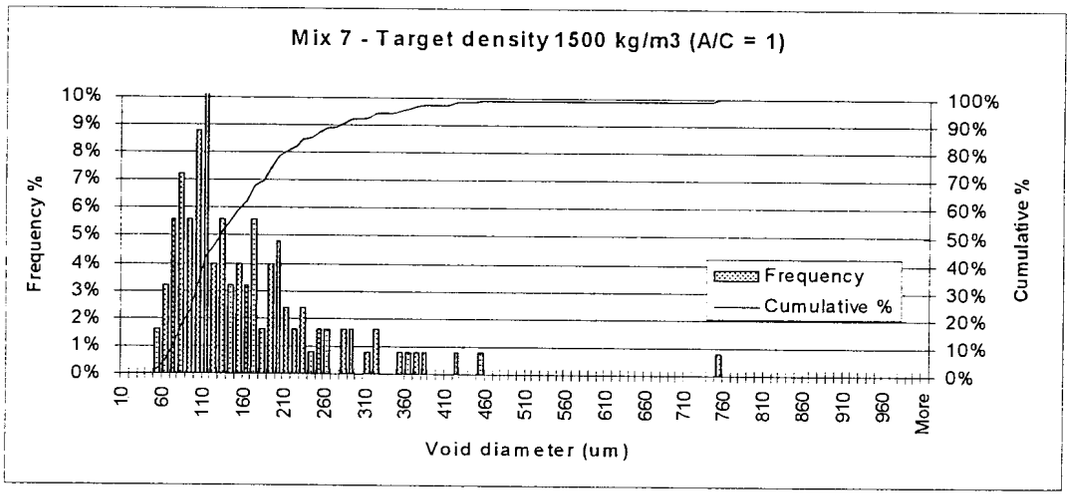
Mix 7 - Target density 1500 kg/m3 (A/C = 1)
Frequency %
Cumulative %
Frequency
Cumulative %
Void diameter (um)
10
60
110
160
210
260
310
360
410
460
510
560
610
660
710
760
810
860
910
960
More

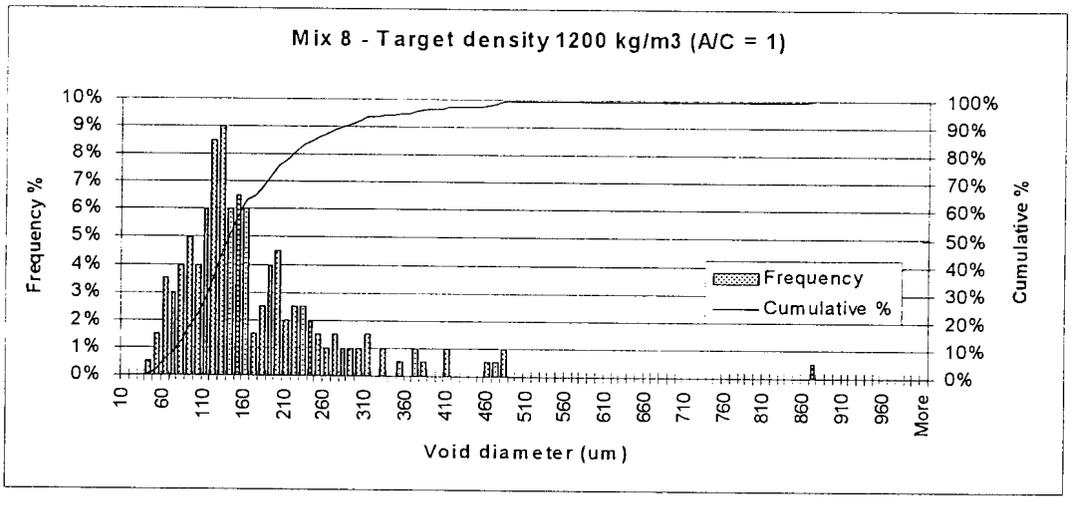
Mix 8 - Target density 1200 kg/m3 (A/C = 1)
Frequency %
Cumulative %
Frequency
Cumulative %
Void diameter (um)
10
60
110
160
210
260
310
360
410
460
510
560
610
660
710
760
810
860
910
960
More

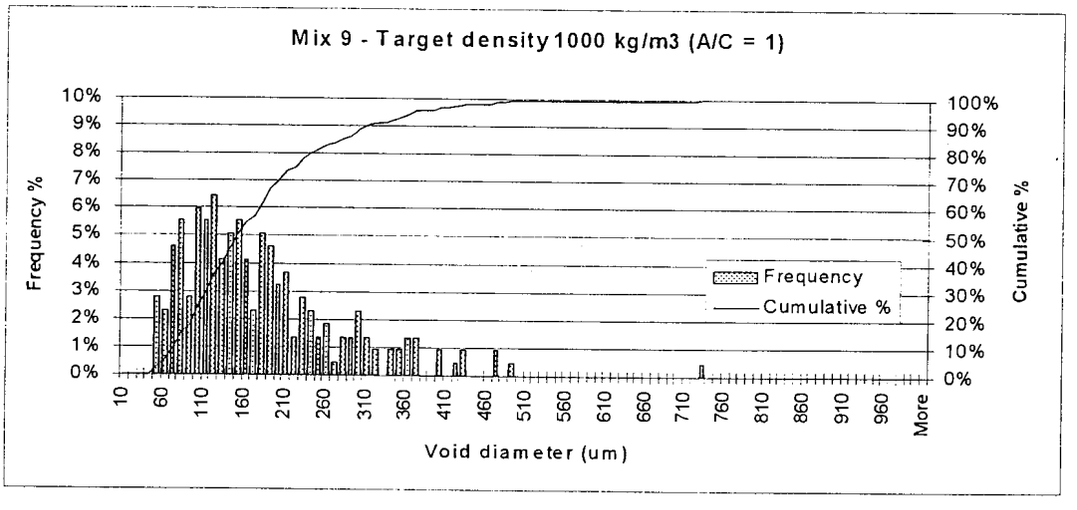
Mix 9 - Target density 1000 kg/m3 (A/C = 1)
Frequency %
Cumulative %
Frequency
Cumulative %
Void diameter (um)
10
60
110
160
210
260
310
360
410
460
510
560
610
660
710
760
810
860
910
960
More

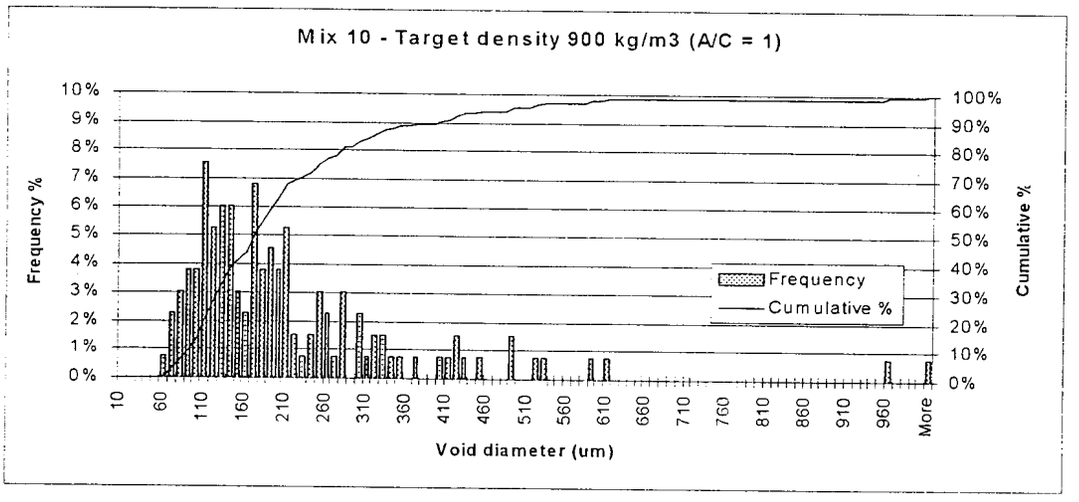
Mix 10 - Target density 900 kg/m3 (A/C = 1)
Frequency %
Cumulative %
Frequency
Cumulative %
Void diameter (um)
10
60
110
160
210
260
310
360
410
460
510
560
610
660
710
760
810
860
910
960
More

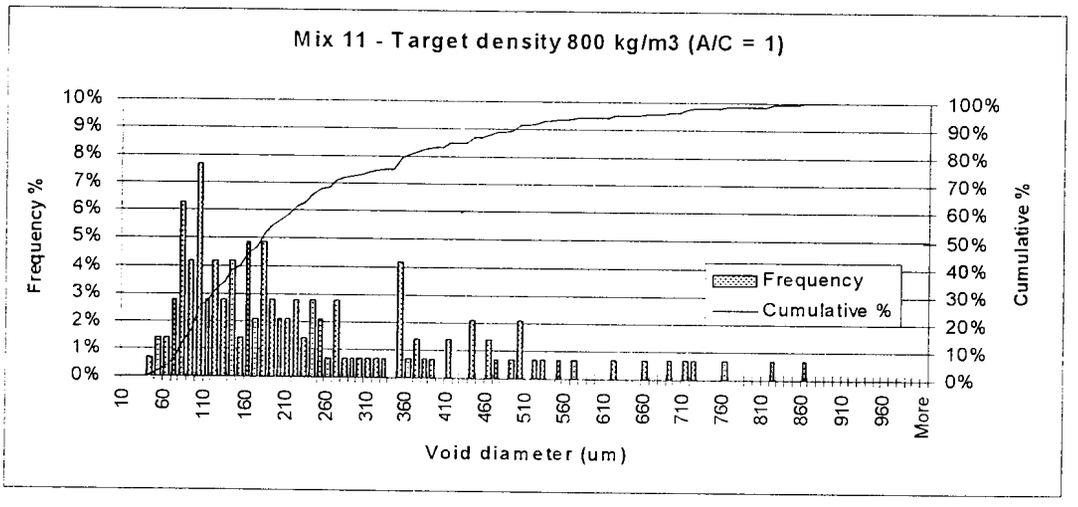
Mix 11 - Target density 800 kg/m3 (A/C = 1)
Frequency %
Cumulative %
Frequency
Cumulative %
Void diameter (um)
10
60
110
160
210
260
310
360
410
460
510
560
610
660
710
760
810
860
910
960
More

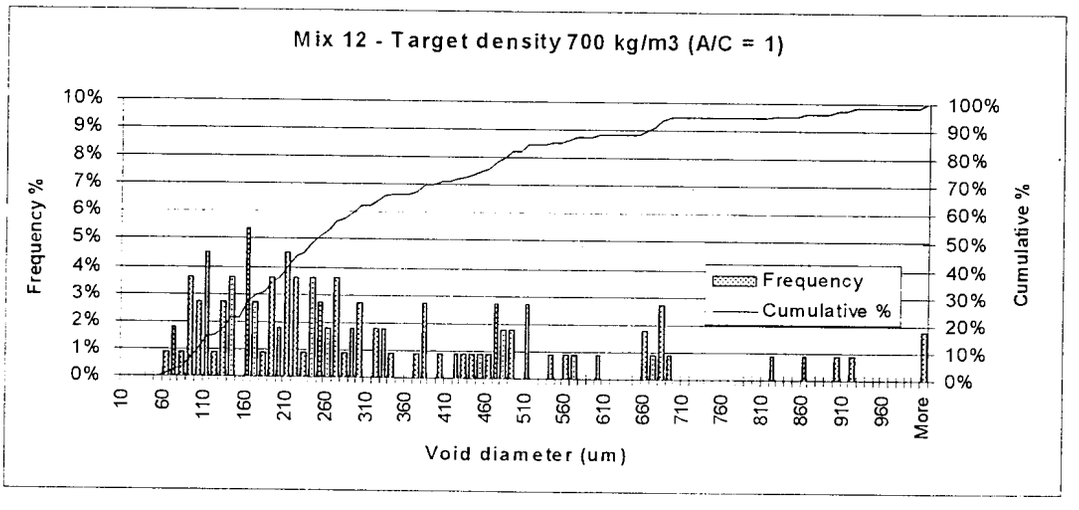
Mix 12 - Target density 700 kg/m3 (A/C = 1)
Frequency %
Cumulative %
Frequency
Cumulative %
Void diameter (um)
10
60
110
160
210
260
310
360
410
460
510
560
610
660
710
760
810
860
910
960
More

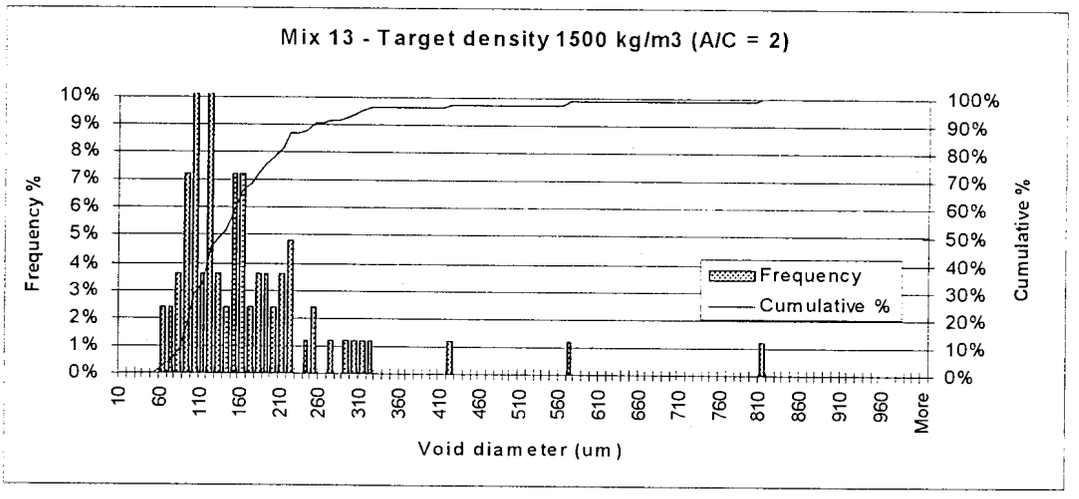
Mix 13 - Target density 1500 kg/m3 (A/C = 2)
Frequency %
Cumulative %
Frequency
Cumulative %
Void diameter (um)
10
60
110
160
210
260
310
360
410
460
510
560
610
660
710
760
810
860
910
960
More

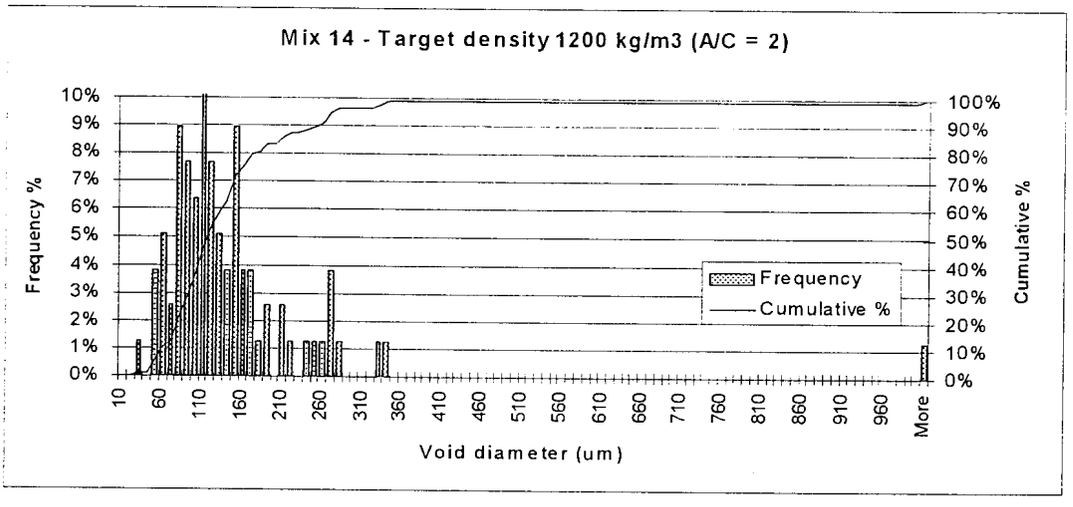
Mix 14 - Target density 1200 kg/m3 (A/C = 2)
Frequency %
Cumulative %
Frequency
Cumulative %
Void diameter (um)
10
60
110
160
210
260
310
360
410
460
510
560
610
660
710
760
810
860
910
960
More

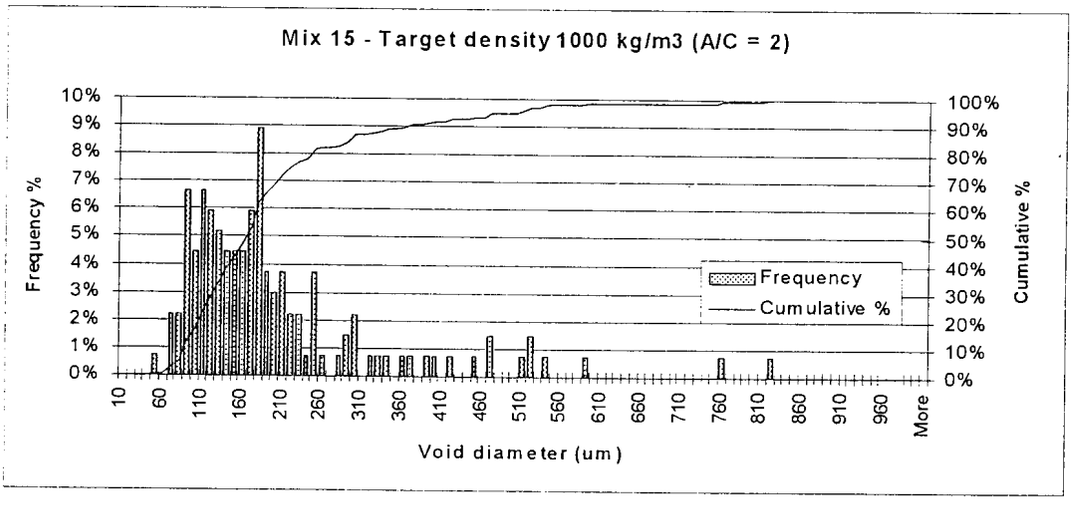
Mix 15 - Target density 1000 kg/m3 (A/C = 2)
Frequency %
Cumulative %
Frequency
Cumulative %
Void diameter (um)
10
60
110
160
210
260
310
360
410
460
510
560
610
660
710
760
810
860
910
960
More

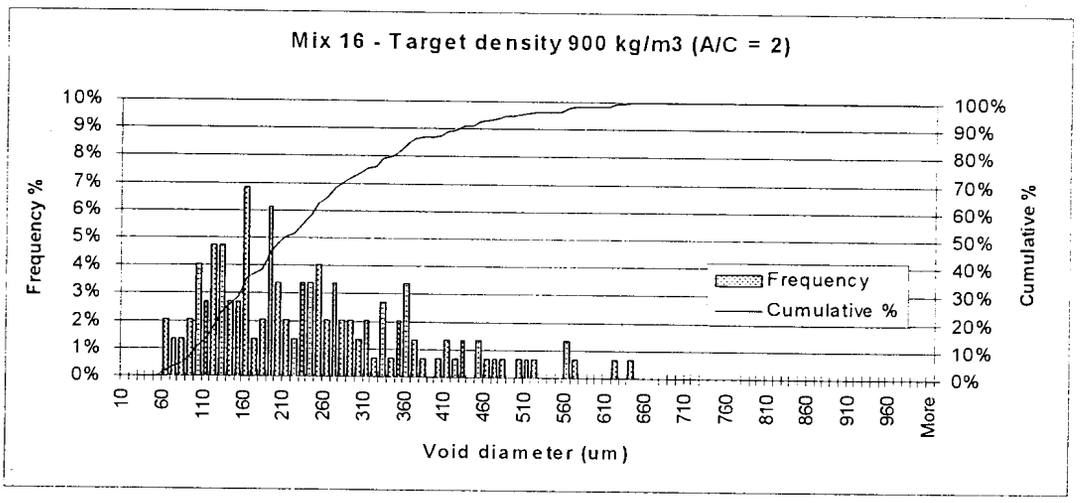
Mix 16 - Target density 900 kg/m3 (A/C = 2)
Frequency %
Cumulative %
Frequency
Cumulative %
Void diameter (um)
10
60
110
160
210
260
310
360
410
460
510
560
610
660
710
760
810
860
910
960
More

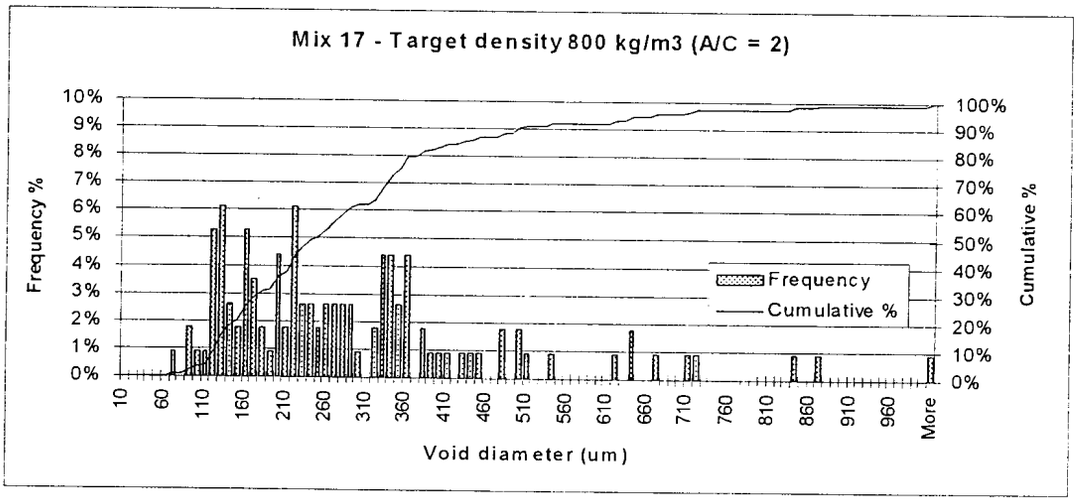
Mix 17 - Target density 800 kg/m3 (A/C = 2)
Frequency %
Cumulative %
Frequency
Cumulative %
Void diameter (um)
10
60
110
160
210
260
310
360
410
460
510
560
610
660
710
760
810
860
910
960
More

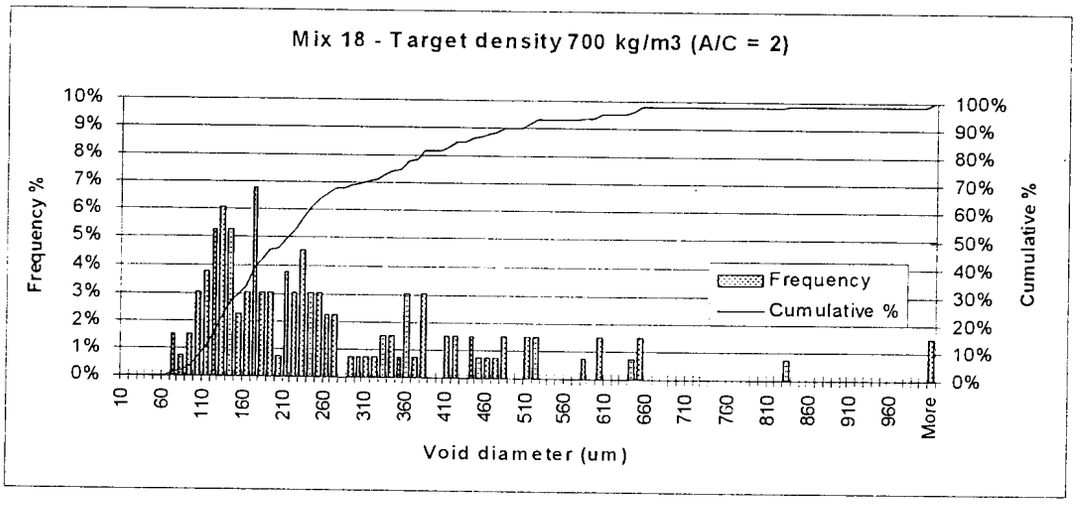
Mix 18 - Target density 700 kg/m3 (A/C = 2)
Frequency %
Cumulative %
Frequency
Cumulative %
Void diameter (um)
10
60
110
160
210
260
310
360
410
460
510
560
610
660
710
760
810
860
910
960
More

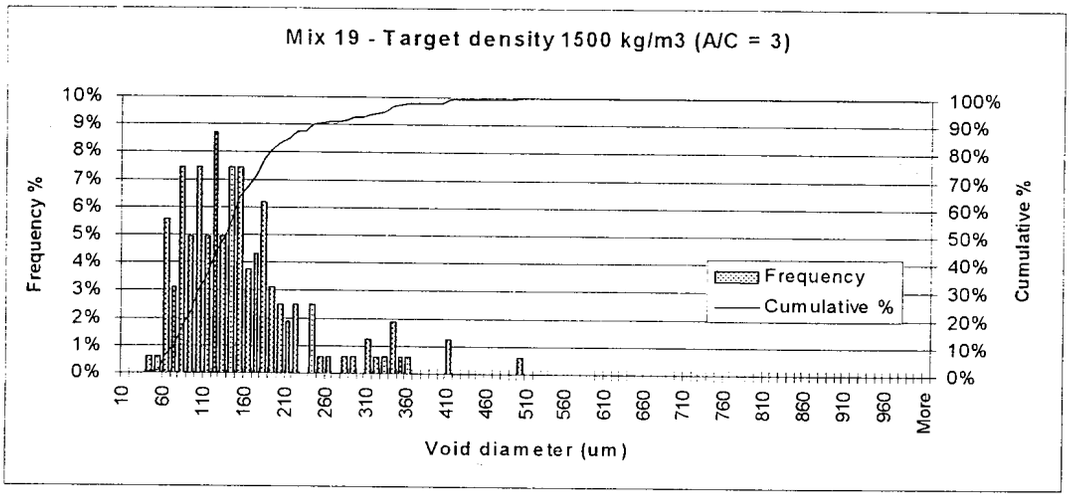
Mix 19 - Target density 1500 kg/m3 (A/C = 3)
Frequency %
Cumulative %
Frequency
Cumulative %
Void diameter (um)
10
60
110
160
210
260
310
360
410
460
510
560
610
660
710
760
810
860
910
960
More

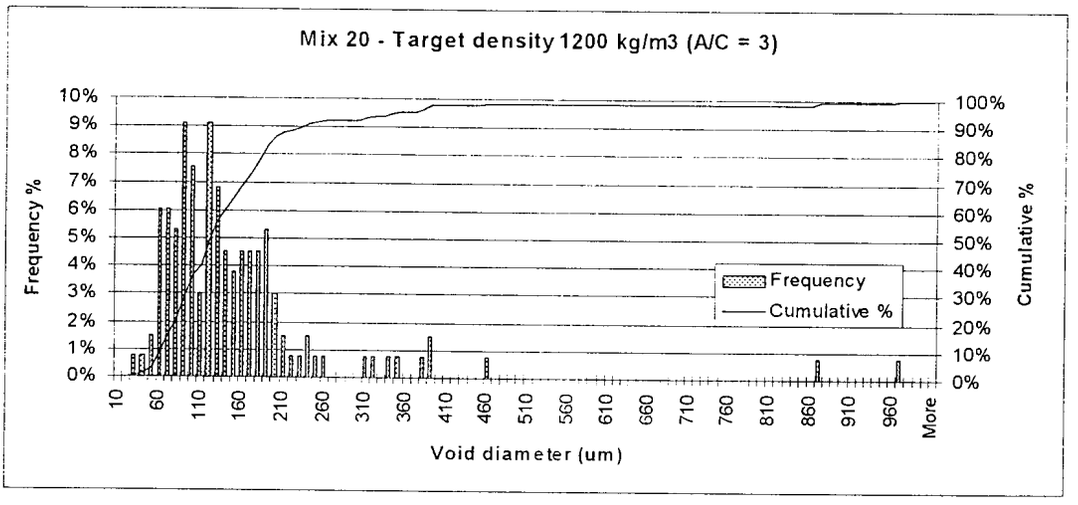
Mix 20 - Target density 1200 kg/m3 (A/C = 3)
Frequency %
Cumulative %
Frequency
Cumulative %
Void diameter (um)
10
60
110
160
210
260
310
360
410
460
510
560
610
660
710
760
810
860
910
960
More

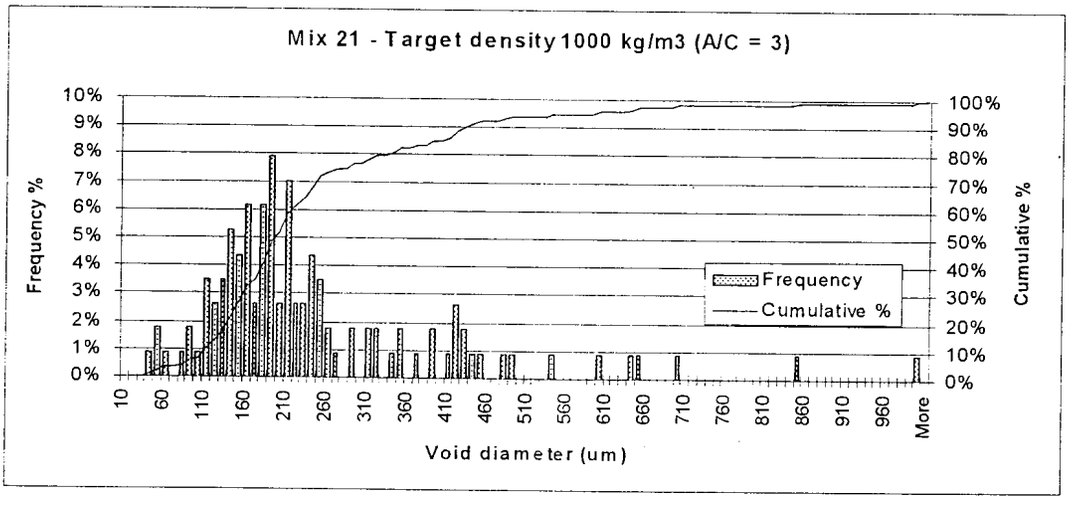
Mix 21 - Target density 1000 kg/m3 (A/C = 3)
Frequency %
Cumulative %
Frequency
Cumulative %
Void diameter (um)
10
60
110
160
210
260
310
360
410
460
510
560
610
660
710
760
810
860
910
960
More

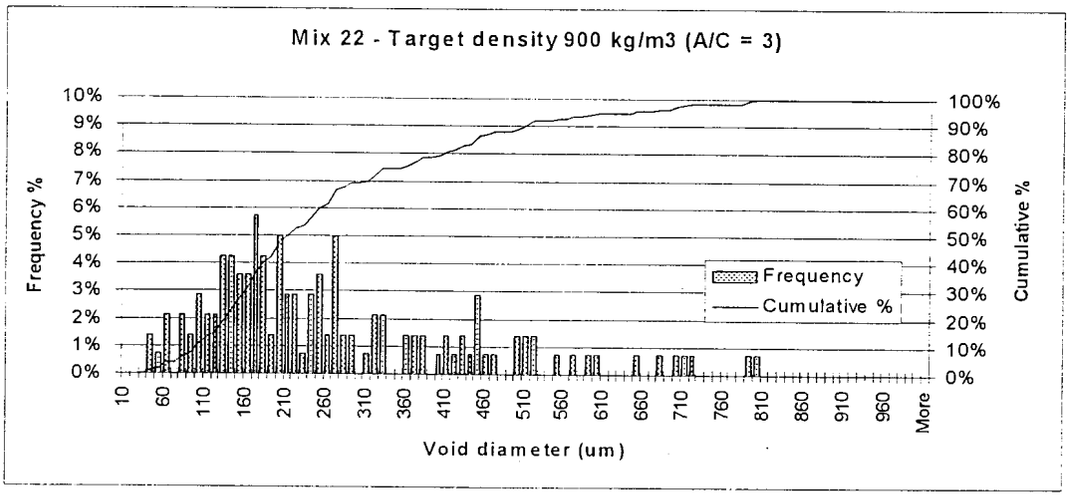
Mix 22 - Target density 900 kg/m3 (A/C = 3)
Frequency %
Cumulative %
Frequency
Cumulative %
Void diameter (um)
10
60
110
160
210
260
310
360
410
460
510
560
610
660
710
760
810
860
910
960
More

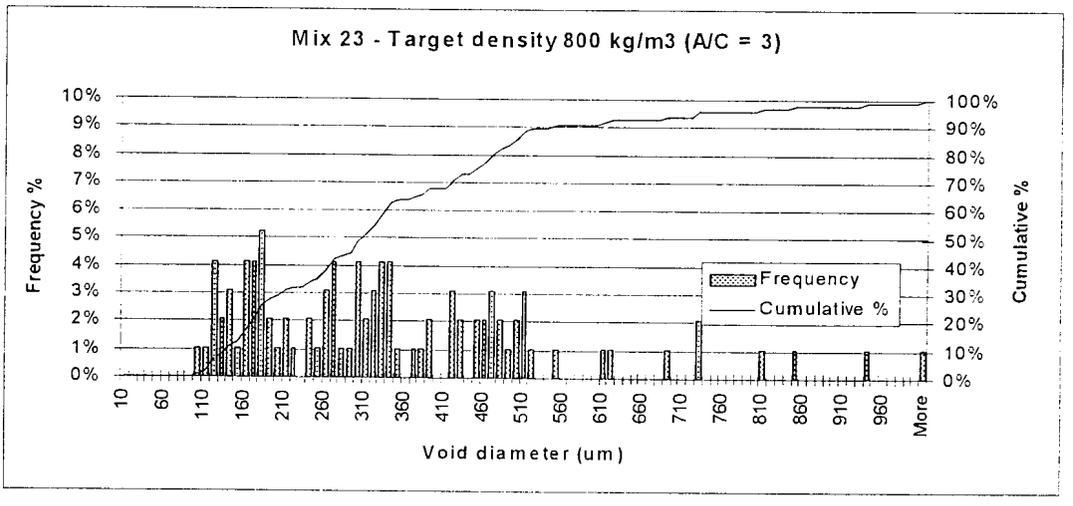
Mix 23 - Target density 800 kg/m3 (A/C = 3)
Frequency %
Cumulative %
Frequency
Cumulative %
Void diameter (um)
10
60
110
160
210
260
310
360
410
460
510
560
610
660
710
760
810
860
910
960
More

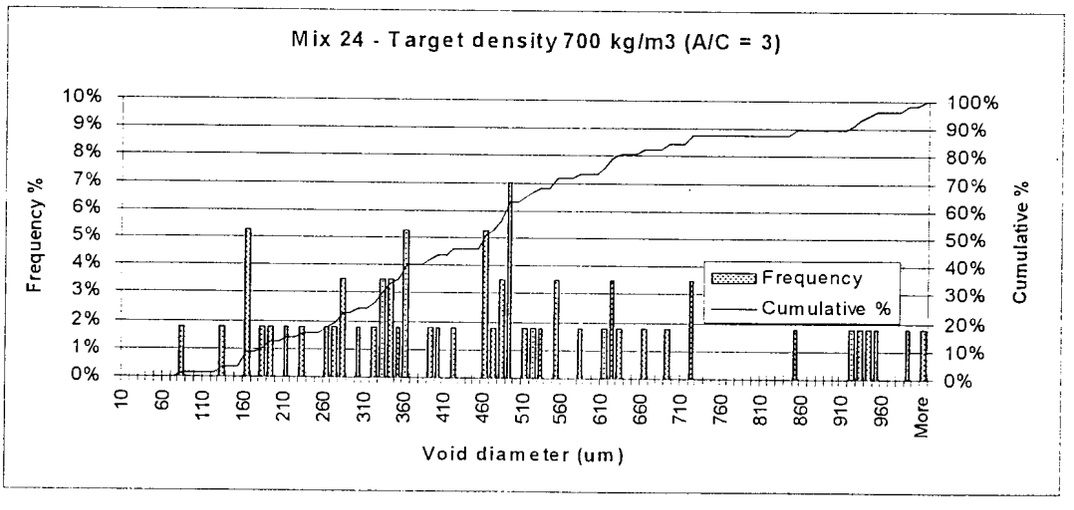
Mix 24 - Target density 700 kg/m3 (A/C = 3)
Frequency %
Cumulative %
Frequency
Cumulative %
Void diameter (um)
10
60
110
160
210
260
310
360
410
460
510
560
610
660
710
760
810
860
910
960
More

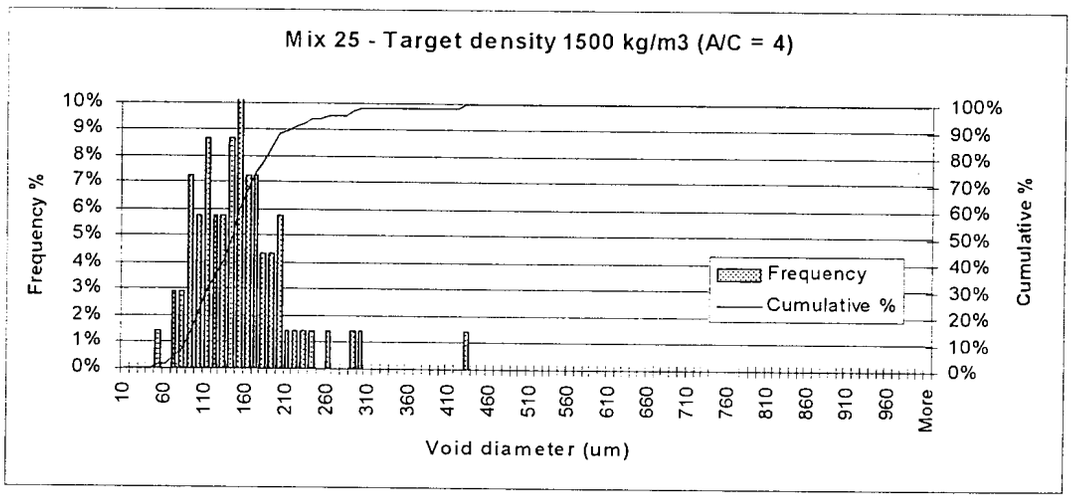
Mix 25 - Target density 1500 kg/m3 (A/C = 4)
Frequency %
Cumulative %
Frequency
Cumulative %
Void diameter (um)
10
60
110
160
210
260
310
360
410
460
510
560
610
660
710
760
810
860
910
960
More

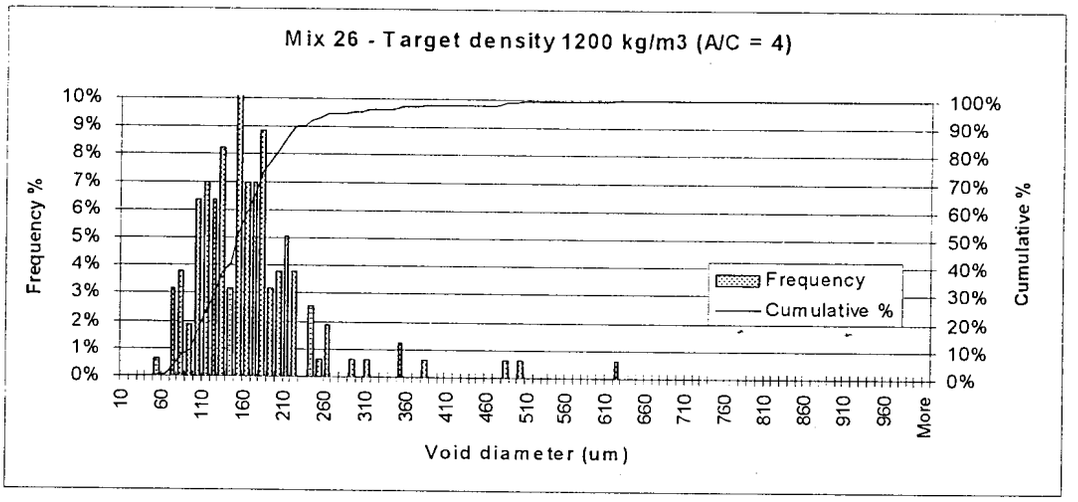
Mix 26 - Target density 1200 kg/m3 (A/C = 4)
Frequency %
Cumulative %
Frequency
Cumulative %
Void diameter (um)
10
60
110
160
210
260
310
360
410
460
510
560
610
660
710
760
810
860
910
960
More

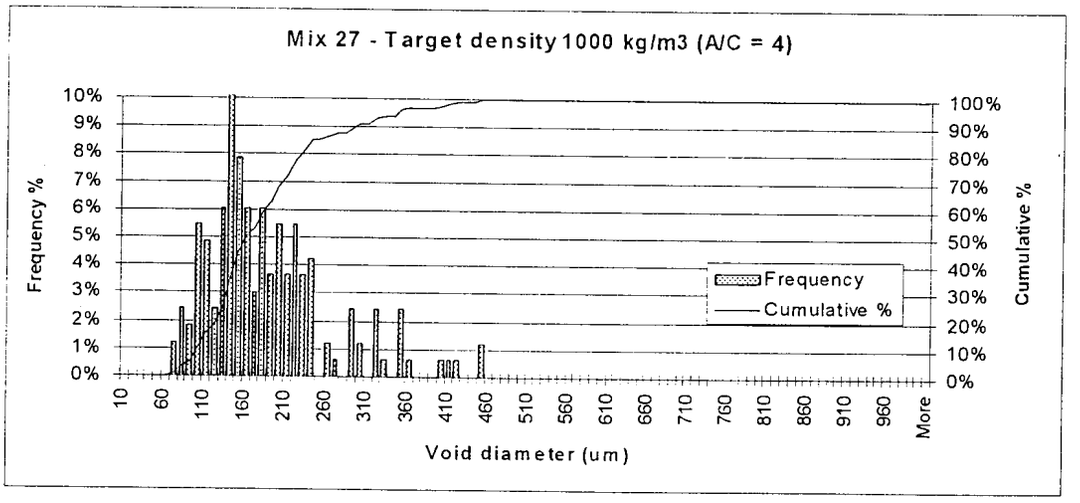
Mix 27 - Target density 1000 kg/m3 (A/C = 4)
Frequency %
Cumulative %
Frequency
Cumulative %
Void diameter (um)
10
60
110
160
210
260
310
360
410
460
510
560
610
660
710
760
810
860
910
960
More

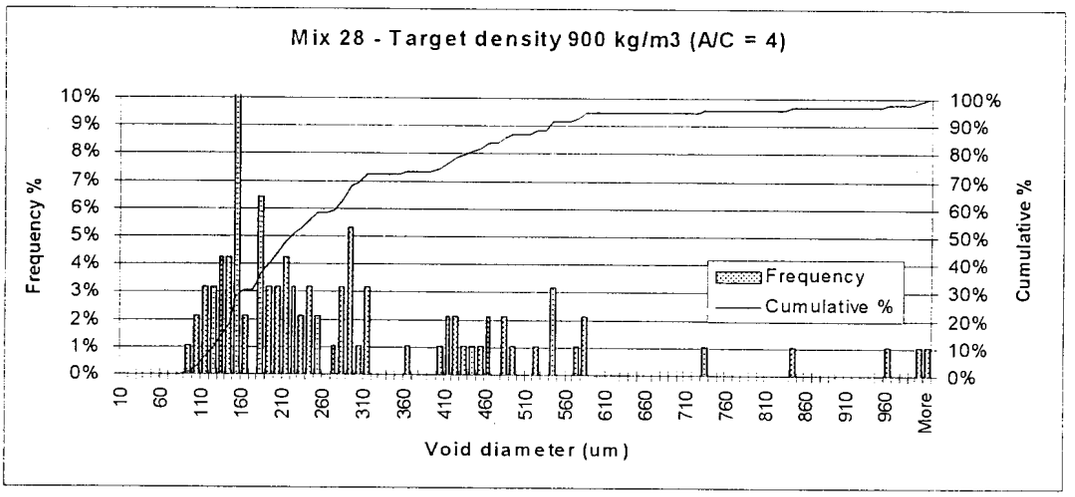
Mix 28 - Target density 900 kg/m3 (A/C = 4)
Frequency %
Cumulative %
Frequency
Cumulative %
Void diameter (um)
10
60
110
160
210
260
310
360
410
460
510
560
610
660
710
760
810
860
910
960
More

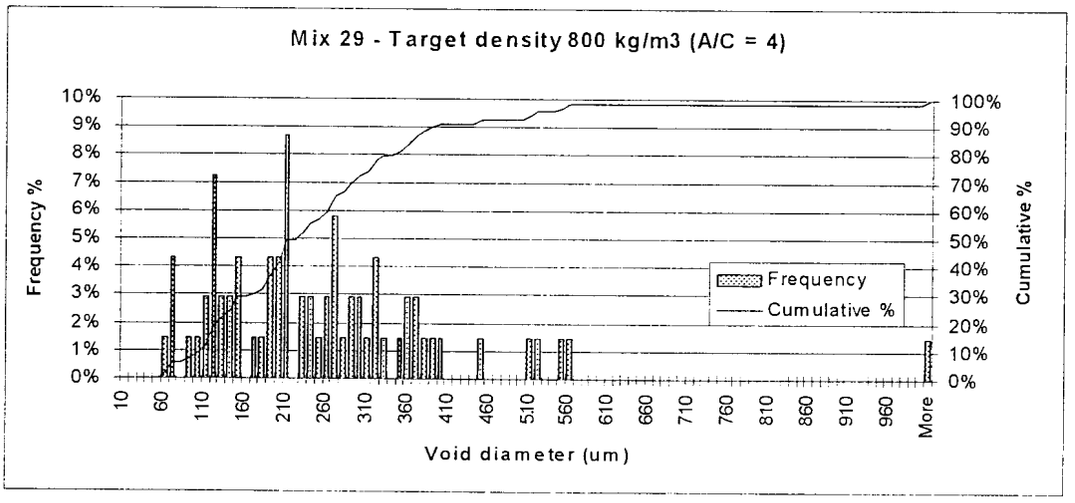
Mix 29 - Target density 800 kg/m3 (A/C = 4)
Frequency %
Cumulative %
Frequency
Cumulative %
Void diameter (um)
10
60
110
160
210
260
310
360
410
460
510
560
610
660
710
760
810
860
910
960
More

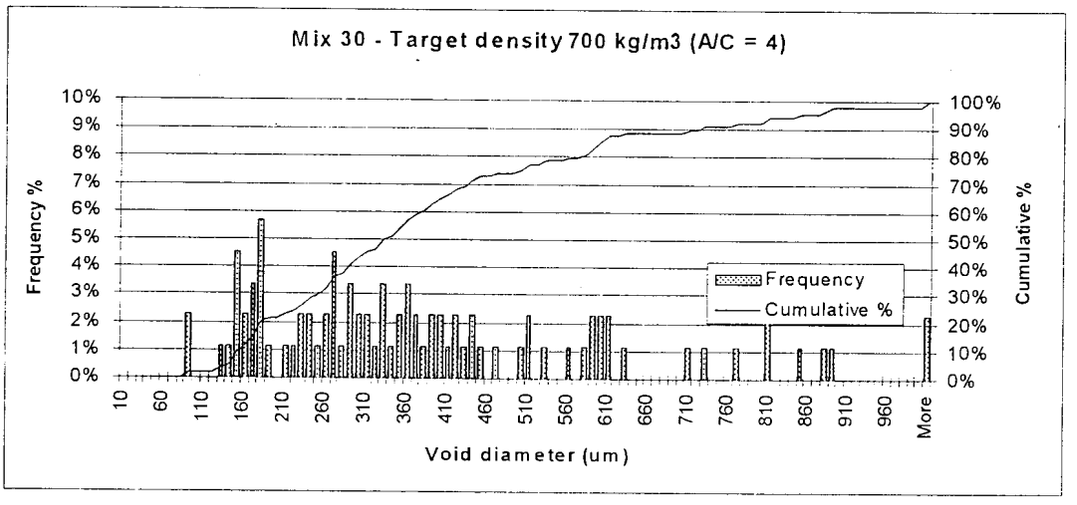
Mix 30 - Target density 700 kg/m3 (A/C = 4)
Frequency %
Cumulative %
Frequency
Cumulative %
Void diameter (um)
10
60
110
160
210
260
310
360
410
460
510
560
610
660
710
760
810
860
910
960
More

APPENDIX B

EXPONENTIAL FIT FOR CUMULATIVE PERCENTAGE OVERSIZE AIR-VOID DIAMETERS OF MIXTURES

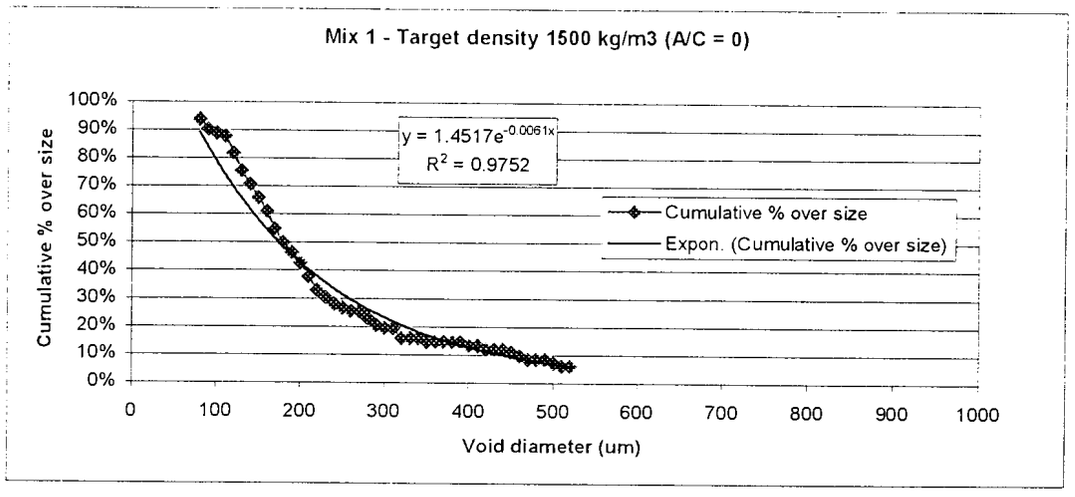

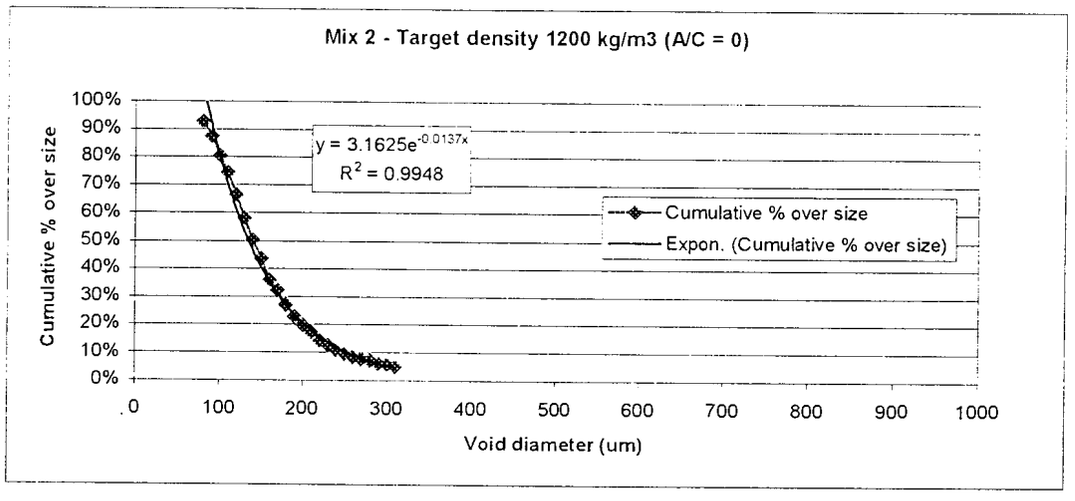

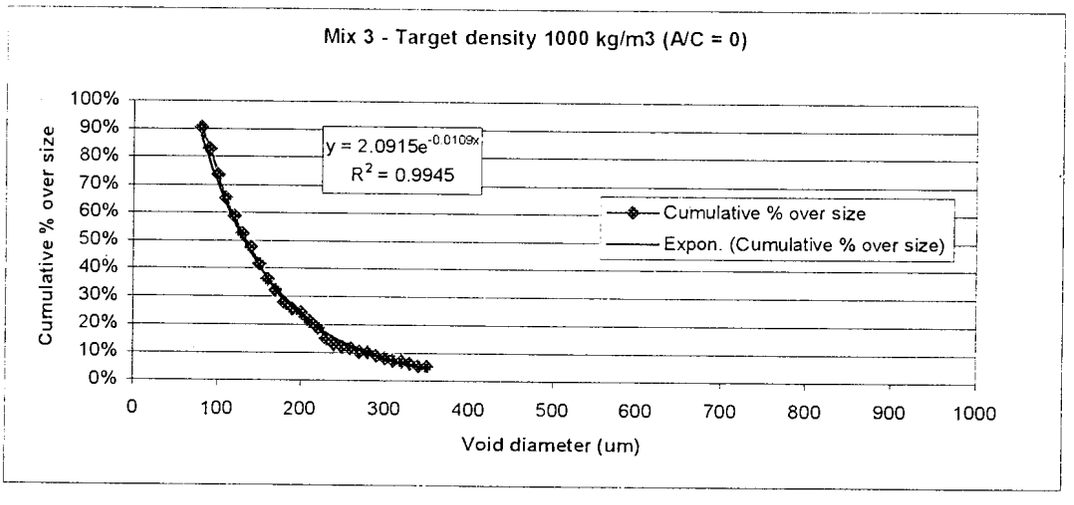

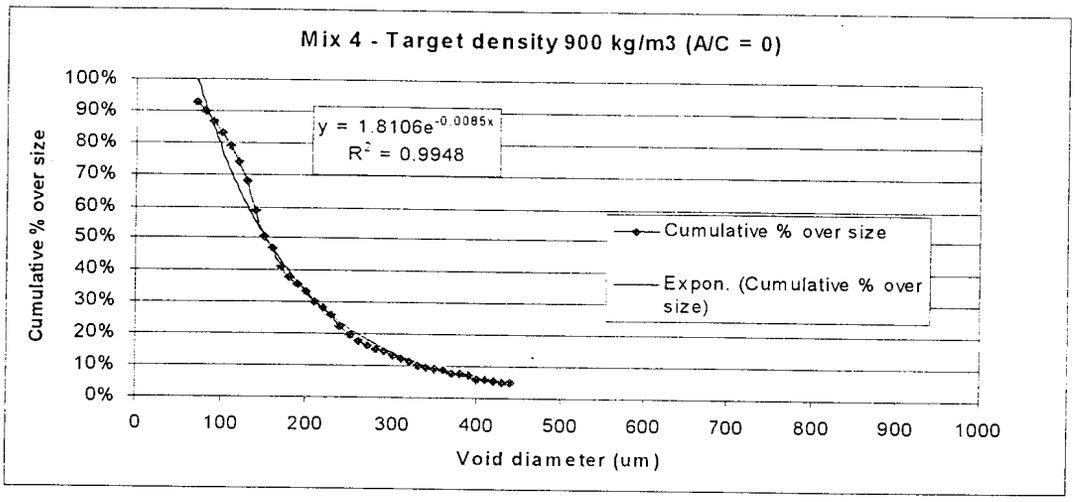
Mix 4 - Target density 900 kg/m3 (A/C = 0)
y = 1.8106e-0.0085x
R2 = 0.9948
Cumulative % over size
Expon. (Cumulative % over size)
Cumulative % over size
100%
90%
80%
70%
60%
50%
40%
30%
20%
10%
0%
0
100
200
300
400
500
600
700
800
900
1000
Void diameter (um)

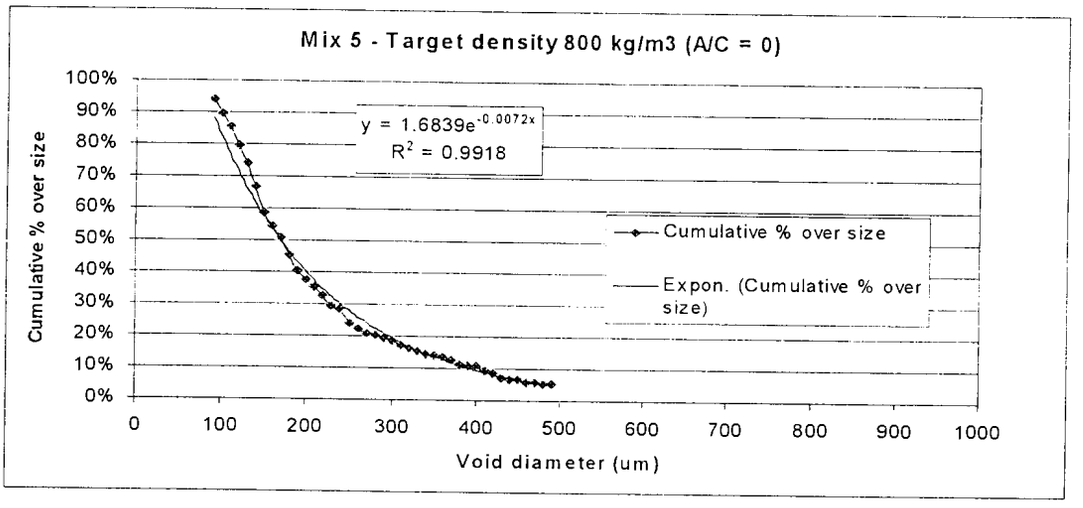
Mix 5 - Target density 800 kg/m3 (A/C = 0)
y = 1.6839e-0.0072x
R2 = 0.9918
Cumulative % over size
Expon. (Cumulative % over size)
Cumulative % over size
100%
90%
80%
70%
60%
50%
40%
30%
20%
10%
0%
0
100
200
300
400
500
600
700
800
900
1000
Void diameter (um)

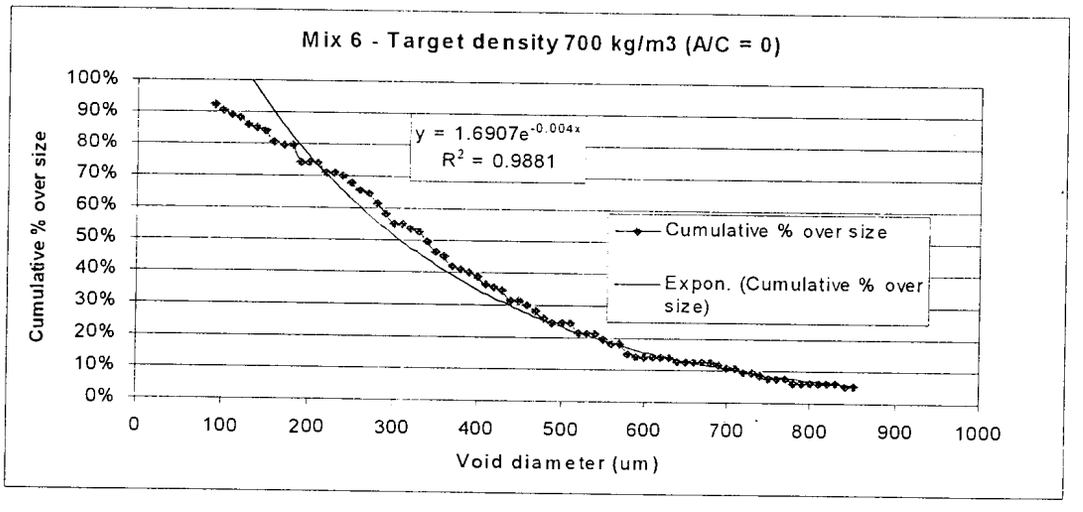
Mix 6 - Target density 700 kg/m3 (A/C = 0)
y = 1.6907e-0.004x
R2 = 0.9881
Cumulative % over size
Expon. (Cumulative % over size)
Cumulative % over size
100%
90%
80%
70%
60%
50%
40%
30%
20%
10%
0%
0
100
200
300
400
500
600
700
800
900
1000
Void diameter (um)

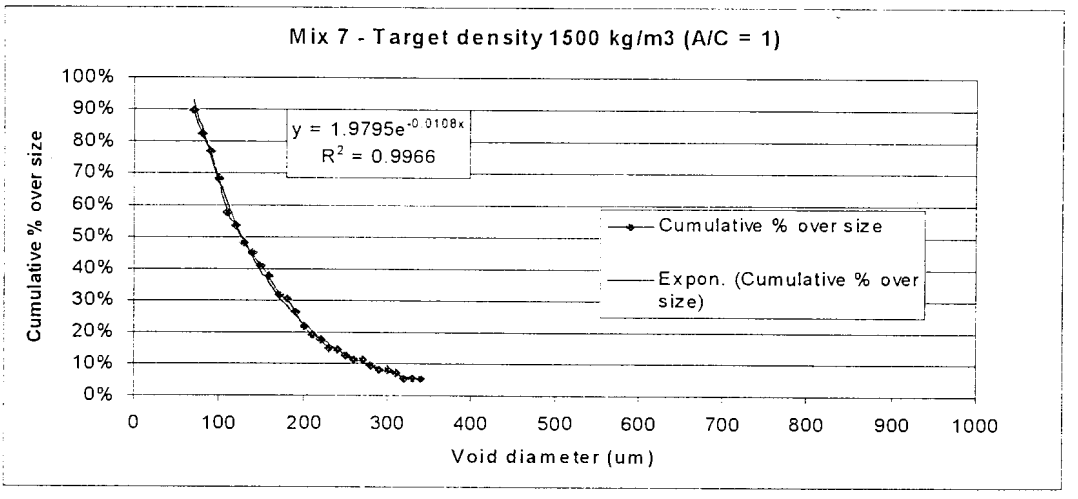

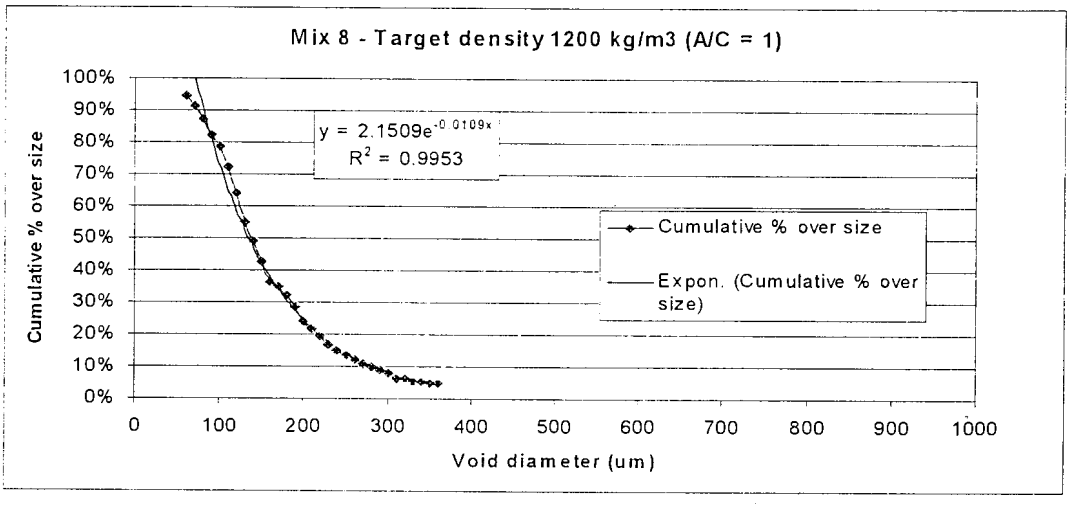

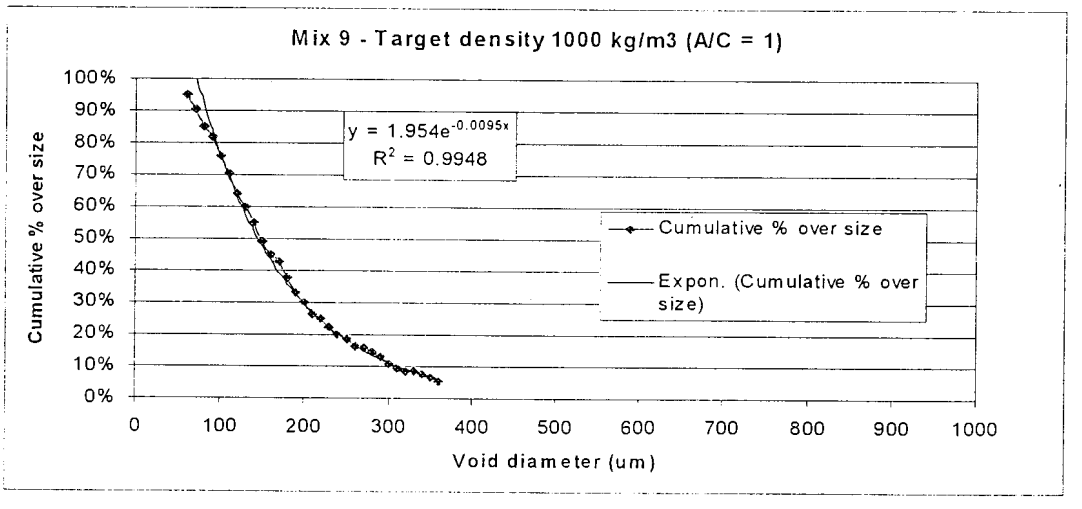

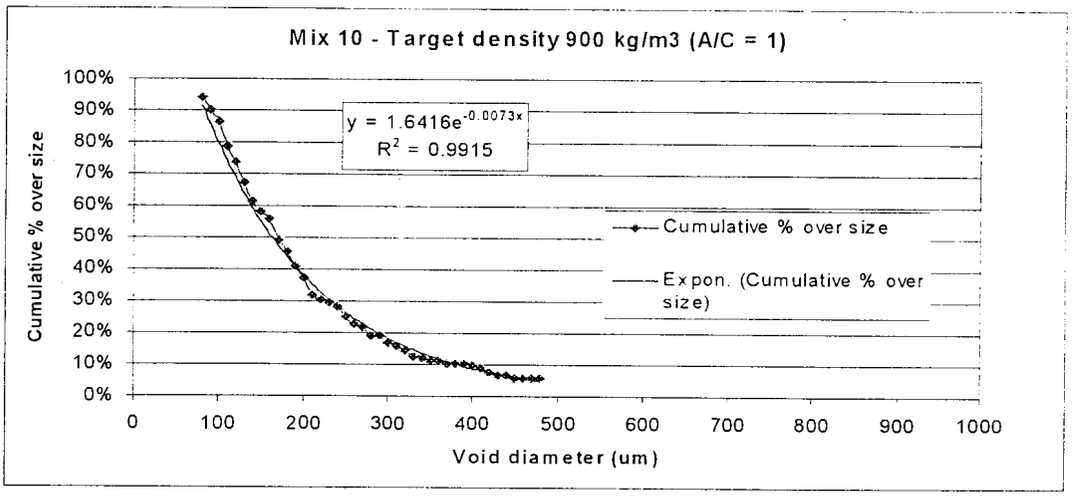
Mix 10 - Target density 900 kg/m3 (A/C = 1)
y = 1.6416e-0.0073x
R2 = 0.9915
Cumulative % over size
Expon. (Cumulative % over size)
Cumulative % over size
Void diameter (um)
100%
90%
80%
70%
60%
50%
40%
30%
20%
10%
0%
0
100
200
300
400
500
600
700
800
900
1000

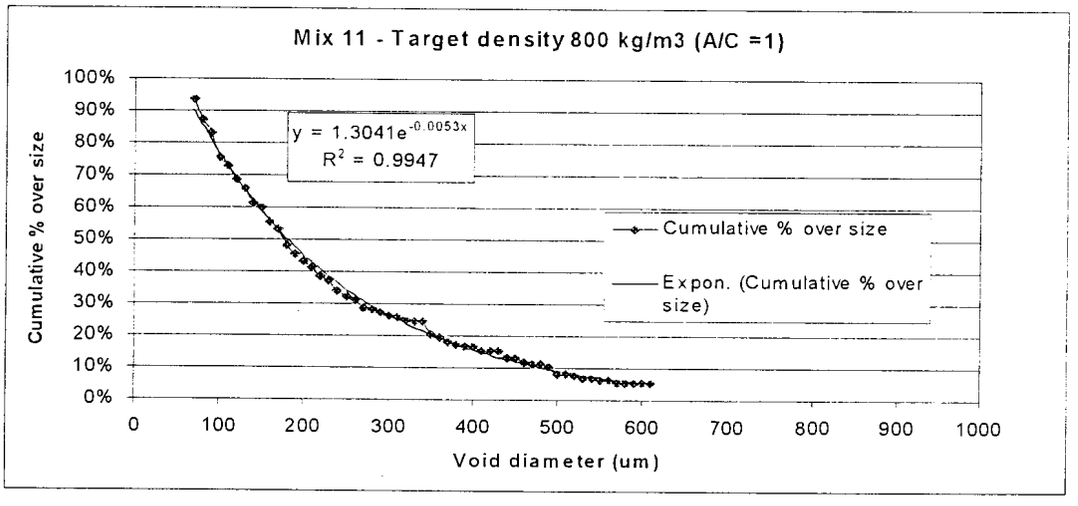
Mix 11 - Target density 800 kg/m3 (A/C =1)
y = 1.3041e-0.0053x
R2 = 0.9947
Cumulative % over size
Expon. (Cumulative % over size)
Cumulative % over size
Void diameter (um)
100%
90%
80%
70%
60%
50%
40%
30%
20%
10%
0%
0
100
200
300
400
500
600
700
800
900
1000

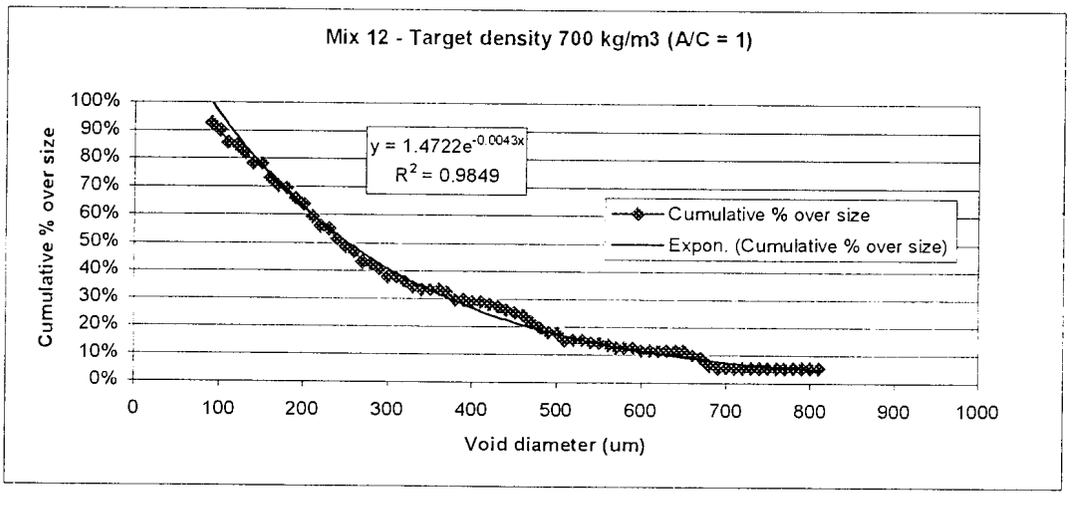
Mix 12 - Target density 700 kg/m3 (A/C = 1)
y = 1.4722e-0.0043x
R2 = 0.9849
Cumulative % over size
Expon. (Cumulative % over size)
Cumulative % over size
Void diameter (um)
100%
90%
80%
70%
60%
50%
40%
30%
20%
10%
0%
0
100
200
300
400
500
600
700
800
900
1000

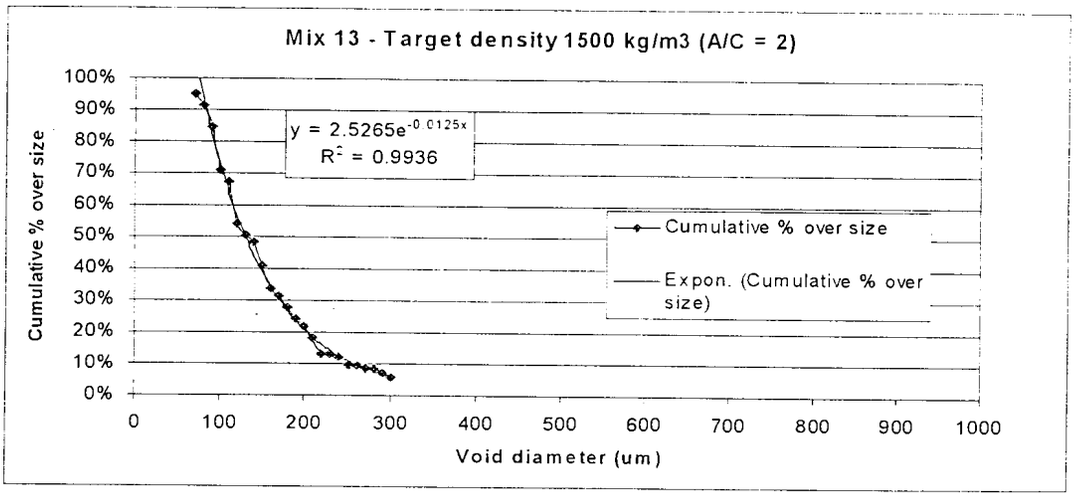
Mix 13 - Target density 1500 kg/m3 (A/C = 2)
y = 2.5265e-0.0125x
R2 = 0.9936
Cumulative % over size
Expon. (Cumulative % over size)
Cumulative % over size
Void diameter (um)
100%
90%
80%
70%
60%
50%
40%
30%
20%
10%
0%
0
100
200
300
400
500
600
700
800
900
1000

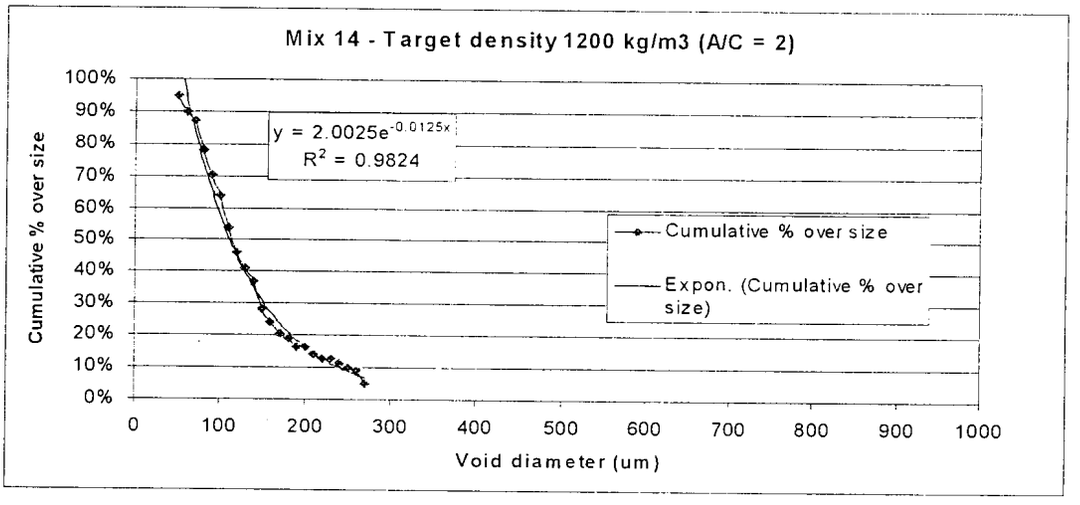
Mix 14 - Target density 1200 kg/m3 (A/C = 2)
y = 2.0025e-0.0125x
R2 = 0.9824
Cumulative % over size
Expon. (Cumulative % over size)
Cumulative % over size
Void diameter (um)
100%
90%
80%
70%
60%
50%
40%
30%
20%
10%
0%
0
100
200
300
400
500
600
700
800
900
1000

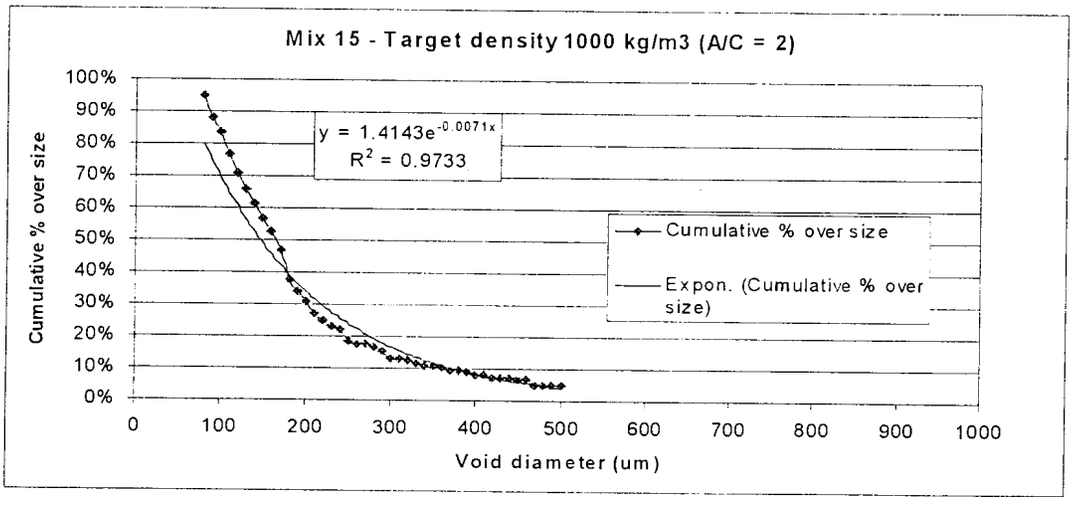
Mix 15 - Target density 1000 kg/m3 (A/C = 2)
y = 1.4143e-0.0071x
R2 = 0.9733
Cumulative % over size
Expon. (Cumulative % over size)
Cumulative % over size
Void diameter (um)
100%
90%
80%
70%
60%
50%
40%
30%
20%
10%
0%
0
100
200
300
400
500
600
700
800
900
1000

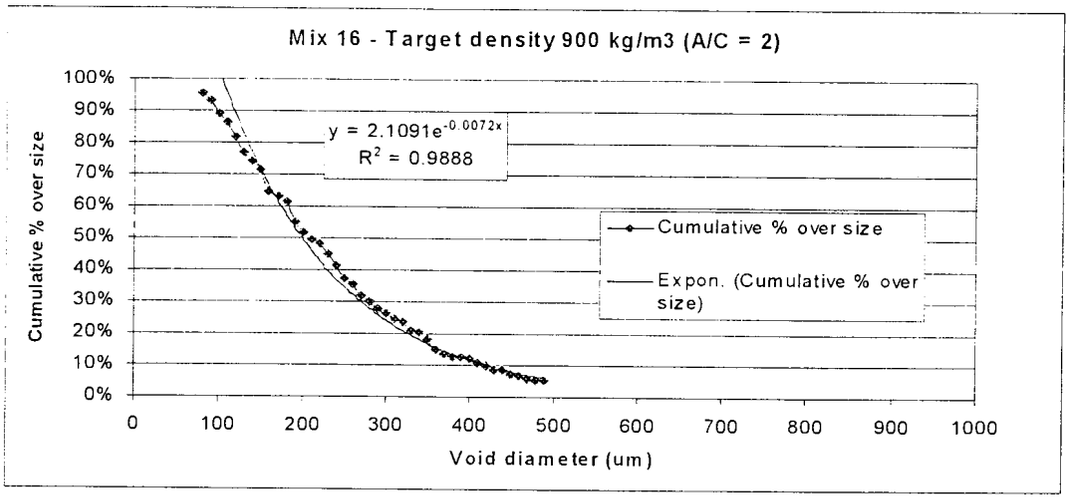
Mix 16 - Target density 900 kg/m3 (A/C = 2)
y = 2.1091e-0.0072x
R2 = 0.9888
Cumulative % over size
Expon. (Cumulative % over size)
Cumulative % over size
Void diameter (um)

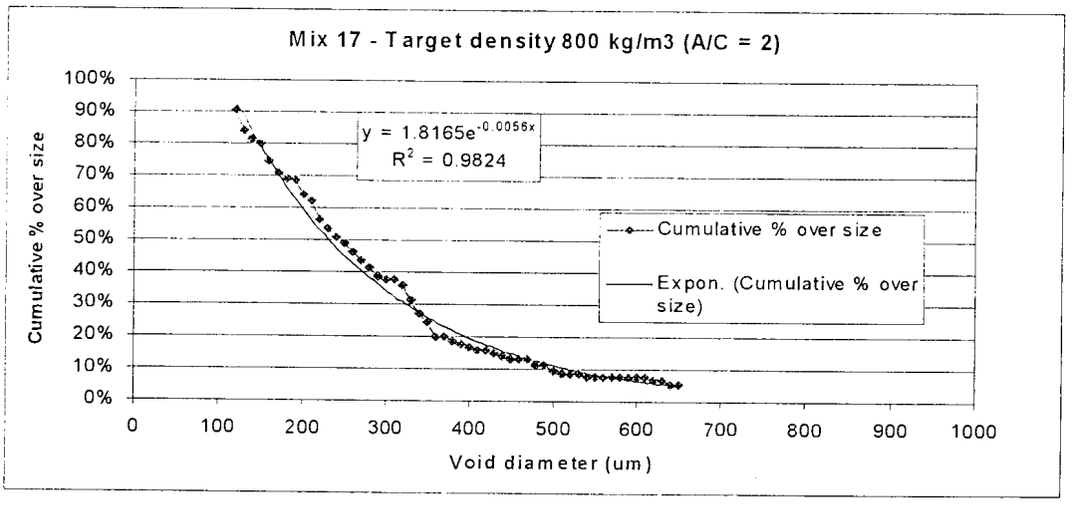
Mix 17 - Target density 800 kg/m3 (A/C = 2)
y = 1.8165e-0.0056x
R2 = 0.9824
Cumulative % over size
Expon. (Cumulative % over size)
Cumulative % over size
Void diameter (um)

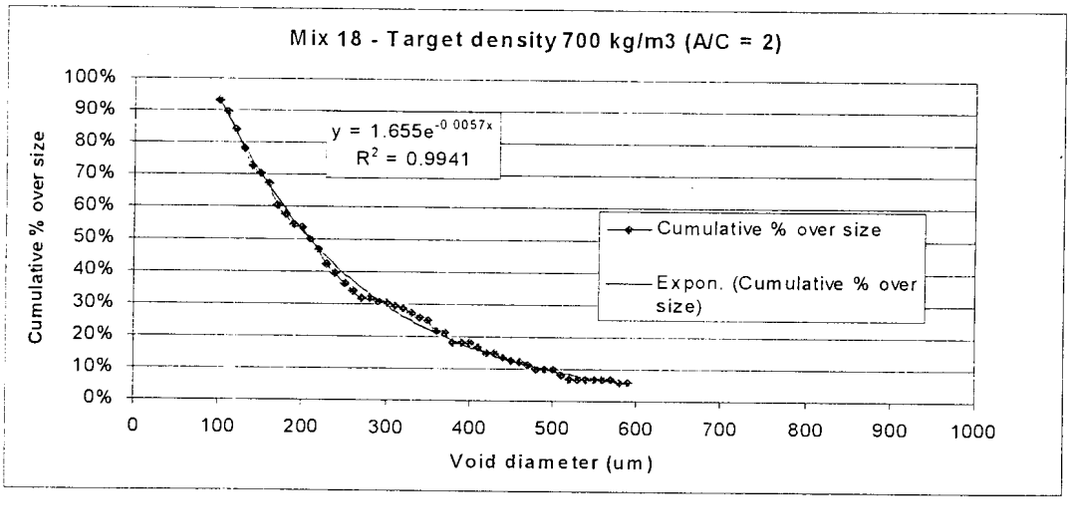
Mix 18 - Target density 700 kg/m3 (A/C = 2)
y = 1.655e-0.0057x
R2 = 0.9941
Cumulative % over size
Expon. (Cumulative % over size)
Cumulative % over size
Void diameter (um)

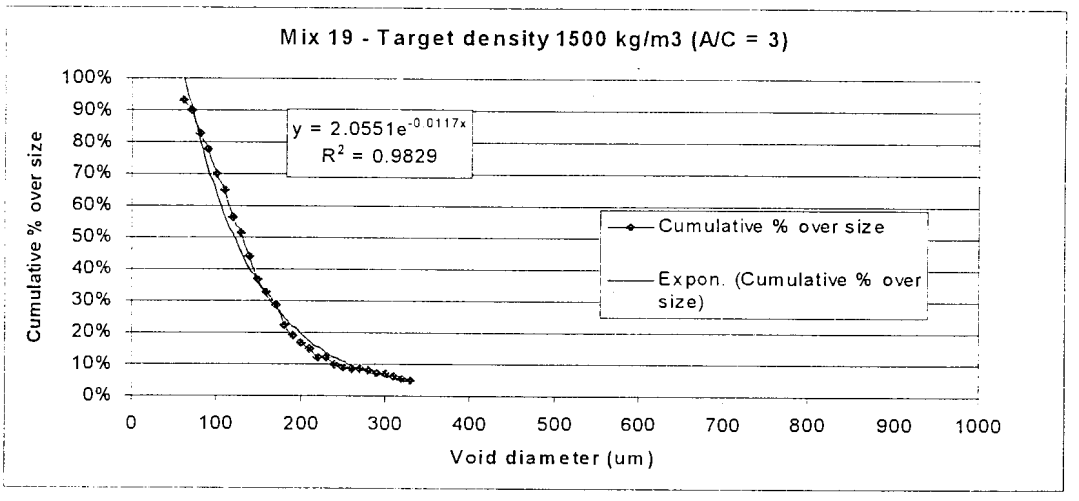
Mix 19 - Target density 1500 kg/m3 (A/C = 3)
y = 2.0551e-0.0117x
R2 = 0.9829
Cumulative % over size
Expon. (Cumulative % over size)
Cumulative % over size
Void diameter (um)

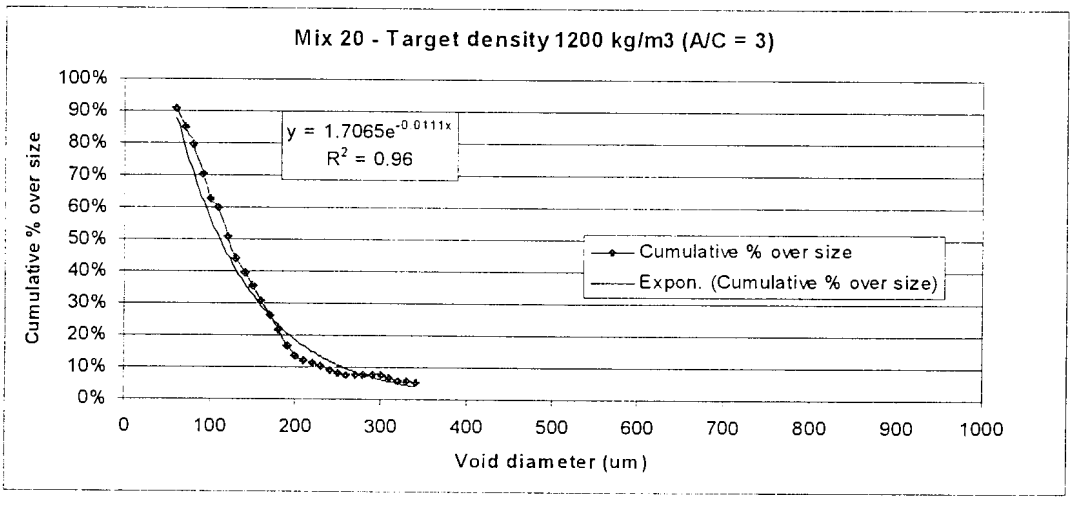
Mix 20 - Target density 1200 kg/m3 (A/C = 3)
y = 1.7065e-0.0111x
R2 = 0.96
Cumulative % over size
Expon. (Cumulative % over size)
Cumulative % over size
Void diameter (um)

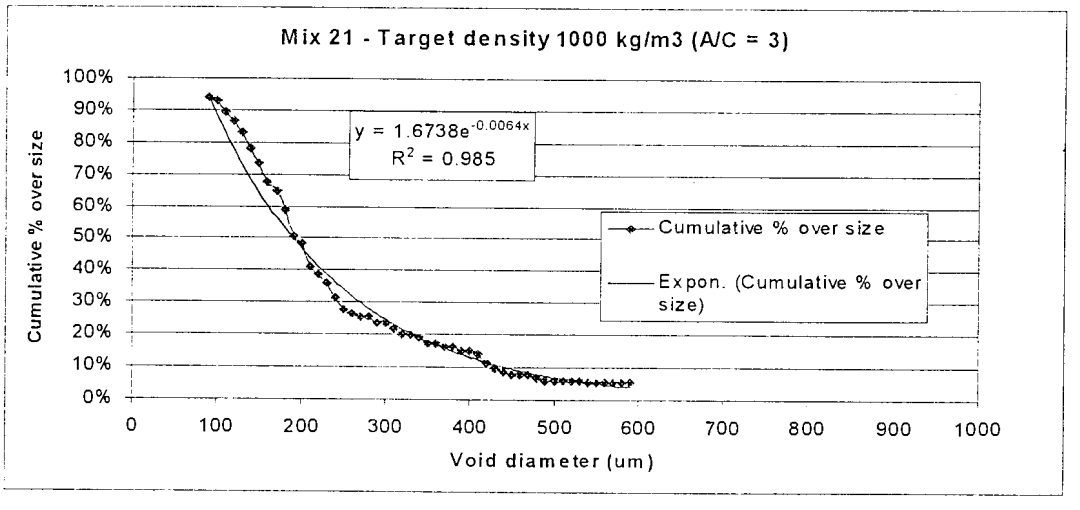
Mix 21 - Target density 1000 kg/m3 (A/C = 3)
y = 1.6738e-0.0064x
R2 = 0.985
Cumulative % over size
Expon. (Cumulative % over size)
Cumulative % over size
Void diameter (um)

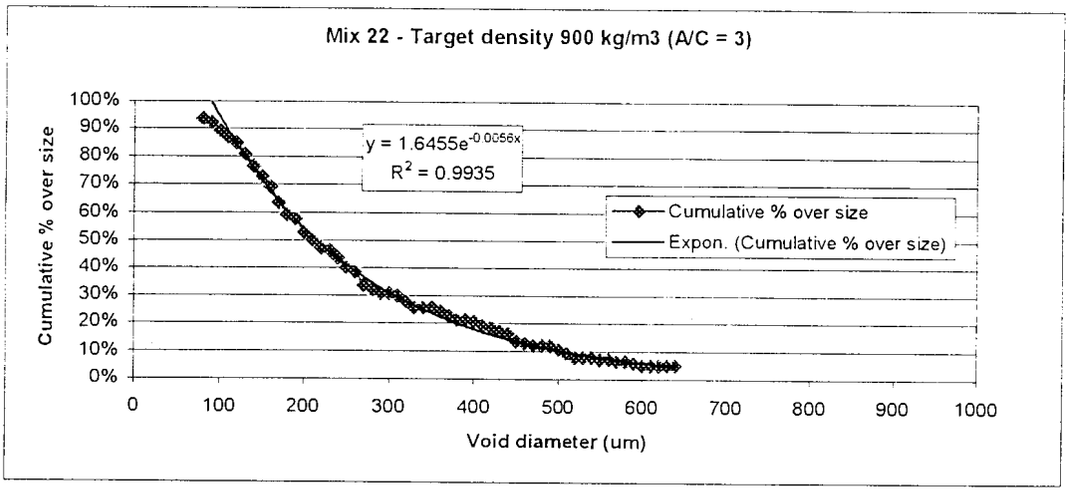
Mix 22 - Target density 900 kg/m3 (A/C = 3)
Cumulative % over size
Void diameter (um)
y = 1.6455e-0.0056x
R2 = 0.9935
Cumulative % over size
Expon. (Cumulative % over size)

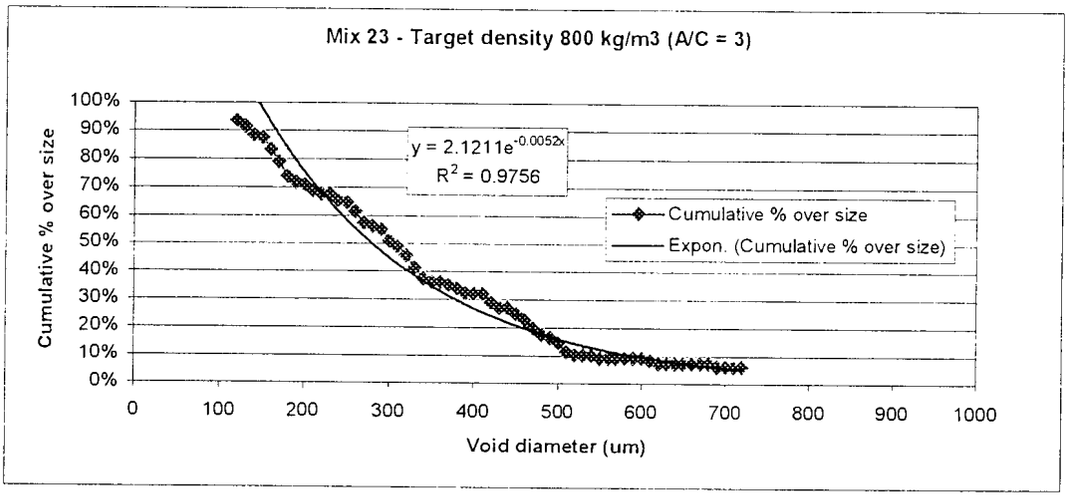
Mix 23 - Target density 800 kg/m3 (A/C = 3)
Cumulative % over size
Void diameter (um)
y = 2.1211e-0.0052x
R2 = 0.9756
Cumulative % over size
Expon. (Cumulative % over size)

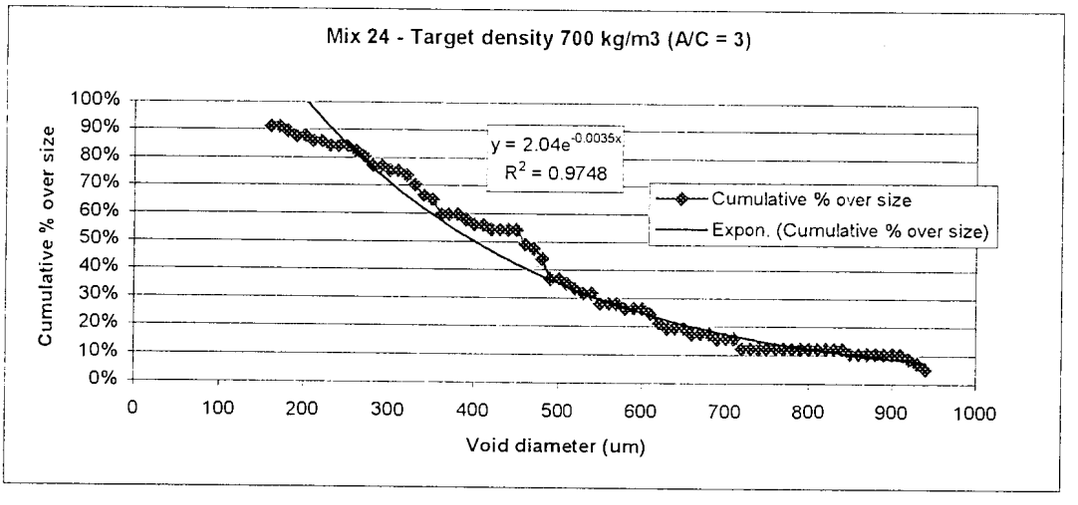
Mix 24 - Target density 700 kg/m3 (A/C = 3)
Cumulative % over size
Void diameter (um)
y = 2.04e-0.0035x
R2 = 0.9748
Cumulative % over size
Expon. (Cumulative % over size)

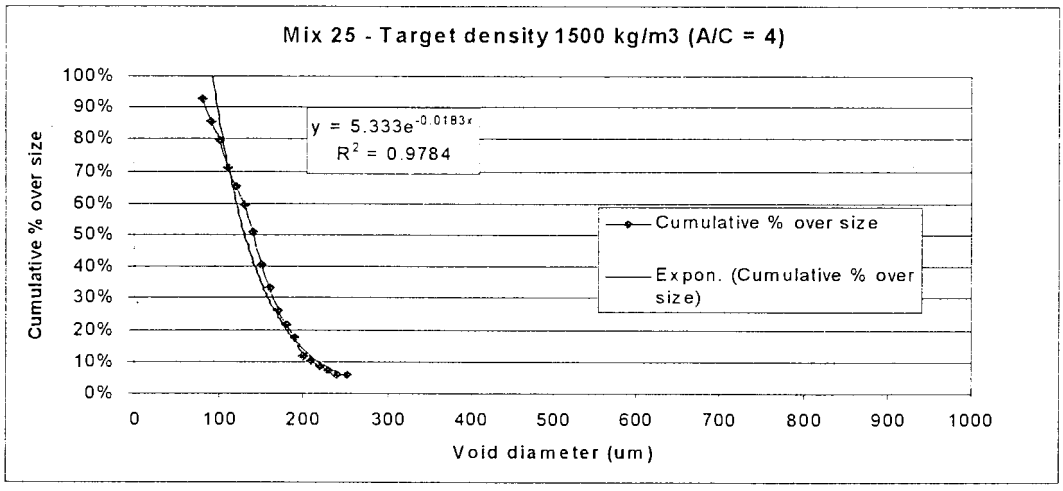
Mix 25 - Target density 1500 kg/m3 (A/C = 4)
y = 5.333e^-0.0183x
R^2 = 0.9784
Cumulative % over size
Expon. (Cumulative % over size)
Cumulative % over size
Void diameter (um)

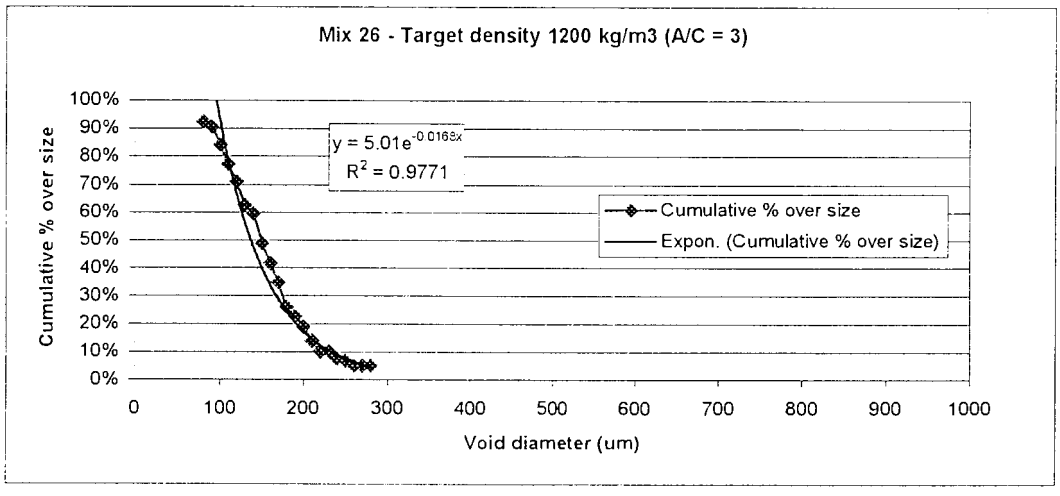
Mix 26 - Target density 1200 kg/m3 (A/C = 3)
y = 5.01e^-0.0168x
R^2 = 0.9771
Cumulative % over size
Expon. (Cumulative % over size)
Cumulative % over size
Void diameter (um)

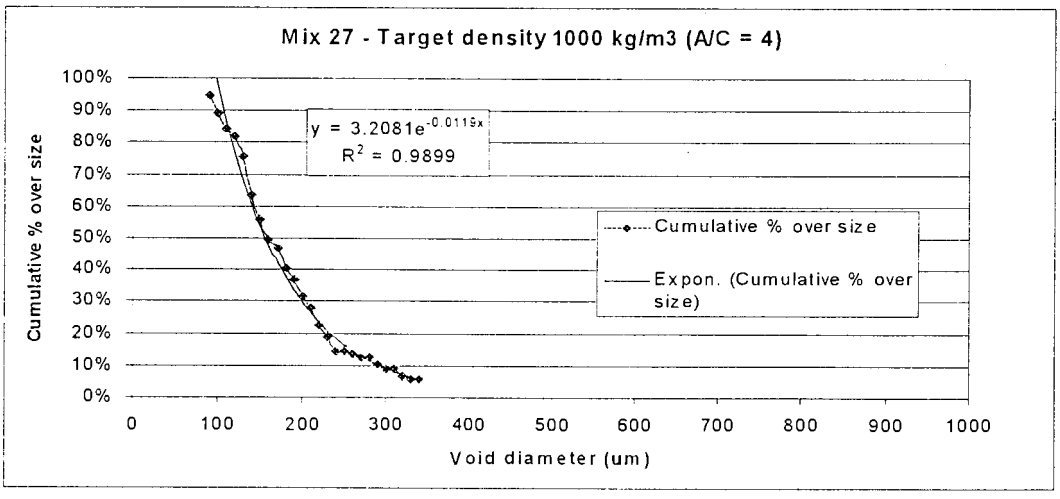
Mix 27 - Target density 1000 kg/m3 (A/C = 4)
y = 3.2081e^-0.0119x
R^2 = 0.9899
Cumulative % over size
Expon. (Cumulative % over size)
Cumulative % over size
Void diameter (um)

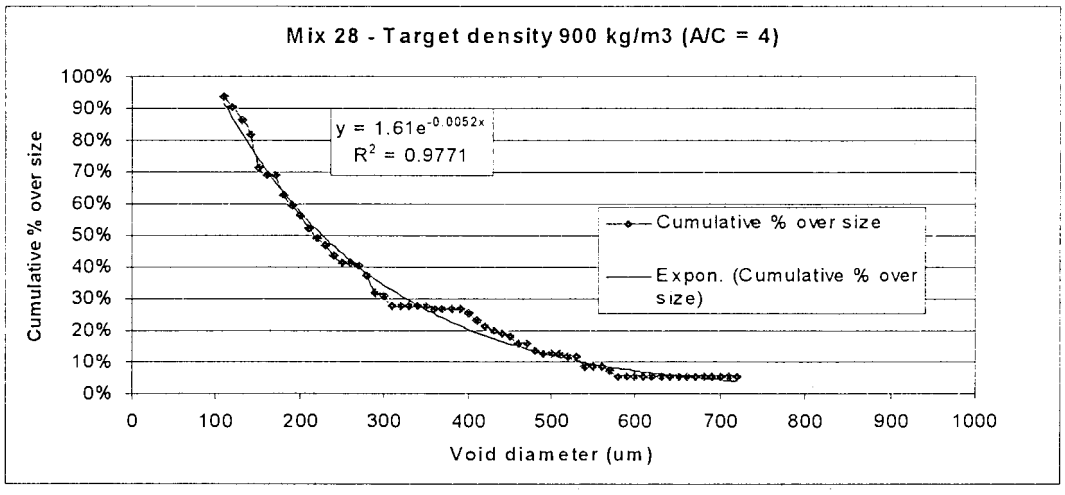
Mix 28 - Target density 900 kg/m3 (A/C = 4)
y = 1.61e-0.0052x
R2 = 0.9771
Cumulative % over size
Expon. (Cumulative % over size)
Cumulative % over size
Void diameter (um)

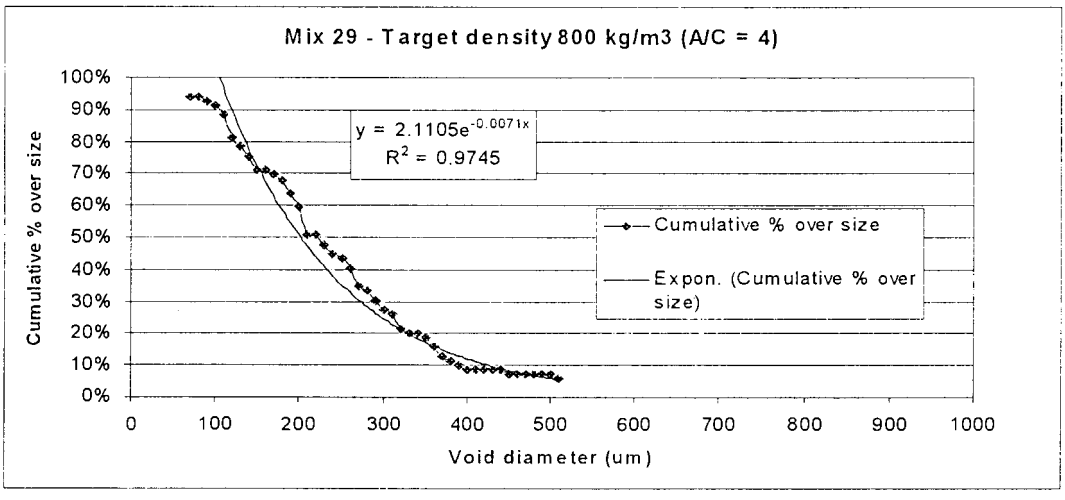
Mix 29 - Target density 800 kg/m3 (A/C = 4)
y = 2.1105e-0.0071x
R2 = 0.9745
Cumulative % over size
Expon. (Cumulative % over size)
Cumulative % over size
Void diameter (um)

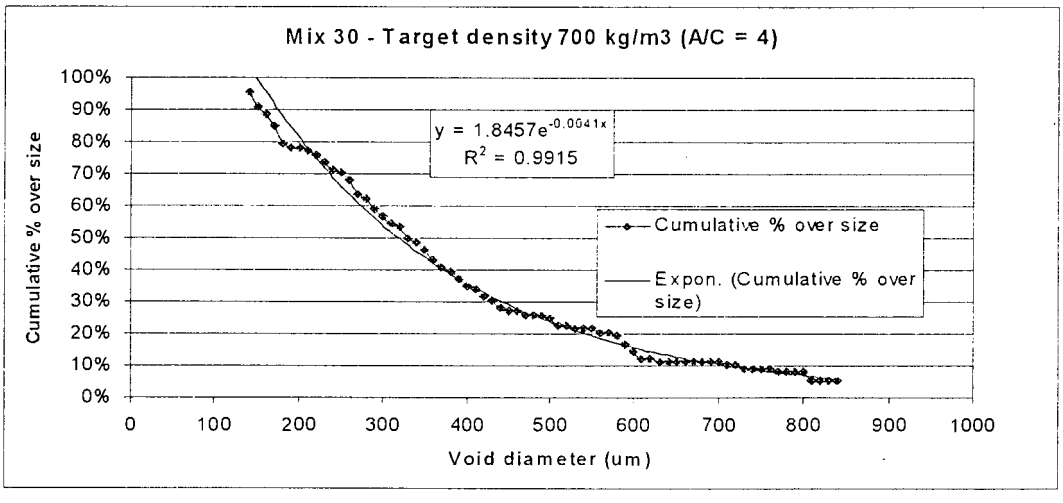
Mix 30 - Target density 700 kg/m3 (A/C = 4)
y = 1.8457e-0.0041x
R2 = 0.9915
Cumulative % over size
Expon. (Cumulative % over size)
Cumulative % over size
Void diameter (um)

APPENDIX C

MODIFIED ROSIN-RAMMLER VOID DISTRIBUTION OF MIXES

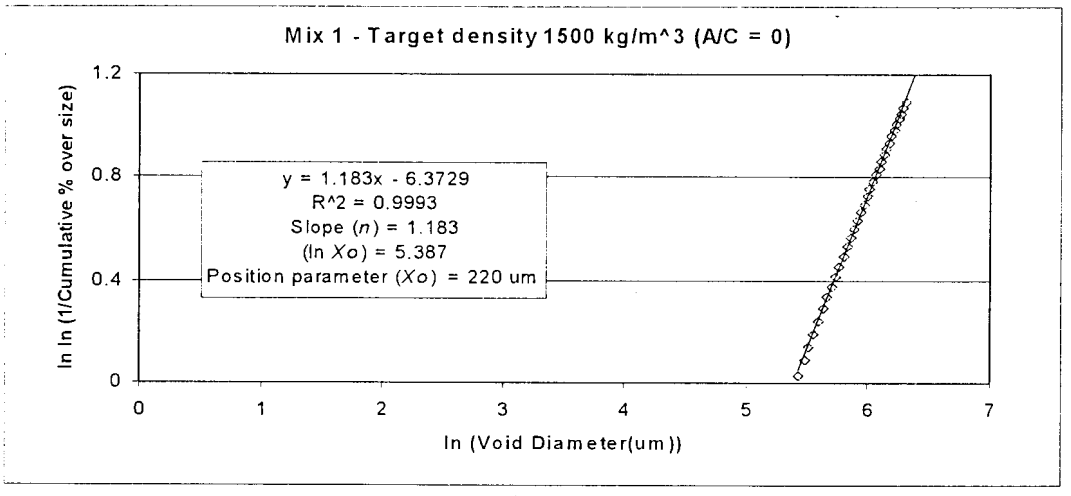

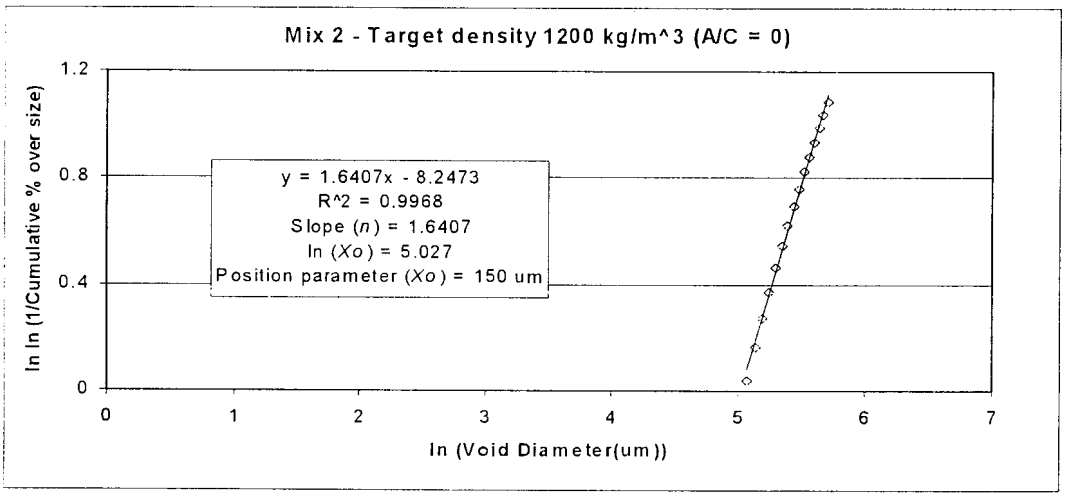

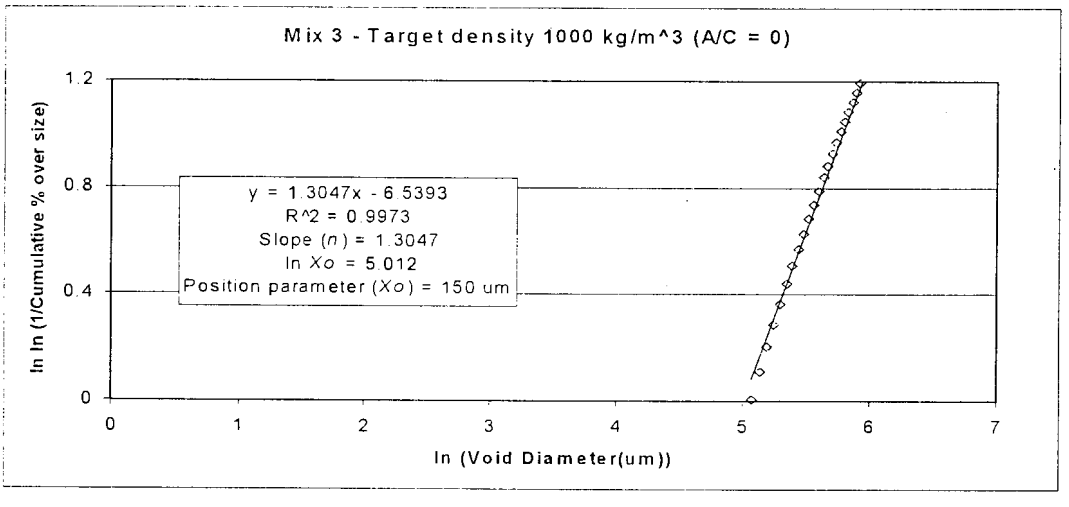

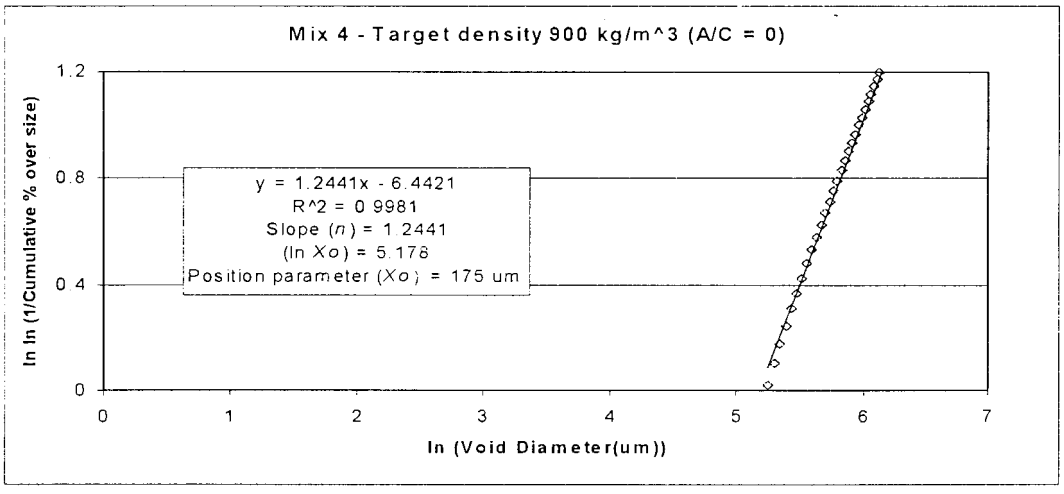
Mix 4 - Target density 900 kg/m^3 (A/C = 0)
y = 1.2441x - 6.4421
R^2 = 0.9981
Slope (n) = 1.2441
(ln Xo) = 5.178
Position parameter (Xo) = 175 um
ln ln (1/Cumulative % over size)
ln (Void Diameter(um))
0
0.4
0.8
1.2
0
1
2
3
4
5
6
7

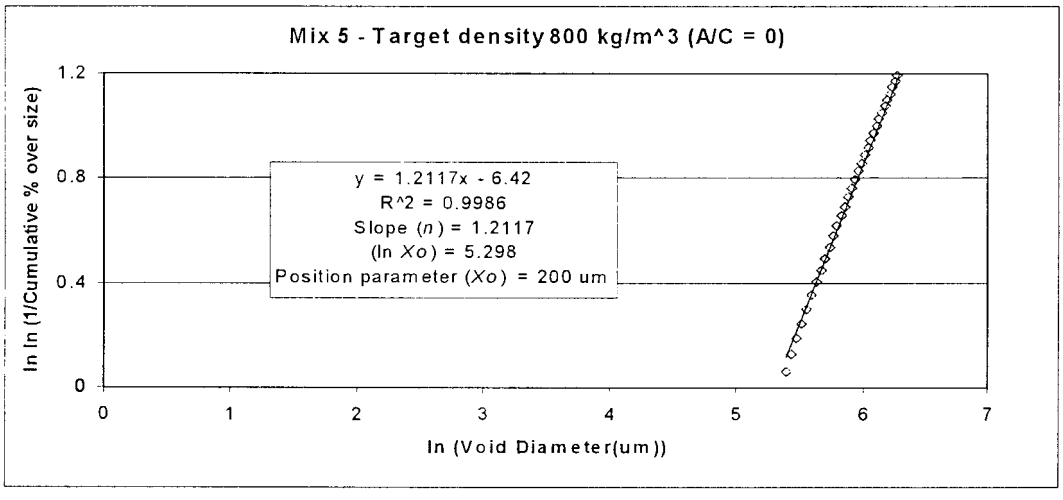
Mix 5 - Target density 800 kg/m^3 (A/C = 0)
y = 1.2117x - 6.42
R^2 = 0.9986
Slope (n) = 1.2117
(ln Xo) = 5.298
Position parameter (Xo) = 200 um
ln ln (1/Cumulative % over size)
ln (Void Diameter(um))
0
0.4
0.8
1.2
0
1
2
3
4
5
6
7

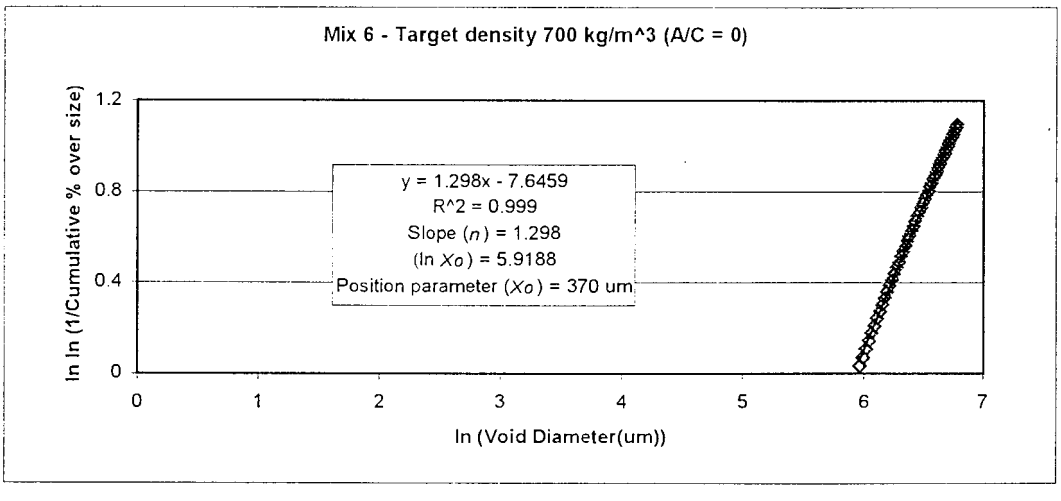
Mix 6 - Target density 700 kg/m^3 (A/C = 0)
y = 1.298x - 7.6459
R^2 = 0.999
Slope (n) = 1.298
(ln Xo) = 5.9188
Position parameter (Xo) = 370 um
ln ln (1/Cumulative % over size)
ln (Void Diameter(um))
0
0.4
0.8
1.2
0
1
2
3
4
5
6
7

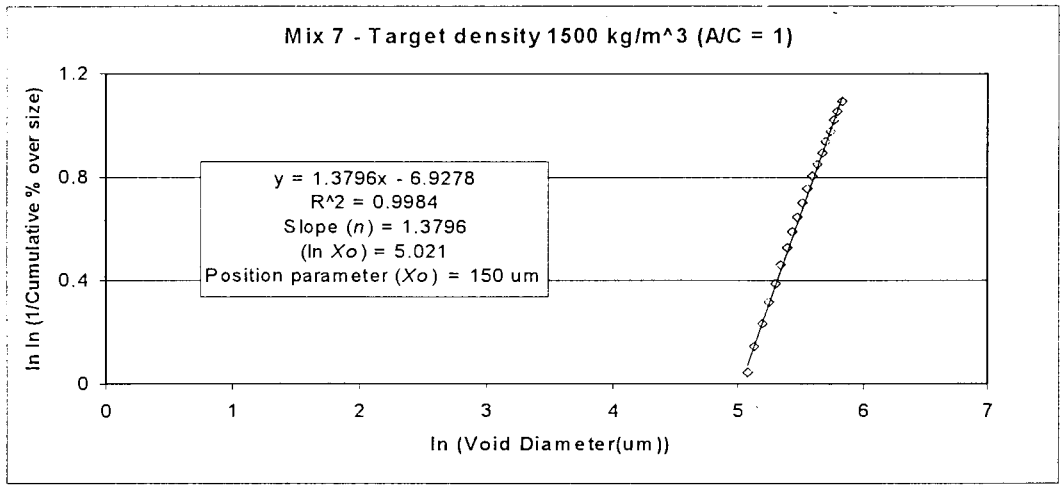
Mix 7 - Target density 1500 kg/m^3 (A/C = 1)
y = 1.3796x - 6.9278
R^2 = 0.9984
Slope (n) = 1.3796
(ln Xo) = 5.021
Position parameter (Xo) = 150 um
ln ln (1/Cumulative % over size)
ln (Void Diameter(um))
0
0.4
0.8
1.2
0
1
2
3
4
5
6
7

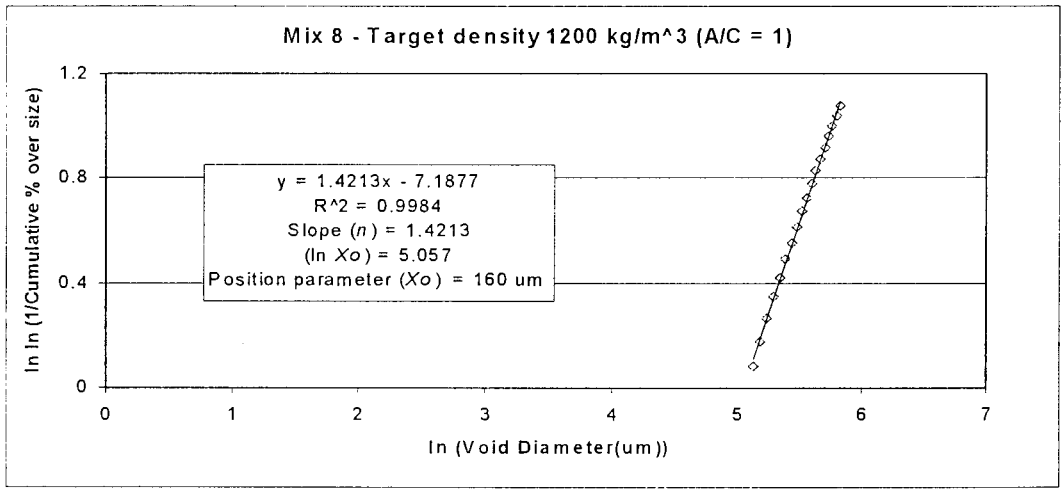
Mix 8 - Target density 1200 kg/m^3 (A/C = 1)
y = 1.4213x - 7.1877
R^2 = 0.9984
Slope (n) = 1.4213
(ln Xo) = 5.057
Position parameter (Xo) = 160 um
ln ln (1/Cumulative % over size)
ln (Void Diameter(um))
0
0.4
0.8
1.2
0
1
2
3
4
5
6
7

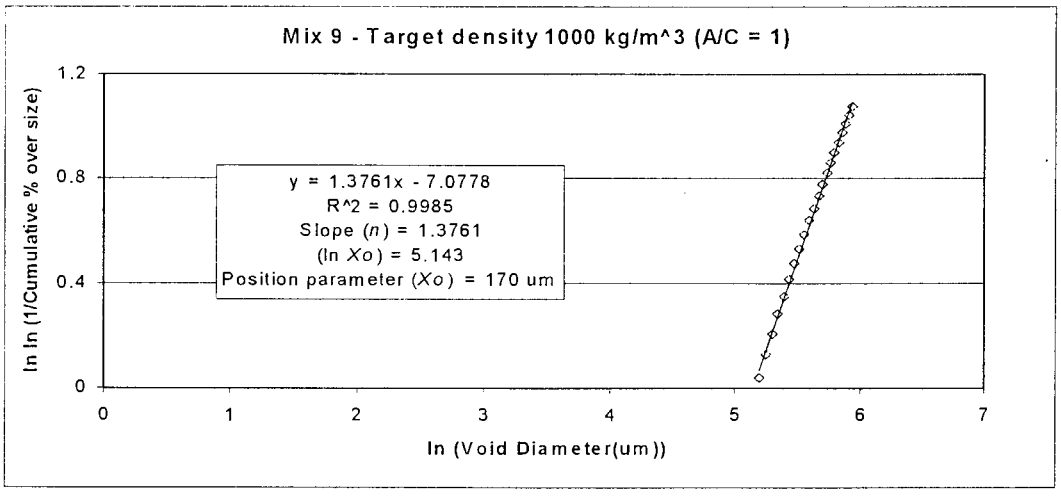
Mix 9 - Target density 1000 kg/m^3 (A/C = 1)
y = 1.3761x - 7.0778
R^2 = 0.9985
Slope (n) = 1.3761
(ln Xo) = 5.143
Position parameter (Xo) = 170 um
ln ln (1/Cumulative % over size)
ln (Void Diameter(um))
0
0.4
0.8
1.2
0
1
2
3
4
5
6
7

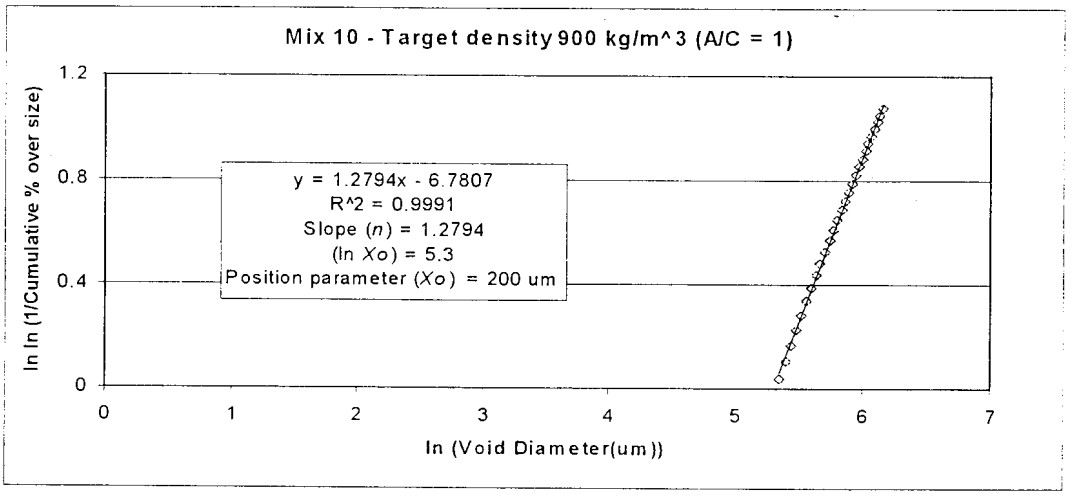

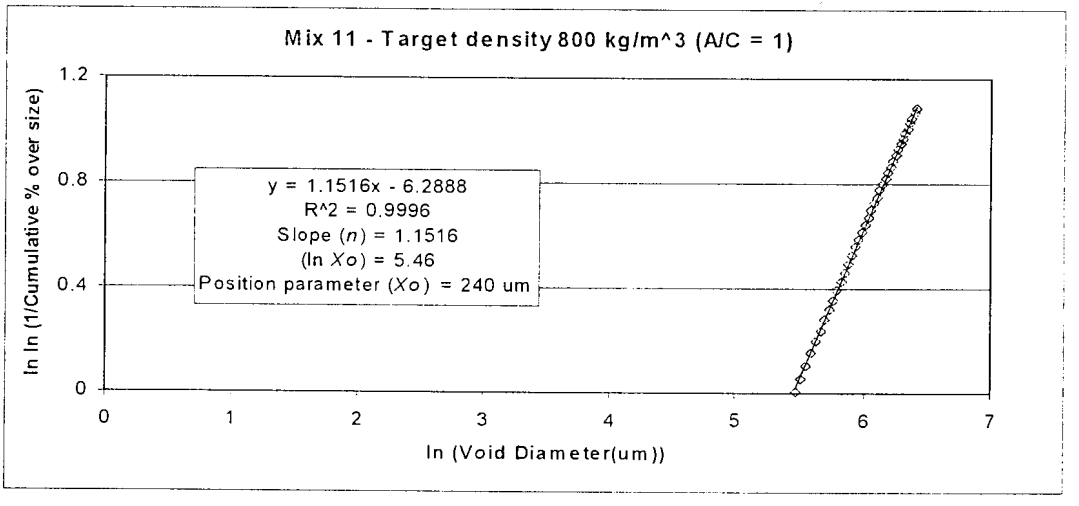

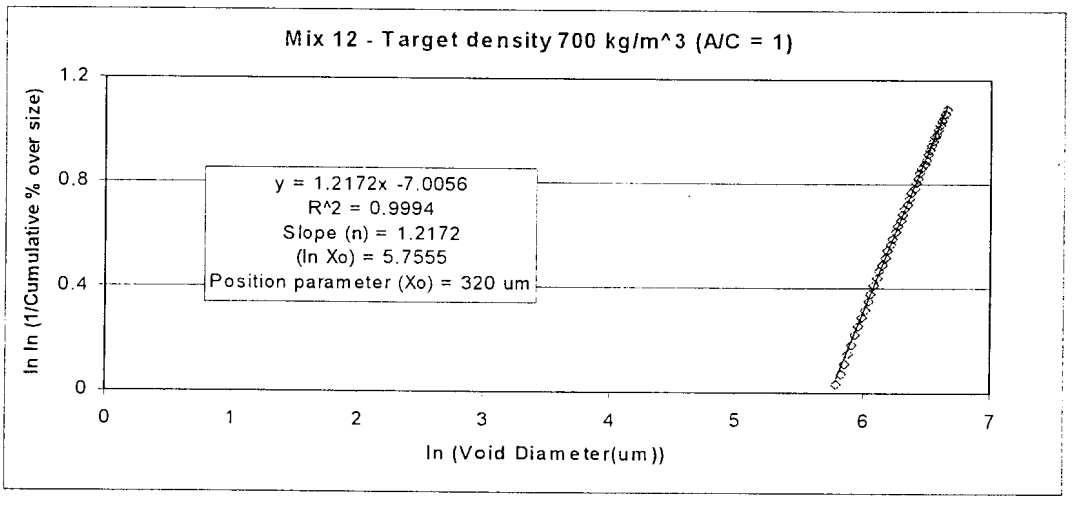

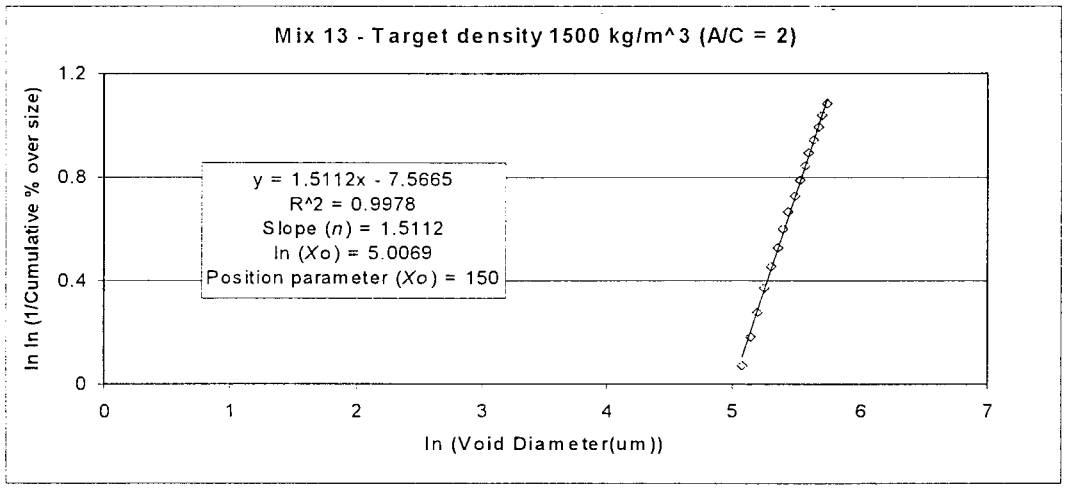
Mix 13 - Target density 1500 kg/m^3 (A/C = 2)
y = 1.5112x - 7.5665
R^2 = 0.9978
Slope (n) = 1.5112
ln (Xo) = 5.0069
Position parameter (Xo) = 150
ln ln (1/Cumulative % over size)
ln (Void Diameter(um))
0
0.4
0.8
1.2
0
1
2
3
4
5
6
7

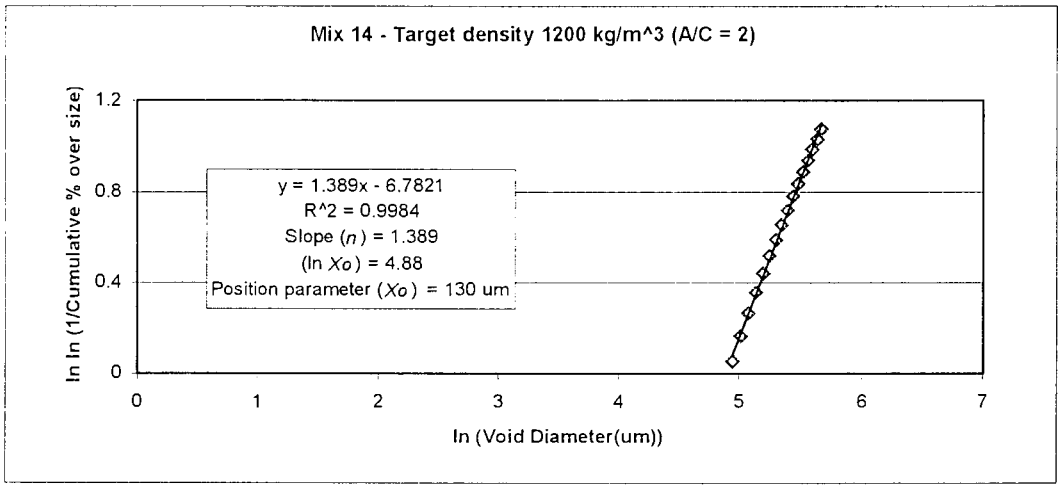
Mix 14 - Target density 1200 kg/m^3 (A/C = 2)
y = 1.389x - 6.7821
R^2 = 0.9984
Slope (n) = 1.389
(ln Xo) = 4.88
Position parameter (Xo) = 130 um
ln ln (1/Cumulative % over size)
ln (Void Diameter(um))
0
0.4
0.8
1.2
0
1
2
3
4
5
6
7

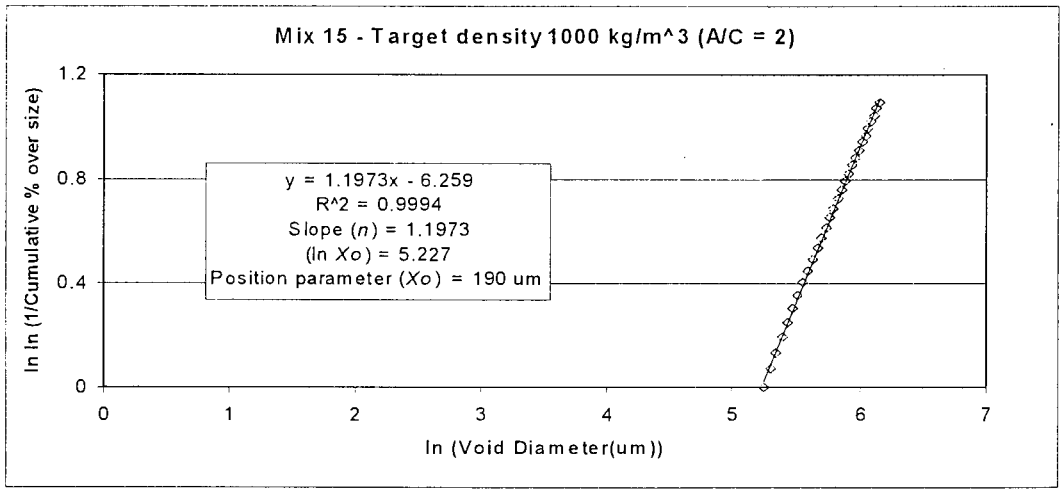
Mix 15 - Target density 1000 kg/m^3 (A/C = 2)
y = 1.1973x - 6.259
R^2 = 0.9994
Slope (n) = 1.1973
(ln Xo) = 5.227
Position parameter (Xo) = 190 um
ln ln (1/Cumulative % over size)
ln (Void Diameter(um))
0
0.4
0.8
1.2
0
1
2
3
4
5
6
7

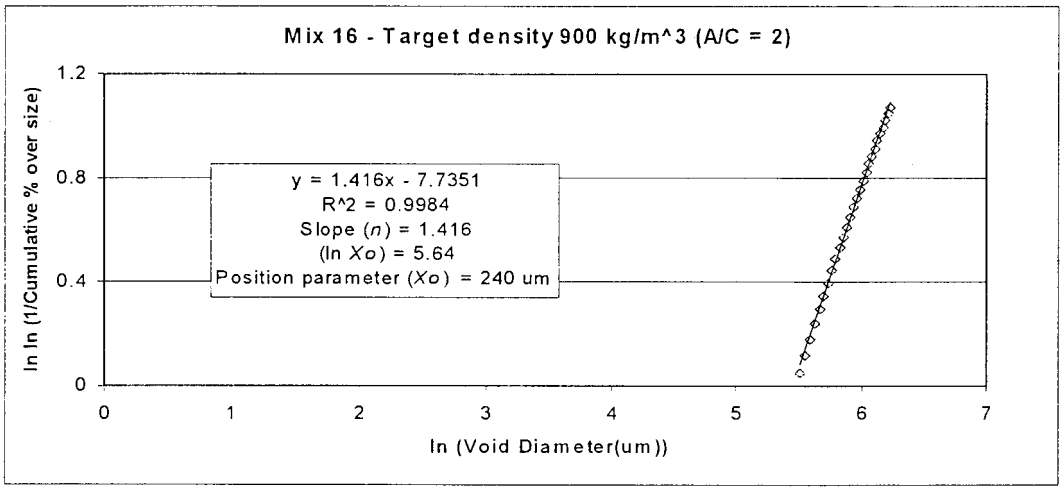
Mix 16 - Target density 900 kg/m^3 (A/C = 2)
y = 1.416x - 7.7351
R^2 = 0.9984
Slope (n) = 1.416
(ln Xo) = 5.64
Position parameter (Xo) = 240 um
ln ln (1/Cumulative % over size)
ln (Void Diameter(um))
0
0.4
0.8
1.2
0
1
2
3
4
5
6
7

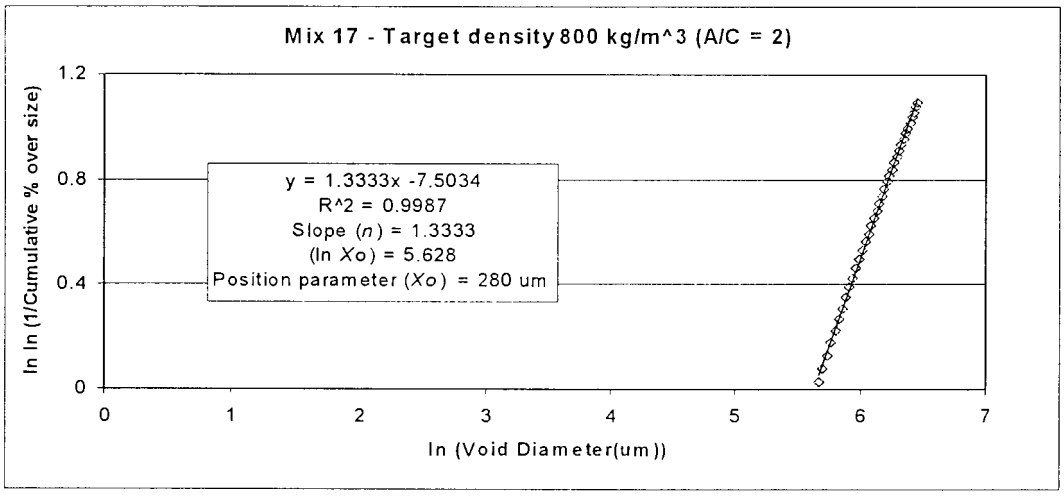
Mix 17 - Target density 800 kg/m^3 (A/C = 2)
y = 1.3333x -7.5034
R^2 = 0.9987
Slope (n) = 1.3333
(ln Xo) = 5.628
Position parameter (Xo) = 280 um
ln ln (1/Cumulative % over size)
ln (Void Diameter(um))
0
0.4
0.8
1.2
0
1
2
3
4
5
6
7

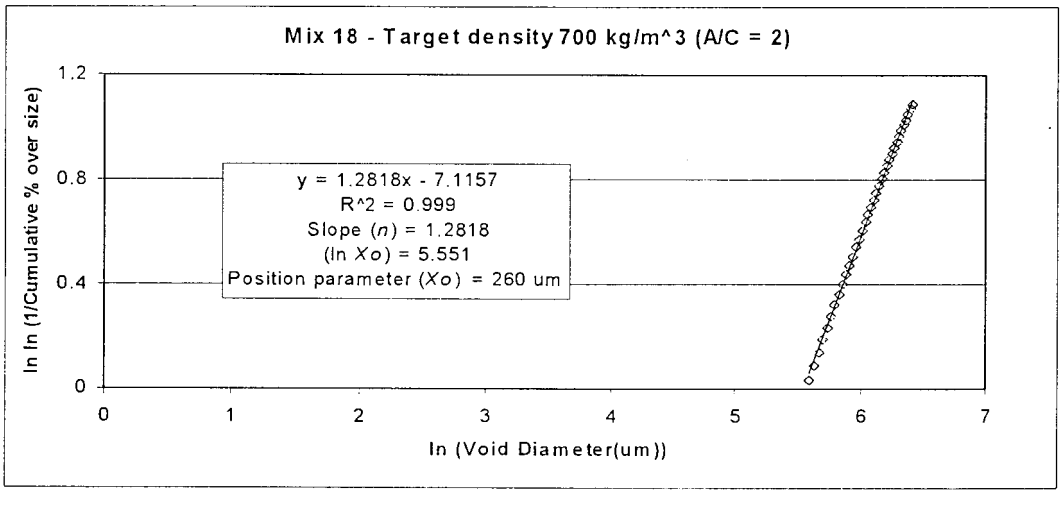
Mix 18 - Target density 700 kg/m^3 (A/C = 2)
y = 1.2818x - 7.1157
R^2 = 0.999
Slope (n) = 1.2818
(ln Xo) = 5.551
Position parameter (Xo) = 260 um
ln ln (1/Cumulative % over size)
ln (Void Diameter(um))
0
0.4
0.8
1.2
0
1
2
3
4
5
6
7

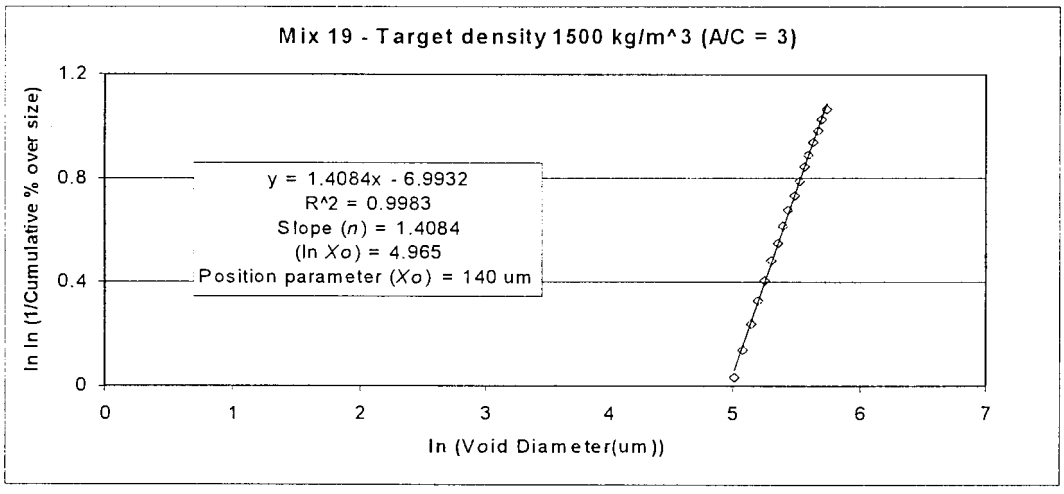
Mix 19 - Target density 1500 kg/m^3 (A/C = 3)
y = 1.4084x - 6.9932
R^2 = 0.9983
Slope (n) = 1.4084
(ln Xo) = 4.965
Position parameter (Xo) = 140 um
ln ln (1/Cumulative % over size)
ln (Void Diameter(um))
0
0.4
0.8
1.2
0
1
2
3
4
5
6
7

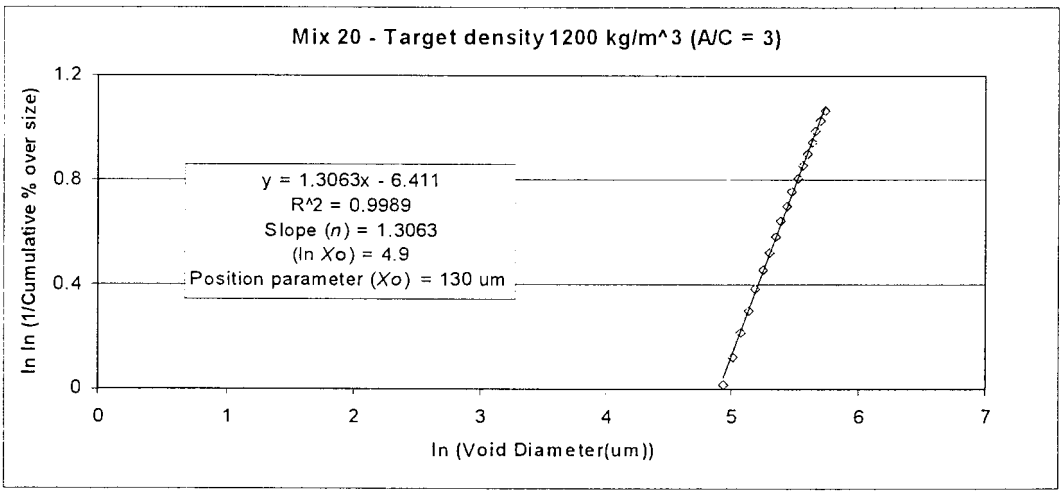
Mix 20 - Target density 1200 kg/m^3 (A/C = 3)
y = 1.3063x - 6.411
R^2 = 0.9989
Slope (n) = 1.3063
(ln Xo) = 4.9
Position parameter (Xo) = 130 um
ln ln (1/Cumulative % over size)
ln (Void Diameter(um))
0
0.4
0.8
1.2
0
1
2
3
4
5
6
7

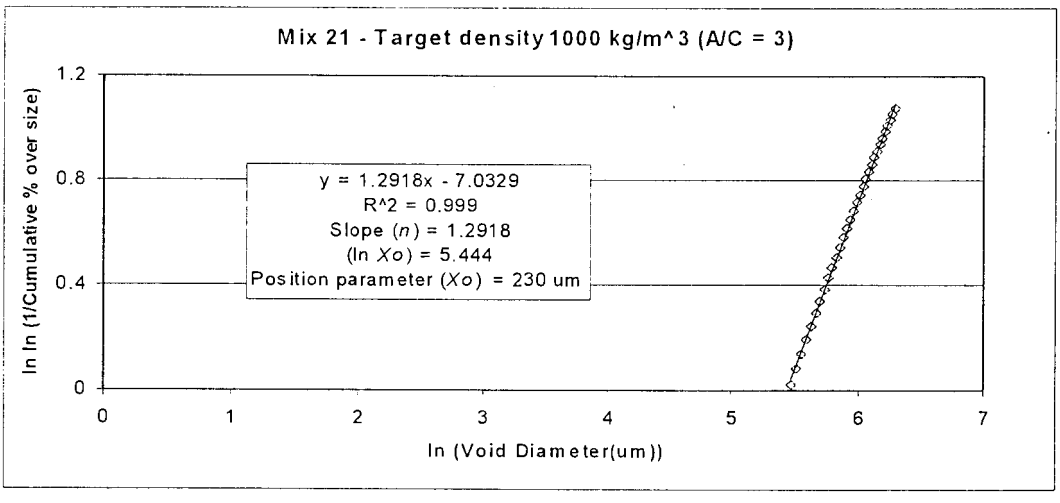
Mix 21 - Target density 1000 kg/m^3 (A/C = 3)
y = 1.2918x - 7.0329
R^2 = 0.999
Slope (n) = 1.2918
(ln Xo) = 5.444
Position parameter (Xo) = 230 um
ln ln (1/Cumulative % over size)
ln (Void Diameter(um))
0
0.4
0.8
1.2
0
1
2
3
4
5
6
7

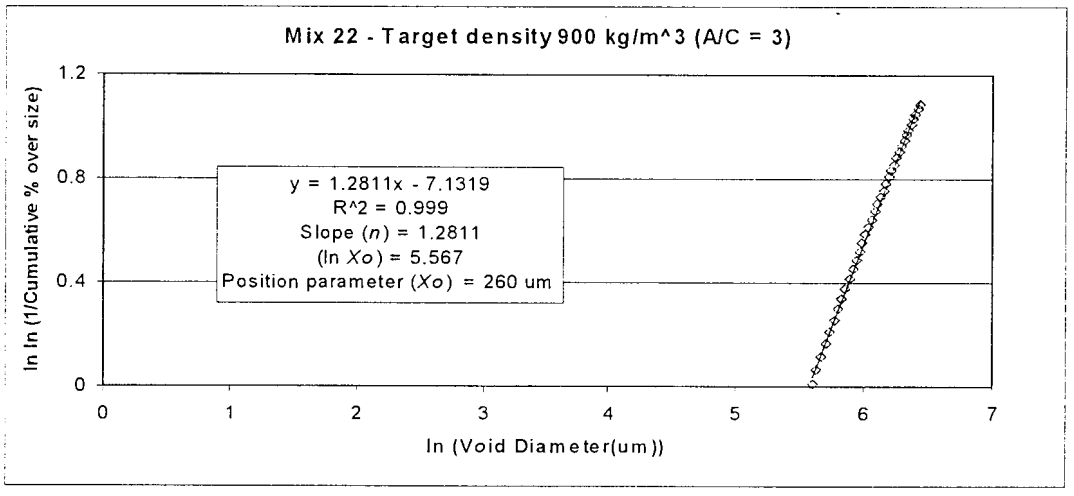
Mix 22 - Target density 900 kg/m^3 (A/C = 3)
y = 1.2811x - 7.1319
R^2 = 0.999
Slope (n) = 1.2811
(ln Xo) = 5.567
Position parameter (Xo) = 260 um
ln ln (1/Cumulative % over size)
ln (Void Diameter(um))
0
0.4
0.8
1.2
0
1
2
3
4
5
6
7

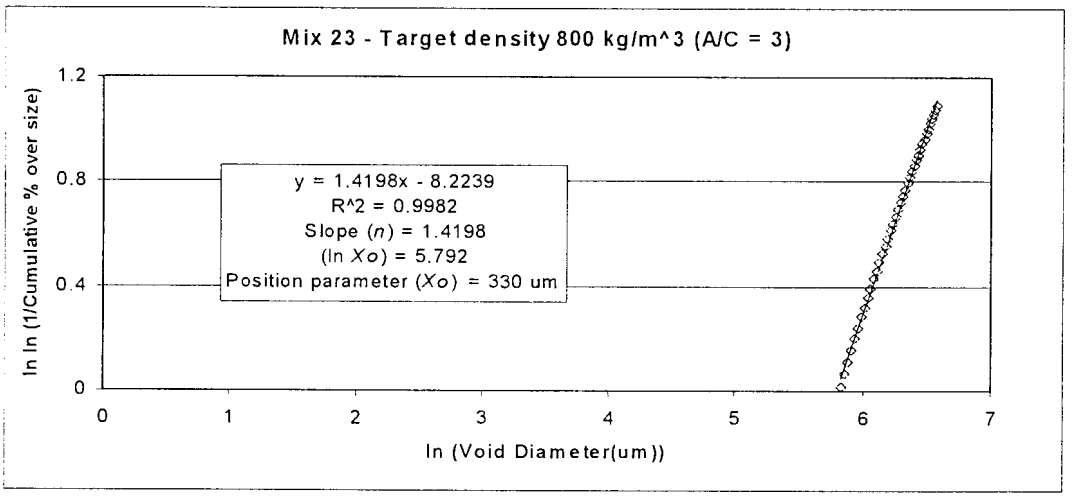
Mix 23 - Target density 800 kg/m^3 (A/C = 3)
y = 1.4198x - 8.2239
R^2 = 0.9982
Slope (n) = 1.4198
(ln Xo) = 5.792
Position parameter (Xo) = 330 um
ln ln (1/Cumulative % over size)
ln (Void Diameter(um))
0
0.4
0.8
1.2
0
1
2
3
4
5
6
7

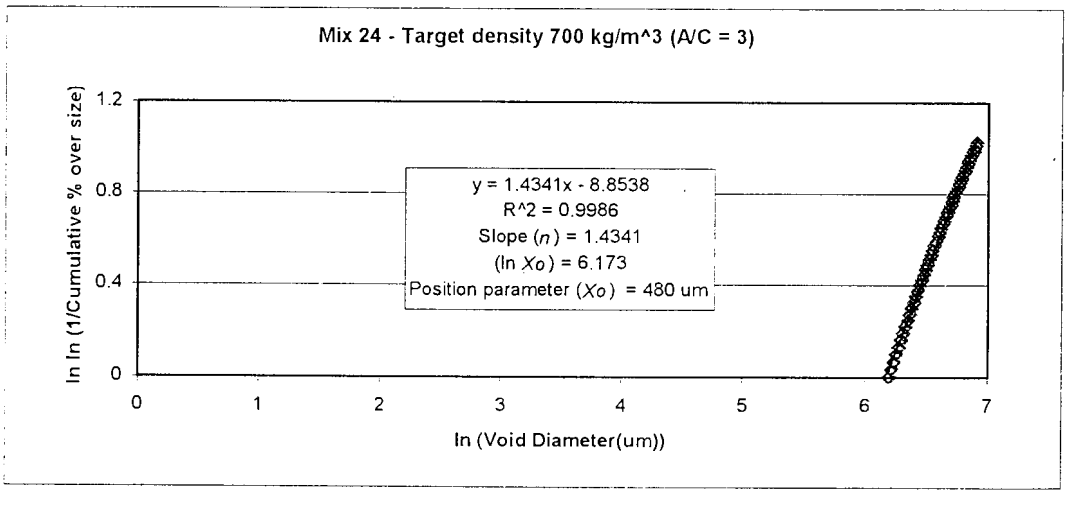
Mix 24 - Target density 700 kg/m^3 (A/C = 3)
y = 1.4341x - 8.8538
R^2 = 0.9986
Slope (n) = 1.4341
(ln Xo) = 6.173
Position parameter (Xo) = 480 um
ln ln (1/Cumulative % over size)
ln (Void Diameter(um))
0
0.4
0.8
1.2
0
1
2
3
4
5
6
7

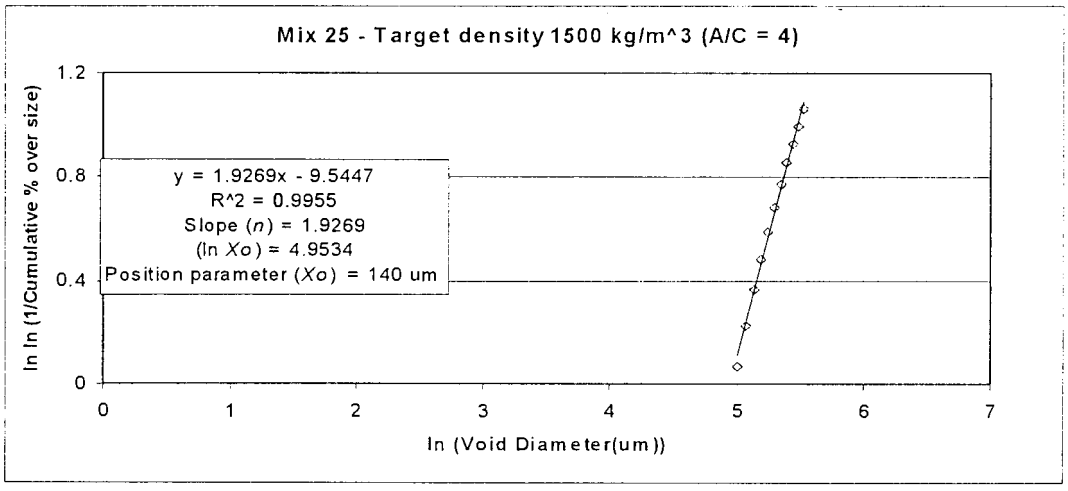
Mix 25 - Target density 1500 kg/m^3 (A/C = 4)
y = 1.9269x - 9.5447
R^2 = 0.9955
Slope (n) = 1.9269
(ln Xo) = 4.9534
Position parameter (Xo) = 140 um
ln ln (1/Cumulative % over size)
ln (Void Diameter(um))
0
0.4
0.8
1.2
0
1
2
3
4
5
6
7

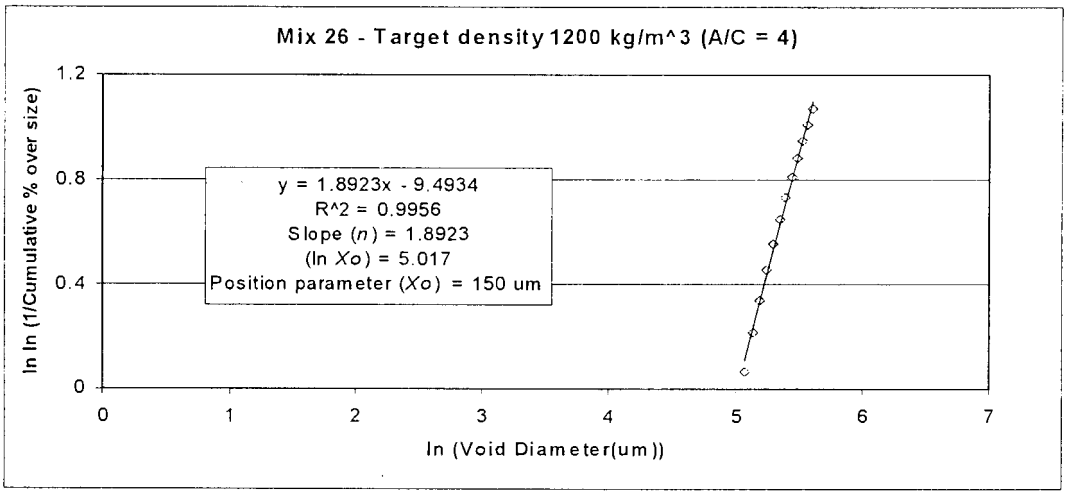
Mix 26 - Target density 1200 kg/m^3 (A/C = 4)
y = 1.8923x - 9.4934
R^2 = 0.9956
Slope (n) = 1.8923
(ln Xo) = 5.017
Position parameter (Xo) = 150 um
ln ln (1/Cumulative % over size)
ln (Void Diameter(um))
0
0.4
0.8
1.2
0
1
2
3
4
5
6
7

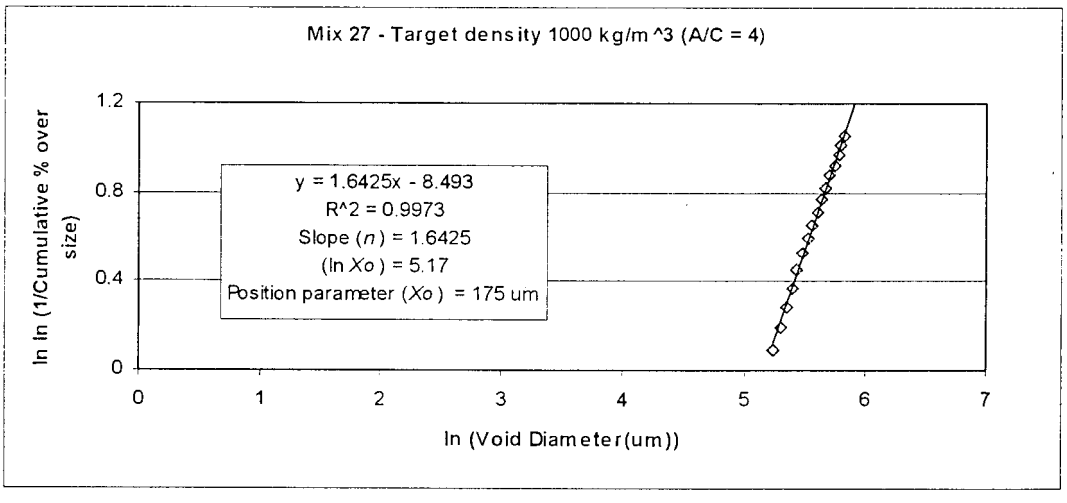
Mix 27 - Target density 1000 kg/m^3 (A/C = 4)
y = 1.6425x - 8.493
R^2 = 0.9973
Slope (n) = 1.6425
(ln Xo) = 5.17
Position parameter (Xo) = 175 um
ln ln (1/Cumulative % over size)
ln (Void Diameter(um))
0
0.4
0.8
1.2
0
1
2
3
4
5
6
7

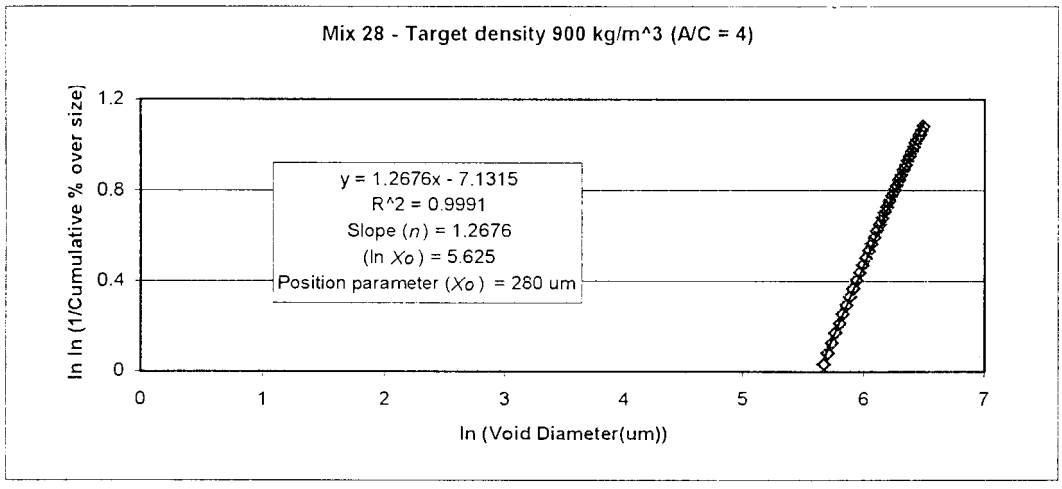
Mix 28 - Target density 900 kg/m^3 (A/C = 4)
y = 1.2676x - 7.1315
R^2 = 0.9991
Slope (n) = 1.2676
(ln Xo) = 5.625
Position parameter (Xo) = 280 um
ln ln (1/Cumulative % over size)
ln (Void Diameter(um))
0
0.4
0.8
1.2
0
1
2
3
4
5
6
7

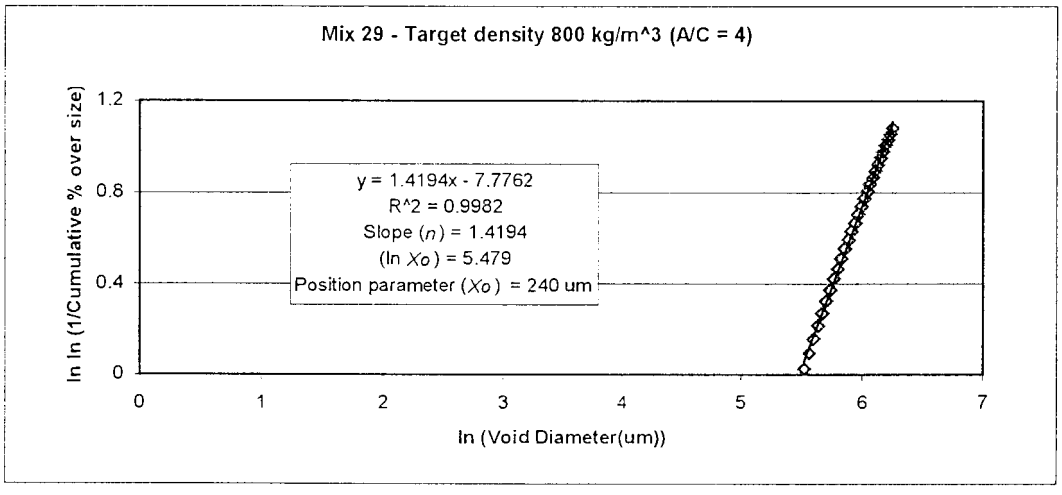
Mix 29 - Target density 800 kg/m^3 (A/C = 4)
y = 1.4194x - 7.7762
R^2 = 0.9982
Slope (n) = 1.4194
(ln Xo) = 5.479
Position parameter (Xo) = 240 um
ln ln (1/Cumulative % over size)
ln (Void Diameter(um))
0
0.4
0.8
1.2
0
1
2
3
4
5
6
7

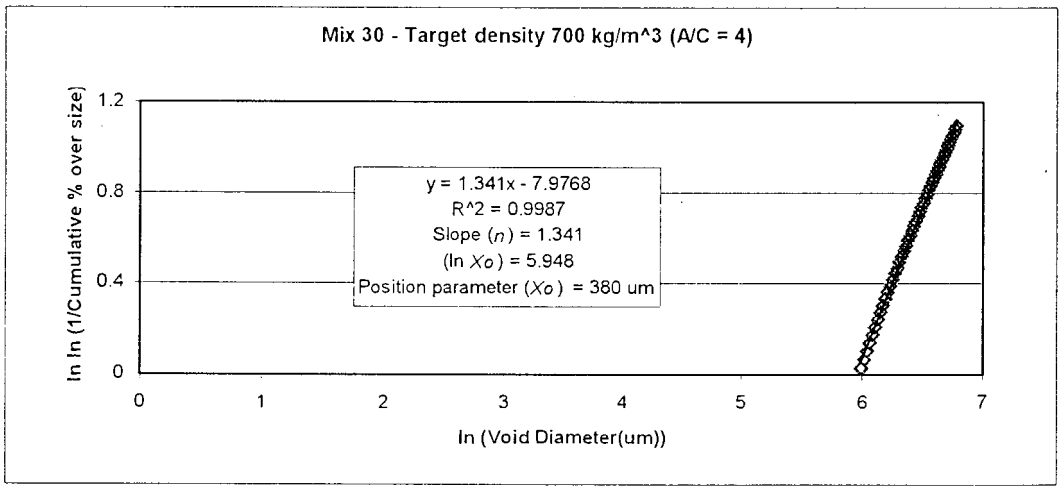
Mix 30 - Target density 700 kg/m^3 (A/C = 4)
y = 1.341x - 7.9768
R^2 = 0.9987
Slope (n) = 1.341
(ln Xo) = 5.948
Position parameter (Xo) = 380 um
ln ln (1/Cumulative % over size)
ln (Void Diameter(um))
0
0.4
0.8
1.2
0
1
2
3
4
5
6
7

APPENDIX D

MACRO IN MICROSOFT EXCEL FOR CALCULATION OF VOID SPACING

Module1 - 1

```
Sub Distance()
'
' distance Macro
' Macro recorded 1999/01/13 by E Kearsley
'
'
nr = ActiveCell.Value
While nr > 0
For i = 1 To nr
    ActiveCell.Offset(i - 1, 1).Range("A1").Select
    xcord = ActiveCell.Value
    ActiveCell.Offset(0, 1).Range("A1").Select
    ycord = ActiveCell.Value
    ActiveCell.Offset(0, 1).Range("A1").Select
    zcord = ActiveCell.Value
    ActiveCell.Offset(1 - i, 3).Range("A1").Select
    ss = 1000
    For n = 1 To nr
        ActiveCell.Offset(n - 1, -5).Range("A1").Select
        xx = ActiveCell.Value
        ActiveCell.Offset(0, 1).Range("A1").Select
        yy = ActiveCell.Value
        ActiveCell.Offset(0, 1).Range("A1").Select
        zz = ActiveCell.Value
        ActiveCell.Offset(-n + 1, 3).Range("A1").Select
        temp = Dist(xcord, ycord, zcord, xx, yy, zz)
        If i > n Or i < n Then
            If temp < ss Then
                ss = temp
                ActiveCell.Offset(i - 1, 0).Range("A1").Select
                ActiveCell.FormulaR1C1 = ss
                ActiveCell.Offset(0, 1).Range("A1").Select
                ActiveCell.FormulaR1C1 = n
                ActiveCell.Offset(1 - i, -1).Range("A1").Select
            Else
            End If
        Else
        End If
    Next
    ActiveCell.Offset(0, -6).Range("A1").Select
  Next
  ActiveCell.Offset(nr, 0).Range("A1").Select
  nr = ActiveCell.Value
Wend
End Sub
Function Dist(xcord, ycord, zcord, xx, yy, zz)
        Dist = (Sqr((xcord - xx) ^ 2 + (ycord - yy) ^ 2) - zcord - zz)
End Function
```

APPENDIX E

AIR-VOID SPACING DISTRIBUTION OF MIXES

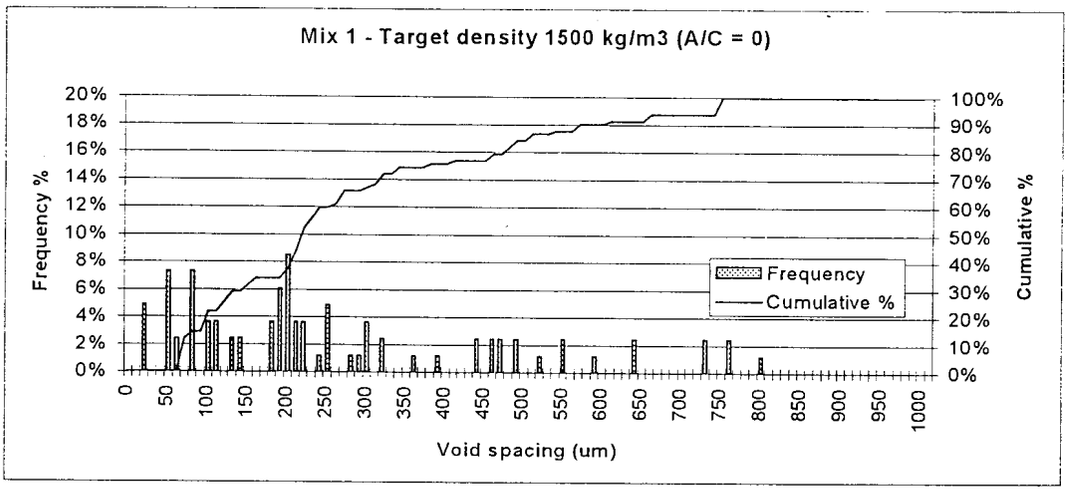
Mix 1 - Target density 1500 kg/m3 (A/C = 0)
Frequency %
Cumulative %
Frequency
Cumulative %
Void spacing (um)

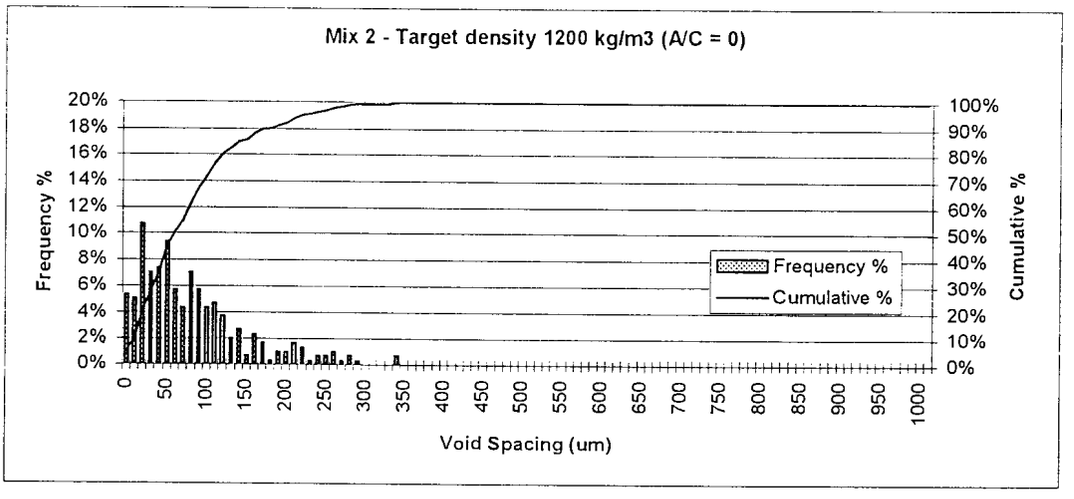
Mix 2 - Target density 1200 kg/m3 (A/C = 0)
Frequency %
Cumulative %
Frequency %
Cumulative %
Void Spacing (um)

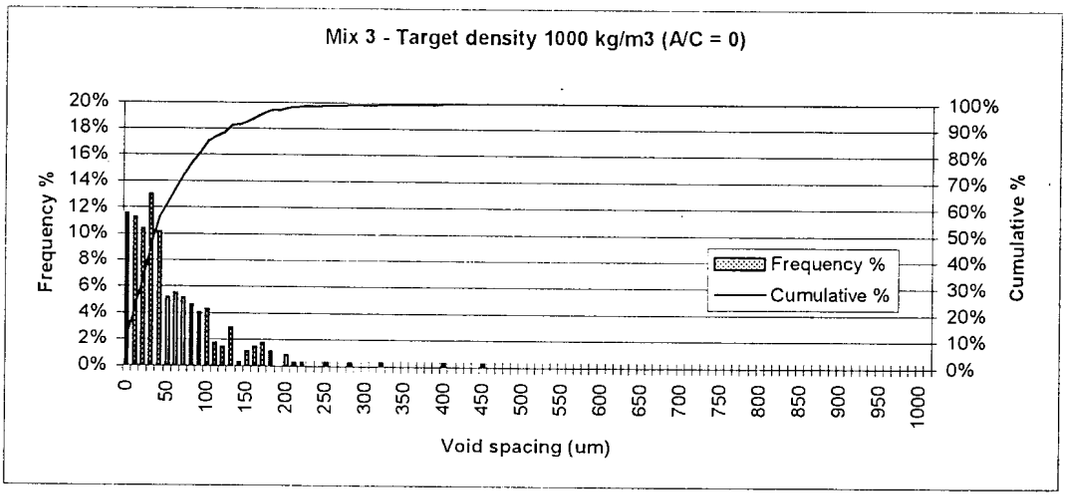
Mix 3 - Target density 1000 kg/m3 (A/C = 0)
Frequency %
Cumulative %
Frequency %
Cumulative %
Void spacing (um)

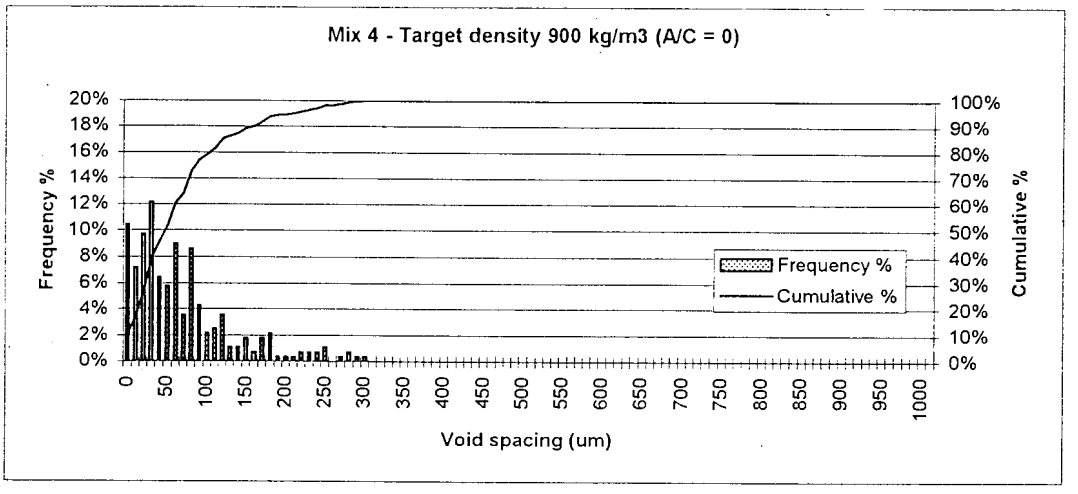
Mix 4 - Target density 900 kg/m3 (A/C = 0)
Frequency %
Cumulative %
Void spacing (um)

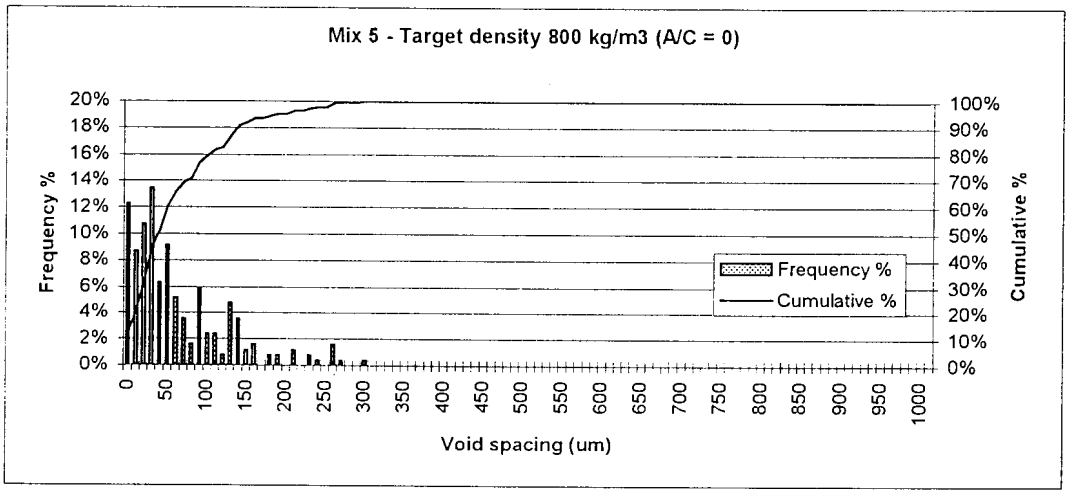
Mix 5 - Target density 800 kg/m3 (A/C = 0)
Frequency %
Cumulative %
Void spacing (um)

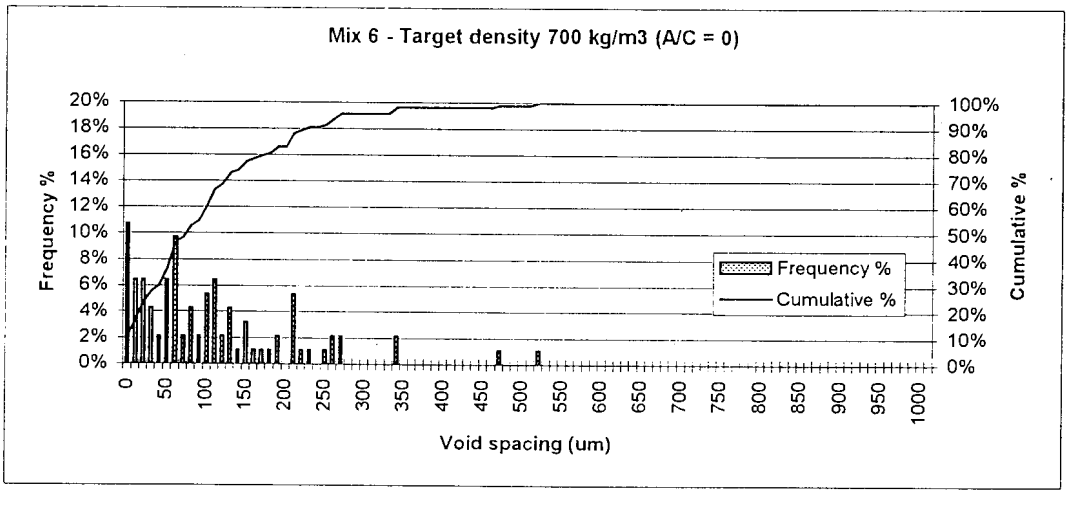
Mix 6 - Target density 700 kg/m3 (A/C = 0)
Frequency %
Cumulative %
Void spacing (um)

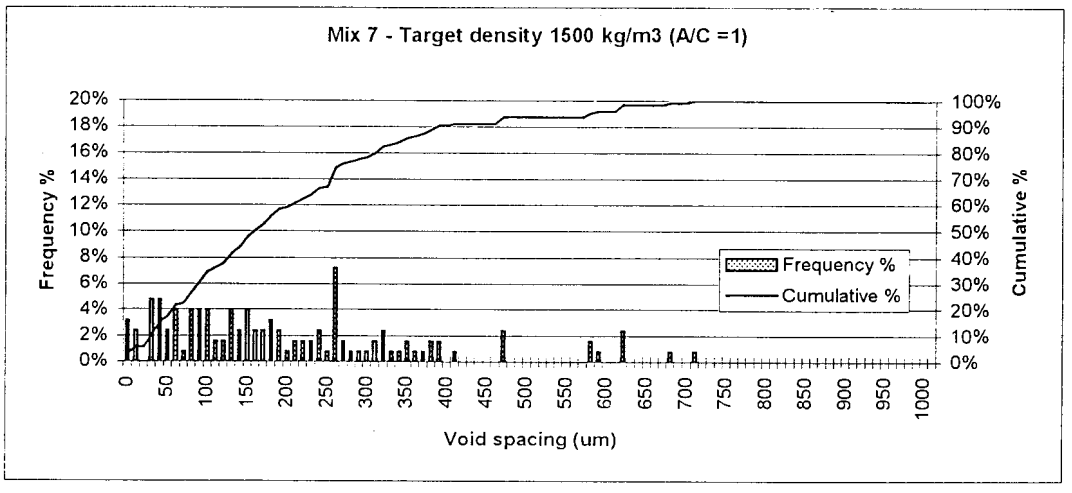
Mix 7 - Target density 1500 kg/m3 (A/C =1)
Frequency %
Cumulative %
Void spacing (um)

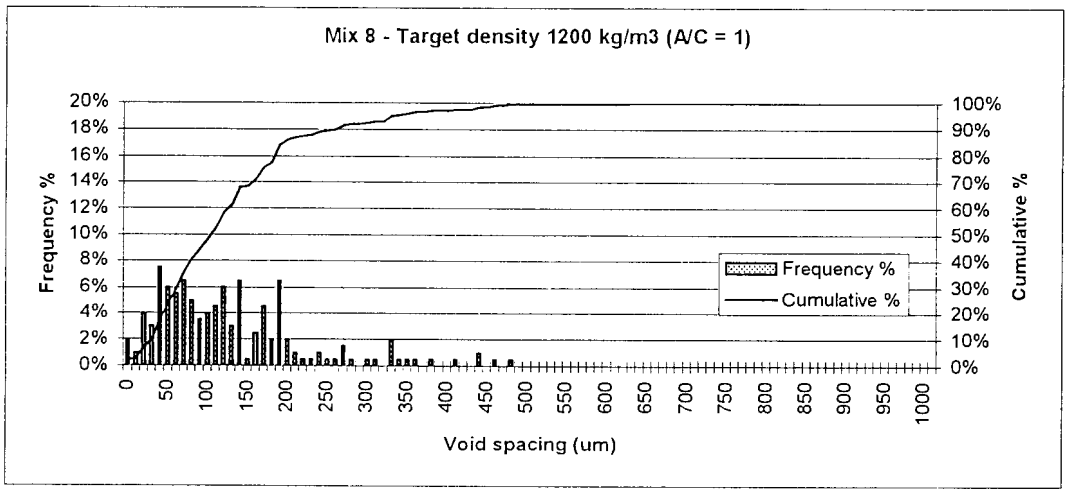
Mix 8 - Target density 1200 kg/m3 (A/C = 1)
Frequency %
Cumulative %
Void spacing (um)

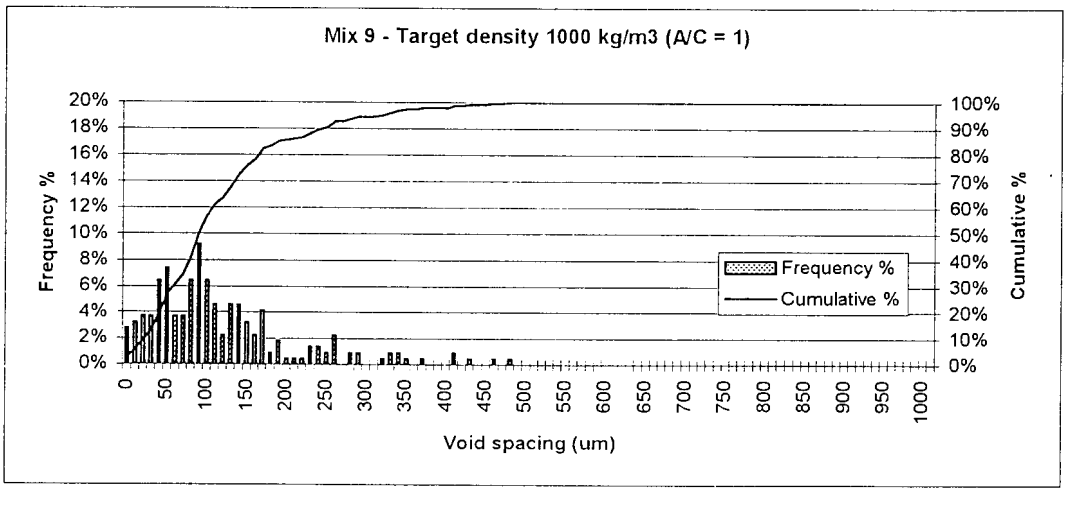
Mix 9 - Target density 1000 kg/m3 (A/C = 1)
Frequency %
Cumulative %
Void spacing (um)

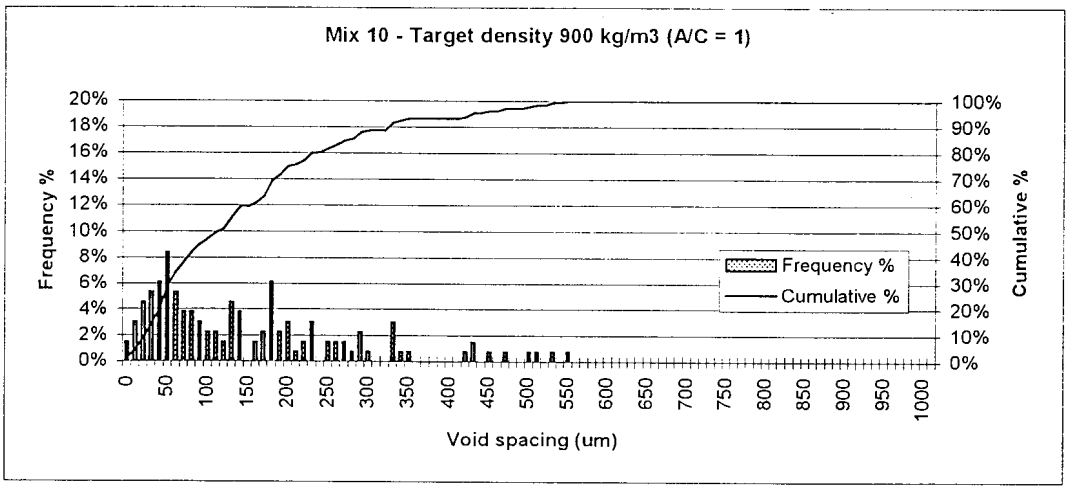
Mix 10 - Target density 900 kg/m3 (A/C = 1)
Frequency %
Cumulative %
Void spacing (um)

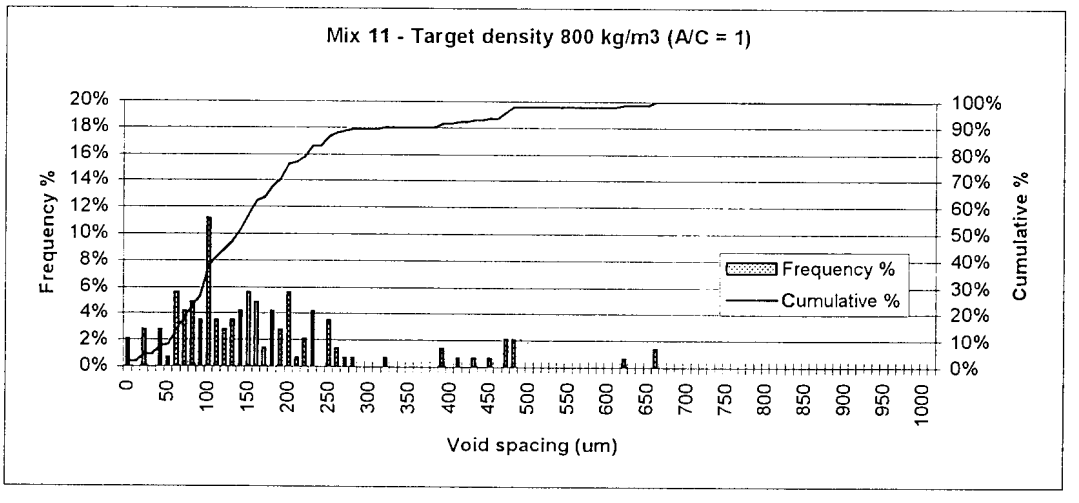
Mix 11 - Target density 800 kg/m3 (A/C = 1)
Frequency %
Cumulative %
Void spacing (um)

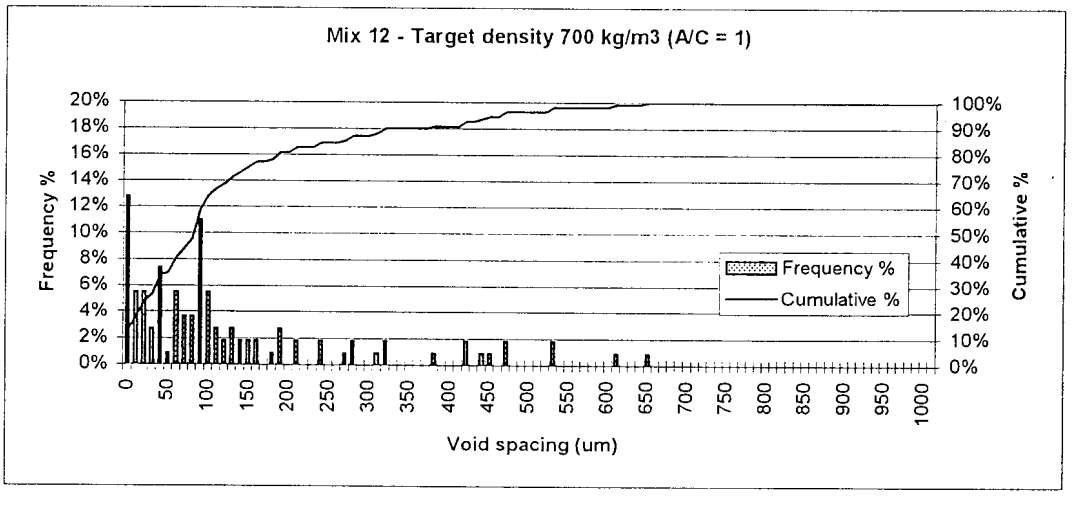
Mix 12 - Target density 700 kg/m3 (A/C = 1)
Frequency %
Cumulative %
Void spacing (um)

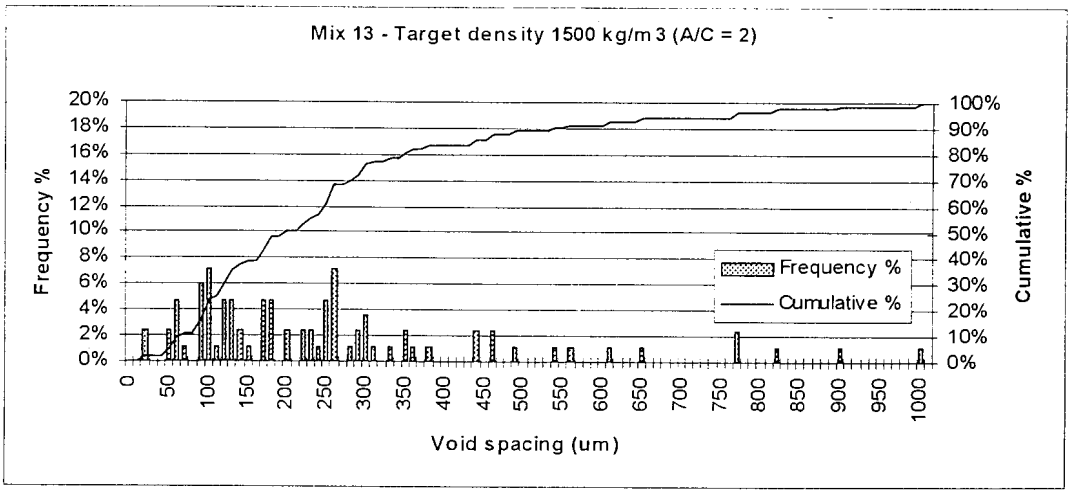
Mix 13 - Target density 1500 kg/m3 (A/C = 2)
Frequency %
Cumulative %
Void spacing (um)

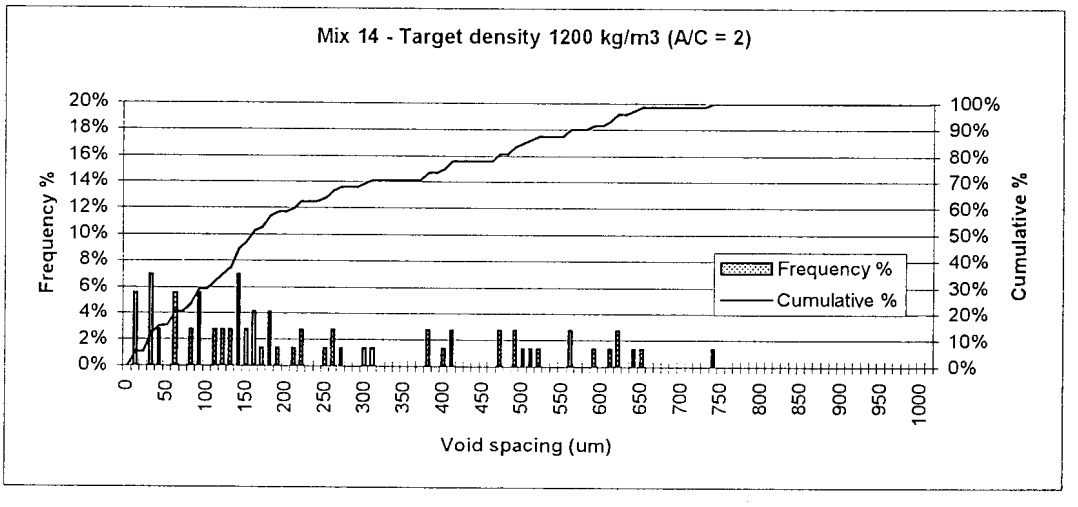
Mix 14 - Target density 1200 kg/m3 (A/C = 2)
Frequency %
Cumulative %
Void spacing (um)

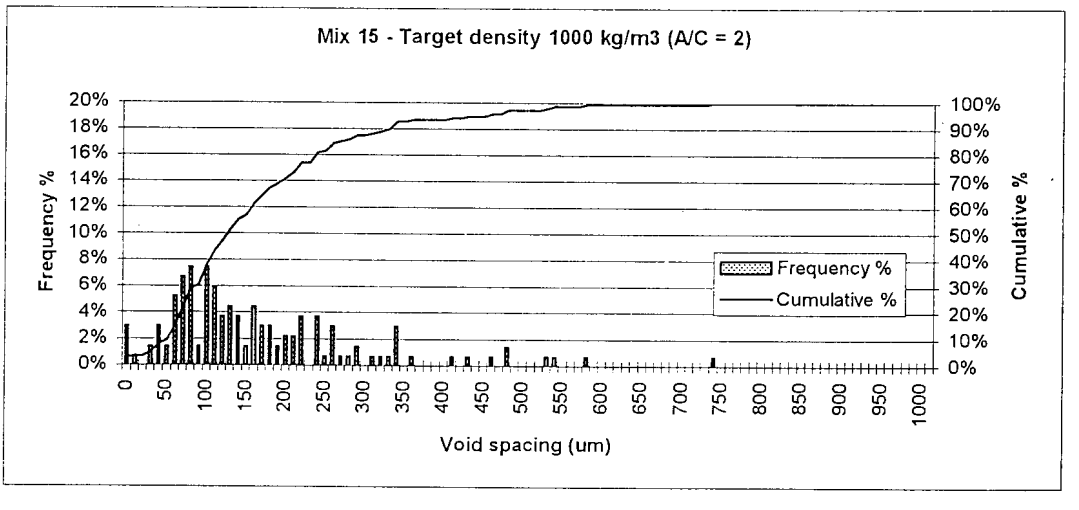
Mix 15 - Target density 1000 kg/m3 (A/C = 2)
Frequency %
Cumulative %
Void spacing (um)

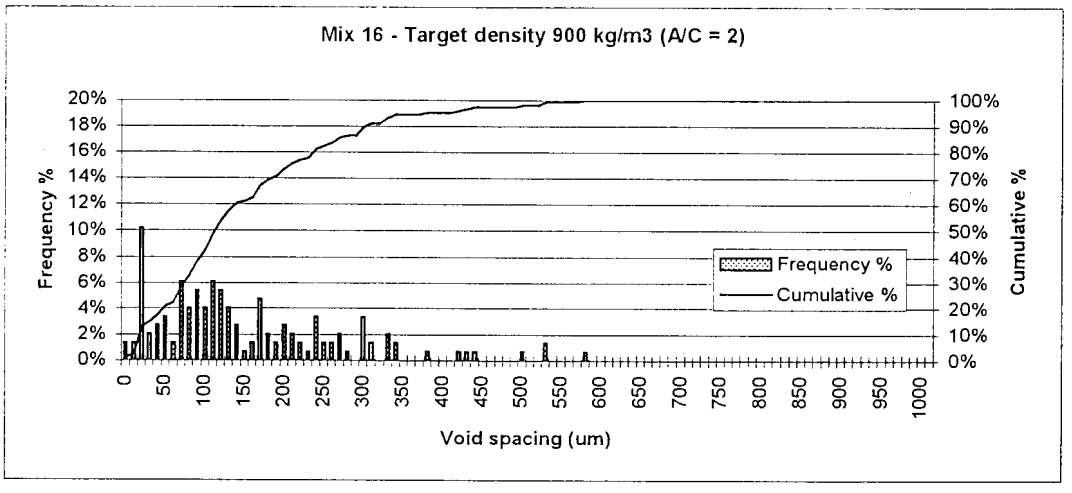
Mix 16 - Target density 900 kg/m3 (A/C = 2)
Frequency %
Cumulative %
Void spacing (um)

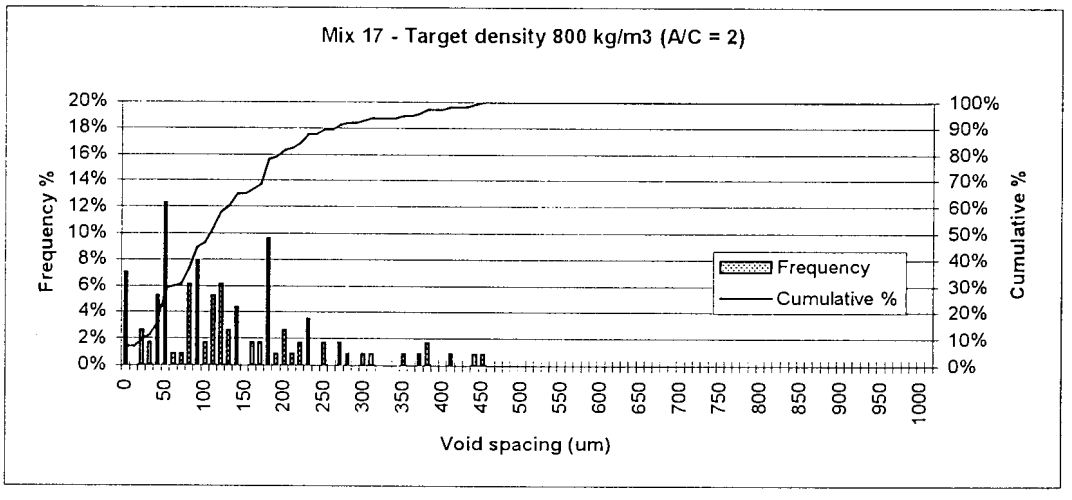
Mix 17 - Target density 800 kg/m3 (A/C = 2)
Frequency
Cumulative %
Void spacing (um)

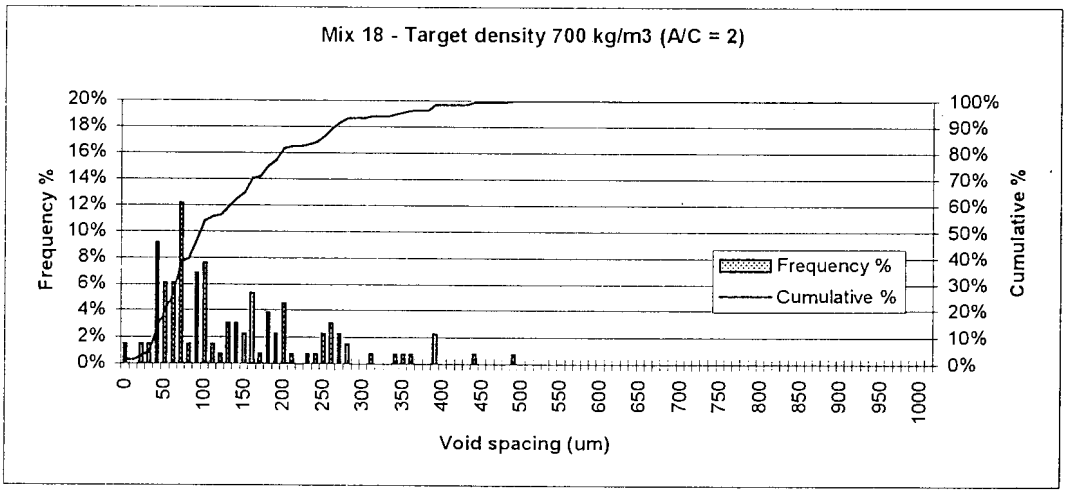
Mix 18 - Target density 700 kg/m3 (A/C = 2)
Frequency %
Cumulative %
Void spacing (um)

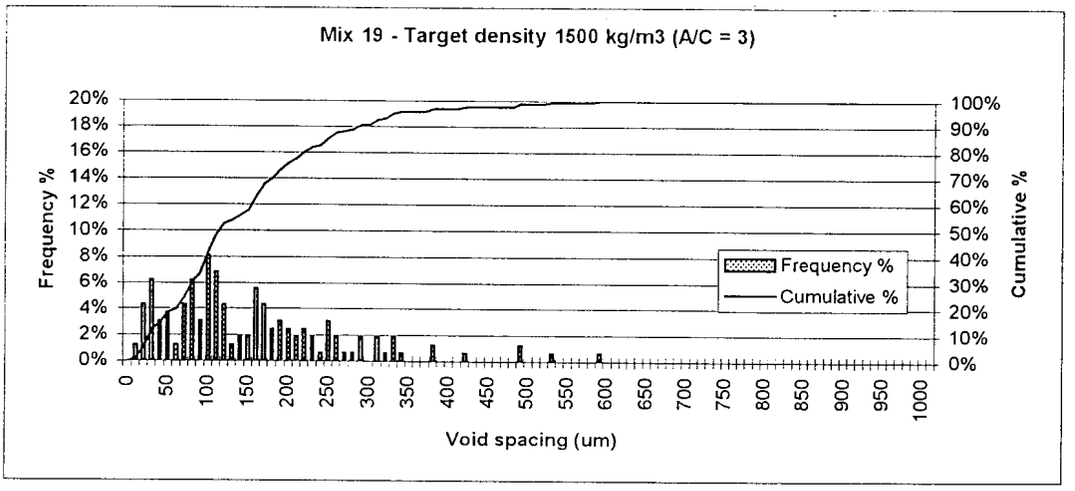
Mix 19 - Target density 1500 kg/m3 (A/C = 3)
Frequency %
Cumulative %
Void spacing (um)

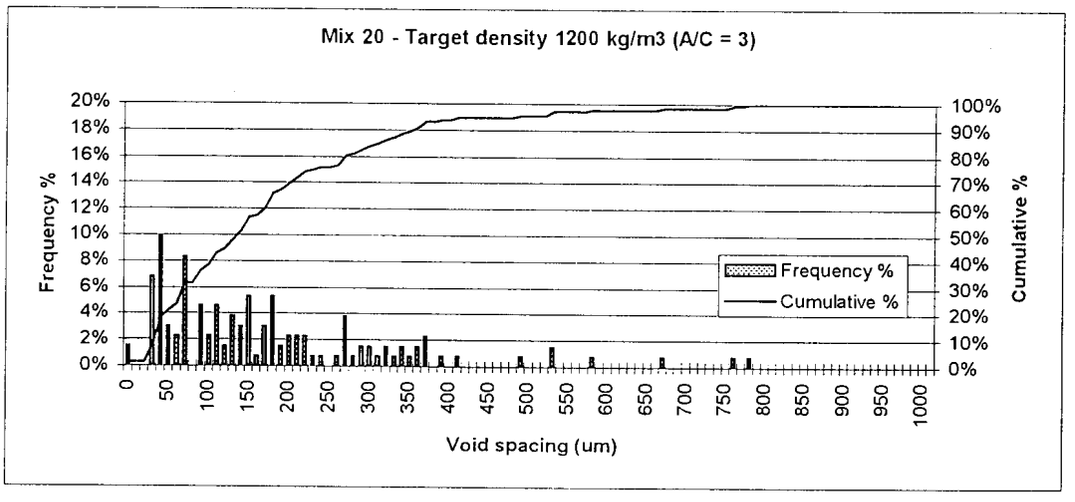
Mix 20 - Target density 1200 kg/m3 (A/C = 3)
Frequency %
Cumulative %
Void spacing (um)

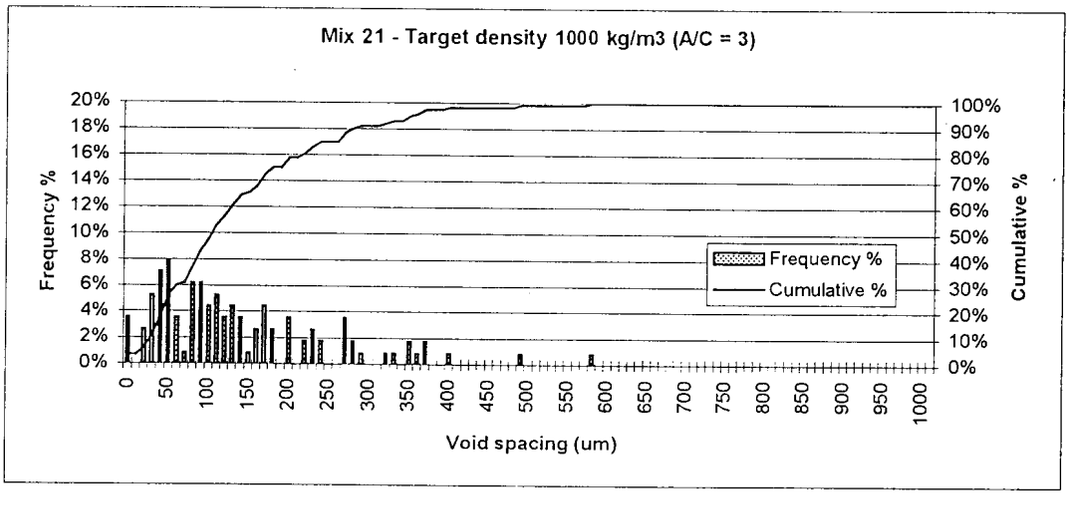
Mix 21 - Target density 1000 kg/m3 (A/C = 3)
Frequency %
Cumulative %
Void spacing (um)

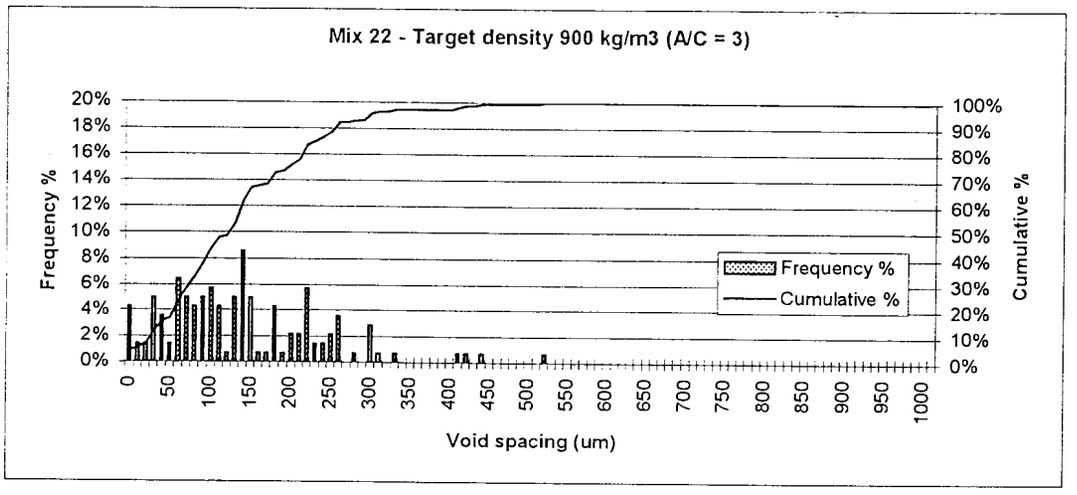
Mix 22 - Target density 900 kg/m3 (A/C = 3)
Frequency %
Cumulative %
Void spacing (um)

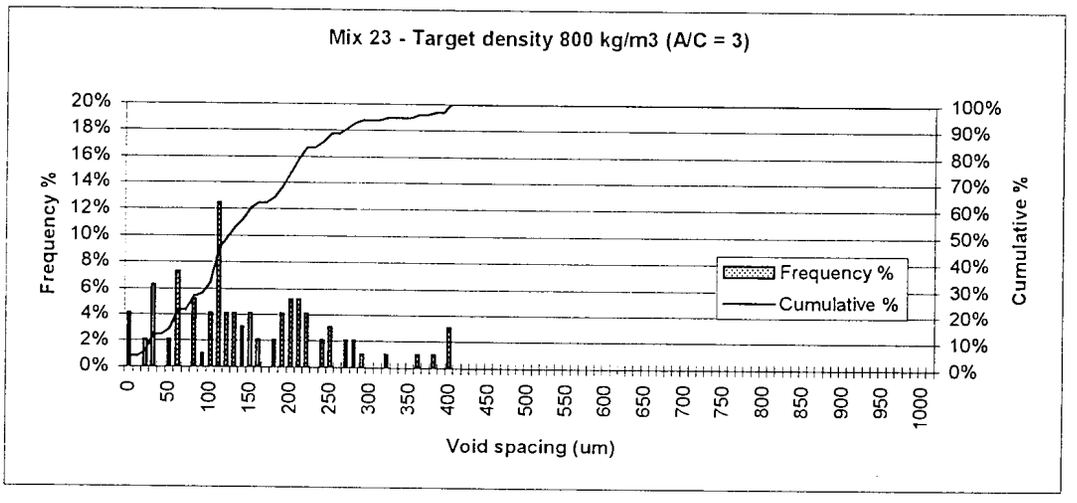
Mix 23 - Target density 800 kg/m3 (A/C = 3)
Frequency %
Cumulative %
Void spacing (um)

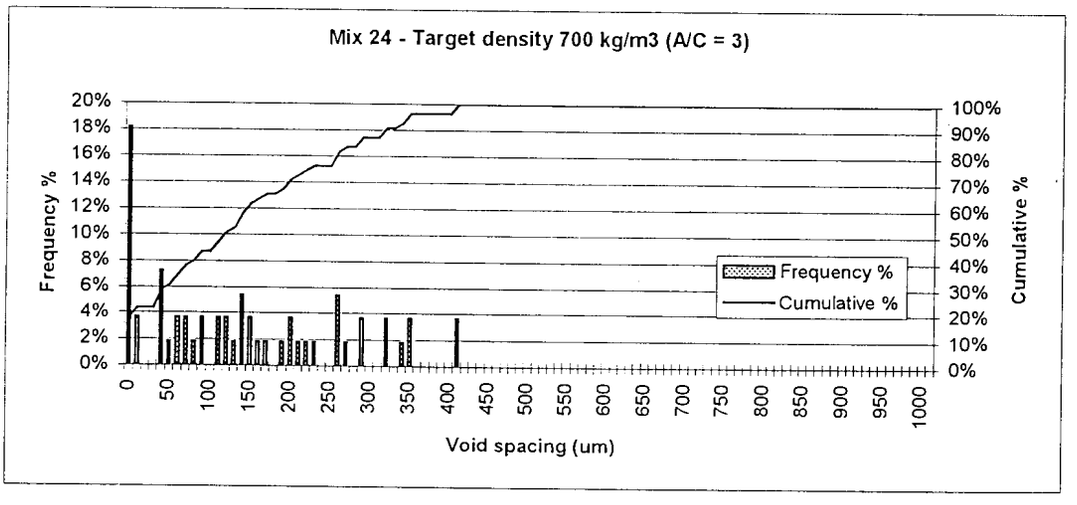
Mix 24 - Target density 700 kg/m3 (A/C = 3)
Frequency %
Cumulative %
Void spacing (um)

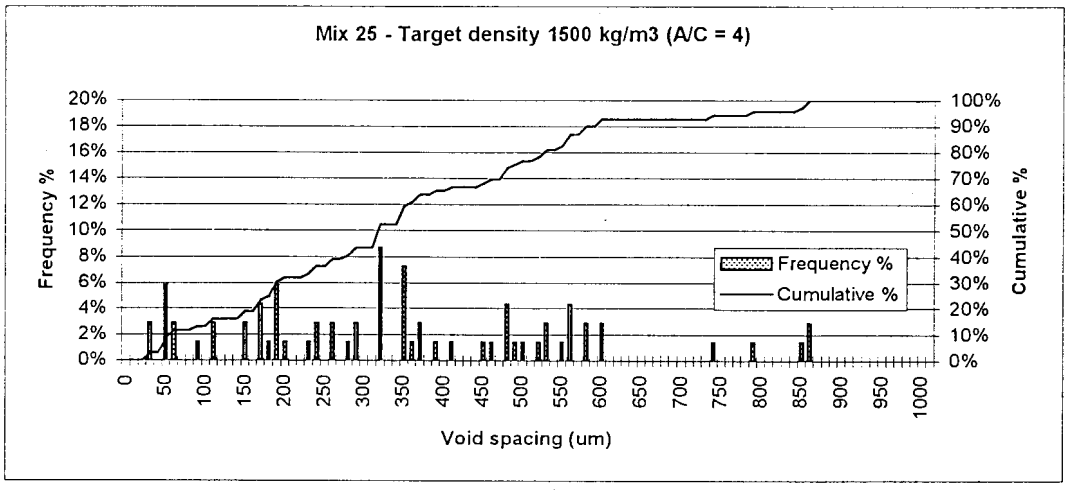
Mix 25 - Target density 1500 kg/m3 (A/C = 4)
Frequency %
Cumulative %
Frequency %
Cumulative %
Void spacing (um)

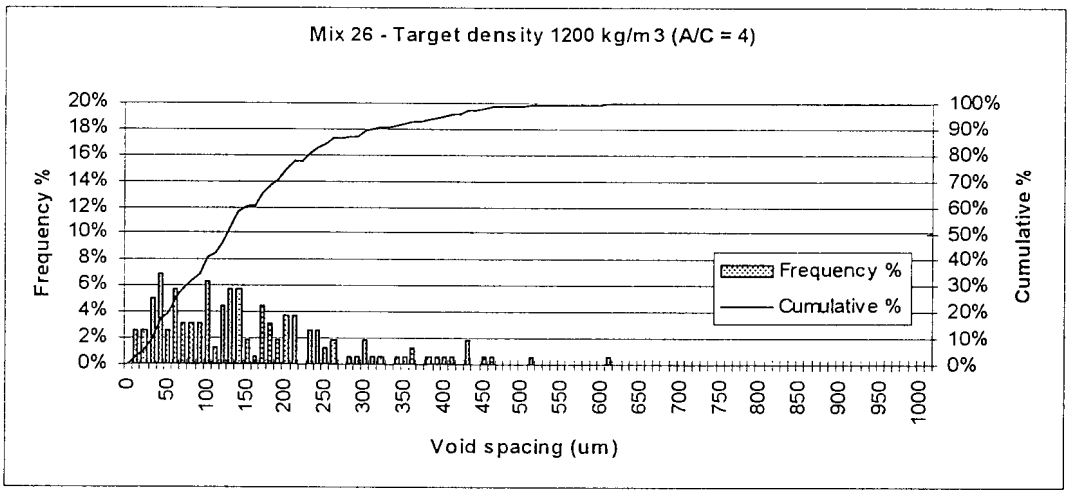
Mix 26 - Target density 1200 kg/m3 (A/C = 4)
Frequency %
Cumulative %
Frequency %
Cumulative %
Void spacing (um)

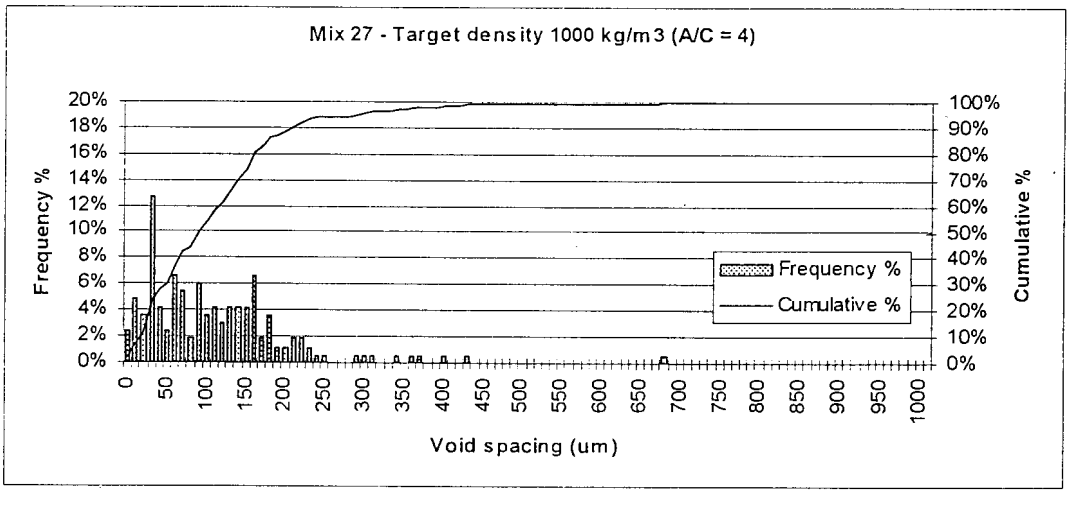
Mix 27 - Target density 1000 kg/m3 (A/C = 4)
Frequency %
Cumulative %
Frequency %
Cumulative %
Void spacing (um)

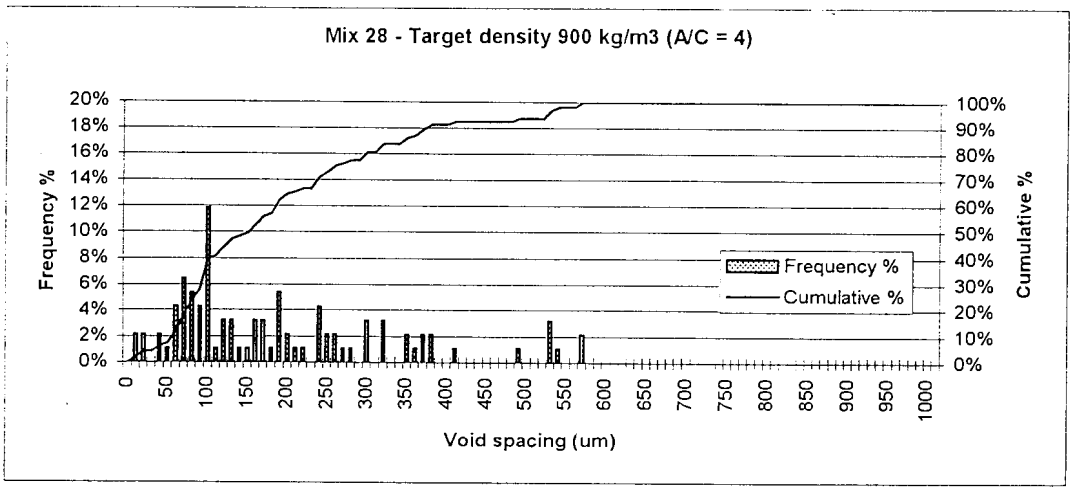
Mix 28 - Target density 900 kg/m3 (A/C = 4)
Frequency %
Cumulative %
Void spacing (um)

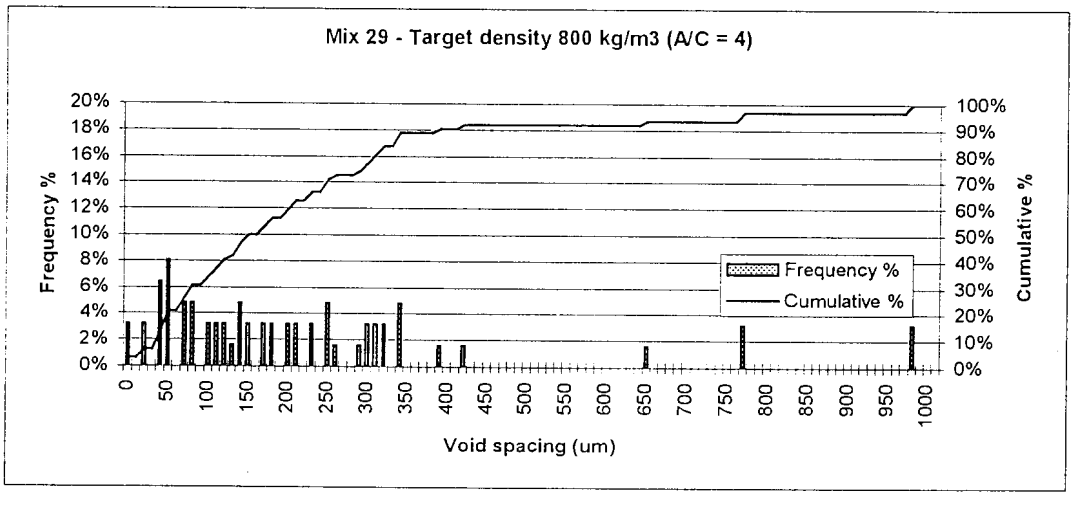
Mix 29 - Target density 800 kg/m3 (A/C = 4)
Frequency %
Cumulative %
Void spacing (um)

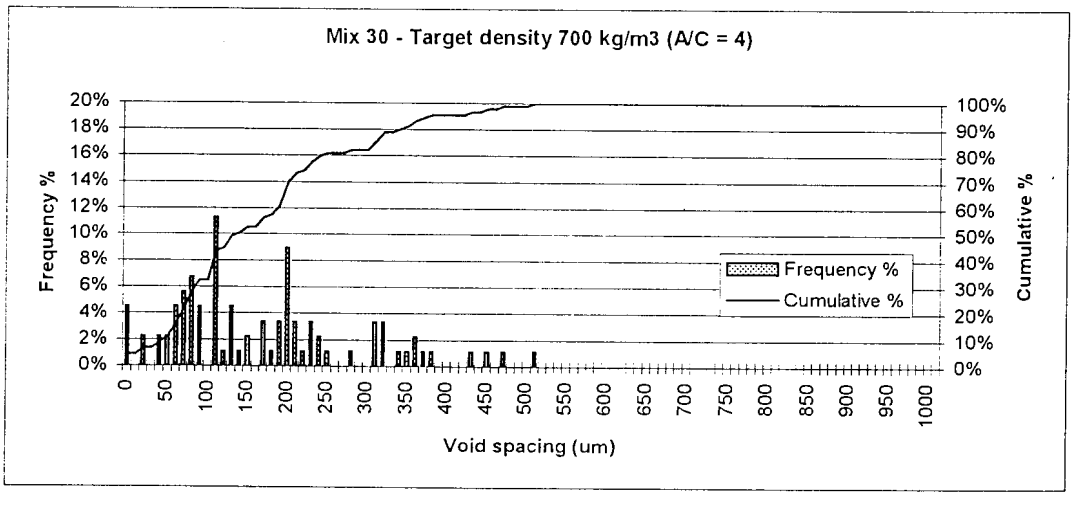
Mix 30 - Target density 700 kg/m3 (A/C = 4)
Frequency %
Cumulative %
Void spacing (um)

APPENDIX F

EXPONENTIAL FIT FOR CUMULATIVE PERCENTAGE OVERSIZE AIR-VOID SPACING OF MIXTURES

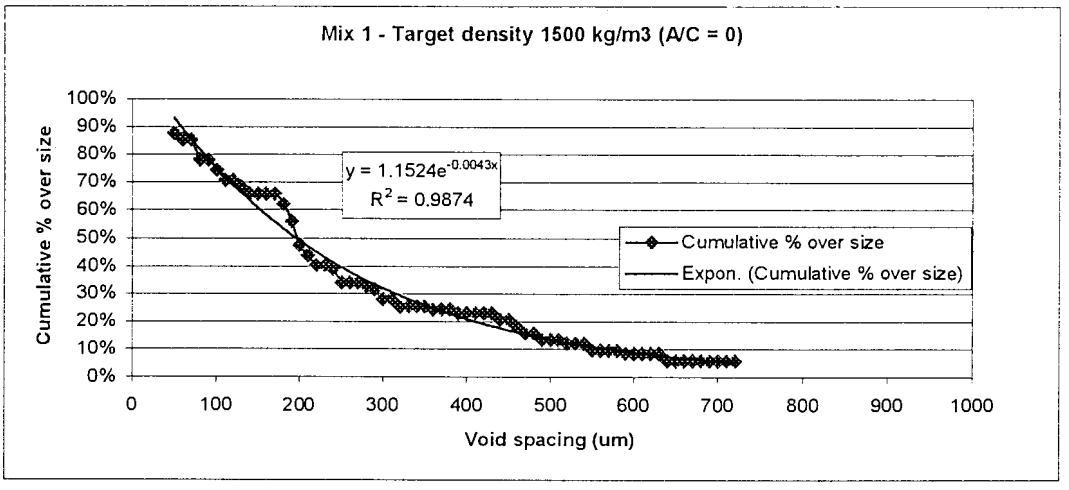
Mix 1 - Target density 1500 kg/m3 (A/C = 0)
Cumulative % over size
100%
90%
80%
70%
60%
50%
40%
30%
20%
10%
0%
y = 1.1524e-0.0043x
R2 = 0.9874
Cumulative % over size
Expon. (Cumulative % over size)
0
100
200
300
400
500
600
700
800
900
1000
Void spacing (um)

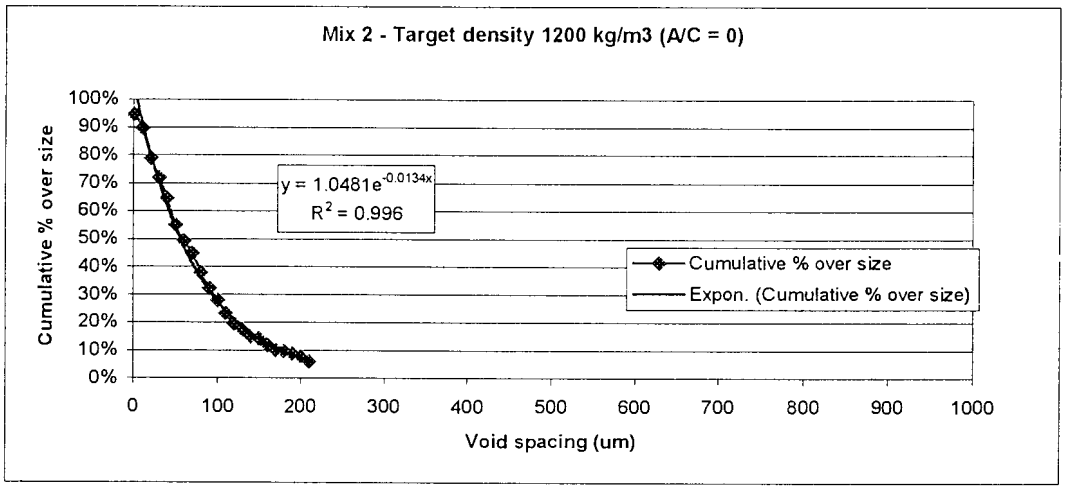
Mix 2 - Target density 1200 kg/m3 (A/C = 0)
Cumulative % over size
100%
90%
80%
70%
60%
50%
40%
30%
20%
10%
0%
y = 1.0481e-0.0134x
R2 = 0.996
Cumulative % over size
Expon. (Cumulative % over size)
0
100
200
300
400
500
600
700
800
900
1000
Void spacing (um)

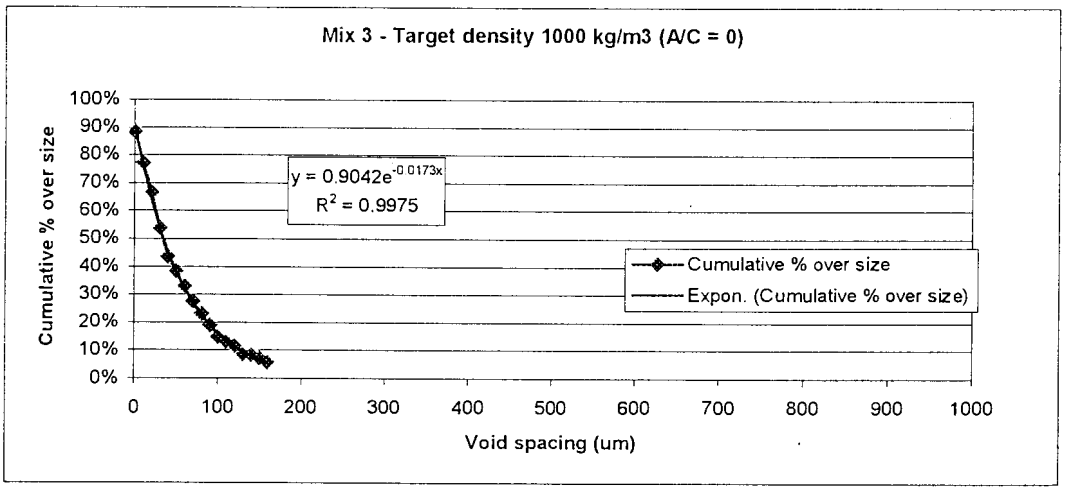
Mix 3 - Target density 1000 kg/m3 (A/C = 0)
Cumulative % over size
100%
90%
80%
70%
60%
50%
40%
30%
20%
10%
0%
y = 0.9042e-0.0173x
R2 = 0.9975
Cumulative % over size
Expon. (Cumulative % over size)
0
100
200
300
400
500
600
700
800
900
1000
Void spacing (um)

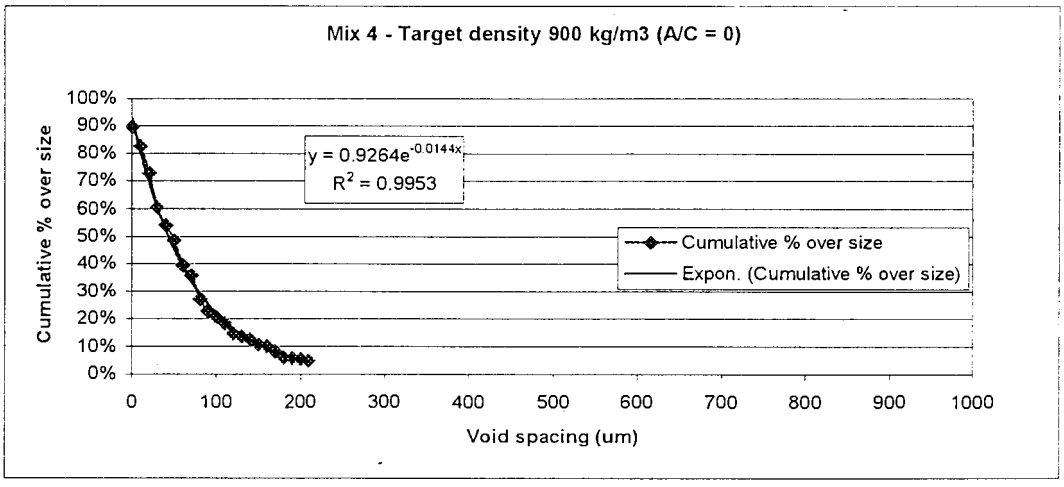
Mix 4 - Target density 900 kg/m3 (A/C = 0)
Cumulative % over size
100%
90%
80%
70%
60%
50%
40%
30%
20%
10%
0%
y = 0.9264e-0.0144x
R2 = 0.9953
Cumulative % over size
Expon. (Cumulative % over size)
0
100
200
300
400
500
600
700
800
900
1000
Void spacing (um)

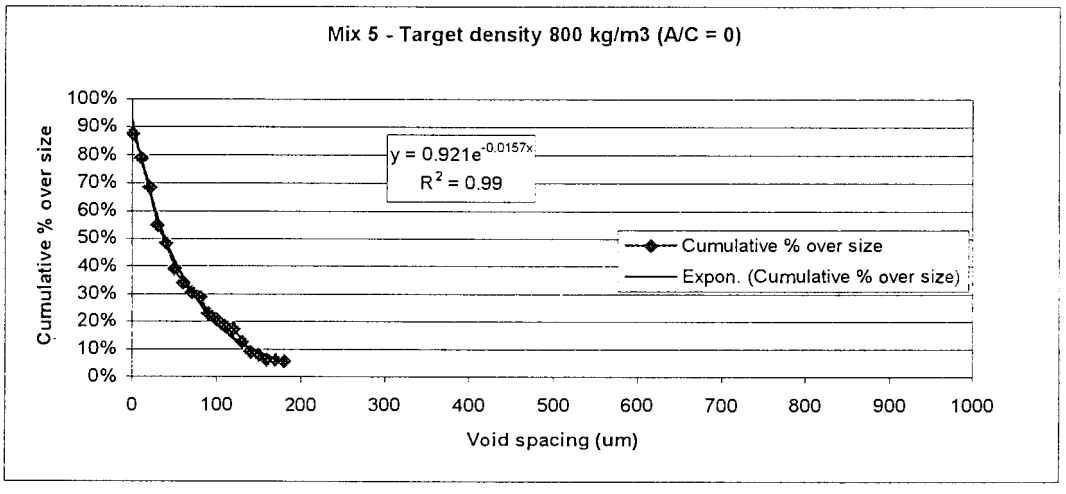
Mix 5 - Target density 800 kg/m3 (A/C = 0)
Cumulative % over size
100%
90%
80%
70%
60%
50%
40%
30%
20%
10%
0%
y = 0.921e-0.0157x
R2 = 0.99
Cumulative % over size
Expon. (Cumulative % over size)
0
100
200
300
400
500
600
700
800
900
1000
Void spacing (um)

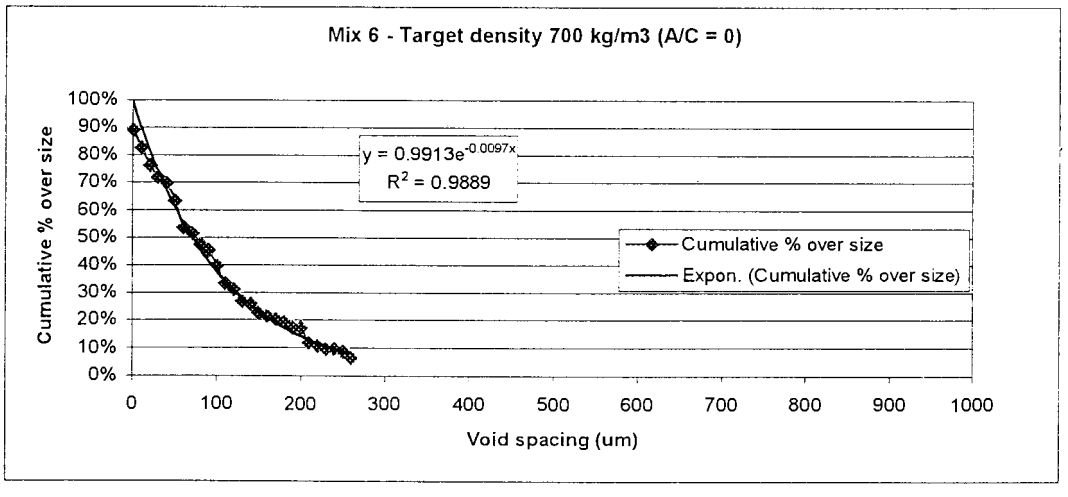
Mix 6 - Target density 700 kg/m3 (A/C = 0)
Cumulative % over size
100%
90%
80%
70%
60%
50%
40%
30%
20%
10%
0%
y = 0.9913e-0.0097x
R2 = 0.9889
Cumulative % over size
Expon. (Cumulative % over size)
0
100
200
300
400
500
600
700
800
900
1000
Void spacing (um)

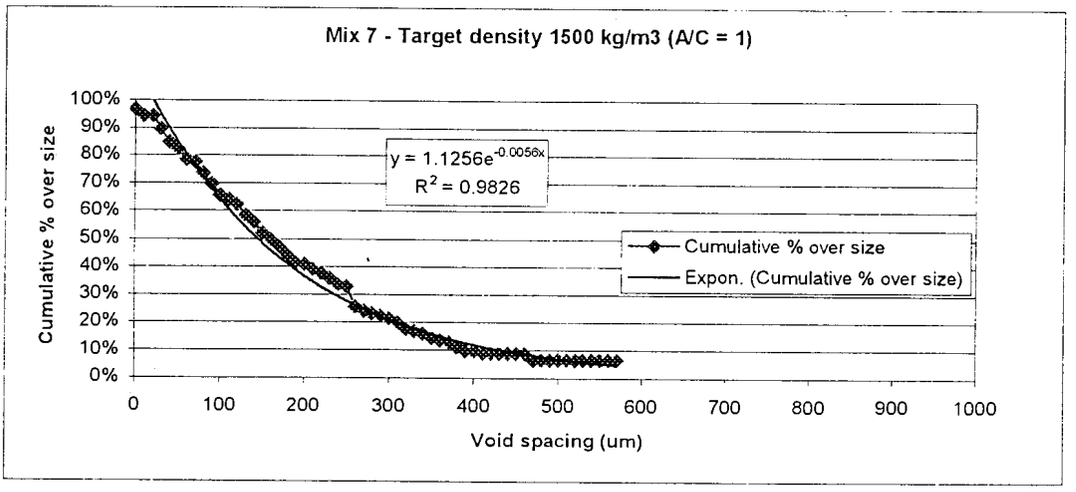
Mix 7 - Target density 1500 kg/m3 (A/C = 1)
Cumulative % over size
100%
90%
80%
70%
60%
50%
40%
30%
20%
10%
0%
y = 1.1256e-0.0056x
R2 = 0.9826
Cumulative % over size
Expon. (Cumulative % over size)
0
100
200
300
400
500
600
700
800
900
1000
Void spacing (um)

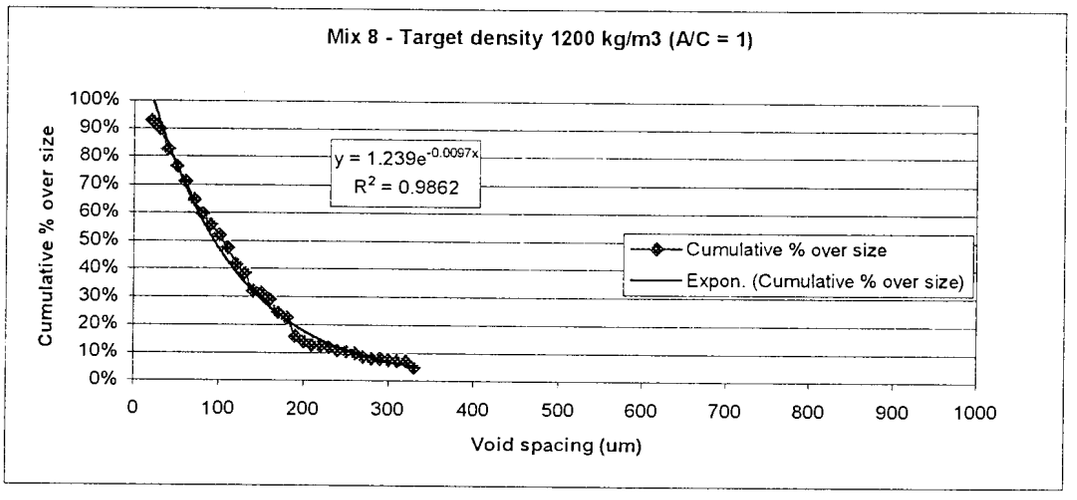
Mix 8 - Target density 1200 kg/m3 (A/C = 1)
Cumulative % over size
100%
90%
80%
70%
60%
50%
40%
30%
20%
10%
0%
y = 1.239e-0.0097x
R2 = 0.9862
Cumulative % over size
Expon. (Cumulative % over size)
0
100
200
300
400
500
600
700
800
900
1000
Void spacing (um)

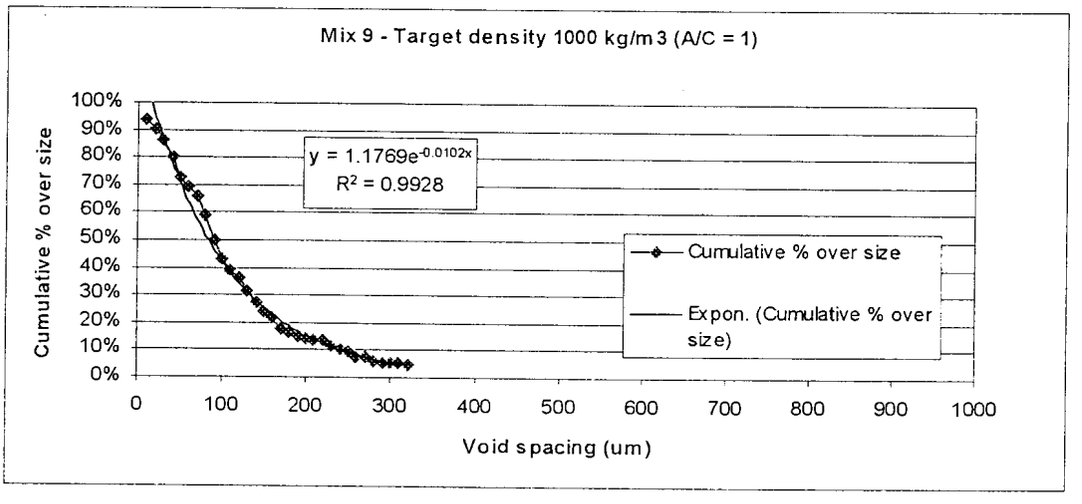
Mix 9 - Target density 1000 kg/m3 (A/C = 1)
Cumulative % over size
100%
90%
80%
70%
60%
50%
40%
30%
20%
10%
0%
y = 1.1769e-0.0102x
R2 = 0.9928
Cumulative % over size
Expon. (Cumulative % over size)
0
100
200
300
400
500
600
700
800
900
1000
Void spacing (um)

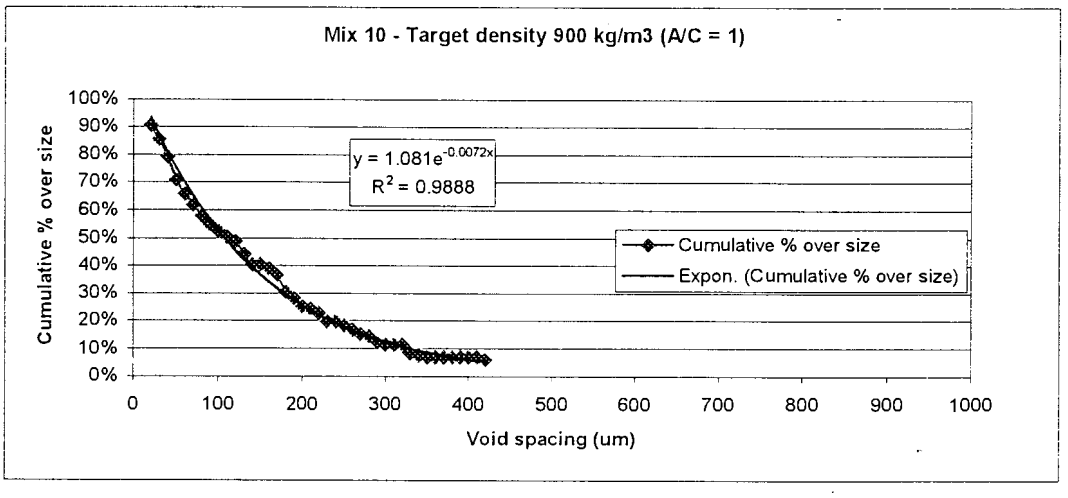
Mix 10 - Target density 900 kg/m3 (A/C = 1)
Cumulative % over size
100%
90%
80%
70%
60%
50%
40%
30%
20%
10%
0%
y = 1.081e-0.0072x
R2 = 0.9888
Cumulative % over size
Expon. (Cumulative % over size)
0
100
200
300
400
500
600
700
800
900
1000
Void spacing (um)

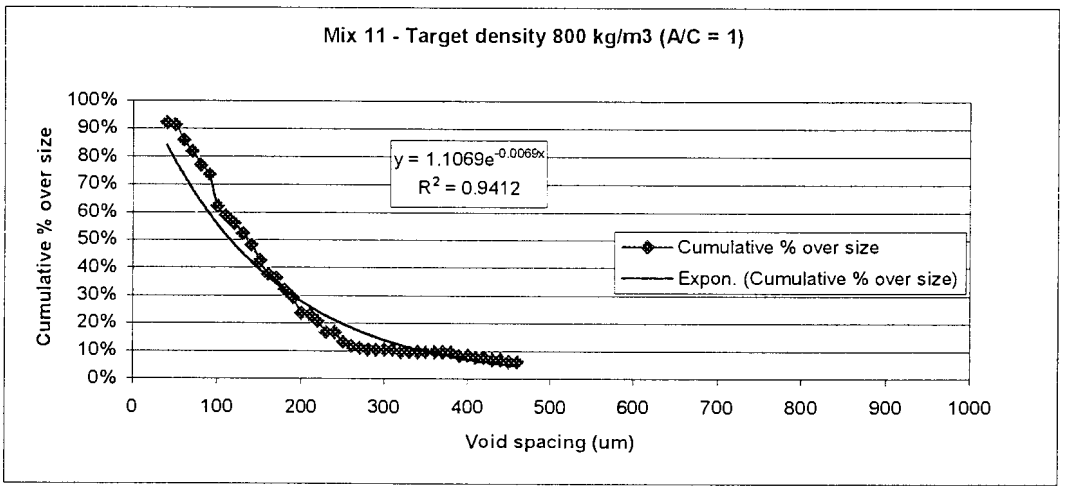
Mix 11 - Target density 800 kg/m3 (A/C = 1)
Cumulative % over size
100%
90%
80%
70%
60%
50%
40%
30%
20%
10%
0%
y = 1.1069e-0.0069x
R2 = 0.9412
Cumulative % over size
Expon. (Cumulative % over size)
0
100
200
300
400
500
600
700
800
900
1000
Void spacing (um)

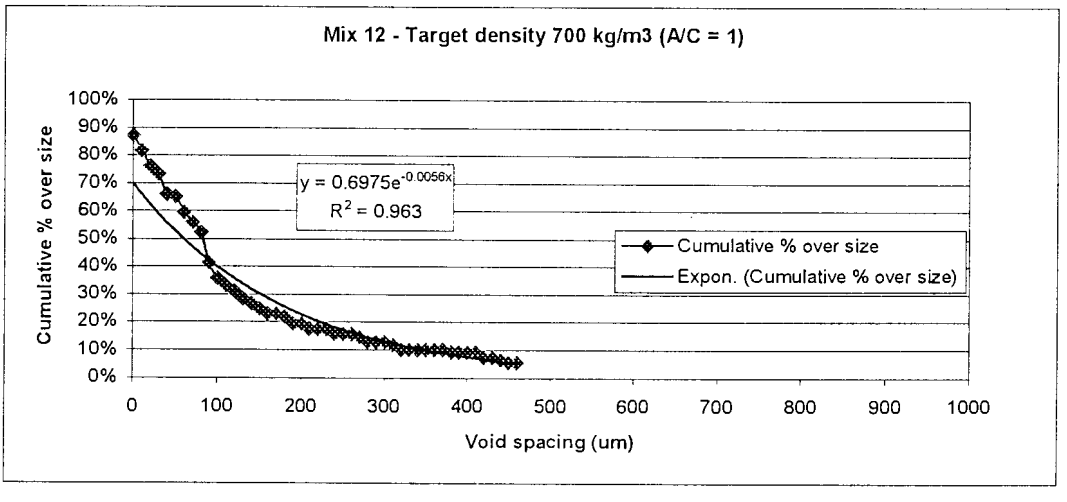
Mix 12 - Target density 700 kg/m3 (A/C = 1)
Cumulative % over size
100%
90%
80%
70%
60%
50%
40%
30%
20%
10%
0%
y = 0.6975e-0.0056x
R2 = 0.963
Cumulative % over size
Expon. (Cumulative % over size)
0
100
200
300
400
500
600
700
800
900
1000
Void spacing (um)

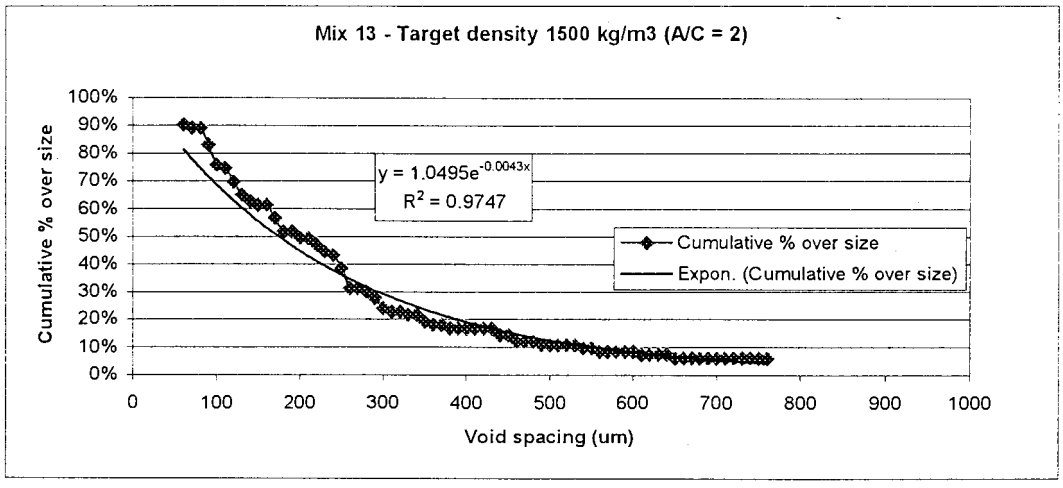
Mix 13 - Target density 1500 kg/m3 (A/C = 2)
Cumulative % over size
100%
90%
80%
70%
60%
50%
40%
30%
20%
10%
0%
y = 1.0495e-0.0043x
R2 = 0.9747
Cumulative % over size
Expon. (Cumulative % over size)
0
100
200
300
400
500
600
700
800
900
1000
Void spacing (um)

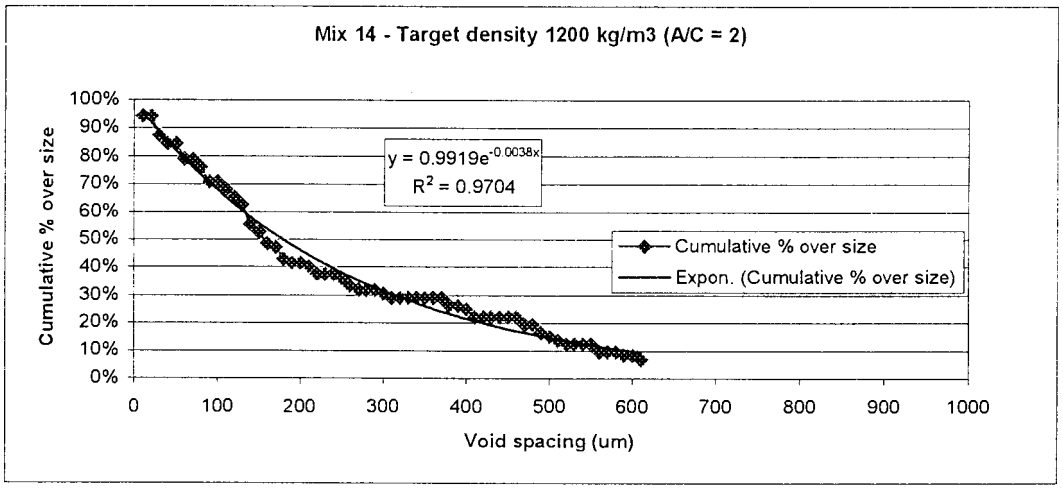
Mix 14 - Target density 1200 kg/m3 (A/C = 2)
Cumulative % over size
100%
90%
80%
70%
60%
50%
40%
30%
20%
10%
0%
y = 0.9919e-0.0038x
R2 = 0.9704
Cumulative % over size
Expon. (Cumulative % over size)
0
100
200
300
400
500
600
700
800
900
1000
Void spacing (um)

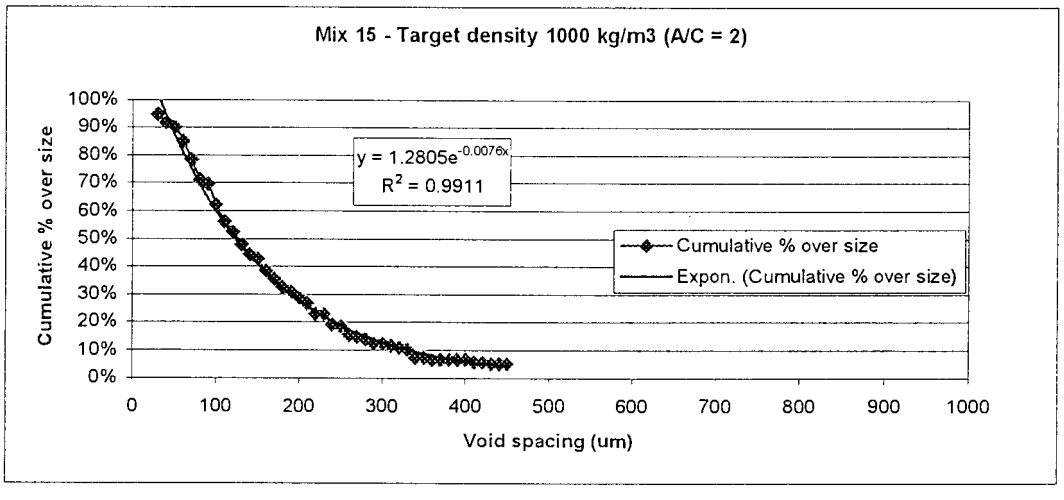
Mix 15 - Target density 1000 kg/m3 (A/C = 2)
Cumulative % over size
100%
90%
80%
70%
60%
50%
40%
30%
20%
10%
0%
y = 1.2805e-0.0076x
R2 = 0.9911
Cumulative % over size
Expon. (Cumulative % over size)
0
100
200
300
400
500
600
700
800
900
1000
Void spacing (um)

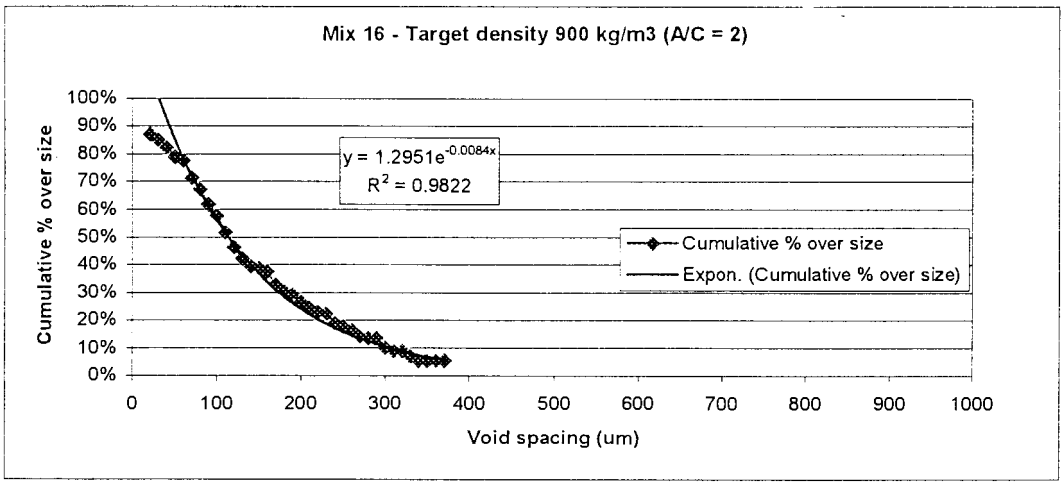
Mix 16 - Target density 900 kg/m3 (A/C = 2)
Cumulative % over size
100%
90%
80%
70%
60%
50%
40%
30%
20%
10%
0%
y = 1.2951e-0.0084x
R2 = 0.9822
Cumulative % over size
Expon. (Cumulative % over size)
0
100
200
300
400
500
600
700
800
900
1000
Void spacing (um)

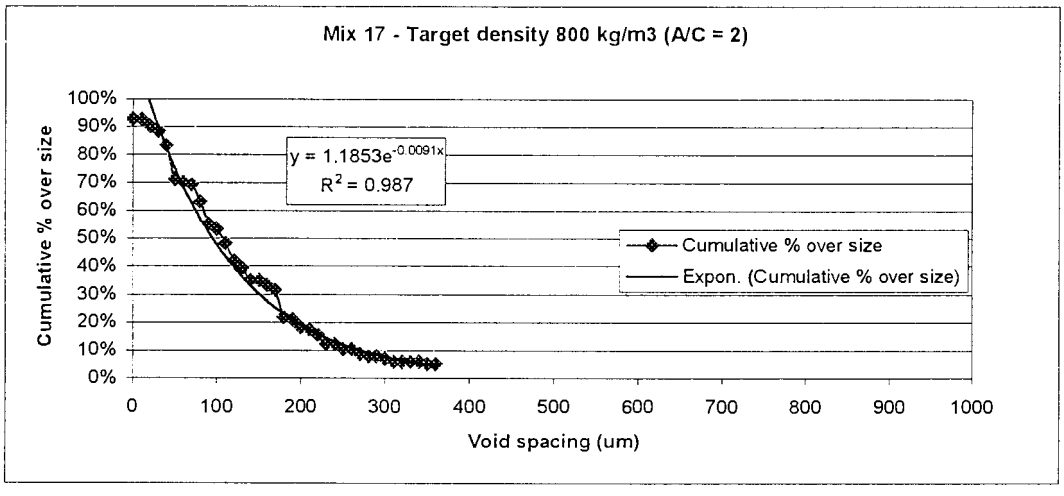
Mix 17 - Target density 800 kg/m3 (A/C = 2)
Cumulative % over size
100%
90%
80%
70%
60%
50%
40%
30%
20%
10%
0%
y = 1.1853e-0.0091x
R2 = 0.987
Cumulative % over size
Expon. (Cumulative % over size)
0
100
200
300
400
500
600
700
800
900
1000
Void spacing (um)

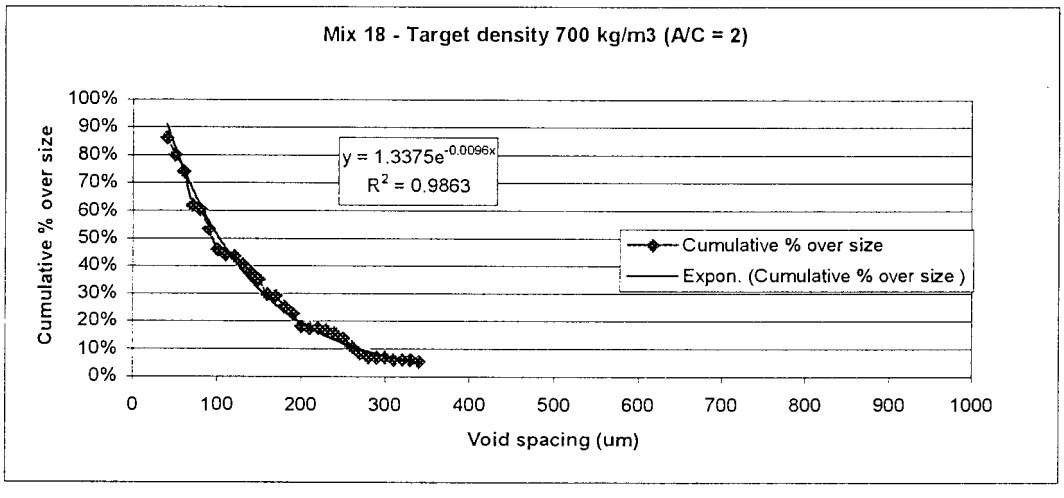
Mix 18 - Target density 700 kg/m3 (A/C = 2)
Cumulative % over size
100%
90%
80%
70%
60%
50%
40%
30%
20%
10%
0%
y = 1.3375e-0.0096x
R2 = 0.9863
Cumulative % over size
Expon. (Cumulative % over size)
0
100
200
300
400
500
600
700
800
900
1000
Void spacing (um)

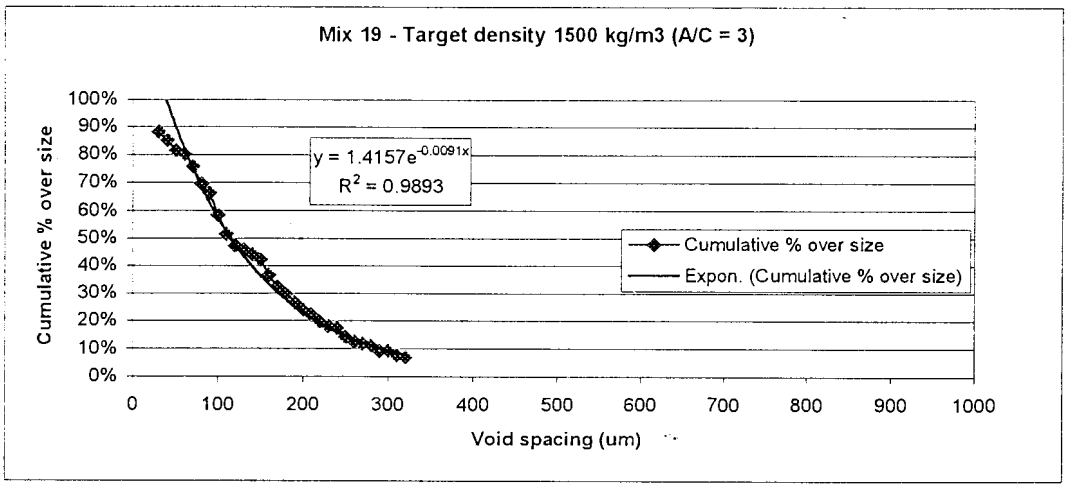
Mix 19 - Target density 1500 kg/m3 (A/C = 3)
Cumulative % over size
100%
90%
80%
70%
60%
50%
40%
30%
20%
10%
0%
y = 1.4157e-0.0091x
R2 = 0.9893
Cumulative % over size
Expon. (Cumulative % over size)
0
100
200
300
400
500
600
700
800
900
1000
Void spacing (um)

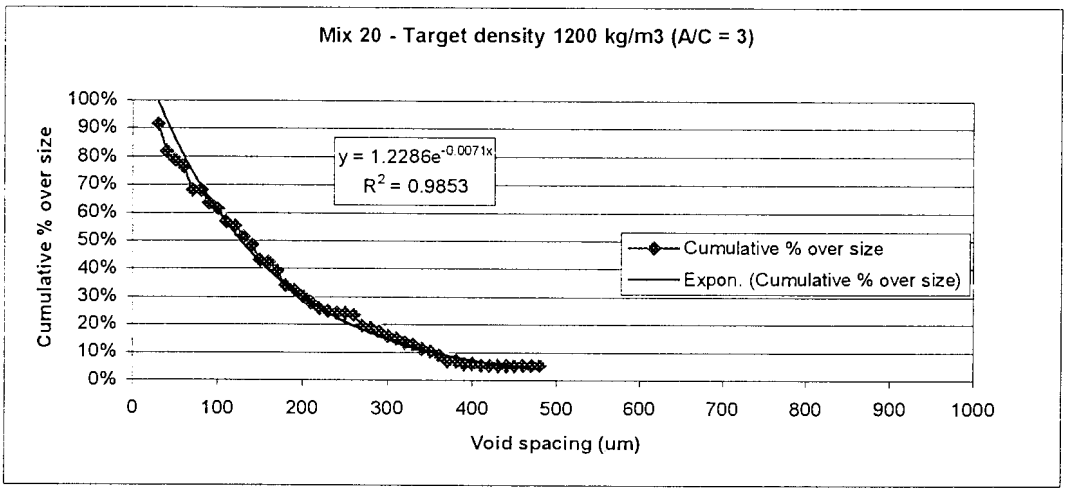
Mix 20 - Target density 1200 kg/m3 (A/C = 3)
Cumulative % over size
100%
90%
80%
70%
60%
50%
40%
30%
20%
10%
0%
y = 1.2286e-0.0071x
R2 = 0.9853
Cumulative % over size
Expon. (Cumulative % over size)
0
100
200
300
400
500
600
700
800
900
1000
Void spacing (um)

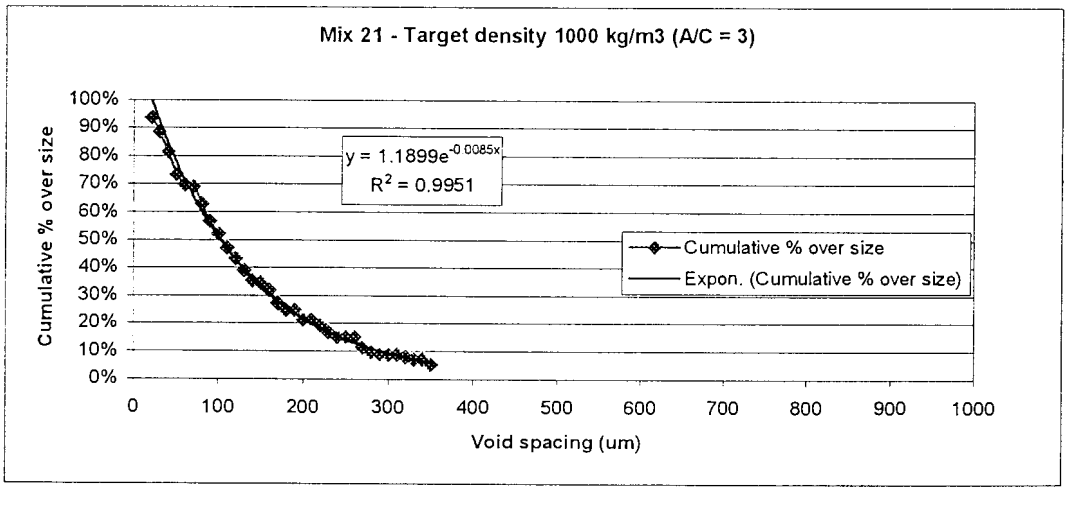
Mix 21 - Target density 1000 kg/m3 (A/C = 3)
Cumulative % over size
100%
90%
80%
70%
60%
50%
40%
30%
20%
10%
0%
y = 1.1899e-0.0085x
R2 = 0.9951
Cumulative % over size
Expon. (Cumulative % over size)
0
100
200
300
400
500
600
700
800
900
1000
Void spacing (um)

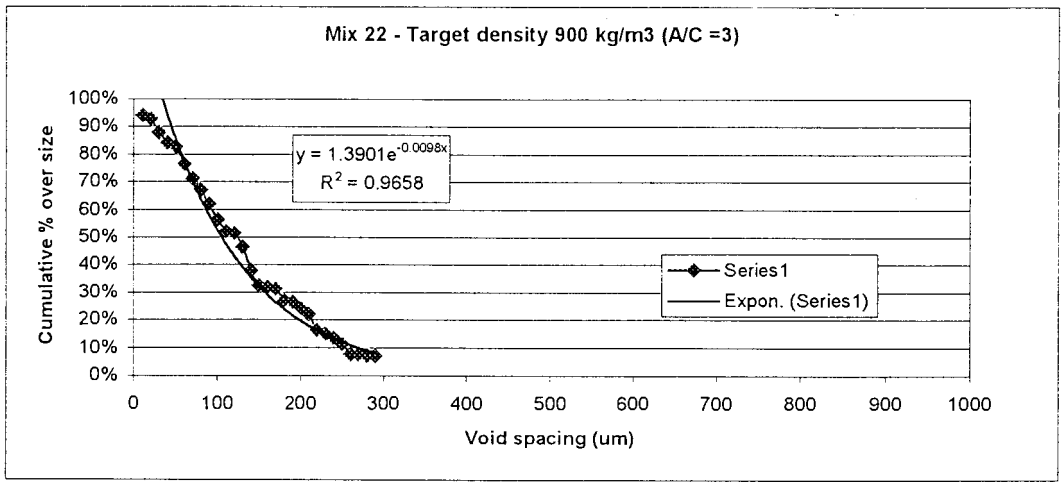
Mix 22 - Target density 900 kg/m3 (A/C =3)
Cumulative % over size
100%
90%
80%
70%
60%
50%
40%
30%
20%
10%
0%
y = 1.3901e-0.0098x
R2 = 0.9658
Series1
Expon. (Series1)
0
100
200
300
400
500
600
700
800
900
1000
Void spacing (um)

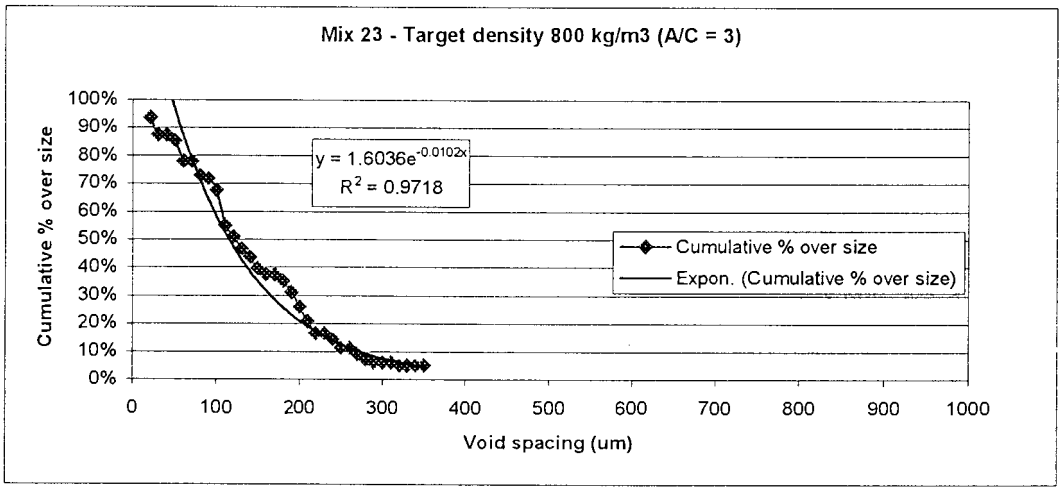
Mix 23 - Target density 800 kg/m3 (A/C = 3)
Cumulative % over size
100%
90%
80%
70%
60%
50%
40%
30%
20%
10%
0%
y = 1.6036e-0.0102x
R2 = 0.9718
Cumulative % over size
Expon. (Cumulative % over size)
0
100
200
300
400
500
600
700
800
900
1000
Void spacing (um)

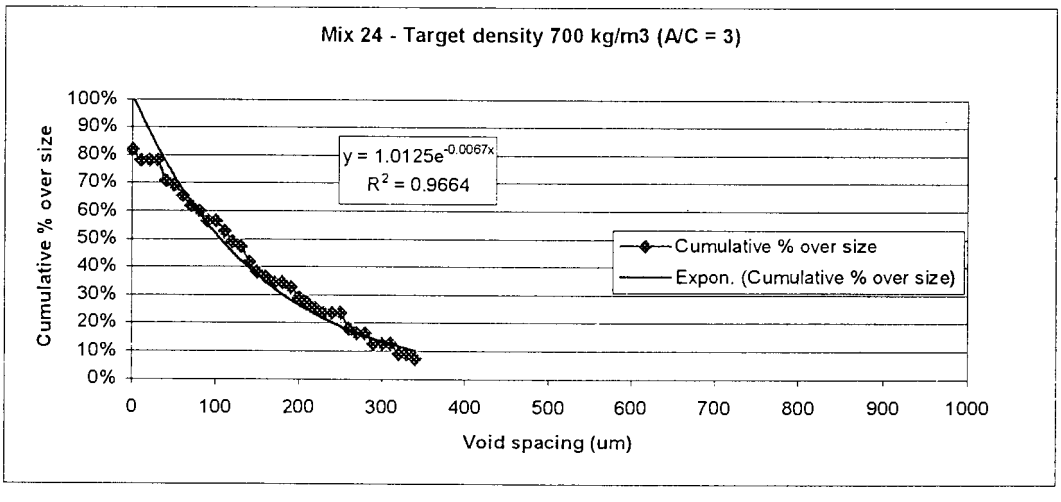
Mix 24 - Target density 700 kg/m3 (A/C = 3)
Cumulative % over size
100%
90%
80%
70%
60%
50%
40%
30%
20%
10%
0%
y = 1.0125e-0.0067x
R2 = 0.9664
Cumulative % over size
Expon. (Cumulative % over size)
0
100
200
300
400
500
600
700
800
900
1000
Void spacing (um)

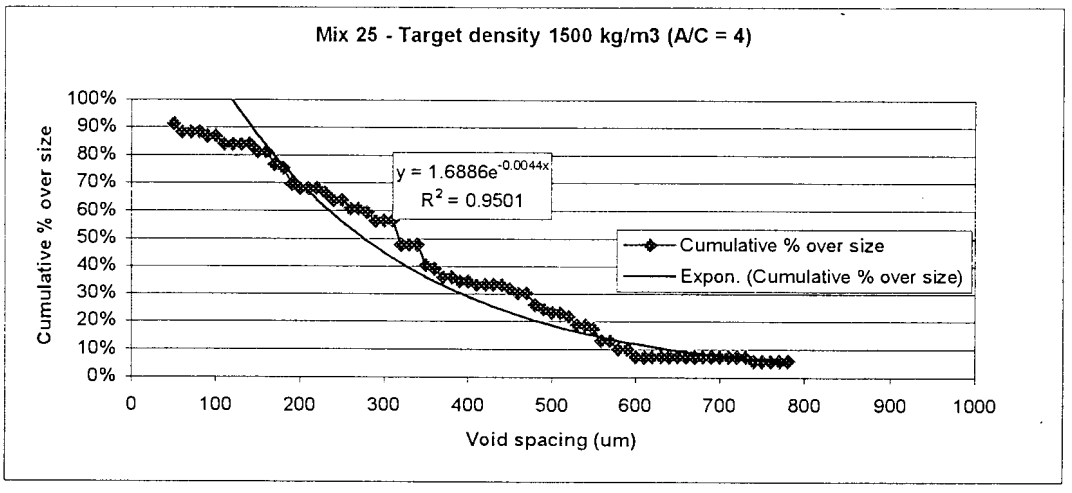
Mix 25 - Target density 1500 kg/m3 (A/C = 4)
Cumulative % over size
100%
90%
80%
70%
60%
50%
40%
30%
20%
10%
0%
y = 1.6886e-0.0044x
R2 = 0.9501
Cumulative % over size
Expon. (Cumulative % over size)
0
100
200
300
400
500
600
700
800
900
1000
Void spacing (um)

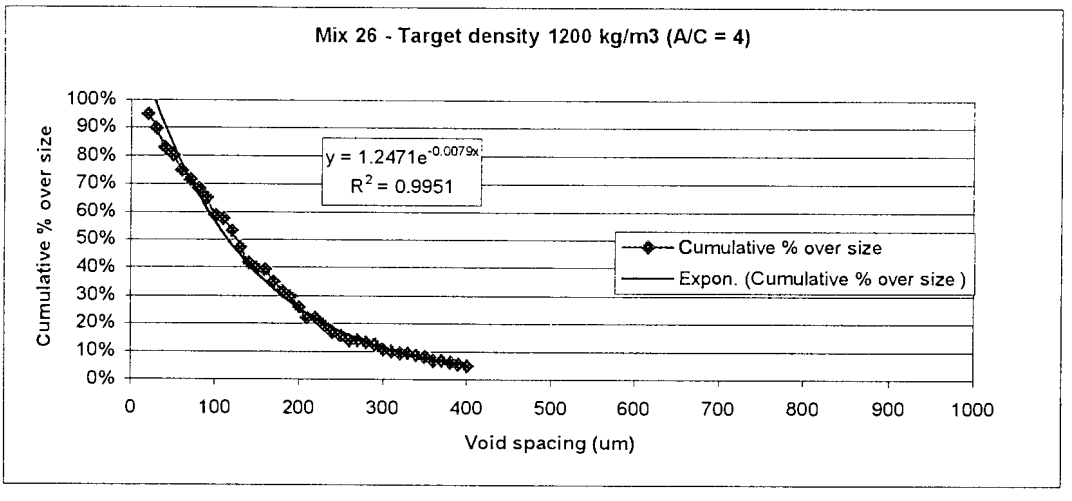
Mix 26 - Target density 1200 kg/m3 (A/C = 4)
Cumulative % over size
100%
90%
80%
70%
60%
50%
40%
30%
20%
10%
0%
y = 1.2471e-0.0079x
R2 = 0.9951
Cumulative % over size
Expon. (Cumulative % over size)
0
100
200
300
400
500
600
700
800
900
1000
Void spacing (um)

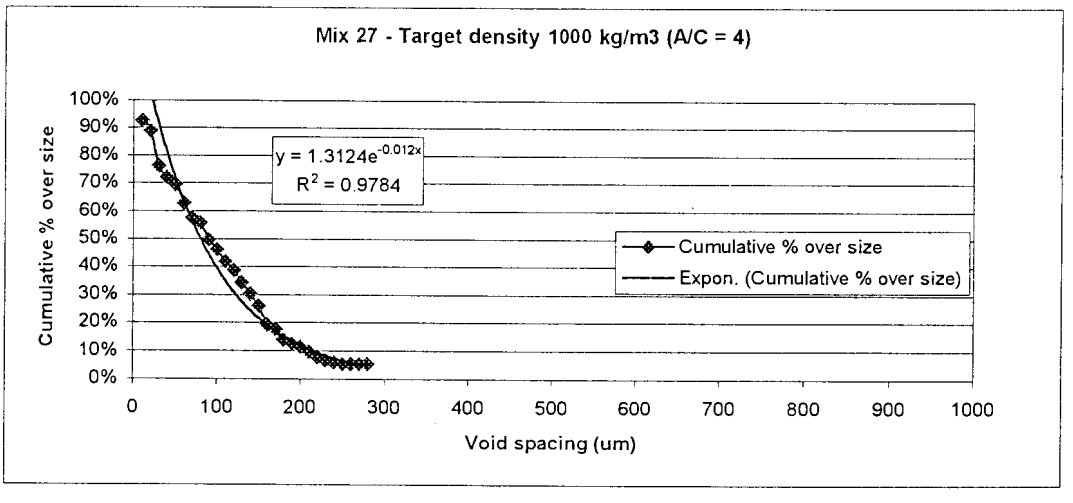
Mix 27 - Target density 1000 kg/m3 (A/C = 4)
Cumulative % over size
100%
90%
80%
70%
60%
50%
40%
30%
20%
10%
0%
y = 1.3124e-0.012x
R2 = 0.9784
Cumulative % over size
Expon. (Cumulative % over size)
0
100
200
300
400
500
600
700
800
900
1000
Void spacing (um)

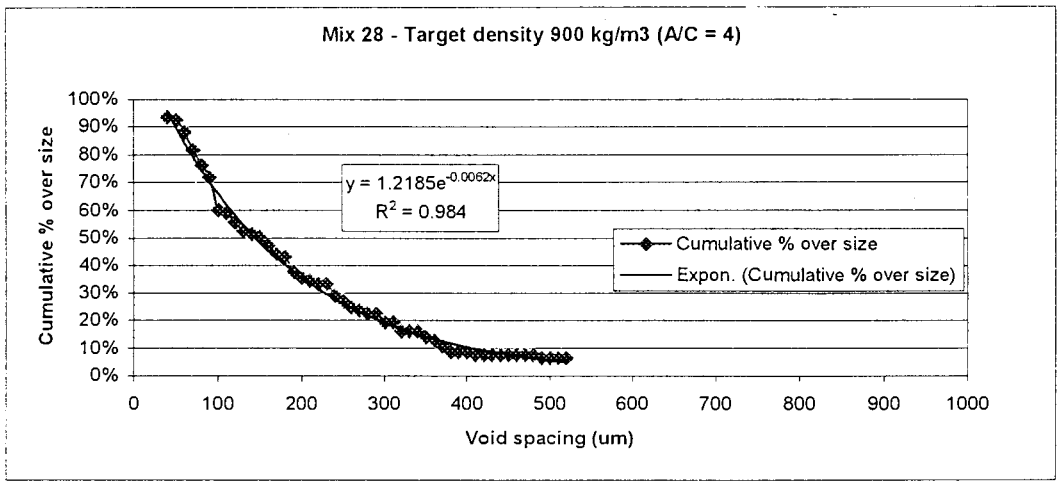
Mix 28 - Target density 900 kg/m3 (A/C = 4)
Cumulative % over size
100%
90%
80%
70%
60%
50%
40%
30%
20%
10%
0%
y = 1.2185e-0.0062x
R2 = 0.984
Cumulative % over size
Expon. (Cumulative % over size)
0
100
200
300
400
500
600
700
800
900
1000
Void spacing (um)

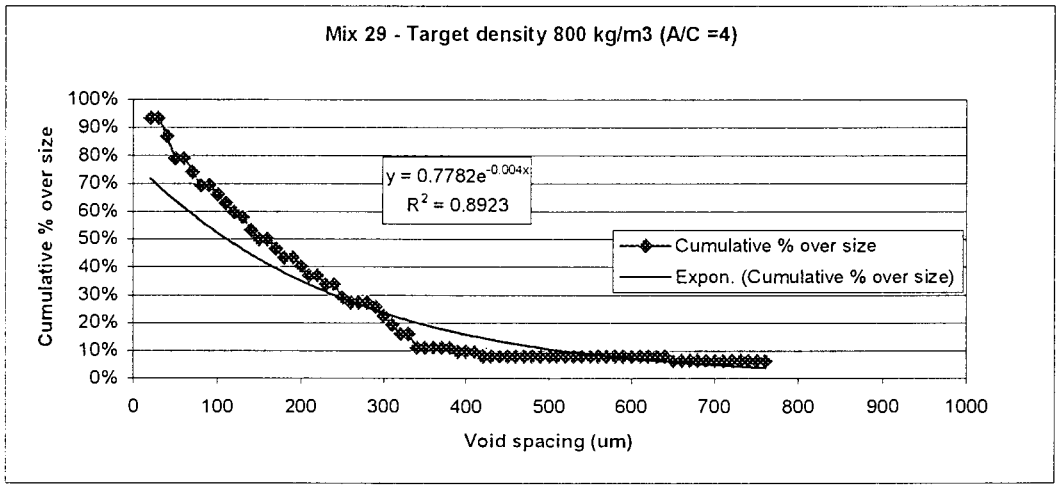
Mix 29 - Target density 800 kg/m3 (A/C =4)
Cumulative % over size
100%
90%
80%
70%
60%
50%
40%
30%
20%
10%
0%
y = 0.7782e-0.004x
R2 = 0.8923
Cumulative % over size
Expon. (Cumulative % over size)
0
100
200
300
400
500
600
700
800
900
1000
Void spacing (um)

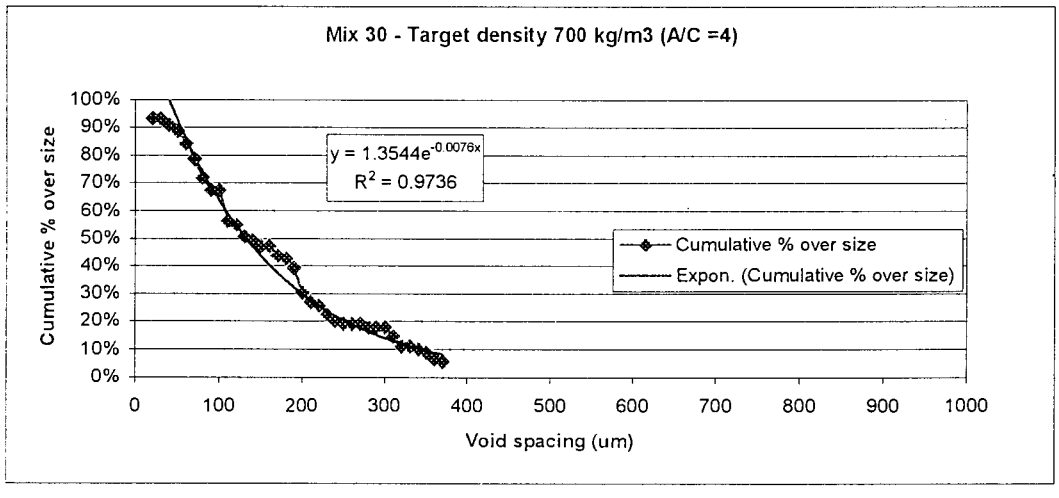
Mix 30 - Target density 700 kg/m3 (A/C =4)
Cumulative % over size
100%
90%
80%
70%
60%
50%
40%
30%
20%
10%
0%
y = 1.3544e-0.0076x
R2 = 0.9736
Cumulative % over size
Expon. (Cumulative % over size)
0
100
200
300
400
500
600
700
800
900
1000
Void spacing (um)

APPENDIX G

SUMMARY OF EXPONENTIAL FITS FOR THE CUMULATIVE % OVERSIZE GRAPHS FOR SPECIFIC ASH / CEMENT RATIOS

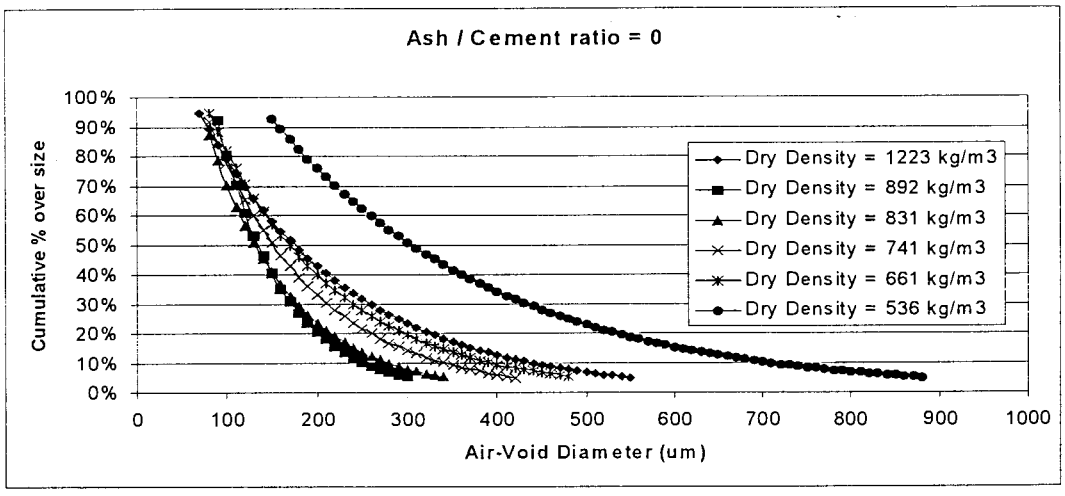
Ash / Cement ratio = 0
Cumulative % over size
100%
90%
80%
70%
60%
50%
40%
30%
20%
10%
0%
0
100
200
300
400
500
600
700
800
900
1000
Air-Void Diameter (um)
Dry Density = 1223 kg/m3
Dry Density = 892 kg/m3
Dry Density = 831 kg/m3
Dry Density = 741 kg/m3
Dry Density = 661 kg/m3
Dry Density = 536 kg/m3

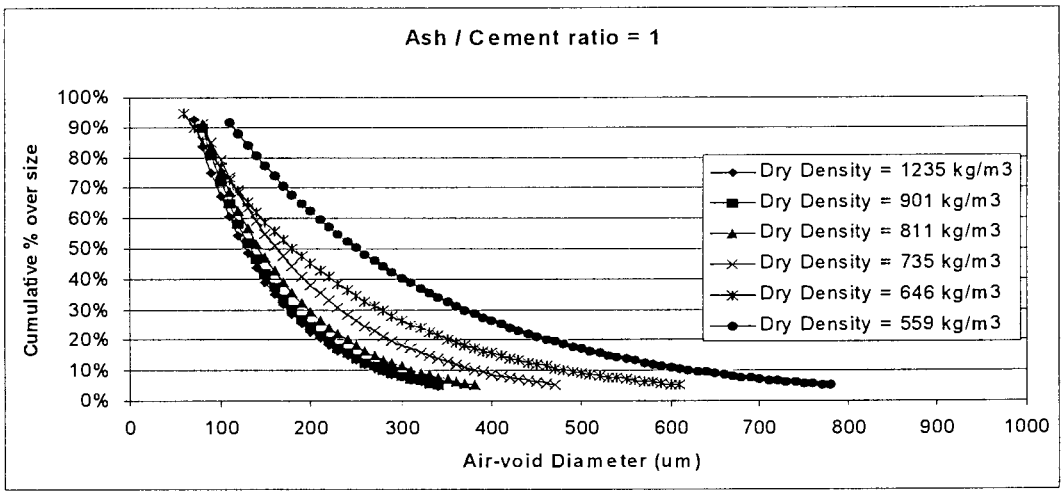
Ash / Cement ratio = 1
Cumulative % over size
100%
90%
80%
70%
60%
50%
40%
30%
20%
10%
0%
0
100
200
300
400
500
600
700
800
900
1000
Air-void Diameter (um)
Dry Density = 1235 kg/m3
Dry Density = 901 kg/m3
Dry Density = 811 kg/m3
Dry Density = 735 kg/m3
Dry Density = 646 kg/m3
Dry Density = 559 kg/m3

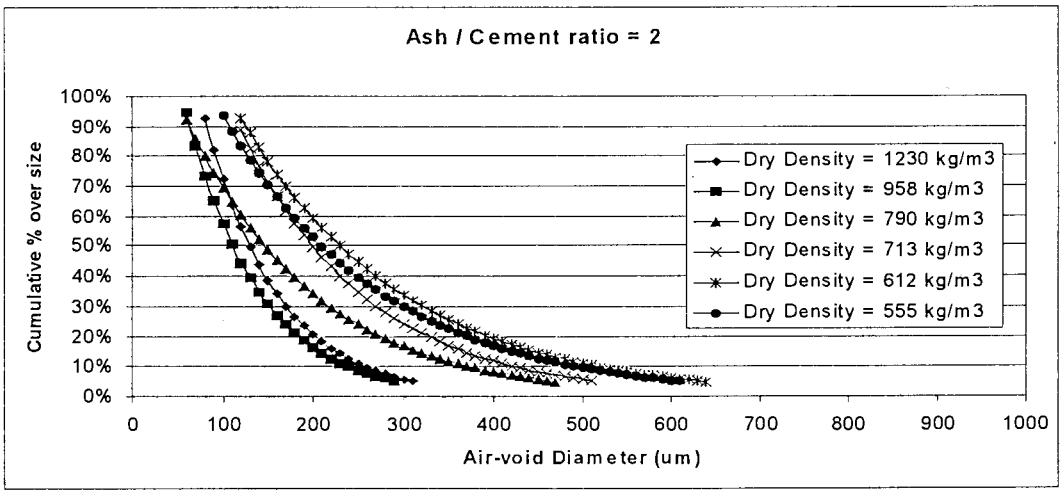
Ash / Cement ratio = 2
Cumulative % over size
100%
90%
80%
70%
60%
50%
40%
30%
20%
10%
0%
0
100
200
300
400
500
600
700
800
900
1000
Air-void Diameter (um)
Dry Density = 1230 kg/m3
Dry Density = 958 kg/m3
Dry Density = 790 kg/m3
Dry Density = 713 kg/m3
Dry Density = 612 kg/m3
Dry Density = 555 kg/m3

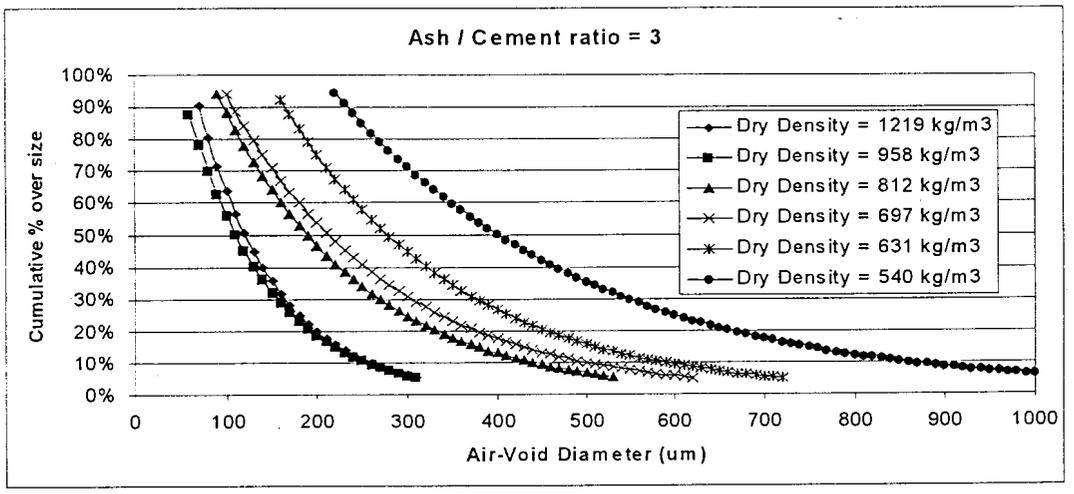
Ash / Cement ratio = 3
Cumulative % over size
100%
90%
80%
70%
60%
50%
40%
30%
20%
10%
0%
0
100
200
300
400
500
600
700
800
900
1000
Air-Void Diameter (um)
Dry Density = 1219 kg/m3
Dry Density = 958 kg/m3
Dry Density = 812 kg/m3
Dry Density = 697 kg/m3
Dry Density = 631 kg/m3
Dry Density = 540 kg/m3

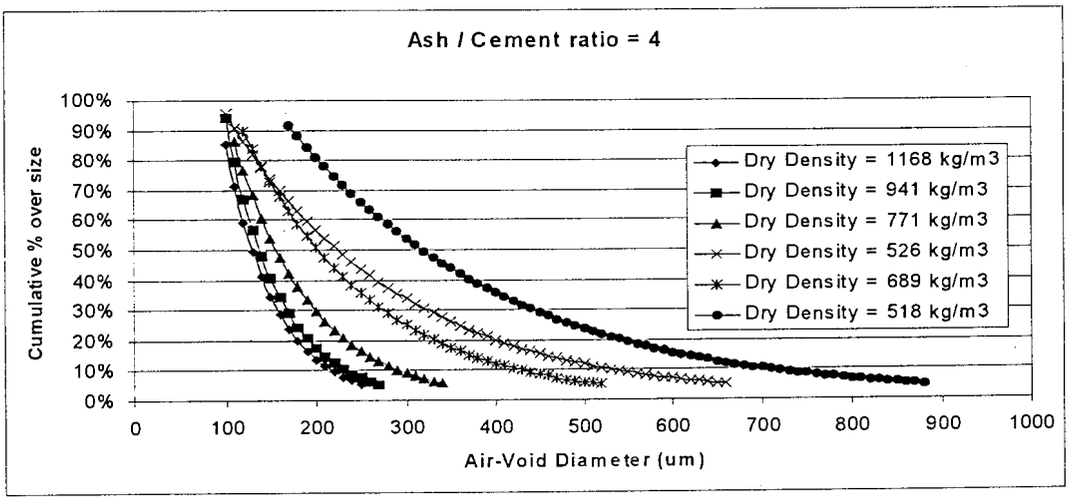
Ash / Cement ratio = 4
Cumulative % over size
100%
90%
80%
70%
60%
50%
40%
30%
20%
10%
0%
0
100
200
300
400
500
600
700
800
900
1000
Air-Void Diameter (um)
Dry Density = 1168 kg/m3
Dry Density = 941 kg/m3
Dry Density = 771 kg/m3
Dry Density = 526 kg/m3
Dry Density = 689 kg/m3
Dry Density = 518 kg/m3